THE UNIVERSITY
of EDINBURGH

Bactericidal mechanisms of nanoparticles and microbial defence strategies

Nimisha Joshi

Doctor of Philosophy

The University of Edinburgh

2013

Declaration

I hereby declare that this thesis has been composed by myself and has not been submitted for any other degree. The work described is my own, except where otherwise stated.

Nimisha Joshi

December 2013

Acknowledgement

I would like to thank my supervisors Dr. Bryne Ngwenya and Dr. Chris French for their guidance and patience during my PhD. I would also like to thank Dr. Andrew Free for his supervision on developing microcosms and microbial community analysis. For supervision on XAS analysis and research facility at Diamond light source, I would like to thank Dr. Fred Mosslemans and also Gbotemi Adedhiran for data processing. I would like to thank Eugene Fletcher for providing me some of his constructs and preliminary characterization data, Steve Mitchell and David Kelly for valuable feedback on microscopy.

I am grateful to Dr Derek Martin and Dr. David Radford for their support and feedback on experiments during my PhD. Thanks to all my friends in Edinburgh for their feedback and lovely company that made it a learning experience.

I am grateful to Rishi Mohan for his love and support and to my parents; this was not possible without you all. This work was supported by the Overseas Research Scholarship (ORSAS) and funding from the School of Geosciences, University of Edinburgh.

Abstract

Manufactured nanoparticles can be toxic to living organisms. This work aims to study the interaction of nanoparticles with bacteria as a model organism. The first objective was, to determine the mechanistic pathways of nanotoxicity with an emphasis on ions and oxidative stress as two key contributors and the second objective, was to investigate what mechanisms bacteria have developed as a strategy to protect themselves against nanotoxicity. The thesis further explores the role of environmental variables such as water chemistry, organic matter and other microorganisms, all of which can potentially change speciation of nanoparticles through their transformation into less toxic species.

KEIO deletion mutants lacking genes encoding proteins which mediate resistance to oxidative stress and ionic toxicity were screened and found to be sensitive to both ionic silver and silver nanoparticles. A bioreporter to detect silver ions was constructed. This was found not to be induced by silver nanoparticles, yet showed reduced viability; this observation also indicates that besides ionic silver there are other toxicity pathways. *E. coli* strains capable of mediating resistance to oxidative stress by overexpression of certain proteins and bio reporters that could detect oxidative stress were constructed. The biosensor cells provide some but not too significant signals. Overexpression of proteins like superoxide dismutase and catalase reduces cell growth, hence, cell viability assays do not provide a realistic measure of protective impact, and thus this strategy is not suited to detect the nature of nanotoxicity.

The protective role of extracellular polymeric substances (EPS) was studied by developing an engineered strain of *E. coli* that overproduces the EPS colanic acid, and use of mutant strains of *Sinorhizobium meliloti*, a free-living N_2 fixing bacterium. Nanoparticle exposure studies reveal that overproduction of EPS mitigates silver nanotoxicity. EPS encapsulates the cells and leads to aggregation of nanoparticles, as shown by microscopy and dynamic light scattering. Furthermore, addition of xanthan, an EPS analogue also produces a similar effect. Lastly, x-ray absorption spectroscopy (XAS) of microcosms amended with silver and zinc oxide nanoparticles show rapid transformation of nanoparticles into corresponding oxides and sulphides. The microcosms show a significant presence of dissimilatory sulphate reducing bacteria (DSRB), and display only marginal change in bacterial community composition on exposure to nanoparticles. These findings suggest that nanomaterials will undergo changes in speciation dependent on the sediment chemistry and the metabolic activities of bacteria in the environment. This process will influence the impact of nanoparticles and the outcomes could be quite different from controlled *in vitro* exposure studies.

Contents

Appendix

List of Figures

List of tables

Abbreviations

^{O}C	degree celsius
µg	microgram
µl	micolitre
µM	micromolar
xg	acceleration due to gravity
CFU	colony forming units
DGGE	Denaturing gradient gel electrophoresis
Diam	diameter
DMEM	dulbecco's Modified Eagle Medium
DNA	deoxyribonucleic acid
Dps	DNA binding protein from starved cells
Eh	Potential difference
EPS	exopolymeric substances
Etbr	ethidium bromide
EXAFS	Extended xray absorption fine structured spectroscopy
FSU	fluorescence unit
g	gram
GFP	green fluorescent protein
HMW	high molecular weight
IPTG	Isopropyl β-D-1-thiogalactopyranoside
KDa	kiloDalton
Km	kanamycin
L	litre

LB	Luria Bertani medium
LCF	Linear combination fitting
LMW	light molecular weight
LPS	lipopolysaccharides
M9	Minimal medium
mg	miligram
ml	mililitre
mM	milimolar
MWCO	molecular weight cut off
nm	nanometer
NMDS	non-metric multidimensional scaling
NP/np	nanoparticles
OD	optical density
OD600	optical density measured at 600 nm
PBS	phosphate buffer saline
PGA	phosphoglyceric acid
ppm	parts per million
RCS	regulation of colanic acid synthesis
RFP	red fluorescent protein
RLU	relative luminescence unit
RNA	ribonucleic acid
ROS	Reactive oxygen species
rpm	revolutions per minute
SD	standard deviation
SEM	scanning electron microscopy
TEM	transmission electron microscopy

UV	ultra violet
W/v	weight per volume
W/w	weight per weight
XANES	X ray absorption near edge structure
XAS	X ray absorption spectroscopy

Chapter 1

Introduction

The current project aims to investigate the interaction of metal nanoparticles with bacteria with a focus on understanding the underlying mechanisms of nanotoxicity and the possible defence mechanisms employed by bacteria against nanoparticle toxicity**.** The study focuses on silver nanoparticles since (a) there is some debate about the relative role of nanoparticles and silver ions in silver nanoparticle toxicity and (b) silver nanoparticles have been shown to undergo rapid transformations with implications for reduction of potential nanotoxicity in the environment. Hence, this chapter starts with a definition of nanoparticles before reviewing previous studies related to their interactions with living organisms. Mechanisms of nanotoxicity including the role of ions and oxidative stress have been discussed further. The chapter concludes with the project outline and the research methodology employed to investigate nanotoxicity.

1.1 Nanoparticles, their sources and applications

A nanoparticle is a broad term that consists of all the particles in the range between 1 to 100 nm in diameter. These could be formed as result of transformations in the earth crust such as volcanic eruptions, by the metabolic activities of the living organisms or could be engineered (Wiesner et al., 2011). Figure 1-1 summarizes different types of nanoparticles based on their origin.

At this small size, the particles behave in a unique manner relative to bulk particles (larger sized) due to their surface area, reactivity and bioavailability. These properties make nanoparticles useful in various industrial applications including health care (Xiao et al., 2012) to develop therapeutics, cosmetics and food industry (Maynard and Michelson, 2006). For instance, titanium based nanoparticles are being extensively used to manufacture sunscreens, toothpaste and skin care cosmetics (Serpone et al., 2007, Weir et al., 2012).

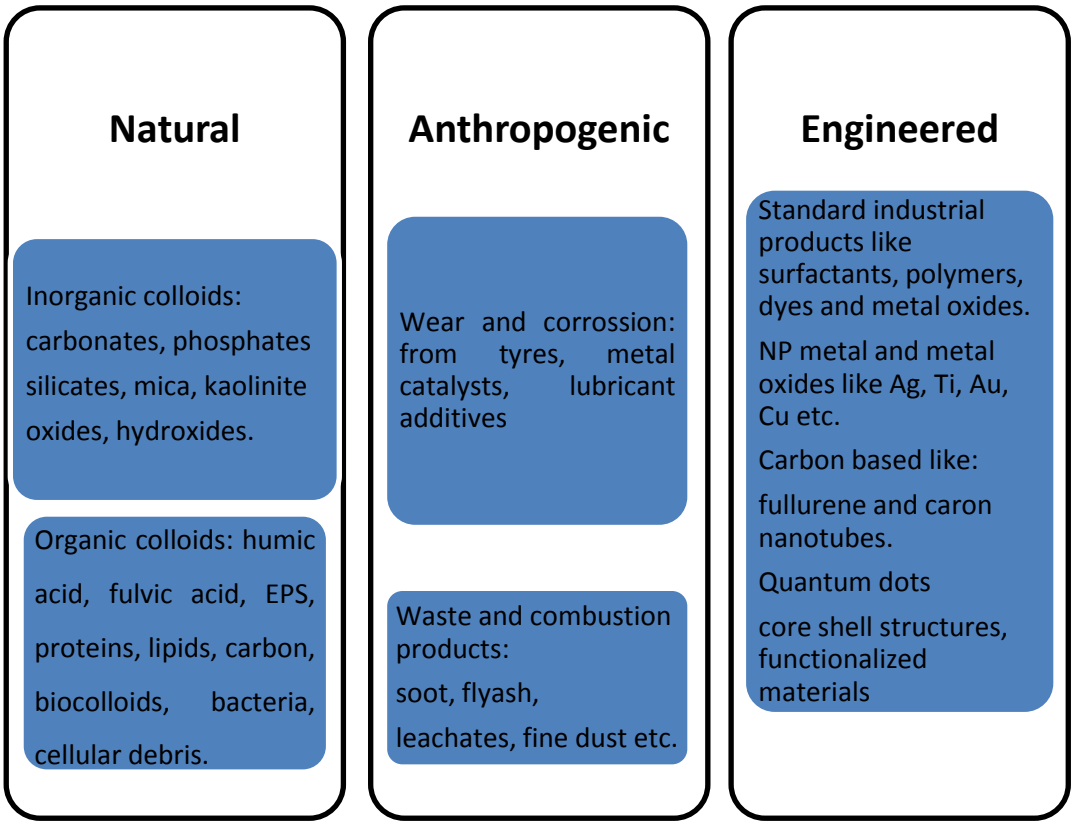

Figure 1-1: Types of nanoparticles and sources of release in the atmosphere

Engineered nanoparticles have been a source of constant attention in the recent past. Iron nanoparticles are used to develop clean up technologies for water purification

(Tratnyek and Johnson, 2006). Metal oxide based nanoparticles are being used in opacifiers, fillers, semiconductors, electronics and prosthetic implants. Besides these applications, studies indicate that fluorescent nanoparticles can be used as biomarkers for effective detection and imaging in cancer diagnostics (Yezhelyev et al., 2006) and drug delivery systems (Tietze et al., 2012). Commonly used engineered nanoparticles and their applications are illustrated in Figure 1-2 (Nel et al., 2006). It is evident that nanoparticles will be extensively used in the future because of their diverse potential applications, likely leading to their release in the environment.

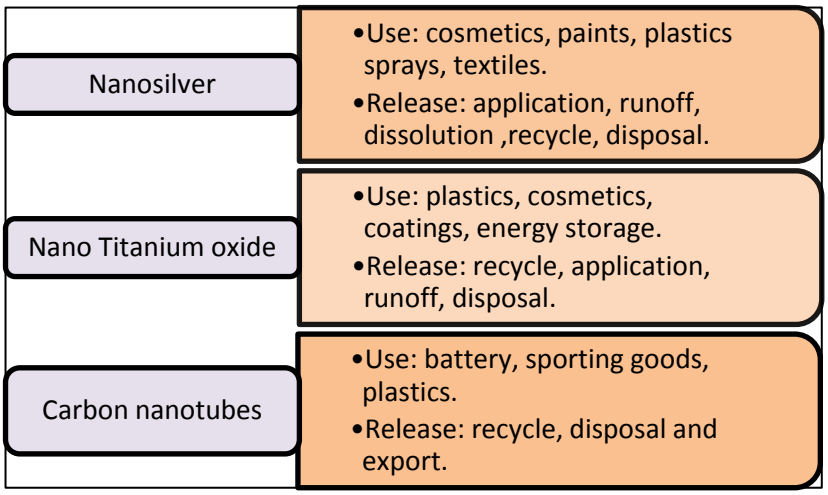

Figure 1-2: Commonly used engineered nanoparticles (Nel et al. 2006)

1.1.1. Interaction of nanoparticles with living organisms: a review

There is a concern amongst scientists about the possible effects of nanoparticles on the atmosphere and the biota and research is being conducted globally to address the safety issues involving their use. Nanoparticles have been shown to have a greater residence time in the atmosphere, thus increasing the chances of direct exposure to living organisms (Nel et al., 2006). As nanoparticles

are small with larger surface area, they can easily diffuse across biological membranes (Urban et al., 2011), disrupt biochemical reactions and produce reactive oxygen species leading to apoptosis (Gou et al., 2010, He et al., 2012). They can accumulate in living organisms and become incorporated in the food chain, and thus cause greater damage to the biota (Lam et al., 2004, Cedervall et al., 2012).

Toxicological studies are being carried out to assess the long term effects of engineered nanoparticles using organisms such as bacteria, nematodes, fungi and mammals. This review summarises the research work conducted on nanotoxicity in order to assess the status and highlight the gaps for future research in this field. Most of the studies indicate that nanoparticles show toxicity by more than one mechanism, it could be ion induced damage or production of oxidative stress (Scown et al., 2010, Johnston et al., 2010, Gaiser et al., 2012, Ma et al., 2013). Figure 1-3 describes possible impact of nanoparticles and associated risks.

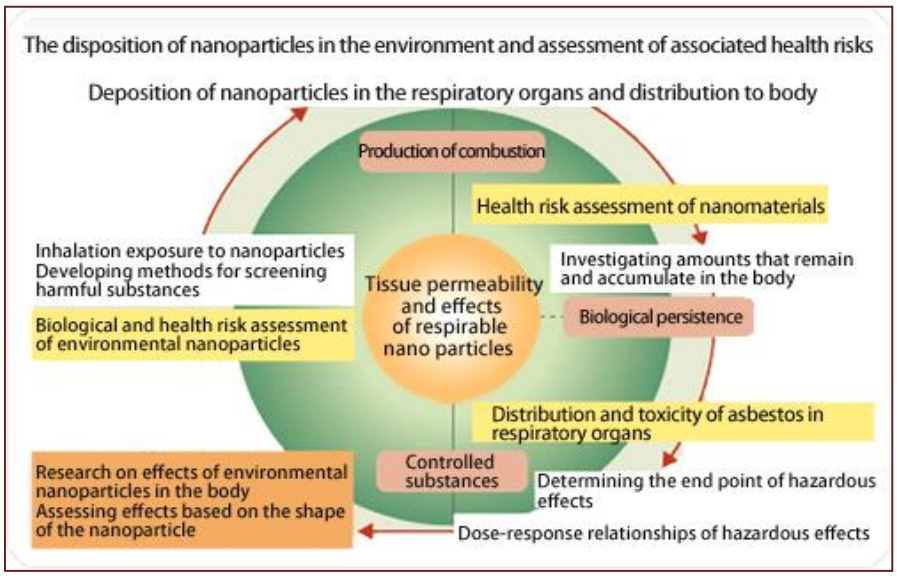

Figure 1-3: Toxicity potential of nanoparticles in environment (Nat. Inst. Env. studies, 2009)

In the next few sections, case studies of nanotoxicity across a range of organisms are discussed to provide background to the relevance of the current study. Table 1-1 in the next section summarizes some of the important nanotoxicity studies conducted so far and their outcomes.

Nanotoxicity studies using mammal as a model organism

Many studies based on eukaryotic cell lines show that engineered nanoparticles can be toxic and cause oxidative stress in mammals (Barillet et al., 2010, Choi et al., 2010, Johnston et al., 2010, Arora et al., 2012, Vandebriel and Jong, 2012). In a study conducted on mice by Lam et al. (2004), mice exposed to carbon nanotubes showed granuloma and necrosis formation in the lungs. In another study by Kenichiro (2008), carbon nanotube exposure led to systemic inflammation in mice. Similarly, a class of nanomaterial called polyaminoamidine dendrimer (PMAM) that is currently being developed for clinical applications was tested on mice (Li et al., 2009). It was found that PMAM has the ability to cause lung injury by inducing autophagic cell death.

Another study done by Bhabra et al. (2009) using human fibroblast cells showed a unique method of toxicity. These cells were exposed to cobalt-chromium nanoparticles (29.5 nm diam) and it was found that nanoparticles could produce a cytotoxic impact without actually crossing the membranes, by transmission of purines such as ATP and cell signalling through gap junction; thereby producing damage to DNA without causing cellular death. Similarly, ZnO nanoparticles were found to be toxic to bronchial epithelial cells and alveolar adenocarcinoma cells by

causing oxidative stress, decreased mitochondrial potential and decrease in production of Interleukin (IL)-8 (Vandebriel and Jong, 2012).

Nanotoxicity studies on invertebrates

A large number of studies have been conducted on the effect of nanoparticles on invertebrates such as crustaceans and nematodes (Lovern and Klaper, 2006, Heinlaana et al., 2008, Poynton et al., 2010, Wani et al., 2011, Tourinho et al., 2012). The common invertebrates studied so far include species of *Daphnia*, Tetrahymena, mussels (*Mytilus edulis*) and annelids such as earthworm (Cattaneo et al., 2009). Dose response experiments have been conducted on these organisms and behavioural changes such as anomalies in swimming rate, feeding and certain physiological aspects have been used as basic parameters to study the effect of C60 fullerenes, quantum dots and metal nanoparticles**.** Results of experiments varied with respect to the species under investigation and the methods employed to synthesize them. For instance, nC60 suspension made by gradual stirring had a lower lethality quotient than those prepared by sonication and LC_{50} (median lethal dose) was reached in less time (Baun et al., 2008). Similarly, *Daphnia magna* was more sensitive to fullerenes than *Daphnia pulex.* It showed an increased heart rate and disruption in swimming and feeding at 10 ppm for nC60 for 48 hours while long term exposure (20 days) reduced the reproduction rate. Exposure to fullerols resulted in oxidative stress in *D. pulex* (Klapera et al., 2009).

Similarly, Blaise et al. (2008) found that the nanotoxicity studies showed varied response with respect to organism and the nanomaterial under investigation.

For instance, amongst all the metal oxides, oxides of copper and titanium in range of 5-50 nm produced adverse impact on physiological processes toxic all three invertebrates *Daphnia pulex***,** *Ceriodaphnia dubia* and *Caenorhabditis elegans*. When bulk salts of silver (silver nitrate) and copper (copper sulphate) were used it was found that *C. elegans* showed most sensitivity amongst the three organisms. Micro-array studies showed that toxicity mechanism varied with each nanoparticle and size used. For instance, Lovern et al. (2006) used different sized titanium dioxide nanoparticles on *D. magna, T. platurus* and *C. spahericus,* and found that the smaller nanoparticles (25 nm or less) were most toxic due to greater surface area and bioavailability.

Nano silver at 125 ppm concentration has been shown to accumulate in the gut of *D. magna* (Oberdörster et. al., 2006) and in the antennae while nano gold particles at 13 nm diameter and 0.75 ppm concentration have been shown to increase stress in digestive glands and hepatocytes in *M. edulis* (Tedesco et al., 2008). Although many toxicological studies have been conducted in invertebrates, the results obtained so far show quite a degree of variability. Therefore, it is necessary to standardize the assays in terms of exposure methods and the nanoparticles being used inorder to derive important conclusions. The invertebrates provide the transitional stage between larger eukaryotes and microorganisms hence they could be used as effective tools to scale observations of the effect of nanotoxicity on prokaryotes to higher organisms (Baun et al., 2008).

Recently Zhang et al. (2012) used Real time quantitative PCR (RT-qPCR) to investigate the impact of copper nanoparticles on the pattern of gene expression in *Caenorhabditis elegans*. The house keeping genes (genes that are normally expressed

for maintaining basic cellular functions in an organism) were used and an oxidative stress sensitive strain of *C. elegans* demonstrated varied impact on the gene expression profile thereby providing vital information on the molecular mechanism of copper oxide nanoparticles.

Nanomaterial	Effects observed	References
Fullerene C60 water suspension	Cytotoxic to human cell lines, Antibacterial, taken up by keratinocytes Morphological changes and adverse effect on larval growth	(Sayes et al., 2004, Lyon and Alvarez, 2005, Waissi-Leinonen et al., 2012)
C60 encapsulated in cyclodextrins, polyethylene glycol	Damages eukaryotic cells, Antibacterial	(Kamat et al., 2000, Yoko et al., 2003, Zhao et al., 2009)
Hydroxylated Fullerene	Oxidative eukaryotic cell damage Reduced growth and apoptosis in multicellular organisms like *C. elegans*	(Kamat et al., 2000) (Cha et al., 2012)
Carboxy fullerene malonic acid derivative	Bactericidal to gram positive cells and human cell lines Induce senescence in cell cycle	(Tsao et al., 1999, Tsao et al., 2001) (Gao et al., 2010)
Fullerene derivative with pyrrolidine groups	Antibacterial, cleaves plasmid DNA	(Tadahiko et al., 2003, Johnston et al., 2010)
Other alkane derivatives of C60	Ant mutagenic, antibacterial, plasmid damage, prevents protein folding	(Tokuyama et al., 1993, Babynin et al., 2002, Johnston et al., 2010)
Metallo fullerene	Accumulates in rats liver Toxicity to plants, oxidative stress	(Cagle et al., 1999) (Long et al., 2012)
Inorganic		
SiO_2	Pulmonary inflammation in rats Cytotoxicity and oxidative stress in lung tissues	(Chen et al., 2004b) (McCarthy et al., 2012)
Anatase (TiO_2)	Pulmonary inflammation in rodents, antibacterial	(Chang et al., 1994, Rehn et al., 2003, Sekar et al., 2011)
Zinc oxide (ZnO)	Antibacterial and pulmonary effects	(Gordon, 1992, Jun et al., 1995) (Vandebriel and Jong, 2012)

Table 1-1: Effect of nanomaterials and associated ions on living organisms (Wiesner et al., 2006) and some recent toxicological studies

Nanotoxicity studies on fungi

Unicellular model organism, *Saccharomyces cerevisiae*, was used to study the effect of nanoparticles of zinc, copper and titanium by Kasmets et al. (2009). In this study both, nanosized and bulk salts of these metals were used in parallel. Titanium dioxide did not cause any toxic effect on yeast in terms of growth while copper and zinc in both bulk and nano sizes were toxic in a dose dependent manner. It was observed that nanoparticles as physical entities could not cause toxicity due to rigid cell wall in yeast but the gradual dissolution of metals in the growth media produced toxicity.

In another study by Kim et al. (2009) nano silver was found to be toxic minimum inhibitory concentration (MIC) of 2 μg/ml to *Candida albicans, S. cervesiase* and *Trichosporon beigelii*. Exposure to nanoparticles caused cell membrane disruption and later stalled binary fission. Chwalibog et al. (2010) investigated the interaction of nanoparticles with *C. albicans* and found that nanoparticles in general with a negative zeta potential (like silver) form a self-assembly around the cell membrane. However, nanoparticles with positive zeta potential (diamond or gold) formed a non-contact interaction that did not cause any damage. Similarly, Bryaskova et al (2011) showed that silver nanoparticles with polyvinyl pyrollidine coating showed a strong antifungal effect on *C. albicans*, C. *capitalis, C. glabrata* and *Aspergillus niger*. Pawlett et al. (2013) used Arbuscular Mycorrhizal fungi and demonstrated that nano zerovalent iron was toxic to fungi but the toxicity was dependent on the soil properties and was least in clayey soils with more organic matter. Humic acid and fulvic acid stabilized the nanoparticles and also

the minerals/clay provided adsorption sites for nanomaterials and prevented the movenement of nanozerovalent iron within the clay structure..

Nanotoxicity and Bacteria

Eukaryotic cells are highly evolved with membranes and sub cellular organelles. The process of sub cellular internalization by phagocytosis and endocytosis (uptake/engulfing of particles) is well studied in them (Xia et al., 2006). The possible impact of nanoparticles as they are ingested and compartmentalized in organelles can provide vital clues about toxicity pathways. Bacterial cells are smaller and establishing reaction mechanism is relatively difficult yet they provide an excellent model to study possible impact of any analyte to the environment. Bacterial models are being widely used to assess the impact of nanoparticles on living organisms. The following studies indicate that the nanoparticles are bactericidal in nature. Investigating the mechanisms of toxicity is the next important step towards a better understanding of microbe-nanoparticle interaction. Bacteria commonly used include *Escherichia coli, Bacillus subtilis, Pseudomonas putida* and *Vibrio fischeri*. The rationale behind using bacterial models is that they can be easily cultured and have shorter life span, are easy to maintain in controlled laboratory conditions and provide excellent models to study cell viability and survival with respect to different nanoparticles and concentrations. They are also at the base of the ecosystem food chain and therefore likely to provide primary information about potential impact of nanoparticles in the natural environment.

Most of the toxicity assays on bacteria rely on calculating the cell viability, using colony forming units and lethality quotient. However, the mechanism of

toxicity is debatable. In a study by Hu et al. (2009), *E. coli* was exposed to nanoparticles of copper oxide (CuO), zinc oxide (ZnO), aluminium oxide (Al_2O_3) and titanium oxide (TiO_2). It was seen that, at a similar concentration and incubation period the ZnO nanoparticles had the lowest toxicity while TiO_2 was most toxic to *E. coli*. In order to study the effect of silver nanoparticles on bacteria, Sondi et al. (2004) exposed *E. coli* to varying concentration of silver and cell viability was determined as shown in Figure 1-4. Silver nanoparticles were bactericidal and deposited in the cell membrane. They released silver ions due to dissolution from their surfaces and affected membrane permeability (figure 1-5a, b).

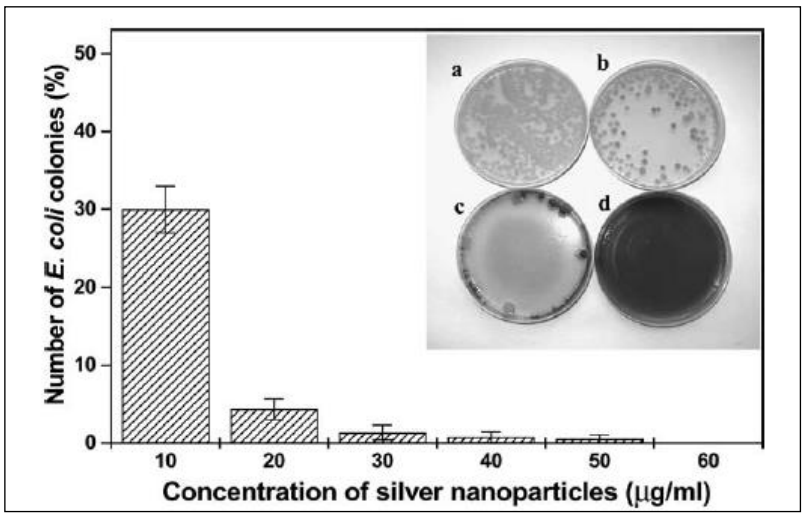

Figure 1-4. Shows the number of viable cells as a function of silver nanoparticle concentration (Sondi et al., 2004)

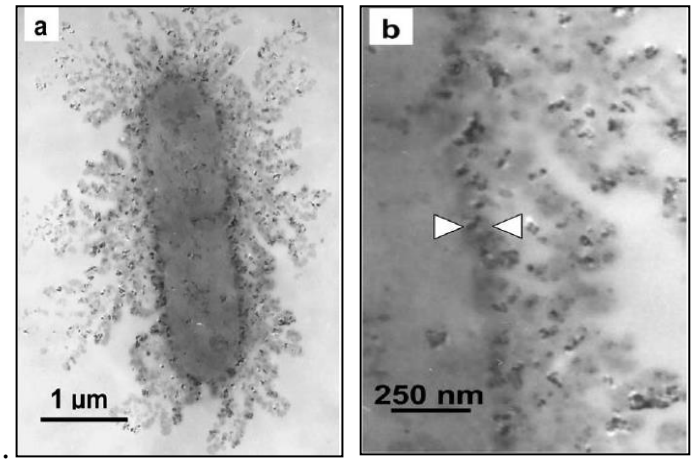

Figure 1-5(a) Shows the transmission electron micrograph of *E.coli* treated with 50µg/cc silver. Figure 1-5(b) shows the membrane damage. (Sondi et al., 2004)

Studies report that gram positive bacteria show a higher viability than the gram negative due to the fact that they form spores (Rincon and Pulgarin, 2005). The variability can also be due to the differences in cell wall composition. Gram positive bacteria have a thick peptidoglycan layer which can trap nanoparticles and prevent cellular uptake (Jin et al., 2010). The negatively charged outer membrane of gram negative bacteria can attract more metal ions than a gram positive one (Valodkar et al., 2010). Morones et al. (2005) reported that under a similar concentration of silver nanoparticles gram positive bacteria showed a higher tolerance level than gram negatives. This effect was seen upto 75 µg/ml of nanoparticle concentration and above this concentration; silver nanoparticles were bactericidal for all the species. Adams et al. (2006) used both, the gram positive (*Bacillus subtilis*) and gram negative bacteria (*E. coli*) as model organisms to study the effect of oxides of silica, zinc and titanium. They found that, silica was least toxic to bacteria and other two nanomaterials exhibited a differential toxicity. *Bacillus subtilis* was more susceptible

to nanotoxicity at low concentrations of metal exposure, for instance 10 ppm of zinc oxide induced 90 percent toxicity in cultures while higher metal concentrations were required to get the same observations in *E. coli.* This study was exceptional in its findings in contrast to others that have been reported earlier. Similarly, nanosized copper and zinc were found to be toxic to bacteria cells (Heinlaana et al., 2008). In another study, Gajjar et al. (2009) developed a recombinant strain of *Pseudomonas putida* with a copper responsive promoter and *lux* as a reporter gene. The bacterium was exposed to nanoparticles and decrease in luminosity was observed with increasing concentration of silver and copper nanoparticles. This study showed that nanoparticles affected the bacteria in terms of growth and viability. The nanoparticles of silver and copper were bactericidal while zinc oxide exhibited more of a bacteriostatic response. In a recent study, both nano TiO_2 and ZnO were found to adversely affect the bacterial population across the whole range of taxa and small sized nanoparticles were found to be more toxic (Ge et al., 2012)

Since bacteria are ubiquitous in nature, the possible impacts of engineered nanoparticles can be studied by using them as model organisms, with emphasis on the features like biofilms, presence of ions, pH of medium and oxidation state can influence the nanoparticle behaviour. Therefore, the factors that can alter the behaviour of nanoparticles need to be addressed. The following section illustrates the importance of these variables in light of the research work conducted in past few years in this field.

1.1.2. Physical properties of stabilized nanoparticles and environmental factors that influence their behaviour and stability

Nanotoxicity depends on two factors one, the physico-chemical properties of the nanoparticles themselves and two, environmental variables like pH of medium, presence of ions, organic matter etc. that can influence the stability and reactivity of nanoparticles. Both these features can have profound effect on toxicity.

1.1.2.1 Physico-chemical properties of engineered nanoparticles

The properties of nanoparticles include shape, size, and chemical properties of nanoparticles. The size of nanoparticles may greatly influence the toxic impact (Auffan et al., 2008, Xia et al., 2008, Simon-Deckers et al., 2009, El Badawy et al., 2010, Lankoff et al., 2012). For instance, in an exposure study using *E. coli* as a model organism, Morones et al (2005) showed that the silver nanoparticles in the range of 1-10 nm diameter were more toxic than larger nanoparticles (50-100 nm diam). Similar results were reported by both Choi (2008) and Raghupati (2011). The nature of nanoparticle also affects the toxicity. Fullerene C60 and some metal nanoparticles both show toxicity but the underlying mechanisms are quite different. Metal nanoparticles like silver, TiO_2 or ZnO show toxicity due to ion-mediated damage upto a point (Jin et al., 2010, Napierska et al., 2012). The C60 suspension on the other hand produced oxidation of proteins in a non-ROS (reactive oxygen species) mediated pathway (Lyon and Alvarez, 2005).

Pal et al. (2007) showed that the shape of silver nanoparticle could affect their toxicity. For instance, the truncated triangular nanoparticles were more biocidal than the spherical or rod shaped nanoparticles because of more active sites or ridges.

Presences of coating agents have been shown to influence the toxicity of nanoparticles too. Presence of cationic stabilizers like cetyl trimethyl ammonium bromide (CTAB) increased the toxicity of silver nanoparticles much more than the anionic chemicals like SDS (sodium dodecyl sulphate) probably because the negative charge on SDS molecules interfered with absorption of bacterial surface on to silver nanoparticle or silver ions by electrostatic effects (Bae et al., 2011).

1.1.2.2 Environmental factors that affect nanotoxicity

Environmental variables such as pH of the exposure medium and experimental conditions, may all contribute to net toxic impact. Divalent cations in medium can affect the behaviour of nanoparticles. For instance, Jin et al. (2010) showed that addition of divalent cations to medium with silver nanoparticles caused differential toxic behaviour. In case of gram-negative bacteria, the divalent cations increased the bactericidal potential of silver nanoparticles probably by acting as bridge between silver nanoparticles and lipopolysaccharide (LPS) layer. This provided a greater attachment of silver nanoparticles on the cell membrane thereby allowing an increase in local concentration of nanoparticles. In contrast, the divalent cations competed with silver ions for bacterial membrane in case of gram-positive bacteria and showed a protective response.

Growth medium components have been shown to affect the nanoparticle behaviour. For example, Li et al. (2011) found that ZnO nanoparticles were most toxic in water, and the presence of ions such as those in phosphate buffer saline (PBS) reduced the toxicity probably by encouraging surface complexation and reducing the concentration of free zinc ions. Xia et al. (2008) observed that use of

Dulbecco's modified eagle medium (DMEM) as a growth medium initiated the agglomeration of polystyrene nanospheres and this clumping action reduced their toxicity potential. A possible reason behind this observation could be that proteins present in the growth medium get adsorbed on the nanospheres resulting in the neutralization of charge and interference in electrostatic repulsion. Fabrega et al. (2009) showed that the toxicity of silver nanoparticles varied with pH and the presence of organic matter such as humic acid. Humic acid altered the nanoparticles behaviour, stabilized them and reduced the short-term toxicity by keeping them in a dispersed form.

It is evident that nanoparticle behaviour and stability is dependent on many variables that can greatly alter their reactivity towards living organisms. Besides these factors, nanoparticles can undergo rapid transformation once released in the environment and this could in turn affect their toxic potential and stability. Recently, realistic experimental models that could mimic natural environments have been used in order to understand the nanoparticle behaviour in a complex environment. It certainly indicates that engineered metal nanoparticles will be rapidly transformed once released in the environment.

For instance, French et al. (2009) have shown that the presence of ions like chlorides can promote rapid aggregation of titanium oxide nanoparticles. Since natural waters have certain levels of chlorides, this can influence the bioavailability of metal nanoparticles. In another study, by Unrine et al. (2012) it was found that the dissolved organic matter released by plants and algal matter in microcosms rapidly complexed to silver ions released by silver nanoparticles. Secondly, Bone et al. (2012) report that the presence of ions like chlorides, and sulphides caused

transformation of silver into silver chlorides and silver sulphides. This in turn reduced the bioavailability of ionic silver and reduced their toxic potential.

1.2 Mechanisms of nanotoxicity

The toxicity of engineered nanoparticles to living organisms has been attributed to a number of mechanisms, including, ion-mediated toxicity, membrane disruption, injury to cells and in some cases production of oxidative stress. For example, **z**inc ions released from zinc oxide nanoparticles influence the activity of dehydrogenases and cause an inhibition of respiratory chain reactions (Mills et al., 2002, Nguyen et al., 2006). Similarly, silver ions formed by surface dissolution from silver nanoparticles have been reported to prevent DNA replication and cause inactivation of proteins carrying sulfhydryl groups (Beard et al., 1995). Oxidative stress has been implicated as a toxicity mechanism in a large number of studies. Hence, the following section deals specifically with oxidative stress mechanism and the possible role of nanoparticles in this process (Note that some nanomaterials like fullerene have been found to be toxic but not directly involved with generation of oxidative stress) (Lyon, 2007). Figure 1-6 illustrates the possible mechanisms by which nanoparticles produce toxicity to living organisms.

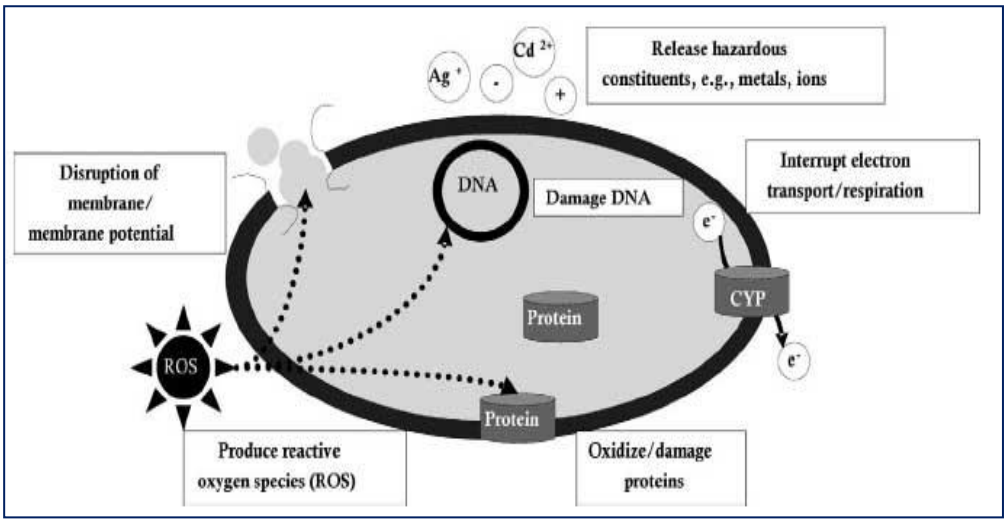

Figure 1-6: Possible mechanisms by which nanoparticles may interact with cells and cause damage (Klaine et al. 2009)

1.2.1 Oxidative stress in organisms: an introduction

Oxygen is a prerequisite for all obligate aerobic organisms of the animal kingdom including mammals, bacteria and other members. The very oxygen that plays a key role in energy production also creates an undesirable array of reactive oxygen species (ROS). These ROS are capable of interfering with biochemical pathways in an organism (Davies, 2000). Thus, this situation creates what is known as "The oxygen paradox" (Davies, 1995). Living organisms including bacteria have evolved an efficient method to deal with stress. This process mediates the activation of many genetic pathways, the resultant reactive oxygen species are converted into less damaging components (scavenged by enzymes and inactivated). Under certain conditions like presence of chemicals, diseases or injury when the rate of generation of ROS is much higher than its removal, a situation known as oxidative stress arises (Farr and Kogoma, 1991).

Active species of oxygen include superoxide radicals ($O_2^{\cdot}$), peroxide (H_2O_2) and hydroxyl radical ($OH^{\cdot}$). In an aerobic organism, these are produced due to metabolic activity like conversion of molecular oxygen to water (electron transport chain). In this process, several enzymes including succinate dehydrogenase, NADPH dehydrogenase and lactase dehydrogenase form superoxide radicals (Imlay and Linn., 1987, Liochev et al., 1999, Imlay, 2003).

Similarly, autoxidation of ubiquinones, catechols and thiols can trigger release of oxyanions. UV radiation triggers peroxide radical formation. Singlet oxygen can be released by decomposition of superoxide anion and some other enzymatic pathways (Farr and Kogoma, 1991). Besides these natural processes, presence of certain chemicals like hydrogen peroxide, paraquat and antibiotics can also lead to production of these ROS. These can be quite harmful to the organisms and found to be involved in DNA damage, mutations, and membrane damage and protein oxidation. The adverse impact of ROS is discussed in the following section.

1. **DNA damage:** When a cell is exposed to hydrogen peroxide, superoxide radicals and ozone, the ROS attack the nitrogen bases and sugar moieties associated with DNA. Peroxide specifically attacks the sugar residues and produces breaks in DNA strands. Bases decompose to form urea-based products. Similarly, oxidation of fatty acids and lipid peroxidation causes further damage by producing compounds that further compromise cellular integrity. These products include several aldehydes and alkenes that later attack the DNA molecules by reactions like alkylation or formation of intrastrand linkages (Saul and Ames., 1986, Imlay and Linn., 1987, Aruoma and Halliwell., 1991.).

2. **Mutagenicity**: ROS are involved in DNA strand breakage and cause harmful mutations. Hydrogen peroxide has a strong mutagenic potential and has been reported to cause mutation in *E. coli* (Fenn et al., 1957).
3. **Membrane damage**: The reactive oxygen species mainly; $OH^{\cdot}$, OOH and singlet oxygen can initiate membrane damage in bacteria. The cell membrane is mainly composed of lipids and proteins and these ROS attack both these components. Lipid chains undergo peroxidation reaction resulting in formation of short chain fatty acids and in this process aldehydes and ketones. All these compounds are mutagenic in nature. These short chain fatty acids are mobile, increase fluidity, and enhance permeability. This diminishes the proton gradient and leads to cell membrane damage and cell leakages (Cabiscol et al., 1999).
4. **Protein damage:** Many enzymes in *E. coli* become inactive or denature when ROS interfere with them. For instance, amino acids such as arginine and proline form their carbonyl derivatives in presence of ROS. Similarly, methionine and cysteine form sulfoxides by disulphide bridge formation (Imlay, 2003).

Oxidative stress is inevitable in many ways, as aerobes require oxygen for metabolism. Living organisms have therefore developed efficient mechanisms to face this crisis and this is robust until overwhelmed by chemicals or environmental stress. For instance, in bacteria such as *E. coli* over 30 genes are up regulated when the bacteria is exposed to hydrogen peroxide or superoxide anions (Spencer B and Tokio, 1991). Figure 1-7 illustrates the enzymatic intervention to mediate oxidative stress in bacteria

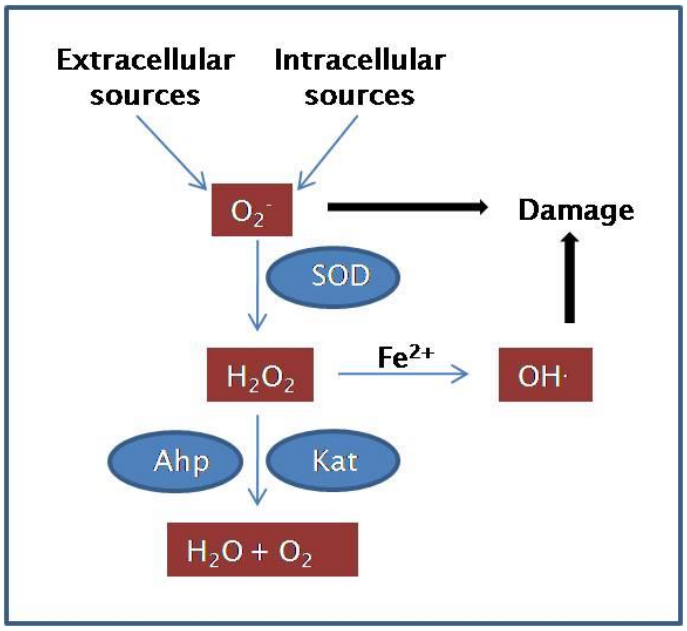

Figure 1-7: Enzymatic response of bacteria to ROS (Mertens, 2008). Superoxide dismutase (SOD), catalase (Kat G) and alkylhydroperoxide reductase (Ahp) mediate ROS (Mertens, 2008).

The oxidative stress response in *E. coli* is well characterized and requires the activation of two regulons namely the OxyR and SOX/SOR. Both of these are specific to the chemical nature of oxidative stress (Cabiscol et al., 1999).

1.2.1.2 Nanoparticles and oxidative stress

Recent studies show that nanoparticles produce oxidative stress in bacteria (He et al., 2012, Ivask et al., 2012). There is much speculation on this issue that is further complicated by the question of whether nanoparticles cause oxidative stress due to small particle size or simply by dissolution from their surfaces. Figure 1-8 illustrates different mechanisms by which nanoparticles induce the formation of ROS.

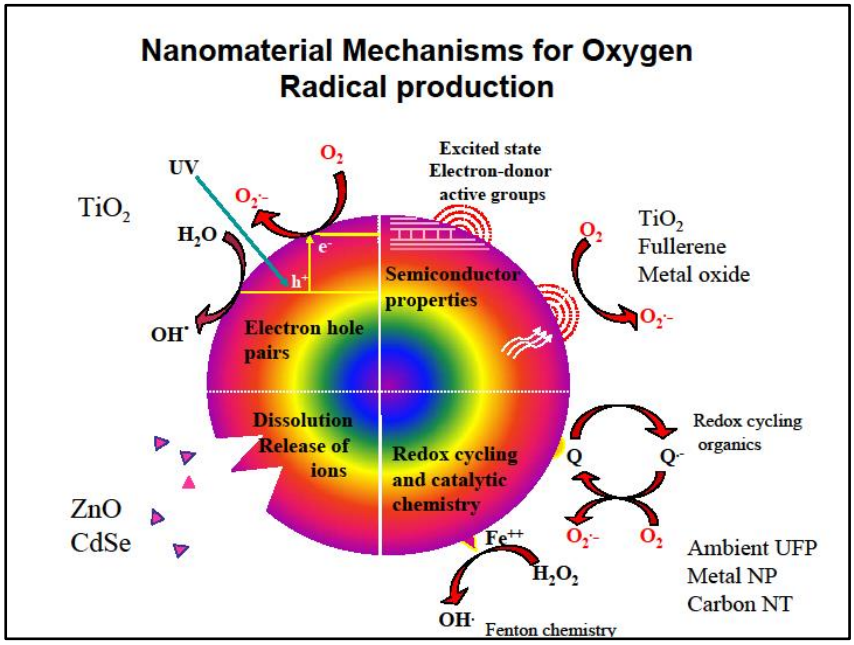

Figure 1-8: Mechanism of reactive oxygen species generation (Nel, 2006)

A large number of studies have focussed on this question but there are some gaps with respect to the findings. The variations due to type of nanoparticles used, exposure methods further complicates the scene. There is debate on the type of ROS generated during nanotoxicity. For instance, one study used special bioreporters and demonstrated that silver nanoparticles are bactericidal to *E. coli* and *S. aureus* due to formation of superoxide radicals and not peroxide (Park et al., 2009). In contrast, the exposure study conducted by Gajjar et al. (2009) states that silver nanoparticle exposure stimulates generation of extracellular hydrogen peroxide. In another study by Choi and Hu (2008), ROS generation was found to be instrumental for some fractions of nanosilver (8-21 nm) only. As for the bulk forms of silver, ROS was not the primary cause of toxicity. Kumar et al. (2011) reported the involvement of zinc oxide and titanium oxide nanoparticles in producing DNA damage and

oxidative stress in *E. coli.* Similarly, an exposure study using titanium oxide showed the production of reactive oxygen species as a dominant mechanism for cytotoxicity (Battin et al., 2009). The screening of deletion mutants of *E. coli* with polystyrene nanoparticles indicated that apart from ROS, other pathways related to cell membrane integrity, DNA repair, flagellar movement were involved. This indicates that bactericidal activity of nanoparticles is a complex response than a simple cause-effect relationship (Ivask et al., 2012). A microarray study conducted recently shows that cerium oxide nanoparticles initiate a global stress response system in *E. coli* (Gou et al., 2010). It can be seen that there is a lack of consensus about the exact nature of ROS formed in different studies. However, it is worth mentioning that most of studies indicate that oxidative stress is a prominent feature associated with nanotoxicity.

1.2.2 Nanoparticles and ionic toxicity

Nanoparticle exposure studies using engineered (metal and metal oxide) nanoparticles demonstrate that ions also contribute to the nanotoxicity. There is a lot of debate about the exact nature of nanotoxicity whether its ions or nanosilver or both (Lubick, 2008). Many exposure studies do provide a significant amount of data that establishes the role of ionic silver in nanotoxicity. For instance, Lok et al. (2007) demonstrated that antibacterial activity of silver nanoparticles was primarily due to chemisorbed silver ions on surface of nanoparticles and the presence of oxygen in the medium accelerated the oxidation of silver and ionic release. Liu et al. (2010) demonstrated that silver nanoparticles release ionic silver and this could be checked by addition of thiol, cysteine and citrate ligand bindings and formation of sulphide

coating. Kittler et al. (2010) studied the dissolution kinetics of stabilized nanoparticles and observed that aged nanoparticles could release as much as 90% of total silver and were more toxic than the fresh batches. In another study, Nagi et al. (2011) also demonstrated that silver nanoparticles embedded in zeolite membrane demonstrated bactericidal properties due to slow release of silver ions. It has been reported that silver nanoparticles are less toxic in anaerobic conditions; partially because low oxygen restricts ionization. This provides circumstantial evidence of the role of ions as a prominent mechanism of silver nanotoxicity (Xiu et al., 2012).

ZnO nanoparticles have been shown to be cytotoxic to eukaryotic organisms due to release of zinc ions (Franklin et al., 2007, Lin et al., 2007). The nanoparticles accumulated in the organs of mice (Wang, 2008) and triggered oxidative stress, membrane damage and mitochondrial injury (George et al. 2009). In case of bacteria, the impact of zinc oxide nanoparticles has been found to be bacteriostatic and many studies show that ionic zinc and internalization of zinc oxide nanoparticles both contribute equally towards the toxicity (Huang et al., 2008, Gajjar et al., 2009, Hu et al., 2009, Li et al., 2011).

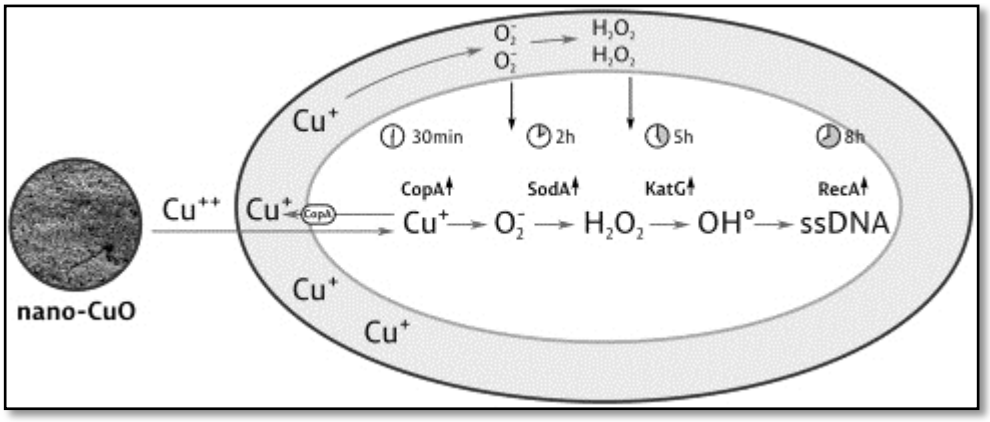

Figure 1-9: Role of copper ions in oxidative stress in *E. coli* bioreporter (Bondarenko et al. 2012), showing ROS generated by copper ions leading to breaks in DNA strands.

Copper nanoparticles are toxic to organisms like algae, mammals and bacteria. The role of copper ions has been found to be instrumental in producing toxicity. In an exposure study using algae, it was shown that particle solubility plays an important role for producing toxicity of oxides of copper, zinc and titanium (Franklin etal.2007). Toxicity of copper oxide nanoparticles has been verified in recent studies by others (Kasmets et al., 2009, Peralta-Videa et al., 2011, Gomes et al., 2012, Ya Nan et al., 2012). Recently, Bonarenko et al (2012) developed oxidative stress responsive probes and showed that dissolution of copper ions from CuO nanoparticles triggered ROS generation and breaks in DNA strands in *E. coli*. The process has been illustrated in Figure 1-9. A global approach that incorporates effect of nanoparticles together with the possible defence mechanisms employed by organisms can help to provide a realistic assessment of nanotoxicity.

1.3 Defence mechanisms against nanotoxicity

Nanoparticles of natural origin like carbon particles, soot and sulphur have been an intrinsic part of the earth's environment (Wisener et al. 2009). Evidence of coexistence of nanoparticles with life suggests that organisms may have features that can enable them to survive exposure to nanoparticles. Therefore, a study of possible defence mechanisms can provide vital information about how life in general, especially bacteria will respond to engineered nanoparticles and the strategies they could use to minimize nanotoxicity. A study in this direction will help to provide a realistic assessment of hazards associated with nanoparticles (Nies and Silver, 1995). Bacteria have special efflux pumps to shuttle undesirable metal ions from the cytoplasm and periplasm (Munson et al., 2000, Petersen and Moller, 2000). Secondly, formation of biofilms has been shown to protect them against desiccation, injury and heat shock (Allison et al., 1998). It is therefore important to investigate if these global stress responses, cell structure (channels like porins) together with protective measures (genetic intervention), can play an important role against nanotoxicity.

1.3.1 Biofilms

Microorganisms have been shown to inhabit environments often as a complex communities and aggregates on the surfaces forming mats, films, flocs and sludges (Flemming and Wingender, 2010). This complex consortium of living organisms is diverse in population and is found embedded in a common matrix known as a biofilm. Biofilms serve many important purposes including providing protection

against abiotic stress such as change in pH, osmolarity, desiccation, presence of chemicals and starvation in microorganisms (Hall-Stoodley et al., 2004). Table 1-2 highlights the key components of EPS and their functions.

Function	Relevance for Biofilm	EPS component involved
Adhesion	Allows the initial steps in colonization of abiotic, biotic surfaces by planktonic cells	Polysaccharides, proteins, DNA and amphiphilic molecules
Aggregation of bacterial cells	Bridging between cells, immobilization, cell-cell recognition	Polysaccharides, proteins, DNA
Cohesion of biofilms	A hydrated matrix that provides mechanistic stability(involves capsules, slime and sheath)	Neutral and charged polysaccharides, proteins and DNA
Retention of water	Maintains a hydrated environment, helps during dessication	Hydrophillic polysaccharides and proteins
Protective barrier	Protects against antibiotics, protozoa and also protects nitrogenase enzyme	polysaccharides and proteins
Sorption of organic and inorganic compounds	Enables accumulation of nutrients and ion exchange, mineral formation	Charged polysaccharides and proteins
Nutrient source	Acts as a source of carbon, nitrogen and phophorous	All EPS components
Sink for excess energy	Excess carbon storage	Polysaccharides
Electron donor/acceptor	Permits redox activity in biofilm	proteins
Exchange of genetic information	Allows horizontal gene transfer	DNA
Enzymatic activity	Enables digestion of macromolecules and degradation of EPS to release cells.	Proteins
Export of cell components	Release of cellular material	Membrane vesicles containing nucleic acis, phospholipids and polysaccharides
Binding of enzymes	Retention and stabilization of enzymes	Polysaccharides and enzymes

Table 1-2: Functions of EPS in Biofilms (Flemming and Wingender, 2010)

1.3.1.1 Biofilms composition and functions

A bacterial biofilm consists of micro colonies made of many cells embedded in a common matrix. This matrix is composed of extracellular polymeric substances (EPS). Besides EPS, the second most prominent feature of a biofilm is the presence of fluid filled channels traversing this matrix. Each of these components has a specific function. For instance, EPS acts as a dynamic scaffold and forms the basis of the consortium and the fluid channels enable influx of nutrients and removal of wastes from the matrix. It also keeps the microbial cells in close proximity to each other thereby allowing cell to cell communication that leads to a synergistic behavioural pattern. The EPS matrix is made up of many components like polysaccharides, lipids, proteins, nucleic acids and natural polymers like humic acids. The composition of EPS is not uniform and depends on the type of microorganisms involved, metabolic state, nitrogen level, nature of environmental stress and the quality of available nutrients (Flemming and Wingender, 2010).

The biofilm matrix offers heterogeneity in terms of microbial composition, phenotypic behaviour and altered gene expression. No two biofilms are alike and within a biofilm the metabolic variations create what could be best described as a micro environmental niche. The overall purpose of such variations is to ensure the selection of the fittest mutants, enhanced tolerance to antibiotics and ensuring a greater resilience within the subpopulations (Stewart and Franklin, 2008). For example, Boles and Singh (2008) found that presence of oxidative stress leads to evolution of resistant species of bacteria within the biofilm of *P. aeruginosa*. The

presence of oxidative stress led to breakage in DNA and repair mechanisms produced antibiotic resistant bacterial communities in the biofilm matrix.

Biofilm formation is a complex process and depends on the nature of the cell surface and the chemical properties of the substratum involved. Hydrophobic surfaces are usually optimum zones for biofilm formation. The initial attachment is a reversible process and presence of pili, flagella or glycocalyx helps in initial attachment when forces of repulsion are high. Once a more permanent attachment is made, then EPS matrix plays a crucial role in maintenance of the structure. In many bacteria, the formation of EPS has been seen to be the first step in biofilm formation (McKenney et al., 1998, Watnick and Kolter, 2000). Surface attachment and associated changes are shown in Figure 1-10

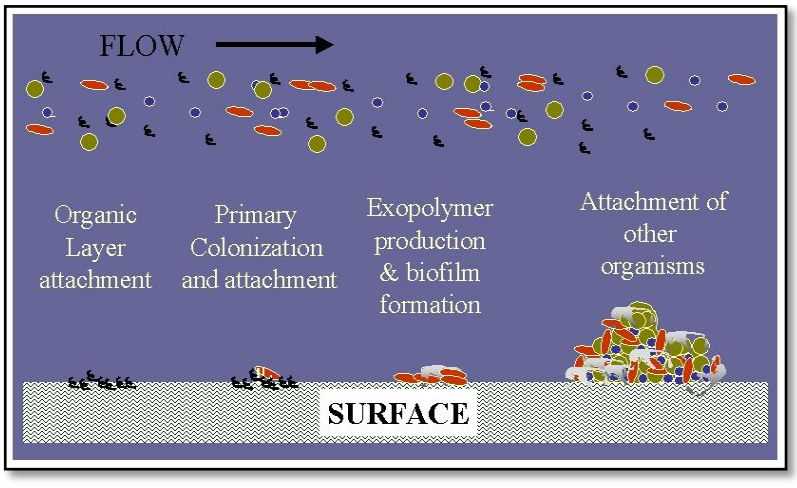

Figure 1-10: Biofilm formation process (Marshall, 1997)

1.3.1.2 Biofilm matrix in bacteria

Polysaccharides form a major component of the biofilm matrix. They are usually branched or linear molecules with a molecular mass of $0.5x10^6$ - $2x10^6$Da. Biofilms can be made of homopolysaccharides like cellulose or hetreopolysaccharides like those formed by bacteria like *Agrobacterium tumefaciens* and Rhizobium. These are composed of a mixture of neutral and charged polysaccharide residues such as alginate, xanthan and colanic acid, which makes them poyanionic in nature. Some polysaccharides are linked with beta N-acetyl glucosamine subunits thus polycationic (Flemming and Wingender, 2010). This matrix could even vary within a bacterial species. For example, in *Pseudomonas aeruginosa*, three types of polysaccharides are involved in EPS formation, each having different monomeric units (Beloin et al., 2008).

Since, two bacteria, *E. coli and Sinorhizobium meliloti* have been used as model organisms to investigate silver nanotoxicity in this project; subsequent sections discuss in detail the synthesis and composition of EPS in these bacteria.

1.3.1.3 EPS in *E. coli*

The *E.coli* biofilm matrix has been characterized extensively and is made up of three polysaccharides (dominant) units: cellulose, colanic acid and Poly- β-1, 6 –N-acetyl glucosamine (PGA).

1. **PGA** enables cell to cell adhesion and attachment to surfaces in *E.coli* (Agladze et al., 2005). The *E. coli* operon, *pgaABCD* is involved in the synthesis, transport and localization of PGA polymers (Wang et al., 2005).

2**. Cellulose:** Cellulose is produced by a wide variety of bacteria including *Salmonella enterica* subsp enterica, *S. typhimurium*, pathogenic and non-pathogenic strains of *E. coli* and *Citrobacter* and Enterobacter species (Solano et al., 2002). The production of cellulose in a biofilm usually occurs at the air-water interphase and depends on the environmental conditions (Beloin et al., 2008).

3**. Colanic acid**: Colanic acid is a negatively charged polymer produced by bacteria like *Acetobacter cloacae, Salmonella typhimurium* and *Escherichia coli*. Colanic acid is made up of glucose, galactose, fucose and glucuronic acid molecules that combine to form hexasaccharide repeating units (Sutherland, 1969) as shown in Figure 1-11. In *E. coli*, colanic acid forms a slimy capsule around the cells and protects them under stressful conditions like osmotic shock, low temperature and desiccation (Sledjeski and Gottesman, 1996, Chen et al., 2004a). Colanic acid synthesis is required to maintain the biofilm structure and provides depth to the maturing biofilm but it is not required for initiation of biofilm formation (Danese et al., 2000). It has been observed that colanic acid production is upregulated in biofilms (Prigent et al., 1999).

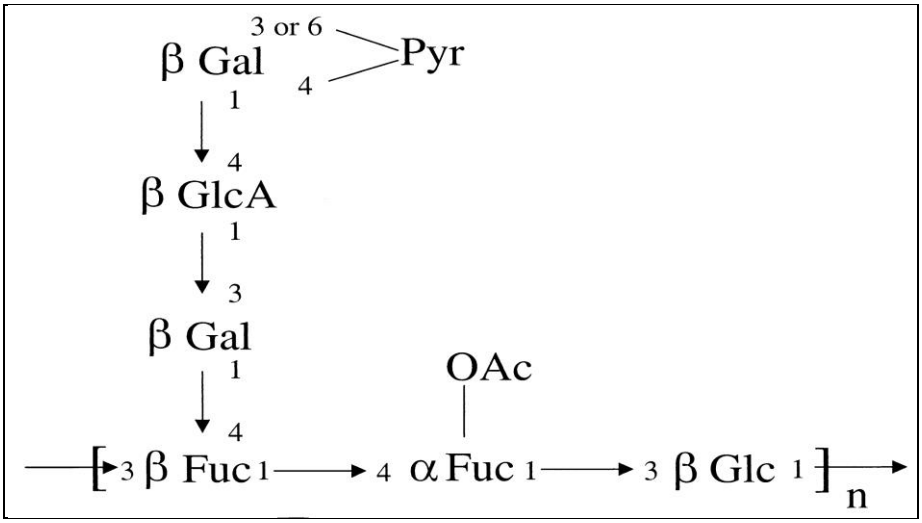

Figure 1-11: Structure of colanic acid monomer (Danese and Kolter, 2000)

1.3.1.4 Genetic regulation of colanic acid synthesis

Colanic acid is a group 1 capsule in terms of its structural organization**.** The capsule expression genes (*cps locus*) are required for the production of colanic acid and consist of a set of 19 genes. Group 1 capsular biosynthesis locus (cps) is made of two regions separated by a transcriptional attenuator (Chung and Goldberg, 1981, Whitfield, 2006). There are four conserved genes namely *wzi*, *wza*, *wzb* and *wzc*. Three of these namely, *wza, wzb and wzc* are involved in polymerization and translocation of polysaccharide to the cell membrane. The other gene belonging to this system codes for regulation of capsular biosynthesis pathway often termed wzy dependent pathway (Obadia et al., 2007). Apart from these genes, the latter part of the circuit includes two inner membrane proteins, Wzx and Wzy. Transcription of this locus is controlled by genes upstream of *wzi*. Colanic acid is not produced under normal growth conditions in *E. coli* and is usually produced by the organism when it is outside the host body (Majdalani and Gottesman, 2005).

The RCS relay system regulates the activity of the genes involved in colanic acid synthesis. It consists of two membrane proteins RcsC, RcsD and a cytoplasmic protein RcsB. When a membrane perturbation occurs or there is some environmental stress, the RcsC auto phosphorylates and this phosphate is subsequently transferred to RcsB as shown in Figure1-12. This process initiates the transcriptional activation by RcsB (Wehland and Bernhard, 1999). The formation of a heterodimer complex between RcsA and RcsB switches on the activation of genes involved in the capsular polysaccharide synthesis (Ebel and Trempy, 1999). This activation in turn regulates the activity of *rcsA* (Stout et al., 1991). Apart from colanic acid synthesis, RcsB is also responsible for inactivation of genes related to curli and fimbriae formation to ensure reduction in motility of bacteria, and contributing to biofilm initiation (Figure1-12 and 1-13). This process is a part of complex regulatory network (Stout, 1996).

The operon shown in Figure 1-13 describes the process of heterodimer formation and transcriptional activation for colanic acid biosynthesis and transport assembly. *wzA* encodes the subunits of a transport apparatus assembly and forms the lipoprotein. *wzb* encodes a tyrosine phosphatase while *wzc* forms a tyrosine kinase required for formation of export assembly of colanic acid (Obadia et al., 2007). WzcA is a glycosyl transferase and WzcB, an acyl transferase for colanic acid synthesis.

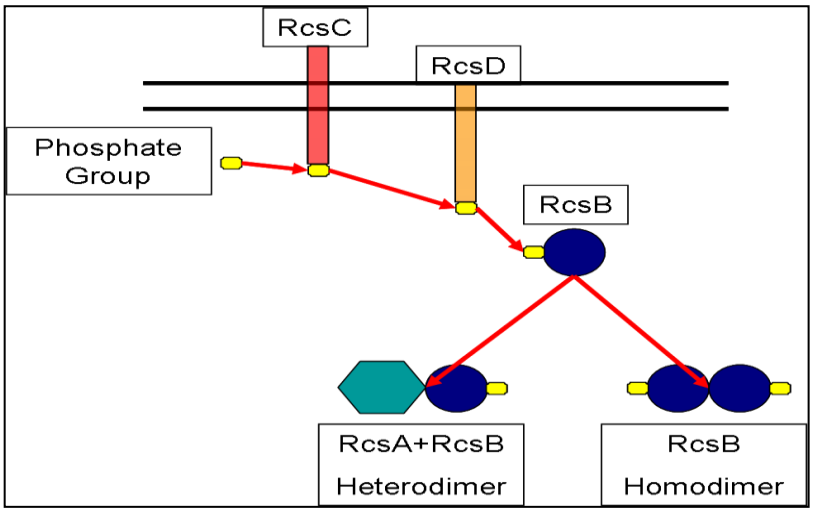

Figure 1-12: Colanic acid production regulation: the RcsAB box (Majdalani and Gottesman, 2005). Formation of dimer switches on the transcription for colanic acid biosynthesis

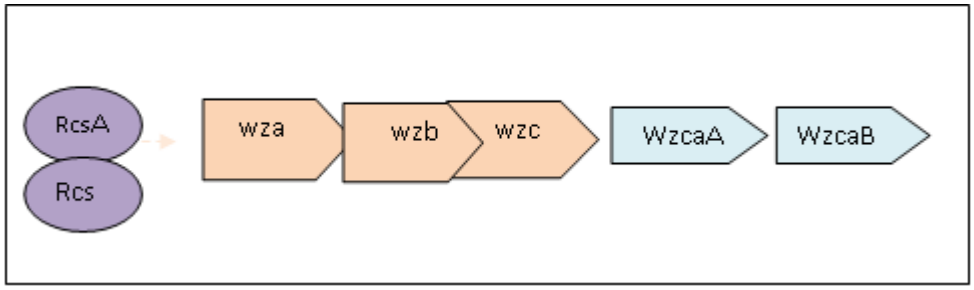

Figure 1-13: Formation of dimer regulates colanic acid production and activity of wzc operon (redrawn from Stevenson et al., 1996).

1.3.1.5 Succinoglycan: EPS synthesized by *Sinorhizobium meliloti*

Apart from *E. coli* and other pathogenic strains of bacteria, many free living bacterial populations also produce biofilms. In most of the cases, this is an effort on the part of microbial communities to survive under environmental stress conditions, but in some cases, it also serves other functions. For instance, in the case of members of genus

Rhizobium, EPS synthesis is a prerequisite for development of infection threads and successful invasion and colonization of the roots of leguminous plants (Janczarek, 2011). This process results in nodule formation in the roots and leads to establishment of a symbiotic relationship between plants and bacteria. There are complex signalling pathways between the bacteria and specific host plants that regulate the whole process. The EPS released by the bacteria plays an important role in biofilm formation that helps to form adhesion and later colonization of host's roots.

Sinorhizobium meliloti is a soil living nitrogen-fixing bacteria present in the roots of plants and requires synthesis of EPS for colonization. Stages in host cell invasion by *S. meliloti* are shown in Figure 1-14. There are three events in this process: (I) the host cell secretes flavonoids that stimulate the release of Nod factor; this process initiates the necessary changes in the plant cells, (II) stage of infection thread formation and (III), bacteria enter by endocytosis and differentiate as bacteroide. (IV) Nitrogen fixation starts (Luyten and Vanderleyden, 2000).

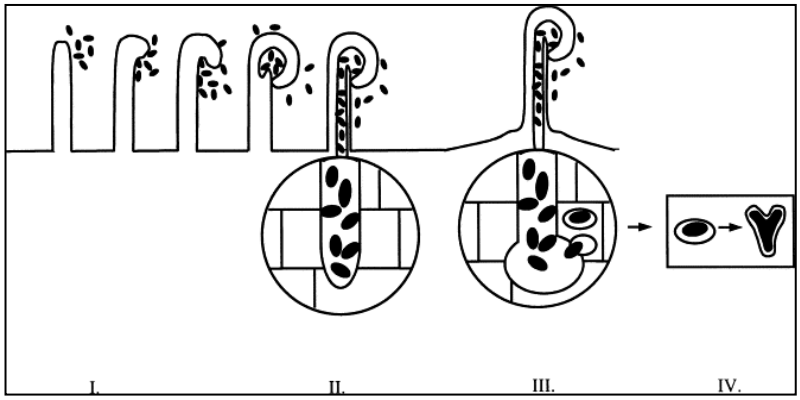

Figure 1-14: Formation of infection thread and Rhizobial invasion (Lyuten et al. 2012)

S. meliloti has been shown to form two types of EPS: type 1 and type 2 based on the molecular weight (Reihnold et al., 1994, Zevenhuizen, 1997). Type 1 EPS is a low molecular weight fraction made up of monomers, dimers/trimers of repeating units. It is the active form of EPS which helps to form a symbiotic relationship with the host plant (Leigh et al., 1985). The high molecular weight (HMW) of type 2 EPS is made of polymers of about 10^6-10^7 Da. The production of EPS is dependent on concentration of nutrients like nitrogen and phosphorus. High salt concentration can also affect the nature of EPS formed. For instance, low nitrogen and sulphur and a high phosphate concentration facilitates type 1 EPS synthesis, whereas phosphate starvation leads to type 2 EPS formations (Reuber and Walker, 1993, Mendrygal and Gonzalez, 2000). Low osmolality promotes type 1 EPS synthesis (Janczarek, 2011). The composition of EPS is strain specific and consists of linear or branched heteroploymers or homopolymers as shown in Figure 1-15. In case of *S. meliloti,* EPS consists of an octameric repeating unit of three glucoses, one galactose, and a side chain of 4 glucose and one pyruvate, acetyl and succinyl modifications all in the ratio of 1:1:1. Succinyl modification is an essential step for colonization of host

tissues (Aman et al., 1981, Müller et al., 1988). Figure 1-16 below shows the chemical configuration of one unit of succinoglycan polymer (both EPS 1 and 2).

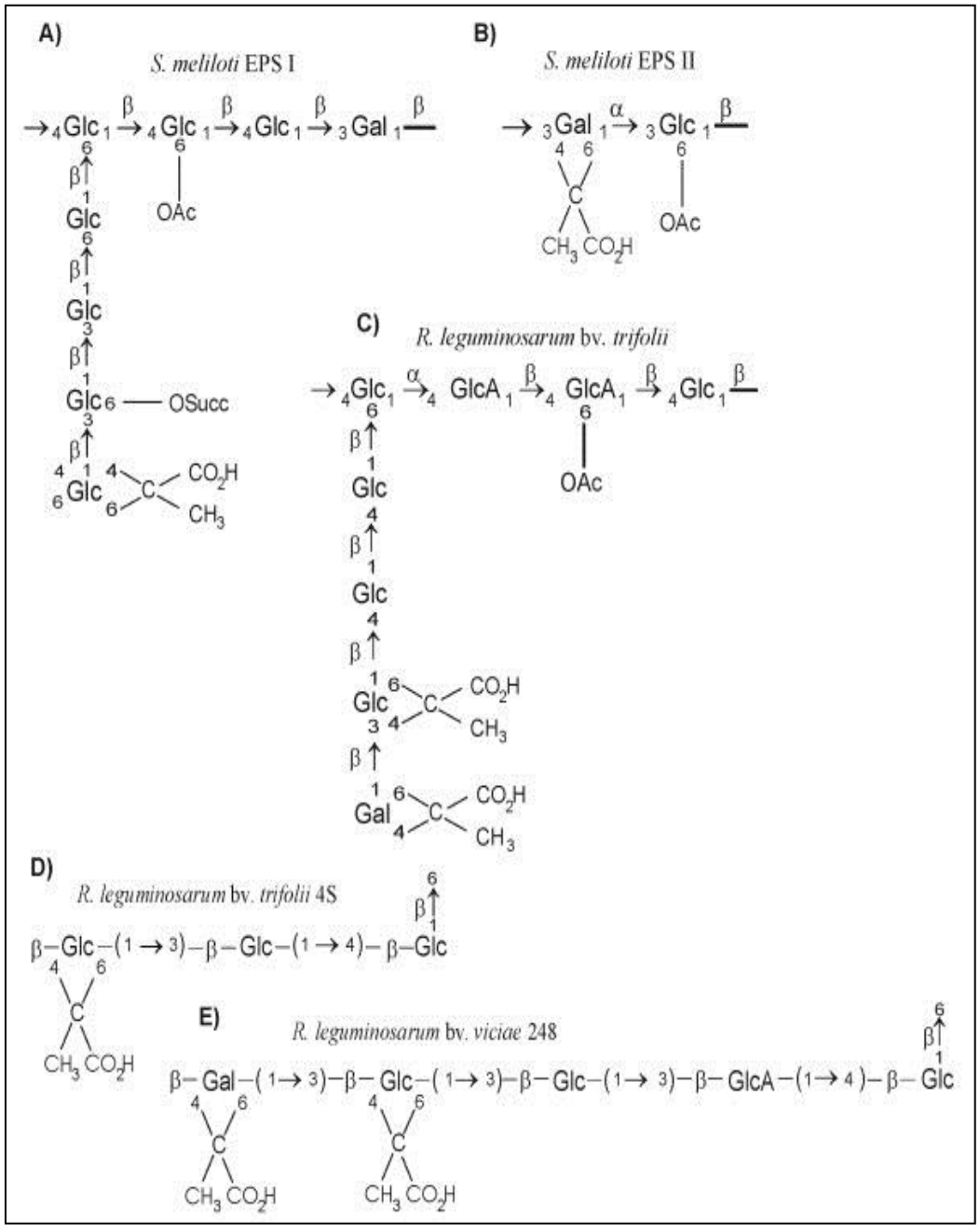

Figure 1-15: EPS types found in members of genus Rhizobium (Skorupska et al., 2006)

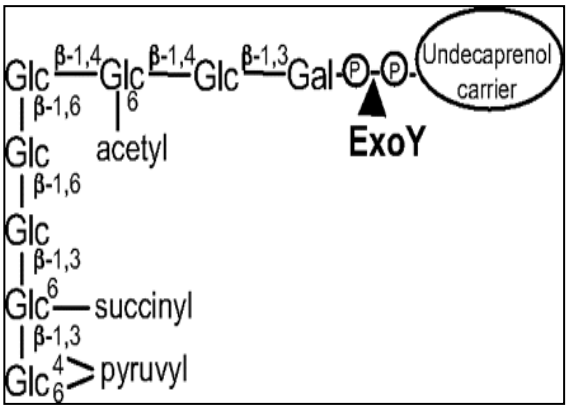

Figure 1-16: Structure of one octameric ring of succinoglycan (Jones et al., 2008)

Genes involved in the synthesis of EPS in *Sinorhizobium meliloti* and their regulation

The genes responsible for EPS synthesis are located on a mega plasmid pSymb as a cluster (Finan et al., 1986). There are about 28 genes organized in various operons that are expressed to facilitate different stages of succinoglycan formation and transport. For example, *exoB* and *exoN* code for enzymes required for production of sugar precursors while *exoL*, *exoM*, *exoA*, *exoO*, *exoU* and *exoW* are involved in assembly.

Polymerization is carried by proteins encoded by genes namely, exoP, *exoT*, *exoQ* and *exoA*. The regulation is carried out by proteins expressed by *exoS*, *exod*, *exoR* and *mucR* which are not present on the mega plasmid but on the chromosome (Doherty et al., 1988, Reuber and Walker, 1993, Keller et al., 1995, Galibert et al., 2001).

Regulation of Succinoglycan production in *Sinorhizobium meliloti*: *exoS* and *exoY*

Type 1 EPS synthesis is negatively regulated by *exoS, exoR, abrA* and *emmc* and *mucR* and *syrM* are the positive regulators. exos encodes an inner membrane protein, ExoS. This protein is a homodimer with sensory properties and is located in the periplasmic space. This protein is responsible for detection of environmental signals required for EPS synthesis (Doherty et al., 1988). ExoS activates another response regulator, ChVI, by phosphorylation. This process modulates EPS synthesis. ExoR is a periplasmic protein that negatively regulates the coordinated activity of ExoS-ChVI (Reed et al., 1991).

Besides EPS synthesis, this complex is also required for bacteria to survive on different carbon sources. Another protein, ExoX, is present on the inner membrane and is required for type 1 EPS synthesis. Besides the Exo, MucR is an important regulator of type 1 EPS synthesis, and a mutation in this gene results in a shift from type1 to type 2 EPS synthesis in *Sinorhizobium meliloti* (Janczarek, 2011).

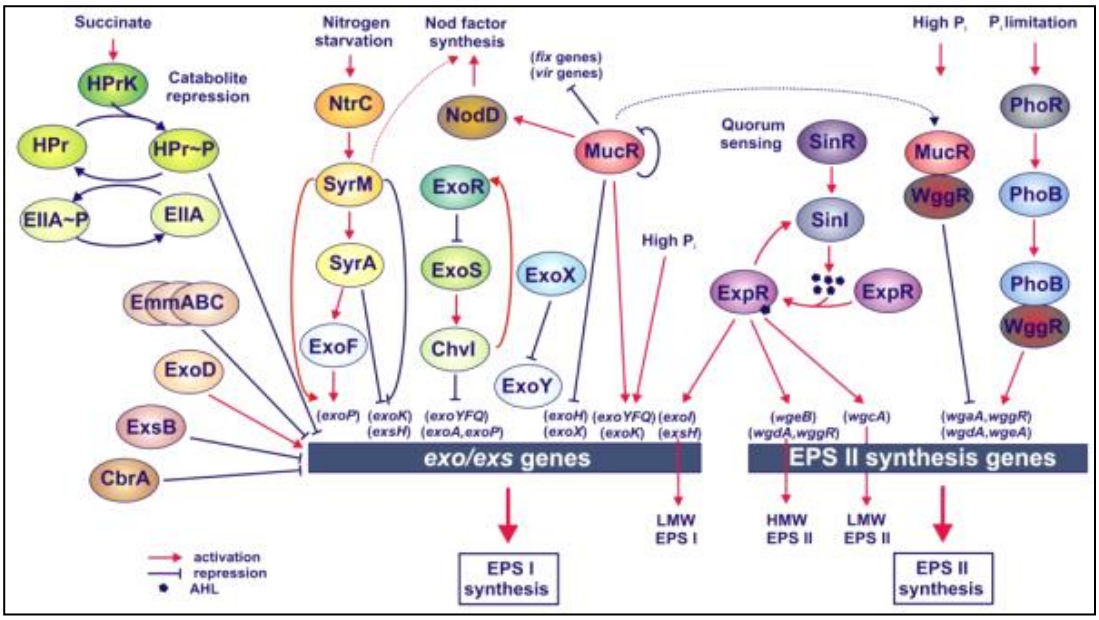

Figure 1-17: Regulation of succinoglycan production in *Sinorhizobium meliloti*

1.3.1.6 Protective role of EPS against nanotoxicity

Biofilms acts as a protective barrier against environmental stress and their potential role against nanotoxicity has become a point of interest. Yang et al. (2007) first reported that bacteria with intact EPS were more resilient against impact of TiO_2 and ZrO_2 nanoparticles than the ones with EPS removed. Similarly, the presence of EPS proteins was shown to promote aggregation of nanoparticles and reduce their dispersal (Moreau et al., 2007). Fabrega et al. (2009) investigated the impact of silver nanoparticles on *Pseudomonas putida* biofilms in the presence of fulvic acid. It was observed that fulvic acid stabilized the nanoparticles by forming a nanoscale film; this reduced the bacterial biofilm and nanoparticle interaction. Battin et al (2009) reported the bacteria embedded in a biofilm matrix have a higher resistance to nanoparticles than the ones in a planktonic state. In another study, it was found that EPS reduced the diffusion coefficient of the nanoparticles by trapping them (Peulen

et al., 2011). Presence of EPS has been shown to reduce the toxicity of silver nanoparticles (Dimkpa et al., 2011, Jiang et al., 2011, Sheng and Liu, 2011).

By using marine biofilms grown *in situ* and silver nanoparticles of varying concentrations, Fabrega et al. (2011) have shown how biofilms could play in an important role in protection against nanotoxicity. They found that even high concentration of silver nanoparticles did not affect the taxa within a heterogeneous sample biofilm. Tadesse et al. (2011) made use of a synthetic biofilm in order to investigate the mechanism of biofilm and nanoparticle interaction. They observed that a hydrated biofilm adsorbed the nanoparticles (TiO_2 in this case) and this limited the diffusion of nanoparticles. Khan et al. (2011) on the other hand report that the EPS provide stability to silver nanoparticles, by increasing the zeta potential of nanoparticles, and preventing their aggregation. This suggests that bacteria within an intact biofilm can resist nanotoxicity, but the presence of EPS and such analogues in aquatic system at neutral pH can increase the residence period of nanoparticles, thereby increasing the probability of exposure of other organisms towards them.

Khan et al. (2011) report that sewage isolates of *Bacillus pumilus* showed similar growth kinetics with and without silver nanoparticles, primarily because the EPS capped the silver nanoparticles and reduced their toxicity. Similarly, Dinesh et al. (2012) also report that besides EPS, the presence of humic acid, fulvic acid and other such organic matter can bind with nanoparticles and greatly reduce bioavailability of NP. Besides bacteria, EPS was shown to protect algae against silver nanotoxicity (Miao et al., 2009). Bovine serum albumin (Peng et al., 2004) and xanthan (Joshi et al., 2012) have also been tested as possible EPS analogues and shown to bind to nanoparticles and reduce toxicity.

1.3.2. Genetic regulation of oxidative stress and enzymatic protection in bacteria

As discussed earlier, living organisms experience oxidative stress during metabolism and also due to changing environmental factors like heat shock, change of pH, UV radiation and also presence of certain stress inducers like peroxides, antibiotics etc. Therefore, bacteria have a range of genes that coordinate in a specific manner and are expressed to produce enzymes that provide protective response. These genes fall in two categories, the OxyR regulon and the SoxR regulon. Each consists of a set of genes that are activated and are specific to the nature of stress.

- **OxyR regulon:** This is up regulated when *E. coli* senses hydrogen peroxide in the vicinity (Yoon et al., 2002). Peroxide stimulon activates *katG*, *katE* and glutathione peroxidase. These genes are expressed to form enzymes that help in the detoxification of peroxide into less harmful species, namely water and oxygen. Besides these, another enzyme called alkylhydroperoxide reductase (synthesized by *ahpC* and *ahpF*), reduces hydroperoxides. The OxyR protein activates the expression of all these genes (Storz et al., 1990).
- **SoxR regulon**: The presence of superoxide anions triggers the defence mechanism in *E. coli* corresponding to superoxide stimulon (under aerobic conditions). It involves activation of 30 proteins, eight of which have been well characterized and are involved in superoxide scavenging. The two SOD enzymes in *E. coli* are the manganese containing Mn-SOD (coded by *sodA*) and Fe-SOD (encoded by *sodB*) (Li and Demple, 1994). Both facilitate the dismutation of superoxide anion to hydrogen peroxide.

Both of these stress responses involve a different set of genes and are ROS specific in nature. It is worth mentioning that the oxidative stress response shows an overlap with some other environmental stress situations like high temperature (heat shock response/Hsp) and SOS response like expression of *recA* or *dnaK* (Zylicz et al., 1983) or DPS(G et al., 2002).

The role of nanoparticles in production of oxidative stress in living organism has been investigated. Studies have shown that nanoparticles promote ROS formation. These studies rely on ROS scavengers like furfuryl alcohol (Xia et al., 2006, Lin et al., 2007, Lin et al., 2008) and ROS detecting probes like dicholorfluorescein. For instance, a study has shown that cerium oxide nanoparticles switch on the expression of Nrf2 pathway in human bronchial cells (Eom et al., 2010). This pathway is a primary defence mechanism against cytotoxic effects of oxidative stress in eukaryotes (Petri et al., 2012). Addition of cysteine has been shown to reduce the toxicity of zinc oxide nanoparticles (Huang et al., 2010). Similarly, a microarray study was conducted by Ivask et al. (2012) and it showed that ROS formed in bacteria on exposure to cerium oxide nanoparticles. Role of oxidative stress in nanotoxicity has been also reported in other works where silver and zinc oxide nanoparticles were used (Xia et al., 2008, Radzig et al., 2012, Gou et al., 2010, Kumar et al., 2011, Napierska et al., 2012). The exogenous addition of enzymes such as catalase and superoxide dismutase has been shown to alleviate silver nanotoxicity in the bacterium, *P.choloraphis* (Gajjar et al., 2011). This protective response is efficient only at low concentration of nanoparticles. This project also intends to investigate if ROS are involved in metal nanotoxicity, by developing overexpression strains capable of producing enzymes that could degrade ROS.

1.3.3 Efflux pumps and ion channels

Bacterial communities that inhabit areas of industrial activities like mining or waste disposal sites often have a higher metal tolerance than their counterparts growing in fresh water or low pollution areas. These bacteria have sophisticated heavy metal regulation system that enables them to survive in environments containing metals such as copper, silver, zinc and nickel.

Often the heavy metal resistance is plasmid mediated and bacteria evolve this strategy with long-term exposure to such analytes. For example, *E. coli* has three systems to remove excess copper ions from the body. First is the P type ATPase, that forms the efflux pump, second, the multi copper oxidase system that removes excess copper ions from the periplasm and third, cus operon that helps to remove both copper and silver ions from the cytoplasm (Nies and Silver, 1995, Petersen and Moller, 2000, Loftin et al., 2005). Figure 1-18 illustrates the cus system in *E. coli*.

The four-part Cus complex consists of the inner membrane pump CusA, the periplasmic protein CusB and the outer membrane protein CusC forming a channel bridging the periplasmic space. Entry of copper may occur from the periplasm (A), from the cytoplasm (B) or via the copper binding chaperone CusF from the periplasm (C) (Rensing et al., 2003).

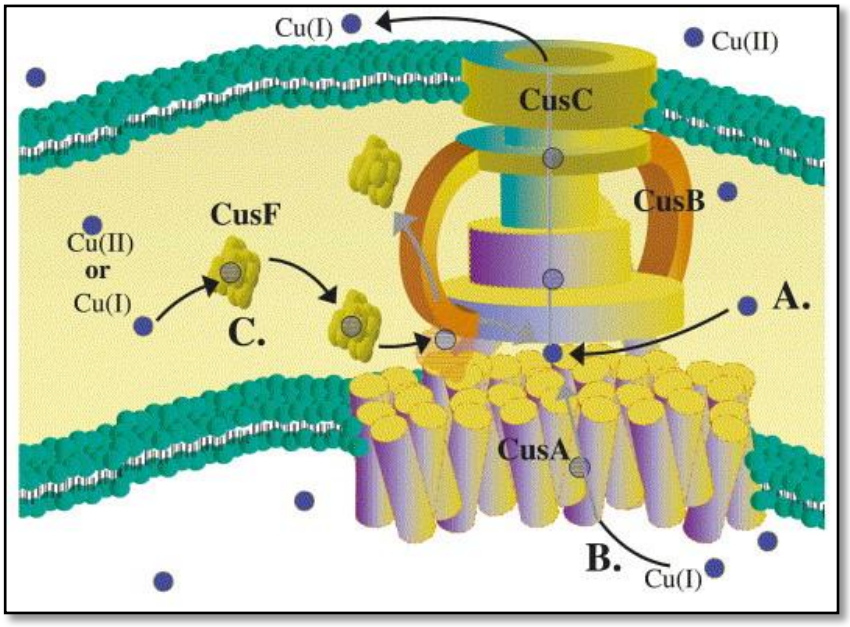

Figure1-18: Functional model of the Cus efflux complex (Rensing et al., 2003)

Besides efflux pumps, gram-negative bacteria have special proteins on the outer membrane surface folded as beta-barrel, called porins. These allow for passive diffusion of solutes and other ions (Schirmer, 1987). *E. coli* has two major porins; OmpC and OmpF (Cowan et al., 1992) that help in passive diffusion of ions into the cytoplasm and at the same time restrict the influx of harmful agents. Absence of porins has been shown to confer metal resistance in some strains of *E. coli* especially to silver ions (Li et al., 1997).

Many studies show that engineered metal and metal oxide nanoparticles like silver and copper oxide cause toxicity by release of ions (Kasemets et al., 2009, Ma et al., 2012). For instance, Radzig et al. (2012) reported that bacterial strain of *E. coli* deficient in membrane proteins like OmpF and OmpC were 5-8 times resistant to silver nanoparticles than the control strain with porins.

Similarly, microarray studies by Gou (2010) showed that genes related to detoxification and efflux of antibiotics and ions were up regulated on exposure to silver nanoparticles. This project also intends to explore the role of ions in causing silver nanotoxicity by exploring the role of ions efflux systems and porins in *E. coli*.

1.3.4. Surface complexation and adsorption of nanoparticles

Environmental variables can play an important role in influencing the behaviour and bioavailability of nanoparticles. Since engineered metal nanoparticles are often stabilized by coatings like sodium citrate or pyrollidine, any factor that can destabilize these coatings can essentially enhance the ionization from their surface (Choi, 2008, Fabrega, 2009, Badawy, 2011). Therefore, it is important to study the role of soil and microbial communities on their speciation. In general, when metal ions are released in soil, the net toxic potential depends on many variables including pH, dissolved organic components and ligands like chloride, sulphides and phosphate that can essentially precipitate them. Besides these abiotic factors, the presence of microbial communities and the metabolic by products also act as active sites for adsorption (Mullen et al., 1989). It has been shown that organisms compete for the metal cations in the soil (Strandberg et al., 1981). Isolated cell envelopes and even bacteria like *Bacillus subtilis, Bacillus licheniformis* and *E. coli* have been shown to bind to large numbers of metal cations like silver, copper, zinc and cadmium (Beveridge and Murray, 1976 , Beveridge and Murray, 1980, Elliott et al., 1986). Bacteria, due to the large surface to volume ratio, provide an excellent sorption site for metal ions (Beveridge and Fyfe, 1985). Gram-positive bacteria, like *Bacillus*

subtlis, have been shown to form surface complexes with metal ions like cadmium and copper and shown to adsorb more ions on the cell surface than gram negative bacteria like *E. coli*. However, the degree of adsorption also depends on the nature of metal. For instance, amongst all metal ions, silver is most easily removable ion. In a study by Mullen et al. (1989), bacteria irrespective of cell wall composition removed 89% silver, however *Bacillus subtilis* showed a preferential adsorption of copper ions.

These findings suggest that toxicity impact levels of metal nanoparticles are dependent on the soil chemistry and biota. Bacteria are often found adhered to surfaces in biofilm matrix in natural environments. The chemical composition of biofilms can also affect nanotoxicity. For instance, succinoglycan, an EPS associated with bacteria like *Sinorhizobium meliloti*, shows a predominance of functional groups like hydroxyl, phosphate, carboxylic and amines on its surface (Reinhold, 1997). This imparts a negative charge to the biofilm and promotes the binding of positively charged metal ions released from metal nanoparticles. Another example is the EPS produced by *Bacillus licheniformis S-86* that shows a high density of functional groups like carboxylic, amine, phoshpodiester and these influence the metal uptake capacity of bacteria (Tourney et al., 2008). Similarly, the EPS produced by *Bacillus subtilis* has been shown to adsorb goethite (Omoike et al., 2004, 2006). The surface complexation of ions released from nanoparticles with polysaccharides, organic acid and other matrix (in the biofilm and environment) (Tadesse, 2012) can therefore influence their bioavailability and overall reduce the toxic potential.

1.3.5 Microbial metabolism driven metal speciation and nanotoxicity

The assessment of the impact of engineered nanoparticles on the environment needs improved experimental designs. Rather than relying on pure cultures and defined growth medium, mixed microbial communities and heterogeneous environment like sediments from natural habitat can perhaps provide more realistic assessment of the effect of nanoparticles on the environment, and also how microbes in the natural environment can detoxify nanoparticles. Experiments that include variables like biofilms, pH, complex microbial community, physicochemical properties of soil should be employed for this purpose. These variables have been incorporated in recent research work that focussed on the effect of microbial activities on metal speciation and nanoparticle behaviour, both in vitro and using microcosms.

The following studies illustrate the importance of environmental chemistry and biotic activities including metabolism that can drive changes in the speciation and transformation of engineered nanoparticles in soil. Microcosms developed from sediments of estuarine origin showed little impact of silver nanoparticles on the bacterial community composition (Kaeriyama et al., 2006, Bekhit et al., 2011). Similarly Tong et al. (2007) showed that C60 fullerene suspension did not produce significant changes in the microbial community structure however; they later reported that fullerene reduced the metabolic activity of some bacterial strains. In contrast, Kanaly et al. (2011) used soil microcosms to investigate the impact of fullerene C60 on biota and found that certain bacterial strains get affected far more than others. He et al. (2012) used microcosms amended with iron oxide magnetic and

found that presence of nanoparticles resulted in greater growth of some members without affecting the total bacterial abundance in general. Yan et al (2009) showed that addition of TiO_2 resulted in reduction in bacterial community population in a dose dependent manner. In another study, it was seen that nano zinc oxide produced a greater toxicity than $nTiO_2$. However, addition of both types of nanoparticles not only led to reduction in total biomass, but also produced significant changes in the bacterial community composition (Yuan et al., 2011). Similar results were reported by Ge et al. (2011) who used microcosms to study the effect of zinc oxide and titanium oxide nanoparticles and found that ZnO nanoparticles caused significant reduction in bacterial community since they were more toxic than TiO_2. The presence of nanoparticles produced adverse impact on microbial population in the microcosms. Rousk et al (2012) also showed that zinc oxide nanoparticles were more toxic to soil bacteria than the copper oxide.

Plant and bacterial metabolic activities affect the stability of nanoparticles. Metabolic activities include release of by-products, organic matter from living organisms, uptake of ions, functional group modifications etc. For instance, Bone et al. (2012) used different types of microcosms, some dosed with only silver nanoparticles, bacterial microcosms and complex microcosms that had both plants and bacteria. The speciation studies of all these microcosms showed that presence of plants significantly affected the bioavailability of silver ions and considerably reduced the silver nanotoxicity. X-ray Absorption Near Edge Structure (XANES) analysis showed that silver speciation led to the formation of silver sulphide. The most important observation was that plant exudates complexed silver ions and reduced their concentration in water and their toxicity levels.

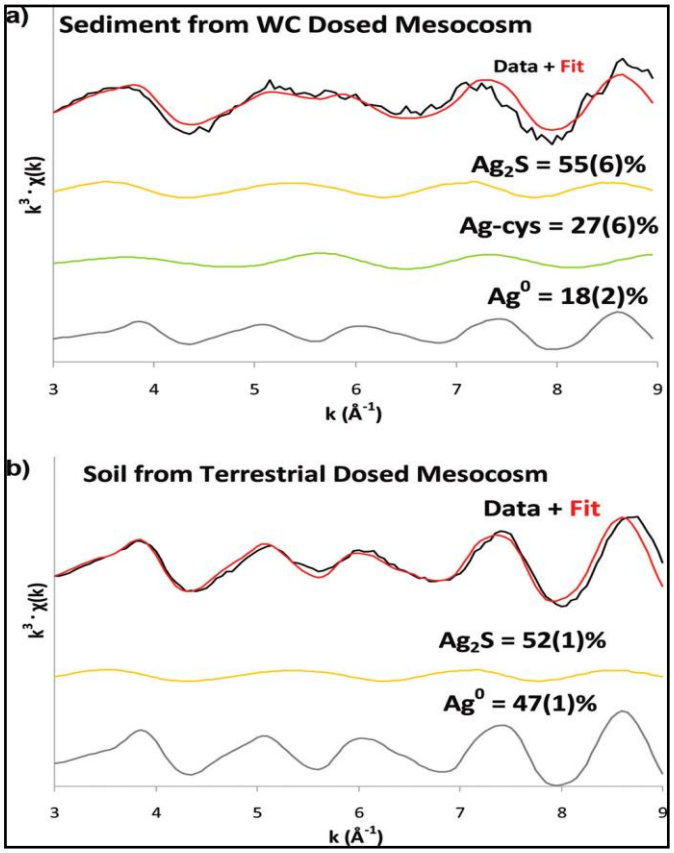

Figure 1-19: Linear Combination Fit model for EXAFS analysis for silver speciation (a) sub aquatic sediment from water mesocosms and (b) sediment from soil microcosm (Lowry, 2012). The EXAFS show that the silver added to microcosm with soil/water transformed into silver sulphide.

Lowry et al. (2012) developed silver nanoparticle amended soil and water mesocosms, and found that 70 per cent of silver was retained in soil (soil microcosm) and (sub aquatic) sediment (Figure 1-19). However, the silver had undergone sulfidation. Recently, Reinsch (2012) demonstrated that sulphidation of silver nanoparticles in the environment is crucial to reducing the toxic potential of nanoparticles. This process was greatly dependent on the initial levels of reduced

sulphur in the system and the X ray absorbition spectroscopy analysis revealed that silver had undergone significant transformations. The soil microcosm had 52% silver, as sulphide and it was even higher in aquatic mesocosms (55% Ag2S) and rest (27%) as Ag-sulphyhydryl complex). There was some accumulation of silver in the plants as well. This work clearly showed that silver nanoparticles underwent rapid transformation in complex environment (such as that of a microcosm) and the mobility of ionic silver was greatly restricted because of the chemical reactions and plant metabolic activity.

It is worth mentioning that physical and chemical properties of soil or water are influenced by the biota and this will also affect the toxicity of nanoparticles indirectly. In a recent study transformation of ZnO nanoparticles under different concentrations of sulphides showed that sulfidation of nanoparticles is in fact a rapid process and formation of zinc sulphide nanoparticles leads to their reduced solubility and promotes their aggregation (Ma et al., 2013). Similarly, investigation into the transformation of silver nanoparticles in waste water showed that most of the silver nanoparticles formed silver sulphide precipitate and there was insignificant percentage of silver nanoparticles in the surface water (Kaegi et al., 2013). These findings suggest that both the abiotic factors and metabolic driven speciation has a great potential to transform and affect the fate of the nanoparticles in the environment. However, the laboratory experiments are important and could be used to develop strategies to study the toxicity pathways of nanoparticles.

Microcosms and nanoparticle exposure studies indicate that nanotoxicity is dependent on many variables. However, they do not provide any indication about the nature of stress produced by the nanoparticles. Development of stress specific

biosensors can certainly help to contribute to our current knowledge about nanoparticles.

1.4 Development of biosensors for studying mechanisms of nanotoxicity

Biosensors or bioreporters are living organisms that can detect the presence of an analyte of interest. This feature enables their wide usage in analysing samples to detect the presence of toxins (French, 2011). The most commonly used biosensors consist of a sensor that can detect presence of analyte and produce a detectable output (Figure 1-20).

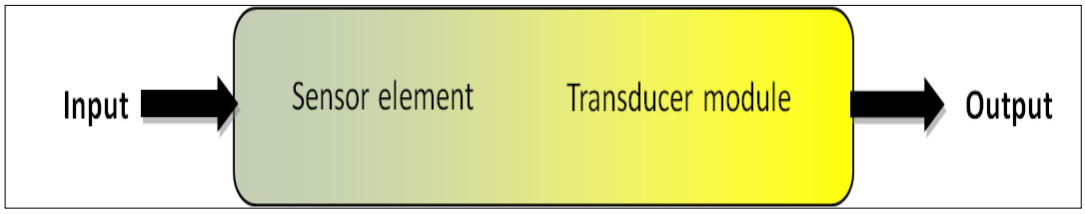

Figure 1-20: Design principle for a synthetic biosensor (Khalil and Collins, 2010)

These are popular devices for environmental monitoring. The output signal could be qualitative like change in colour or quantitative such as change in fluorescence. Table 1-3 summarizes different reporter genes and various signal outputs that could be used to develop a whole cell biosensor.

Reporter protein	Advantage	Disadvantage	Detection methods
β-galactosidase	Sensitive and stable, could be used in anaerobic conditions.	Requires addition of a substrate	Colorimetric, histochemical, electrochemical
Firefly luciferase	High sensitivity, linear range	Requires substrate, ATP and aerobic conditions	Bioluminescence
Bacterial luciferase	Sensitive, no substrate addition required if *luxCDABE* used	Heat sensitive	Bioluminescence
Aequorin	Sensitive	Needs calcium ion and substrate	Bioluminescence
Green fluorescent protein	Stable at biological pH, no substrate needed shows auto fluorescence	Background fluorescence may interfere, not sensitive, may be cytotoxic to some organisms	Fluorescence

Table 1-3: Reporter genes used to develop whole cell biosensors (Daunert et al., 2000)

Biosensors could be roughly grouped into two categories; in the first, are simple biosensors that are non-specific and simply provide a measurable output in presence of a contaminant and in the second category are the stress specifc biosensors. For example, a biosensor that senses a toxin and shows a drop in fluorescence thereby provides indications of presence of harmful/toxic substance.

In the context of nanotoxicity studies conducted so far non-specific biosensors have been extensively used against a range of engineered nanoparticles. For instance, the soil bacterium, *Pseudomonas putida* KT2440 was transformed with a *lux* plasmid and the impact of metal nanoparticles like silver, copper oxide and zinc oxide was established (Gajjar et al., 2009). In another study, *Pseudomonas*

putida BS566 was fused to *luxCDABE* (Dams et al., 2011). The silver nanotoxicity was investigated by measuring the changes in luminescence value of biosensor cells.

In the second category are the biosensors that are highly specific to an analyte. They have a sensor element that responds only to a known toxin like a promoter specific to metal like copper or arsenic. To develop such a biosensor, genes related to ion efflux and metal homeostasis are exploited. For instance, bacteria can survive in high concentrations of heavy metal ions like copper and silver as they contain efficient efflux mechanisms to pump out the ions. These shuttle mechanisms are dependent on the activity of promoters specific to heavy metal ions. Once induced, they regulate the expression of proteins that form efflux channels. This property of the bacteria is utilized, while designing a whole cell biosensor. Microbial biosensors have been generated to detect metals like arsenic, cobalt, antimony, chromium, copper and zinc. Besides metals, biosensors have been made for compounds like benzene, toluene and certain sugars and amino acids. The basic design of a biosensor consists of the promoter that is responsive to a certain compound, a reporter gene (summarized in Table 1-3) and a transducer. When the analyte is taken up by the biosensor organism it activates the promoter and in turn the reporter gene is expressed (Van der Meer et al., 2004). The user can perceive a visible response of this reaction in various forms depending on the choice of reporter gene (Figure 1-20). The following section discusses the biosensors developed in the past to investigate nanotoxicity.

Nanotoxicity has been investigated by developing specific biosensor by Gu et al. (2010). An extensive library of genes fused to *gfp* was developed in order to understand the mechanism of nanotoxicity. It was observed that silver and titanium dioxide nanoparticles stimulated a global SOS response in cells. It also showed that

oxidative stress and membrane damage were the two key mechanisms associated with nanotoxicity. Recently, Bondarenko et al (2012) developed three types of biosensors, one that detects hydrogen peroxide (*lux* integrated to *katG* in chromosome); second was the *recA* fused to *lux* in a plasmid and third *copA* integrated to *lux and* exposed them to copper oxide (CuO) nanoparticles (np). Exposure to CuO np induced all three types of biosensors. It showed that all of these factors, formation of reactive oxygen species, DNA damage and ionic toxicity (copper) contributed total toxicity. Further development in the field of biosensor design and optimization can thus help establish a better understanding of nature of nanotoxicity.

1.5 Project

This project is interdisciplinary, both molecular biology and geochemistry has been extensively used to study the mechanism of nanotoxicity and genetic as well as biomolecular defence mechanisms deployed by bacteria against nanotoxicity. The role of microbes and sediment chemistry as a driving force behind transformation and speciation of nanoparticles has been investigated.

1.5.1 Research rationale

The project aims to investigate the defense mechanisms developed by bacteria against nanotoxicity. In the course of evolution, microorganisms have been exposed to natural nanoparticles like fullerenes (detected in geological material dating back 1.85 billion years). Fullerenes have been observed in clays from the Cretaceous and

Permo-Triassic boundary and are believed to have been produced in fires resulting from the meteorite impact (Heymann et al., 1994). Thus, geochemical processes have been constantly producing natural nanoparticles. Figure 1-21 shows the various nanoparticulate of natural origin.

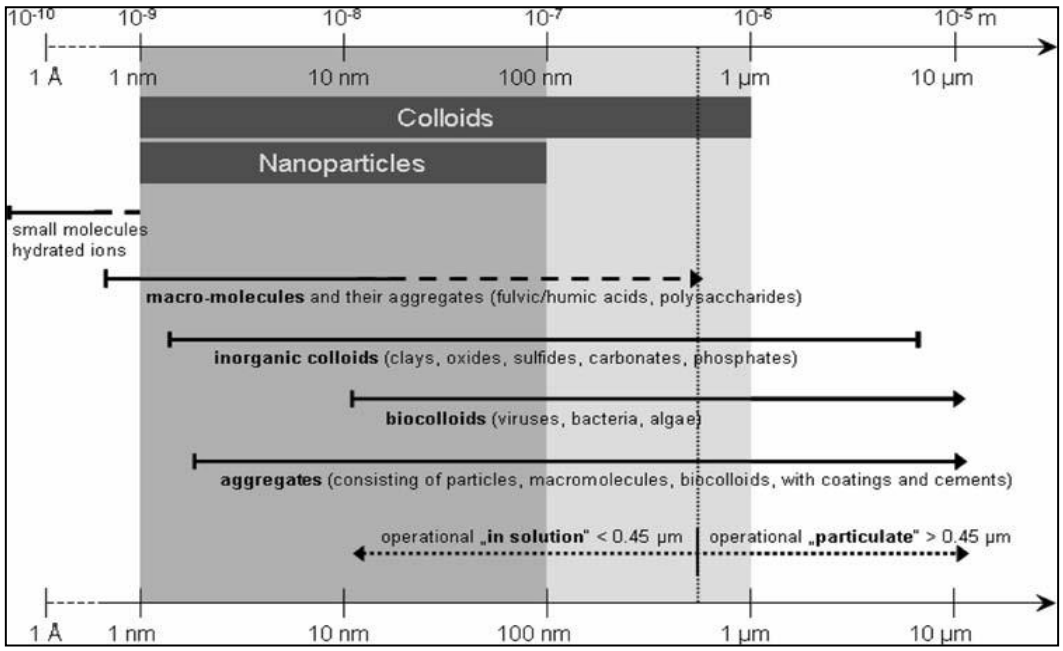

Figure 1-21: Nanoparticles of natural origin

Therefore, it can be said that microbes must have developed protective mechanisms against possible deleterious effects of the nanoparticles. Secondly, the stability and reactivity of nanoparticles are affected by environmental parameters such as pH and ionic oxidation state, as shown in many studies (Fabrega et al., 2009, Peulen et al., 2011). These factors influence the aggregation of nanoparticles thereby affecting their bioavailability and reactivity with other chemical entities (Lowry et al., 2012). It has been shown that in contrast to metal toxicity studies, nanotoxicity seems to show lesser impact at the ecological scale (Tong et al., 2007, Bone et al., 2012,

Calder et al., 2012). Hence, this project aims to study the possible defence mechanisms employed by bacteria against nanoparticles and the environmental factors that could influence the nanoparticle behaviour.

Microorganisms such as bacteria largely exist as biofilms in the environment. A typical biofilm consists of extracellular polymeric substance (EPS) and has been shown to provide protection to bacteria against compounds including metal oxides. For instance, Moreau et al. (2007), demonstrated that extracellular proteins played a crucial role in lowering the metal availability by trapping the nanoparticles and reducing their toxicity. Similarly, it has been observed that the presence of EPS delayed photo catalytic degradation caused by N doped TiO_2 (Liu et al., 2007). Therefore, first objective of the project is to study the role of EPS with respect to nanoparticle aggregation and toxicity. The microbe and nanoparticle interaction has been studied and the hypothesized role of EPS examined by using soil bacteria such as *Sinorhizobium meliloti.* The mutated strain overproducing EPS have been used to study nanoparticle- microbe interactions to investigate if the EPS producing bacteria offer co protection to non-EPS producers.

Research to date indicates generation of reactive oxygen species and ionic toxicity as two possible mechanisms of nanotoxicity (Lyon and Alvarez, 2005, Park et al., 2009, Ma et al., 2012, Napierska et al., 2012). Hence, the second objective of the project is to investigate the dominant mechanisms of silver nanotoxicity by using synthetic biology to develop overexpression strains and stress responsive probes that could detect ions like copper and oxidative stress in bacteria. The third objective is to identify the environmental variables that can drive changes in speciation of ions and render nanoparticles less bioavailable by developing sediment microcosm.

1.5.2 The following strategies have been developed in order to address these questions

1. **What are the mechanisms of nanotoxicity?**

In order to investigate the possible role of nanoparticles in producing oxidative stress, deletion mutants from the KEIO collection (Baba et al., 2006) have been used in exposure studies. Besides these, overexpressing strains that could produce protective enzymes such as catalase and superoxide dismutase have been developed. *E. coli* has been used to make bioreporters to detect oxidative stress and ions like copper and silver. Results of these findings constitute chapter 2 and 3 of the thesis and a manuscript is ready for submission

2. **Do biofilms provide protection against nanotoxicity?**

To investigate the possible role of EPS against silver nanotoxicity, an EPS overexpressing strain of *E. coli*, JM109/pRcsA2 has been developed. This modified strain produces colanic acid. Secondly, mutants of *Sinorhizobium meliloti*, a bacterium belonging to genus Sinorhizobium have been used for nanoparticle exposure studies. Findings of this study have been published (Joshi et al., 2012) and are presented in detail in Chapter 4.

3. **Do metabolically induced transformations of nanoparticles affect its toxic potential?**

   The impact of nanoparticles has been further studied by developing microcosms. Winogradsky columns have been developed using sediment and water from Blackford pond, a representative example of an urban pond. These have been

amended with silver and zinc oxide nanoparticles. The objectives of this experiment are (a) to assess the impact of metal nanoparticles on the microbial community composition, (b) to study the speciation of metal ions in sediment samples. This could provide valuable information about the factors that can influence the mobility of metal nanoparticles in the environment and help provide a realistic assessment of their bioavailability to biota. This is in contrast to laboratory settings where pure cultures and defined medium are used. These have serious limitations while identifying the variables that could influence the stability and toxicity of nanoparticles. Results of this study form chapter 5 of the thesis.

1.5.3 Summary of general research methodology

In order to pursue research on the project a wide range of analytical techniques have been used including, surface characterization studies, microscopic techniques and molecular biology.

A. Microscopy and Dynamic Light scattering

Detailed microscopic studies related to interaction of nanoparticles with bacterial membranes have been done by using Scanning Electron Microscopy (SEM), Transmission Electron Microscopy (TEM) and Fluorescence Microscopy. Microscopic studies, in particular TEM have been used to assess grain size distribution and aggregation status of nanoparticles. Dynamic light scattering (DLS) has been used to study the stability of nanoparticle characteristics under different conditions.

B. Molecular biology

Molecular biology techniques including Synthetic biology have been used to develop biosensors and overexpression strains. The assembly approach and advantage of using synthetic biology are discussed in the following paragraph.

The parts of the biosensors have been made in a specific format as described in the Registry of Standardized Biological Parts (Registry, 2003). The metal specific promoters and reporter genes (pieces of DNA) have been designed with certain restriction sites attached to them (French et al., 2011). The advantage of using this format is that it allows the freedom of recombining each part to optimize the system and provides functional units that could also be incorporated into other projects. BioBrick assembly method is shown in Figure 1-22.

For this, project synthetic biology tools have been employed to achieve three objectives:

- ✓ Developing metal ion and oxidative stress responsive biosensors
- ✓ Developing an EPS overexpressing system in *E. coli*
- ✓ Developing overexpression strains that produce enzymes like catalase and superoxide dismutase.

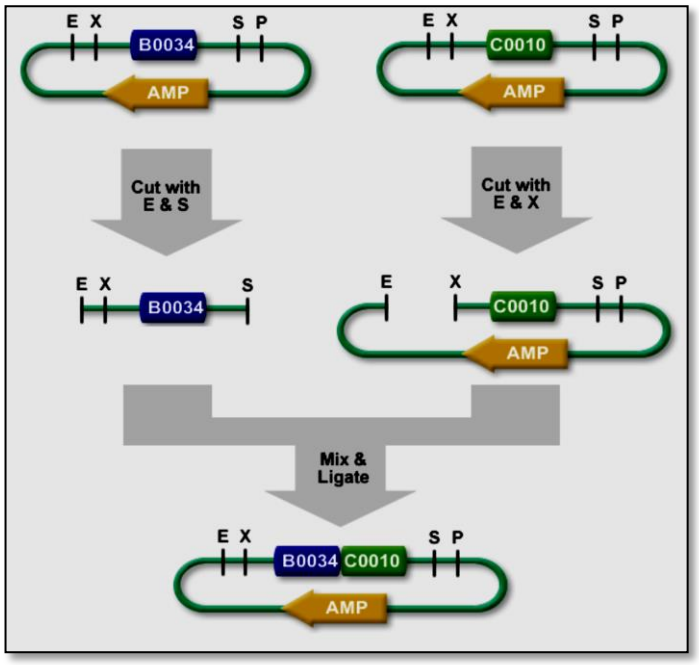

Figure 1-22: Design of a BioBrick: E (EcoR1), X (Xba1), S (Spe1) and P (Pst1) denote the restriction sites that are added to each part to facilitate the assembly of BioBricks

C. Microbiological tools

Microbial tool related to developing and conducting eco toxicological assays, calculating cell viability using colony forming units (CFU/ml), growth curves and characterization assays for gene expression studies have been used.

D. Development of microcosm and microbial community analysis

Sediment and water microcosms have been developed using lake water and amended with different concentration of silver and zinc oxide nanoparticles. These microcosms have been made sulphate rich in order to ensure the growth of sulphate reducing bacteria (dsrB). This experiment has been set up in order to realistically assess the fate and speciation of engineered nanoparticles if they find release in

environment. The following techniques are used to study the microbial communities and the transformation of nanoparticles:

Microbial community composition has been determined by using 16sRNA and denaturing gradient gel electrophoresis (DGGE). Subsequent gel analysis has been conducted by using software's like Bionumerics and Primer6 (to determine population characteristics and similarity).

E. X-ray spectroscopy analysis for determination of transformation rates and fate of nanoparticles in the microcosms

Fate of nanoparticles (silver and zinc oxide) added to the microcosm has been analysed by using K edge X-ray absorption spectroscopy (XAS). The samples have been analysed at Synchrotron Research Facility at Diamonds, UK. Reference standards like chlorides, carbonates, sulphates and sulphides of the silver and zinc oxide were analysed in XAS. Sub samples from three zones, top, bottom and a bulk (homogeneous) mixture within microcosms have been used to study the spatial heterogeneity that might exist. These variations can possibly arise either due to the variations in pH and aeration or due to the microbial activities in different layers within the column. The data collected from the beam line were analysed by using a dedicated software, Athena and after normalization, the data were processed in a Linear combination fitting model (LCF) along with mixture of the standards so as to estimate the proportion of different ionic species the nanoparticles could have transformed into within the incubation period.

1.5.4 Thesis structure

The mechanisms of nanotoxicity have been investigated and its major findings constitute the first two results chapters. It was found that silver nanotoxicity operates by multiple pathways (chapter two) and that nanoparticles were involved in oxidative stress response in bacteria (chapter three) however, the nature of ROS could not be established. Presence of EPS and analogues like xanthan reduced nanotoxicity and these findings form chapter four of the thesis. Finally the stability of nanoparticles in the environment was investigated by development of sediment microcosms and it was seen that nanoparticles rapidly transformed into metal sulphides, this constitutes chapter five and thesis concludes with a summary.

References

1. A, N., Harrison, A., Sabbani, S., Munson, R. S., Jr., Dutta, P. K. & Waldman, W. J. 2011. Silver nanoparticles embedded in zeolite membranes: release of silver ions and mechanism of antibacterial action. *Int J Nanomedicine.*, 6**,** 1833-52.

2. Adams, L. K., Lyon, D. Y. & Alvarez, P. J. J. 2006. Comparative eco-toxicity of nanoscale TiO2, SiO2, and ZnO water suspensions. *Water Res.*, 40**,** 3527-3532.

3. Agladze, K., Wang, X. & Romeo, T. 2005. Spatial periodicity of *Escherichia coli* K-12 biofilm microstructure initiates during a reversible, polar attachment phase of development and requires the polysaccharide adhesin PGA. *J. Bacteriol*, 187(24)**,** 8237-46.

4. Allison, D. G., Sutherland, I. (eds.Macbain, A) 1998. In biofilm communities: order from chaos? *Bioline Cardiff***,** 381-387.

5. Aman, P., McNeil, M., Franzén, L.E., Darvill, A. G. & Albersheim, P. 1981. Structural elucidation, using h.p.l.c.-m.s. and g.l.c.-m.s., of the acidic polysaccharide secreted by *Rhizobium meliloti* strain 1021. *Carbohydrate Res.*, 95**,** 263–282.

6. Arora, S., Rajwade, J. M. & Paknikar, K. M. 2012. Nanotoxicology and in vitro studies: The need of the hour. *Toxicol Appl Pharmacol.* 258**,** 151-165.

7. Aruoma, I. & Halliwell., B. 1991. DNA damage and free radicals. *Chem. Br,* 2**,** 149-152.

8. Auffan, M. l., Achouak, W., Rose, J. r., Roncato, M.A., Chanéac, C., Waite, D. T., Mason, A., Woicik, J. C., Wiesner, M. R. & Bottero, J.-Y. 2008. Relation between the redox state of Iron based nanoparticles and their cytotoxicity toward *Escherichia coli. Environ. Sci Technol.*, 42**,** 6730-6735.

9. Baba, T., Ara, T., Hasegawa, M., Takai, Y., Okumura, Y., Baba, M., Datsenko, K. A., Tomita, M., Wanner, B. L. & Mori, H. 2006. The construction of systematic in-frame, single-gene knockout mutant collection in *Escherichia coli* K-12. *Mol.Syst.Biol*.[Accessed 9June2009]

10. Babynin, E. V., Nuretdinov, I. A., Gubskaya, V. P. & Barabanshchikov, B. I. 2002. Study of mutagenic activity of Fullerene and aome of its derivatives using His+ reversions of *Salmonella typhimurium* as an example.*Genetika,* 38**,** 453–457.

11. Badawy, El.,Silva, R.J.,Morris, B.,Schekel, K.G.,Suidan,M.,Tolayamat, T.M. 2011.Surface charge dependent toxicity of silver nanoparticles. *Environ. Sci.Technol*.45,283-287.

12. Bae, E., Park, H., Park, J., Yoon, J., Kim, Y.H., Choi, K., Yi, J.. 2011. Effect of Chemical Stabilizers in Silver Nanoparticle Suspensions on Nanotoxicity. *Bull.Korean.Chem.Soc*.32,613-619.

13. Barillet, S., Deckers, A.S, Herlin-Boime, N., Reynaud, C., Cassio, D., Gouget, B. & Carriere, M. 2010. Toxicological consequences of TiO2, SiC nanoparticles and multi-walled carbon nanotubes exposure in several mammalian cell types: an in vitro study. *J. Nanopart. Res.,* 12**,** 61-73.

14. Battin , T., Frank, V. D., Weilhartner, A., Ottofuelling, S. & Hofmann, T. 2009. Nanostructured TiO2: transport behavior and effects on aquatic microbial communities under environmental conditions. *Environ. Sci. Technol.,* 43**,** 8098-8104.

15. Baun, A., Hartmann, N. B., Grieger, K. & Kusk, K. O. 2008. Ecotoxicity of engineered nanoparticles to aquatic invertebrates: a brief review and recommendations for future toxicity testing. *Ecotoxicol.,* 17**,** 387-395,.

16. Beard, S. J., Hughes, M. N. & Poole, R. K. 1995. Inhibition of the cytochrome bd-terminated NADH oxidase system in *Escherichia coli* K-12 by divalent metal cations. *FEMS microbiol lett.,* 131**,** 205-210.

17. Bekhit, A., Fukamachi, T., Saito, H. & Kobayashi, H. 2011. The role of OmpC and OmpF in acidic resistance in *Escherichia coli*. *Biol Pharm Bull.*. 34**,** 330-4.

18. Beloin, C., Roux, A. & Ghigo, J. 2008. Escherichia coli biofilms. *Curr Top Microbiol Immunol. ,* 322**,** 249-89.

19. Beveridge, T. J. & Fyfe, W. S. 1985. Metal fixation by bacterial cell walls. *Canadian J Earth Sci,* 22(12)**,** 1893-1898.

20. Beveridge, T. J. & Murray, R. G. 1976 Uptake and retention of metals by cell walls of *Bacillus subtilis*. *J. Bacteriol.,* 127**,** 1502-1518.

21. Beveridge, T. J. & Murray, R. G. 1980. Sites of metal deposition in the cell wall of *Bacillus subtilis*. *J. Bacteriol.* 141(2)**,** 876–887.

22. Bhabra, G., Sood, A., Fisher, B., Cartwright, L., Saunders, M., Evans, W. H., Surprenant, A., Castejon, G., Mann, S., Davis, S. A., Hails, L. A., Ingham, E., Verkade, P., Lane, J., Heesom, K., Newson, R. & Case, C. P. 2009. Nanoparticles can cause DNA damage across a cellular barrier. *Nature Nanotechnol.***,** 873-883.

23. Blaise, C., Gagné, F., Férard, J. F. & Eullaffroy, P. 2008. Ecotoxicity of selected nano-materials to aquatic organisms. *Environ. Toxicol.,* 23**,** 591-598.

24. Bondarenko, O., Ivask, A., Käkinen, A. & Kahru, A. 2012. Sub-toxic effects of CuO nanoparticles on bacteria: kinetics, role of Cu ions and possible mechanisms of action. *Environ. Pollut.,* 169**,** 81-90.

25. Bone, A. J., Colman, B. P., Gondikas, A. P., Newton, K. M., Harrold, K. H., Cory, R. M., Unrine, J. M., Klaine, S. J., Matson, C. W. & Di Giulio, R. T. 2012. Biotic and abiotic interactions in aquatic microcosms determine fate and toxicity of Ag nanoparticles: part 2-toxicity and Ag speciation. *Environ. Sci.Technol.*, 46(13)**,** 6925-33.

26. Bryaskova, R., Pencheva, D., Nikolov, S. & Kantardjiev, T. 2011. Synthesis and comparative study on the antimicrobial activity of hybrid materials based on silver nanoparticles (AgNps) stabilized by polyvinylpyrrolidone (PVP). *J.Chem.Biol.*, 4**,** 185-191.

27. Cabiscol, E., Tamarit, J. & Ros, J. 1999. Oxidative stress in bacteria and protein damage by reactive oxygen species. *Int. J Microbiol.*, 3**,** 3-8.

28. Cagle, D. W., Kennel, S. J., Mirzadeh, S., Alford, J. M. & Wilson, L. J. 1999. *In Vivo* Studies of fullerene based materials using endohedral metallofullerene radiotracers.*Proc. Natl. Acad. Sci. U.S.A.*, 96**,** 5182–5187.

29. Calder, A., Dimkpa, C., McLean, J., Britt, D., Johnson, W. & Anderson, A. 2012 Soil components mitigate the antimicrobial effects of silver nanoparticles towards a beneficial soil bacterium, *Pseudomonas chlororaphis* O6. *Sci Total Environ.*, 429**,** 215-22.

30. Cattaneo, A., Gornati, R., Chiriva-Internati, M. & Bernardini, G. 2009. Ecotoxicology of nanomaterials: the role of invertebrate testing. *ISJ* 6**,** 78-97.

31. Cedervall, T., Hansson, L.A., Lard, M., Frohm, B. & Linse, S. 2012. Food chain transport of nanoparticles affects behaviour and fat metabolism in fish. *PLoS ONE,* 7(2): e32254. doi:10.1371/journal.pone.0032254.

32. Cha, Y. J., Lee, J. & Choi, S. 2012. Apoptosis-mediated *in vivo* toxicity of hydroxylated fullerene nanoparticles in soil nematode *Caenorhabditis elegans. Chemosphere,* 87**,** 49-54.

33. Chang, W., Wen, Y., Lin, Z., Zainal, N., E. Williams, Zhu, K., Kruzic, A. P., Smith, R. L. & Rajeshwar, K. 1994. Bactericidal activity of TiO2 photocatalyst in aqueous media: toward a solar-sssisted water disinfection system. *Environ. Sci. Technol.* , 28**,** 934–938.

34. Chen, J., Lee, S. M. & Mao, Y. 2004a. Protective effect of exopolysaccharide colanic acid of *Escherichia coli* O157:H7 to osmotic and oxidative stress. *Int. Journal Food microbiol.*, 3**,** 281-286.

35. Chen, Y., Chen, J., Dong, J. & Jin, Y. 2004b. Comparing study of the effect of nanosized silicon dioxide and microsized silicon dioxide on fibrogenesis in rats. *Toxicol. Ind. Health* 20**,** 21-27.

36. Choi, J.Y., Lee, S.H., Na, H.B., An, K., Hyeon, T., Seo, T.S. 2010. In vitro cytotoxicity screening of water-dispersible metal oxide nanoparticles in human cell lines. *Bioprocess Biosyst Eng.*, 33**,** 21-30.

37. Choi, O. & Hu, Z. 2008. Size dependent and reactive oxygen species related nanosilver toxicity to nitrifying bacteria. *Environ. Sci Technol.,* 42**,** 4583-4588.

38. Chung, C. & Goldberg, A. 1981. The product of the lon (capR) gene in *Escherichia coli* is the ATP-dependent protease, protease La. *Proc Natl Acad Sci,* 78**,** 4931-5.

39. Chwalibog, A., Sawosz, E., Hotowy, A., Szeliga, J., Mitura, S., Mitura, K., Grodzik, M., Orlowski, P. & Sokolowska, A. 2010. Visualization of interaction between inorganic nanoparticles and bacteria or fungi. *Int. J Nanomed.*, 5**,** 1085-94.

40. Cowan, S. W., Schirmer, T., Rummel, G., Steiert, M., Ghosh, R., Pauptit, R. A., Jansonius, J. N. & Rosenbusch, J. P. 1992. Crystal structures explain functional properties of two *E. coli* porins. *Nature,* 358(6389)**,** 727-33.

41. Dams , R., Biswas, A., Olesiejuk, A., Fernandes, T. & Christofi, N. 2011. Silver nanotoxicity using a light-emitting biosensor *Pseudomonas putida* isolated from a wastewater treatment plant. *J. Hazard. Mater.*, 195**,** 68-72.

42. Danese, P. & Kolter, R. 2000. Exopolysaccharide production is required for development of *Escherichia coli* K-12 biofilm architecture. *J Bacteriol.,* 182(12)**,** 3593-6.

43. Danese, P. N., Pratt, L. A. & Kolter, R. 2000. Exopolysaccharide production is required for development of *Escherichia coli* K-12 biofilm architecture. *J. Bacteriol. ,* 182**,** 3593-3596.

44. Daunert, S., Barrett, G., Feliciano, J., Shetty, R., Shrestha, S. & Smith-Spencer, W. 2000. Genetically engineered whole-cell sensing systems: coupling biological recognition with reporter genes. *Chem Review,* 100(7)**,** 2705-38.

45. Davies, K. J. 1995. Oxidative stress: the paradox of aerobic life. *Biochem Soc Symp.,* 61**,** 1-31.

46. Davies, K. J. A. 2000. Oxidative Stress, antioxidant defenses, and damage removal, repair, and replacement systems. *IUBMB Life,* 50**,** 279–289.

47. Dimkpa, C., Calder, A., Gajjar, P., Merugu, S., Huang, W., Britt, D., McLean, J., Johnson, W. & Anderson, A. J. 2011. Interaction of silver nanoparticles with an environmentally beneficial bacterium, *Pseudomonas chlororaphis*. *J. Hazard.Mater,* 188**,** 428-435.

48. Dinesh, R., Anandaraj, M., Srinivasan, V. & Hamza, S. 2012. Engineered nanoparticles in the soil and their potential implications to microbial activity. *Geoderma,* 173-174**,** 19-27.

49. Doherty, D., Leigh, J. A., Glazebrook, J. & Walker, G. C. 1988. *Rhizobium meliloti* mutants that overproduce the *R. meliloti* acidic calcofluor-binding exopolysaccharide. *J Bacteriol.,* 170(9)**,** 4249-4256.

50. Ebel, W. & Trempy, J. E. 1999. *Escherichia col*i RcsA, a positive activator of colanic acid capsular polysaccharide synthesis, functions To activate its own expression. *J Bacteriol.,* 181(2)**,** 577-584.

51. El Badawy, A. M., Silva, R. G., Morris, B., Scheckel, K. G., Suidan, M. T. & Tolaymat, T. M. 2010. Surface Charge-Dependent Toxicity of Silver Nanoparticles. *Environ. Sci Technol.,* 45**,** 283-287.

52. Elliott, H. A., Liberati, M. R. & Huang, C. P. 1986. Competitive adsorption of heavy metals by soils. *J. Environ Qual.,* 15 214-219.

53. Eom, H. J. & Choi, J. 2010. Oxidative stress of CeO2 nanoparticles via p38-Nrf-2 signaling pathway in human bronchial epithelial cell Beas-2B. *Toxicol Lett.,* 187**,** 187, 77- 83.

54. Fabrega, J., Renshaw, J. C. & Lead, J. R. 2009. Interactions of silver nanoparticles with *Pseudomonas putida* biofilms. *Environ Sci Technol.,* 43**,** 9004-9009.

55. Fabrega, J., Shona, R., Fawcett, S., Renshaw, J. C. & Lead, J. R. 2009. Silver nanoparticle impact on bacterial growth: effect of pH, concentration, and organic matter. *Environ. Sci. Technol.,* 43(19)**,** 7285-90.

56. Fabrega, J., Zhang, R., Renshaw, J. C., Liu, W. T. & Lead, J. R. 2011. Impact of silver nanoparticles on natural marine biofilm bacteria. *Chemosphere,* 85**,** 961-966.

57. Farr, S. B. & Kogoma, T. 1991. Oxidative stress responses in *Escherichia coli* and *Salmonella typhimurium*. *Microbiol Rev. ,* 55(4)**,** 561–585.

58. Fenn, W. O., Gerschman, G., Gilbert, D. L., D. E. Terwilliger & Cothran., F. V. 1957. Mutagenic effects of high oxygen tensions on *Escherichia coli*. *Proc. Natl. Acad. Sci. USA,* 43:**,** 1027-1032.

59. Finan, T., Kunkel, B., De Vos, G. & Signer, E. 1986. Second symbiotic megaplasmid in *Rhizobium meliloti* carrying exopolysaccharide and thiamine synthesis genes. J. Bacteriol.**,** 66-72.

60. Flemming, H. C. & Wingender, J. 2010. The biofilm matrix. *Nature Reviews,* 8**,** 623-633.

61. Franklin, N. M., Rogers, N. J., Apte, S. C., Batley, G. E., Gadd, G. E. & Casey, P. S. 2007. Comparative toxicity of nanoparticulate ZnO, bulk ZnO, and ZnCl2 to a freshwater microalga *Pseudokirchneriella subcapitata*: the importance of particle solubility. *Eniron. Sci.Technol.,* 15**,** 8484-90.

62. French, C. E., Mora, K. d., Joshi, N., Elfick, A., Haseloff, J. & Ajioka, J. 2011. Synthetic biology and the art of Biosensor design. *National Academies Press*.

63. French, R. A., Jacobson, A. R., Kim, B., Isley, S. L., Penn, R. L. & Baveye, P. C. 2009. Influence of ionic strength, pH, and cation valence on aggregation kinetics of titanium dioxide nanoparticles. *Environ. Sci Technol,* 43**,** 1354-1359.

64. G, Z., Cecil, P., Ilari, A., Giangiacomo, L., Laue, T. M., Chiancone, E. & Chasteen, N. D. 2002. Iron and hydrogen peroxide detoxification properties of DNA-binding protein from starved cells: a ferritin-like DNA-binding protein of *Escherichia coli. J Biol Chem.*, 277(31)**,** 27689-96.

65. Gaiser, B. K., Fernandes, T. F., Jepson, M. A., Lead, J. R., Tyler, C. R., Baalousha, M., Biswas, A., Britton, G. J., Cole, P. A., Johnston, B. D., Ju-Nam, Y., Rosenkranz, P., Scown, T. M. & Stone, V. 2012. Interspecies comparisons on the uptake and toxicity of silver and cerium dioxide nanoparticles. *Environ Toxicol Chem.,* 31**,** 144-154.

66. Gajjar, P., Pettee, B., Britt, D., Huang, W., Johnson, W. & Anderson, A. 2009. Antimicrobial activities of commercial nanoparticles against an environmental soil microbe, *Pseudomonas putida* KT2440. *J Biol.Eng.*, 3**,** 1611-1754.

67. Galibert, F., Finan, T., Long, S., Puhler, A., Abola, P., Ampe, F., Barloy-Hubler, F., Barnett, M., Becker, A., Boistard, P., Bothe, G., Boutry, M., Bowser, L., Buhrmester, J., Cadieu, E., Capela, D., Chain, P., Cowie, A., Davis, R., Dreano, S., Federspiel, N., Fisher, R., Gloux, S., Godrie, T., Goffeau, A., Golding, B., Gouzy, J., Gurjal, M., Hernandez-Lucas, I., Hong, A., Huizar, L., Hyman, R., Jones T, Kahn, D., Kahn, M., Kalman, S., Keating, D., Kiss, E., Kom, C., Lelaure, V., Masuy, D., Palm, C., Peck, M., Pohl, T., Portetelle, D., Purnelle, B., Ramsperger, U., Surzycki, R., Thebault, P., Vandenbol, M., Vorholter, F., Weidner, S., Wells, D., Wong, K., Yeh, K. & Batut, J. 2001. The composite genome of the legume symbiont *Sinorhizobium meliloti*. *Science,* 293(5530)**,** 668-72.

68. Gao, J., Wang, H. L., Shreve, A. & Iyer, R. 2010. Fullerene derivatives induce premature senescence: a new toxicity paradigm or novel biomedical applications. *Toxicol Appl Pharmacol. ,* 244**,** 130-43.

69. Ge, Y., Schimel, J. P. & Holden, P. A. 2011. Evidence for negative effects of TiO2 and ZnO nanoparticles on soil bacterial communities. *Environ. Sci .Technol.,* 45**,** 1659-1664.

70. Ge, Y., Schimel, J. P. & Holden, P. A. 2012. Identification of soil bacteria susceptible to TiO_2 and ZnO nanoparticles. *Appl. Environ Microbiol.,* 78**,** 6749-58.

71. George, S., Pokhrel, S., Xia, T., Gilbert, B., Ji, Z., Schowalter, M., Rosenauer, A., Damoiseaux, R., Bradley, K. A., Mädler, L. & Nel, A. E. 2009. Use of a rapid cytotoxicity screening approach to engineer a safer zinc oxide nanoparticle through iron doping. *ACS Nano,* 4**,** 15-29.

72. Gomes, T., Pereira, C. G., Cardoso, C., Pinheiro, J. P., Cancio, I. & Bebianno, M. J. 2012. Accumulation and toxicity of copper oxide nanoparticles in the digestive gland of *Mytilus galloprovincialis*. *Aquat. Toxicol.,* 111-112**,** 72-79.

73. Gordon, T. 1992. Pulmonary effects of inhaled zinc oxide in human subjects, guinea pigs, rats and rabbits. *Am. Ind. Hyg. Assoc. J. ,* 54**,** 503–509.

74. Gou, N., Hayden, A. O. & Gu, A. Z. 2010. Mechanistic toxicity assessment of nanomaterials by whole-cell-array stress genes expression analysis. *Environ. Sci. Technol.,* 44**,** 5964–5970.

75. Lowry, G.V., Espinasse, B.P., Badireddy, A.R, Richardson, C.J., Reinsch, B.C., Bryant, L.D., Bone,A.J., Deonarine,A., Chae,S., Therezien,M., Colman, B.P., Hsu Kim, H.,Bernhardt, E.S., Matson, C.W., Wiesner, M.R. 2012. Long term transformation and fate of manufactured Ag nanoparticles in a simulated large scale freshwater emergent wetland. *Environ.Sci.Technol.,* 46**,** 7027-36.

76. Hall-Stoodley, L., Costerton, J. W. & Stoodley, P. 2004. Bacterial biofilms: from natural environments to infectious disease. *Nature Reviews,* 2**,** 95-108.

77. He, D., Garg, S. & Waite, T. D. 2012. H2O2-mediated oxidation of zero-valent silver and resultant interactions among silver nanoparticles, silver ions, and reactive oxygen species. *Langmuir,* 28(27)**,** 10266-75.

78. He, S., Feng, Y., Ren, H., Zhang, Y., Gu, N. & Lin, X. 2011. The impact of iron oxide magnetic nanoparticles on the soil bacterial community. *J Soils Sedim,* 11**,** 1408-1417.

79. Heinlaana, M., Ivaska, A., Blinovaa, I., Dubourguier, H.C. & Kahru, A. 2008. Toxicity of nanosized and bulk ZnO, CuO and TiO2 to bacteria *Vibrio fischeri* and crustaceans *Daphnia magna* and *Thamnocephalus platyurus*. *Chemosphere,* 71**,** 1308–1316.

80. Heymann, D., Chibante, L. P. F., Brooks, R. R., Wolbach, W. S. & Smalley, R. E. 1994. Fullerenes in the cretaceous tertiary boundary layer. *Science,* 29**,** 645-647.

81. http://medicine.tamhsc.edu/basic-sciences/mmp/faculty/katja-mertens.html Untitled. [online] [Accessed: 30 Apr 2013].

82. Hu, X., Cook, S., Wang, P. & Hwang, H. M. 2009. In vitro evaluation of cytotoxicity of engineered metal oxide nanoparticles. *Sci.Total Environ.,* 407**,** 3070-3072.

83. Huang, C. C., Aronstama., R. S., Chen, D. R. & Huang, Y. W. 2010. Oxidative stress, calcium homeostasis, and altered gene expression in human lung epithelial cells exposed to ZnO nanoparticles. *Toxicology in Vitro,* 24**,** 45–55.

84. Huang, Z., Zheng, X., Yan, D., Yin, G., Liao, X., Kang, Y., Yao, Y., Huang, D. & Hao, B. 2008. Toxicological Effect of ZnO nanoparticles based on bacteria. *Langmuir,* 24**,** 4140-4144.

85. Imlay, J. A. 2003. Pathways of oxidative damage. *Annu Rev Microbiol. ,* 57**,** 395-418.

86. Imlay, J. A. & Linn., S. 1987. Mutagenesis and stress responses induced in *Escherichia coli* by hydrogen peroxide. *J.Bacteriol.,* 169**,** 2967-2976.

87. Ivask, A., Suarez, E., Patel, T., Boren, D., Ji, Z., Holden, P., Telesca, D., Damoiseaux, R., Bradley, K. A. & Godwin, H. 2012. Genome wide bacterial toxicity screening uncovers the mechanisms of toxicity of a cationic polystyrene nanomaterial. *Environ. Sci. Technol.,* 46**,** 2398–2405.

88. Janczarek, M. 2011. Environmental signals and regulatory pathways that influence exopolysaccharide production in rhizobia. *Int J Mol Sci,* 12**,** 7898-933.

89. Jiang, G., Shen, Z., Niu, J., Bao, Y., Chen, J. & He, T. 2011. Toxicological assessment of TiO2 nanoparticles by recombinant *Escherichia coli* bacteria. *J. Env. Monit.,* 13**,** 42-48.

90. Jin, X., Li, M., Wang, J., MarambioJones, C., Peng, F., Huang, X., Damoiseaux, R. & Hoek, E. M. V. 2010. High-Throughput screening of silver nanoparticle stability and bacterial inactivation in aquatic media: influence of specific ions. *Environ. Sci Technol.,* 44**,** 7321-7328.

91. Johnston, H. J., Hutchison, G. R., Christensen, F. M., Aschberger, K. & Stone, V. 2010. The biological mechanisms and physicochemical characteristics responsible for driving fullerene toxicity. *Toxicol Sci.,* 114**,** 162–182

92. Johnston , H. J., Semmler-Behnke, M., Brown, D. M., Kreyling, W., Tran, L. & Stone, V. 2010. Evaluating the uptake and intracellular fate of polystyrene nanoparticles by primary and hepatocyte cell lines in vitro. *Toxicol. Appl. Pharmacol.,* 242**,** 66-78.

93. Jones, K. M., Sharopova, N., Lohar, D. P., Zhang, J. Q., VandenBosch, K. A. & Walker, G. C. 2008. Differential response of the plant Medicago truncatula

to its symbiont *Sinorhizobium meliloti* or an exopolysaccharide-deficient mutant *PNAS* 105**,** 704-709.

94. Joshi, N., Ngwenya, B. & French, C. E. 2012. Enhanced resistance to nanoparticle toxicity is conferred by overproduction of extracellular polymeric substances. *J. Hazard. Mater.,* 241–242**,** 363-370.

95. Jun, S., Hideo, I., Hashimoto, A., Kokugan, T. & Shimizu, M. 1995. Effect of ceramic powders on spores of *Bacillus subtilis*. *J. Chem. Eng. Jpn,* 28**,** 288–293.

96. Rogers,K.R. & Lin, J.N. 1992. Biosensors for environmental monitoring. *Biosensors and Bioelectronics,*7, 317-321.

97. Kaeriyama, M., Machida, K., Kitakaze, A., Wang H, L. Q., Fukamachi, T., Saito, H. & Kobayashi, H. 2006. OmpC and OmpF are required for growth under hyperosmotic stress above pH 8 in *Escherichia coli*. *Lett Appl Microbiol.,* 42(3)**,** 195-201.

98. Kamat, J. P., Devasagayama, T. P. A., Priyadarsini, K. I. & Mohan, H. 2000. Reactive oxygen species mediated membrane damage induced by fullerene derivatives and its possible biological implications. *Toxicology,* 155**,** 55-61.

99. Kanaly, R. A., Maeda, A. H., Kunihiro, M. & Hamamura, N. 2011. Application of denaturing gradient gel electrophoresis as an ecotoxicological tool to investigate the effects of aqu-Fullerene on a bacterial community. *Interdiscip Enviriron Chem.***,** 79-88.

100. Kasemets, K., Ivask, A., Dubourguier, H.C. & Kahru, A. 2009. Toxicity of nanoparticles of ZnO, CuO and TiO2 to yeast *Saccharomyces cerevisiae*. *Toxicology in vitro,* 23**,** 1116-1122.

101. Kasmets, K., Ivask, A., Dubourgier, H. & Kahru, A. 2009. Toxicity of nanoparticles TiO2,ZnO,SiO2 to yeast *Saccharomyces cerevisiae*. *Toxicity invitro,* 23**,** 1116-1122.

102. Keller, M., Roxlau, A., Wenig, W. M., Schmidt, M., Quandt, J., Niehaus, K., Jording, D., Arnold, W. & Pühler, A. 1995. Molecular analysis of the Rhizobium meliloti mucR gene regulating the biosynthesis of the exopolysaccharides succinoglycan and galactoglucan. *Mol. Plant Microbe interact.,* 8**,** 267-277.

103. Khalil, A. S. & Collins, J. J. 2010. Synthetic biology: applications come of age. *Nat Rev Genet.,* 11**,** 367-379

104. Khan, S., Mukherjee, A. & Chandrasekaran, N. 2011. Silver nanoparticles tolerant bacteria from sewage environment. *J. Environ. Sci,* 23(2)**,** 346-352.

105. Khan, S. S., Mukherjee, A. & Chandrasekaran, N. 2011. Impact of exopolysaccharides on the stability of silver nanoparticles in water. *Water Res.,* 45**,** 5184-5190.

106. Khan, S. S., Srivatsan, P., Vaishnavi, N., Mukherjee, A. & Chandrasekaran, N. 2011c. Interaction of silver nanoparticles (SNPs) with bacterial extracellular proteins (ECPs) and its adsorption isotherms and kinetics. *J. Hazard Mater.,* 192**,** 299-306.

107. Kim , K., Sung, W. S., Suh, B. K., Moon, S. K., Choi, J. S., Kim, G. J. & Li, D. J. 2009. Antifungal activity and mode of action of silver nanoparticles on *Candida albicans*. *Biometals,* 22**,** 235-242.

108. Kittler, S., Greulich, C., Diendorf, J., Köller, M. & Epple, M. 2010. Toxicity of silver nanoparticles increases during storage because of slow dissolution under release of silver ions. *Chem. Mate,* 22**,** 4548–4554.

109. Klapera, R., Cragoa, J., Barra, J., Arndta, D., Setyowatib, K. & Jian Chenb 2009. Toxicity biomarker expression in daphnids exposed to manufactured nanoparticles: Changes in toxicity with functionalization. *Environ. Pollut.*157**,** 1152–1156.

110. Knight, T. 2003. Idempotent Vector Design for Standard Assembly of Biobricks, . *mit.edu/handle/1721.1/21168 1–11*.

111. Kumar, A., Pandey, A. K., Singh, S. S., Shanker, R. & Dhawan, A. 2011. Engineered ZnO and TiO2 nanoparticles induce oxidative stress and DNA damage leading to reduced viability of *Escherichia coli*. *Free Radical Bio Med.,* 52**,** 1872-1881.

112. Lam, C., James, J. T., McCluskey, R. & Hunter, R. L. 2004. Pulmonary toxicity of single-wall carbon nanotubes in mice 7 and 90 days after intratracheal instillation. *Toxicol. Sci.,* 77**,** 126-134.

113. Lankoff, A., Sandberg, W., Wegierek-Ciuk, A., Lisowska, H., Refsnes, M., Sartowska, B., Schwarze, P., Meczynska-Wielgosz , S., Wojewodzka, M. & Kruszewski, M. 2012. The effect of agglomeration state of silver and titanium dioxide nanoparticles on cellular response of HepG2, A549 and THP-1 cells. *Toxicol. Lett.,* 208**,** 197-213.

114. Leigh, J., Signer, E. & Walker, G. 1985. Exopolysaccharide-deficient mutants of Rhizobium meliloti that form ineffective nodules. *Proc Natl Acad Sci,* 82**,** 6231-5.

115. LiYana, C., Qia, W. & Ru Honga, M. 2009. Effect of nanoparticles on the bacterial community of the cucumber phyllosphere. *Chinese J Agri Biotechnol,* 6**,** 141-145.

116. Li, C., Liu, H., Sun, Y., Wang, H., Guo, F., Rao, S., Deng, J., Zhang, Y., Miao, Y., Guo, C., Meng, J., Chen, X., Li, L., Li, D., Xu, H., Wang, H., Li,

B., Jiang, C. 2009. PAMAM nanoparticles promote acute lung injury by inducing autophagic cell death through the Akt-TSC2-mTOR signaling pathway. *J. Mol.Cell Biol.,* 1**,** 37-45.

117. Li, H., Nikaido, H. & Williams, K. E. 1997. Silver-resistant mutants of *Escherichia coli* display active efflux of Ag+ and are deficient in porins. *J Bacteriol.* , 179(19)**,** 6127–6132.

118. Li, M., Zhu, L. & Lin, D. 2011. Toxicity of ZnO nanoparticles to *Escherichia coli*: mechanism and the influence of medium components. *Environ. Sci.Technol.,* 45**,** 1977-1983.

119. Li, Z. & Demple, B. 1994. SoxS, an activator of superoxide stress genes in *Escherichia coli* purification and interaction with DNA. *J Biol Chem.,* 269(28)**,** 18371-7.

120. Lin, W., Stayton, I., Huang, Y. W., Zhou, X. D. & Ma, Y. 2008. Cytotoxicity and cell membrane depolarization induced by aluminum oxide nanoparticles in human lung epithelial cells A549.*Toxicol Environ.Chem,* 90**,** 983-996.

121. Lin, W. S., Xu, Y., Huang, C. C., Ma, Y., Shannon, K. B., Chen, D. R. & Huang, Y. W. 2007. Toxicity of nano- and micro-sized ZnO particles in human lung epithelial cells. *J Nanopart Res.,* 11**,** 25-29.

122. Liochev, S. I., Benov, L., Touati, D. & Fridovich, I. 1999. Induction of the soxRS Regulon of *Escherichia coli* by superoxide. *J Biol. Chem.,* 274**,** 9479-9481.

123. Liu, Y., Li, J., Qiu, X. & Burda, C. 2007. Bactericidal activity of nitrogen-doped metal oxide nanocatalysts and the influence of bacterial extracellular polymeric substances (EPS). *J Photochem Photobiol A: Chem,* 190**,** 94-100.

124. Loftin, I., Franke, S., Roberts, A., Weichsel, A., Heroux, A., Montfort, W. R., Rensing, C. & McEvoy, M. M. 2005. A novel copper-binding fold for the periplasmic copper resistance protein CusF. *Biochem,* 44**,** 10533-40.

125. Lok, C.N., Ho, C.M., Chen, R., He, Q.Y., Yu, W.Y., Sun, H., Tam, P.K., Chiu, J.F., Che, C.M. 2007. Silver nanoparticles: partial oxidation and antibacterial activities. *J..Biol Inorg.Chem.,* 12**,** 527-534.

126. Long, Z., Ji, J., Yang, K., Lin, D. & Wu, F. 2012. Systematic and quantitative investigation of the mechanism of carbon nanotubes' toxicity toward Algae. *Environ. Sci.Technol.,* 46**,** 8458–8466

127. Lovern, S. B. & Klaper, R. 2006. *Daphnia magna* mortality when exposed to titanium dioxide and fullerene (C60) nanoparticles. *Environ Toxicol Chem.* , 25(4)**,** 1132-7.

128. Lowry, G. V., Gregory, K. B., Apte, S. C. & Lead, J. R. 2012. Transformations of nanomaterials in the environment. *Environ. Sci.Technol.,* dx.doi.org/10.1021/es300839e.

129. Lubick, N. 2008. Nanosilver toxicity: ions, nanoparticlesor both? *Environ. Sci.Technol.,* 42**,** 8617.

130. Luyten, E. & Vanderleyden, J. 2000. Survey of genes identified in *Sinorhizobium meliloti* spp., necessary for the development of an efficient symbiosis. *Eur J Soil Biol,* 36**,** 1-26.

131. Lyon, D. & Alvarez, P. J. 2005. Fullerene water suspension (nC60) exerts antibacterial effects via ROS-independent protein oxidation. *Environ.Sci.Technol.,* 42**,** 8127-8132.

132. Ma, H., Williams, P. L. & Diamond, S. A. 2013a. Ecotoxicity of manufactured ZnO nanoparticles – a review. *Environ. Pollut.,* 172**,** 76–85.

133. Ma, R., Levard, C., Marinakos, S. M., Cheng, Y., Liu, J., Michel, F. M., Brown, G. E. & Lowry, G. V. 2012. Size-controlled dissolution of organic-coated silver nanoparticles. *Environ. Sci Technol,* 46**,** 752-759.

134. Ma, R., Levard, C., Michel, F. M., Brown, G. E. J. & Lowry, G. V. 2013b. Sulfidation mechanism for zinc oxide nanoparticles and the effect of sulfidation on their solubility. *Environ. Sci.Technol.,* 19;47(6)**,** 2527-34. .

135. Majdalani, N. & Gottesman, S. 2005. The Rcs phosphorelay: A complex signal transduction system. *Annu Rev Microbiol.,* 59**,** 379-405.

136. Marshall, K.C. 1997. Colonization, Adhesion, and Biofilms. pp. 358-365. In Hurst J.C. (ed.) Manual of Environmental Microbiology. ASM Press, Washington DC

137. Maynard, A. & Michelson, E. 2006. The nanotechnology consumer productsi nventory. Washington, DC: Project on emerging nanotechnologies, Woodrow Wilson International Center for Scholars.*Available from:<http://nanotechproject.org/44>; March 2006 [accessed 12.09.2009]*.

138. McCarthy, J., Inkielewicz-Stepniak, I., Corbalan, J. J. & Radomski, M.W. 2012. Mechanisms of toxicity of amorphous silica nanoparticles on human lung submucosal cells in vitro: protective effects of fisetin. *Chem. Res. Toxicol.,* 25**,** 2227–2235.

139. McKenney, D., Hubner, J., Muller, E., Wang, Y., Goldmann, D. A. & Pier., G. B. 1998. The ica locus of Staphylococcus epidermidis encodes production of the capsular polysaccharide adhesin. Infect. *Immun. ,* 66**,** 4711-4720.

140. Mendrygal, K. E. & Gonzalez, J. E. 2000. Environmental regulation of exopolysaccharide production in *Sinorhizobium meliloti*. *J Bacteriol.,* 182**,** 599-606.

141. Miao, A. J., Schwehr, K. A., Xu, C., Zhang, S. J., Luo, Z., Quigg, A. & Santschi, P. H. 2009. The algal toxicity of silver engineered nanoparticles and detoxification by exopolymeric substances. *Environ. Pollut.,* 157(11)**,** 3034-41.

142. Mills, D. A., Schmidt, B., Hiser, C., Westleya, E. & Ferguson-Miller, S. 2002. Membrane potential-controlled inhibition of cytochromec oxidase by Zinc. *J. Biolog. Chem.,,* 277**,** 14894-14901.

143. Moreau, J., Weber, P., Michael, C., Martin, M., Gilbert, B., Hutcheon, I. & Banfield, J. F. 2007. Extracellular proteins limit the dispersal of biogenic nanoparticles. *Science,* 316**,** 1600-1603.

144. Mullen, M. D., Wolf, D. C., Ferris, F. G., Beveridge, T. J., Flemming, C. A. & Bailey, G. W. 1989 Bacterial sorption of heavy metals. *Appl Environ Microbiol.,* 55(12)**,** 3143–3149.

145. Müller, P., Hynes, M., Kapp, D., Niehaus, K. & Pühler, A. 1988. Two classes of *Rhizobium meliloti* infection mutants differ in exopolysaccharide production and in co inoculation properties with nodulation mutants. *Mol Gen Genet.,* doi: 10.1007/BF00338388.

146. Munson, G., Lam, D. L., Outten, F. W. & O'Halloran, T. V. 2000. Identification of a copper-responsive two-component system on the chromosome of *Escherichia coli* K-12. *J Bacteriol.,* 182(20)**,** 5864-71.

147. Napierska, D., Rabolli, V., Thomassen, L. C. J., Dinsdale, D., Princen, C., Gonzalez, L., Poels, K. L. C., Kirsch-Volders, M., Lison, D., Martens, J. A. & Hoet, P. H. 2012. Oxidative stress induced by pure and iron-doped amorphous silica nanoparticles in subtoxic conditions. *Chem. Res Toxicol.,* 25(4), 828-37.

148. Nat.Inst.Env.studies 2009. http://www.nies.go.jp/gaiyo/bunya/penvironmrisk-e.html.[accessed 21/4/2009]

149. Nel, A., Xia, T., Mädler, L. & Li, N. 2006. Toxic potential of materials at the nanolevel. *Science,* 311**,** 622-627.

150. Nguyen, T., Phuong, M., Nghia, P. T. & Marquis, R. E. 2006. Zinc effects on oxidative physiology of oral bacteria. *Adv in Natul Sci.,* 7**,** 131-138.

151. Nies, D. & Silver, S. 1995. Ion efflux systems involved in bacterial metal resistances. *J. Ind. Microbiol.,* 14**,** 186-99.

152. Obadia, B., Lacour, S., Doublet, P., Baubichon-Cortay, Cozzone, A. J. & Grangeasse, C. 2007. Influence of tyrosine-kinase Wzc activity on colanic acid production in *Escherichia coli* K12 cells. *J. Mol.Biol.,* 367**,** 42-53.

153. Oberdörster, E., Zhu, S., Blickley, T. M., McClellan-Green, P. & Haasch., M. L. 2006. Ecotoxicology of carbon-based engineered nanoparticles: Effects of fullerene (C60) on aquatic organisms. *Carbon. ,* 44(6):**,** 1112-1120.

154. Omoike, A. & Chorover, J. 2004. Spectroscopic study of extracellular polymeric substances from *Bacillus subtilis*: aqueous chemistry and adsorption effects. *Biomacromol.,* 5**,** 1219-1230.

155. Omoike, A. & Chorover, J. 2006. adsorption of geothite to extracellular polymeric substances from *Bacillus subtilis*. *Geochem.Cosmochim.Acta,* 70**,** 827-838.

156. Pal, S., Tak, Y. & Song, J. M. 2007. Does the antibacterial activity of silver nanoparticles depend on the shape of the nanoparticle? A study of the Gram-negative bacterium *Escherichia coli*. *Appl. Environ. microbiol.,* 73**,** 1712-1720.

157. Park, H. J., Kim, J. Y., Kim, J., Lee, J. H., Hahn, J. S., Gu, M. B. & Yoon, J. 2009. Silver-ion-mediated reactive oxygen species generation affecting bactericidal activity. *Water Res.,* 43(4)**,** 1027-32.

158. Pawlett, M., Ritz, K., Dorey, R. A., Rocks, S., Ramsden, J. & Harris, J. A. 2013. The impact of zero-valent iron nanoparticles upon soil microbial communities is context dependent. *Environ. Sci. Pollution,* 20**,** 1041–1049.

159. Peng, Z. G., Hidajat, K. & Uddin, M. S. 2004. Adsorption of bovine serum albumin on nanosized magnetic particles. *J.Colloid. Interphase Sci.,* 15**,** 277-83.

160. Peralta-Videa, J. R., Zhao, L., Lopez-Moreno, M. L., de la Rosa, G., Hong, J. & Gardea-Torresdey, J. L. 2011. Nanomaterials and the environment: A review for the biennium 2008-2010. *J Hazard Mater.,* 186**,** 1-15.

161. Petersen, C. & Moller, L. B. 2000. Control of copper homeostasis in *Escherichia coli* by a P-type ATPase, CopA, and a MerR-like transcriptional activator, CopR. *Gene,* 261**,** 289-298.

162. Petri, S., Körner, S. & Kiaei, M. 2012. Nrf2/ARE Signaling pathway: key mediator in oxidative stress and potential therapeutic target in ALS. *Neurology Research International*.

163. Peulen T & Wilkinson, K. J. 2011. Diffusion of nanoparticles in a biofilm. *Environ. Sci. Technol.,* 45**,** 3367-3373.

164. Peulen, T. O. & Wilkinson, K. J. 2011. Diffusion of nanoparticles in a biofilm. *Environ Sci Technol.,* 45**,** 3367-3373.

165. Poynton, H. C., Lazorchak, J. M., Impellitteri, C. A., Smith, M. E., Rogers, K., Patra, M., Hammer, K. A., Allen, H. J. & Vulpe, C. D. 2010. Differential gene expression in *Daphnia magna* suggests distinct modes of action and

bioavailability for ZnO nanoparticles and Zn ions. *Environ Sci Technol.,* 45**,** 762-768.

166. Prigent, C., Vidal, O., Dorel, C. & Lejeune, P. 1999. Abiotic surface sensing and biofilm-dependent regulation of gene expression in *Escherichia coli*. *J Bacteriol.,* 181(19)**,** 5993-6002.

167. Radzig, M. A., Nadtochenko, V. A., Koksharova, O. A., Kiwi, J., Lipasova, V. A. & Khmel, I. A. 2012. Antibacterial effects of silver nanoparticles on Gram-negative bacteria: Influence on the growth and biofilms formation, mechanisms of action. *Colloids Surface B.* doi: 10.1016/j.colsurfb.2012.07.039.

168. Reed, J. W., Glazebrook, J. & Walker, G. C. 1991. The exoR gene of Rhizobium meliloti affect RNA levels of other exo genes but lacks homology to known transcriptional regulators. *J Bacteriol,* 173**,** 3789–3794.

169. Registry http://partsregistry.org/Catalog.[accessed 20September, 2012]

170. Rehn, B., Seiler, F., Rehn, S., Bruch, J. & Maier, M. 2003. Investigations on the inflammatory and genotoxic lung effects of two types of titanium dioxide: untreated and surface treated. *Toxicol. Appl. Pharmacol.,* 189**,** 84–95.

171. Reihnold, B. R., Chan, S. Y., Reuber, L., Marra, A., Walker, G. C. & Reinhold, V. N. 1994. Detailed structural characterization of succinoglycan, the major exopolysaccharide of *Rhizobium meliloti* Rml021. *J Bacteriol.,* 176**,** 1997-2002.

172. Reinsch, B. C., Levard, C., Li, Z., Ma, R., Wise, A., Gregory, K. B., G. E. Brown, J. & Lowry, G. V. 2012. Sulfidation of silver sanoparticles secreases *Escherichia coli* growth inhibition. *Environ. Sci. Technol.,* 46**,** 6992-7000.

173. Reuber, T. & Walker, G. C. 1993. Biosynthesis of succinoglycan, a symbiotically important exopolysaccharide of *Rhizobium meliloti*. *Cell,* 74(2)**,** 269-280.

174. Rincon, A. & Pulgarin, C. 2005. Use of coaxial photocatalytic reactor (CAPHORE) in the TiO2 photo-assisted treatment of mixed *Escherichia coli* and *Bacillus subtilis* and the bacterial community present in wastewater. *Catal. Today.,* 101**,** 331-344.

175. Rousk, J., Ackermann, K., Curling, S. F. & Jones, D. L. 2012. Comparative toxicity of nanoparticulate CuO and ZnO to soil bacterial communities. *PLoS ONE,* 7(3)**,** e34197.

176. Tedesco, S., Doyle, H., Redmond, G., Sheehan, D. 2008. Gold nanoparticles and oxidative stress in *Mytilus edulis*. *Mar Environ Res.* ,66**,** 131-3.

177. Sahle-Demessie, E. & Tadesse, H. 2011. Kinetics and equilibrium adsorption of nano-TiO2 particles on synthetic biofilm. *Surface Science,* 605**,** 1177-1184.

178. Saul, R. L. & Ames., B. N. 1986. Background levels of DNA damage in the population, p. in M. Simic and L. Grossman (ed.), Mechanisms of DNA damage and repair. Plenum Publishing Corp., New York.**,** 529-535.

179. Sayes, C. M., Fortner, J. D., Guo, W., Lyon, D., Boyd, A. M., Ausman, K. D., Tao, Y. J., Sitharaman, B., Wilson, L. J., Hughes, J. B., West, J. L. & Colvin, V. L. 2004. The differential cytotoxicity of water-soluble Fullerenes. *Nano Lett.***,** 1881-1887

180. Scown, T. M., Santos, M. E., Eduarda, M., Johnston, B. D., Gaiser, B., Baalousha, M., Mitov, S., Lead, J. R., Stone, V., Fernandes, T. F., Jepson, M., Aerle, R. & Tyler, C. R. 2010. Effects of aqueous exposure to silver nanoparticles of different sizes in rainbow trout. *Toxicol. Sci.,* 115(2)**,** 521-534.

181. Sekar, D., Falcioni, M. L., Barucca, G. & Falcioni, G. 2011. DNA damage and repair following in vitro exposure to two different forms of Titanium dioxide nanoparticles on trout erythrocyte. *Env. Toxicol.,* 10.1002/tox.20778.

182. Serpone, N., Dondi, D. & Albini, A. 2007. Inorganic and organic UV filters: Their role and efficacy in sunscreens and suncare products. *Inorganica Chimica Acta,* 360**,** 794-802.

183. Sheng, Z. & Liu, Y. 2011. Effects of silver nanoparticles on wastewater biofilms. *Water Res.***,** 879-2448 (Electronic) doi: 10.1016/j.watres.2011.08.065.

184. Simon-Deckers, A. l., Loo, S., Mayne-L'hermite, M., Herlin-Boime, N., Menguy, N., Reynaud, C. c., Gouget, B. & Carrière, M. 2009. Size-, composition and shape-dependent toxicological impact of metal oxide nanoparticles and carbon nanotubes toward bacteria. *Environ Sci Technol.,* 43**,** 8423-8429.

185. Skorupska, A., Janczarek, M., Marczak, M., Mazur, A. & Król, J. 2006. Rhizobial exopolysaccharides: genetic control and symbiotic functions. *Microbial Cell Factories*.

186. Sledjeski, D. & Gottesman, S. 1996. Osmotic shock induction of capsule synthesis in *Escherichia coli* K-12. *J Bacteriol.,* 178(4)**,** 1204-6.

187. Solano, C., García, B., Valle, J., Berasain, C., Ghigo, J., Gamazo, C. & Lasa, I. 2002. Genetic analysis of *Salmonella enteritidis* biofilm formation: critical role of cellulose.*Mol Microbiol.,* 43(3)**,** 793-808.

188. Sondi, I. & Sondi, B. S. 2004. Silver nanoparticles as antimicrobial agent: a case study on *E. coli* as a model for Gram-negative bacteria. *J.Colloid. Interphase Sci.,* 275**,** 177-182.

189. Spencer B, F. & Tokio, K. 1991. Oxidative Stress Responses in *Escherichia coli* and *Salmonella typhimurium*. *ASM***,** 561-585.

190. Stevenson, G., Adrianopoullouys, K., Hobbs, M. & Revves, P. R. 1996. Organization of the *Escherichia coli* K-12 gene cluster responsible for production of the extracellular polysaccharide colanic acid. *J.Bacteriol.,* 178**,** 4885-4893.

191. Stewart, P. S. & Franklin, M. J. 2008. Physiological heterogeneity in biofilms. *Nat Rev Microbiol., 6,*199-210

192. Storz, G., Tartaglia, L. A. & Ames, B. N. 1990. The OxyR regulon. *Antonie Van Leeuwenhoek,* 58(3)**,** 157-161.

193. Stout, V. 1996. Identification of the promoter region for the colanic acid polysaccharide biosynthetic genes in *Escherichia coli K*-12. *J Bacteriol,* 178**,** 4273-80.

194. Stout, V., Torres-Cabassa, A., Maurizi, M. R., Gutnick, D. & Gottesman, S. 1991. RcsA, an unstable positive regulator of capsular polysaccharide synthesis. *J Bacteriol.,* 173**,** 1738-1747.

195. Strandberg, G., Shumate, S. & Parrott, J. 1981. Microbial cells as biosorbents for heavy metals: accumulation of uranium by *Saccharomyces cerevisiae* and *Pseudomonas aeruginosa. Appl Environ Microbiol. ,* 41(1)**,** 237-45.

196. Sutherland, I. 1969. Structural studies on colanic acid, the common exopolysaccharide found in the Enterobacteriaceae, by partial acid hydrolysis. *J.Biol.Chem.,* 115**,** 935-945.

197. Tadahiko, M., Nishikawa, D., Takahashi, K., Usui, N., Yamori, T., Seki, M., Endo, T. & Mochizuki, M. 2003. Antibacterial and antiproliferative activity of cationic fullerene derivatives. . 2003, 13 (24), . *Bioorg. Med. Chem. Lett,* 13**,** 4395–4397.

198. Tietze, R., Lyer, S., Dürr, S. & Alexiou, C. 2012. Nanoparticles for cancer therapy using magnetic forces. *nanomed(Lond),* 7**,** 447-57.

199. Tokuyama, H., Yamago, S. & Nakamura, E. 1993. Photoinduced biochemical activity of fullerene carboxylic acid. *J. Am. Chem. Soc.,* 115**,** 7918–7919.

200. Tong, Z., Bischoff.M, Nies, L., Applegate, B. & Turco, R. F. 2007. Impact of fullerene (C60) on a soil microbial community. *Environ Sci.Technol.,* 41**,** 2985-2991.

201. Tourinho, P. S., Gestel, C. A. M. v., Lofts, S., Svendsen, C., Soares, A. M. V. M. & Loureiro, S. 2012. Metal-based nanoparticles in soil: Fate, behavior, and effects on soil invertebrates. *Environ Toxicol Chem.,* 31**,** 1679-1692.

202. Tourney, J., Ngwenya, B. T., Mosselmans, J. W. F., Tetley, L. & Cowie, G. L. 2008. The effect of extracellular polymers (EPS) on the proton adsorption characteristics of the thermophile *Bacillus licheniformis* S-86. *Chemical Geology,* 247**,** 1-15.

203. Tratnyek, P. G. & Johnson, R. L. 2006. Nanotechnologies for environemntal cleanup. *Nanotoday*.

204. Tsao, N., Luh, T.Y., Chou, C.K., Wu, J.J., Lin, Y.S. & Lei, H.-Y. 1999. Inhibition of *Escherichia coli* induced meningitis by carboxyfullerene. *Antimicrob. Agents Chemother.,* 43**,** 2273-2277.

205. Tsao, N., Luh, T.Y., Chou, C.K., Wu, J.J., Lin, Y.S. & Lei, H.Y. 2001. Inhibition of group A Streptococcus infection by carboxyfullerene. *Antimicrob. Agents Chemother.,* 45**,** 1788–1793.

206. Unrine, J. M., Colman, B., Bone, A. J., Gondikas, A. P. & Matson, C. W. 2012. Biotic and abiotic interactions in aquatic microcosms determine fate and toxicity of Ag nanoparticles. Part 1. aggregation and dissolution. *Environ. Sci.Technol.,* 46**,** 6915–6924.

207. Urban, A. S., Pfeiffer, T., Fedoruk, M., Lutich, A. A. & Feldmann, J. 2011. Single-step injection of gold nanoparticles through phospholipid membranes. *ACS Nano,* 24**,** 3585-90.

208. Valodkar, M., Bhadoria, A., Pohnerkar, J., Mohan, M. & Thakore, S. 2010. Morphology and antibacterial activity of carbohydrate-stabilized silver nanoparticles. *Carbohydrate Res.,* 345**,** 1766-1773.

209. Van der Meer, J., Tropel, D. & Jaspers, M. 2004. Illuminating the detection chain of bacterial bioreporters. *Environ Microbiol,* 6**,** 1005-1020.

210. Vandebriel, R. J. & Jong, W. H. D. 2012. A review of mammalian toxicity of ZnO nanoparticles. Aip Conf Proc**.,** http://dx.doi.org/10.2147/NSA.S23932.

211. Waissi-Leinonen, G. C., Petersen, E. J., Pakarinen, K., Akkanen, J., Leppänen, M. T. & Kukkonen, J. V. K. 2012. Toxicity of fullerene (C60) to sediment-dwelling invertebrate Chironomus riparius larvae. *Env. Toxicol and chem.,* 10.1002/etc.1926.

212. Wang, B., Feng, W. Y., Wang, M., Wang, T. C., Gu, Y. Q., Zhu, M. T., Ouyang, H., Shi, J. W., Zhang, F., Zhao, Y. L., Chai, Z. F., Wang, H. F. & Wang, J. 2008. Acute toxicological impact of nanoand submicro-scaled zinc oxide powder on healthy adult mice. *J. Nanopart. Res.,* 10**,** 263–276.

213. Wang, X., Dubey, A., Suzuki, K., Baker, C., Babitzke, P. & Romeo, T. 2005. CsrA post-transcriptionally represses pgaABCD, responsible for synthesis of a biofilm polysaccharide adhesin of *Escherichia coli*. *Mol Microbiol.,* 56(6)**,** 1648-63.

214. Wani, M. Y., Hashim, M. A., Nabi, F. & Malik, M. A. 2011. Nanotoxicity: dimensional and morphological concerns. *Adv Physic Chemis.,* 2011.

215. Watnick, P. & Kolter, R. 2000. Biofilm, city of microbes. *182(10)***,** 2675-9.

216. Wehland, M. & Bernhard, F. 1999. The RcsAB box. Characterization of a new operator essential for the regulation of exopolysaccharide biosynthesis in enteric bacteria. *J.Biol.Chem.,* 275**,** 7013-7020.

217. Weir, A., Westerhoff, P., Fabricius, L., Hristovski, K. & Goetz, N. V. 2012. Titanium dioxide nanoparticles in food and personal care products. *Environ. Sci.Technol.,* 45**,** 224202250.

218. Whitfield, C. 2006. Biosynthesis and assembly of capsular polysaccharides in *Escherichia coli. Annu Rev Biochem.,* 75**,** 39-68.

219. Wiesner, M., Lowry, G., Alvarez, P., Dionysiou, D. & Biswas, P. 2006. Assessing the risks of manufactured nanomaterials. *Environ Sci Technol.* , 40(14)**,** 4336-45.

220. Wiesner, M. R., Lowry, V. G., Casman, E., Bertsch, P. M., Matson, C. W., Giulio, T. D., Liu, J. & Hochella, M. F. 2011. Meditations on the ubiquity and mutability of nano-sized materials in the environment. *ACS Nano,* 7**,** 2466-70.

221. Xia, T., Kovochich, M., Brant, J., Hotze, M., Sempf, J., Oberley, T., Sioutas, C., Yeh, J. I., Wiesner, M. R. & Nel, A. E. 2006. Comparison of the abilities of ambient and manufactured nanoparticles to induce cellular toxicity according to an oxidative Stress paradigm. *Nano Letters,* 6**,** 1794-1807.

222. Xia, T., Kovochich, M., Liong, M., Mädler, L., Gilbert, B., Shi, H., Yeh, J. I., Zink, J. I. & Nel, A. E. 2008. Comparison of the mechanism of toxicity of zinc Oxide and cerium oxide nanoparticles based on dissolution and oxidative stress properties. *ACS Nano,* 2**,** 2121-2134.

223. Xiu , Z. M., Zhang, Q. B., Puppala, H. L., Colvin, V. L. & Alvarez, P. J. 2012. Negligible particle-specific antibacterial activity of silver nanoparticles. *Nano Lett.,* 12(8)**,** 4271-5.

224. YaNan, C., Mingyi, Z., Lin, X., Jun, Z. & Gengmei, X. 2012. The toxic effects and mechanisms of CuO and ZnO nanoparticles. *Materials,* 5**,** 2850-2871.

225. Yezhelyev, M. V., Gao, X., Xing, Y., Al-Hajj, A., Nie, S. & O'Regan, R. M. 2006. Emerging use of nanoparticles in diagnosis and treatment of breast cancer. *Lancet Oncol* 7**,** 657-67.

226. Yoko, K., Yuka, K., Atsuko, M., Naoki, M. & Yoko, Y. 2003. Fullerene as a novel photoinduced antibiotic. *Fullerenes, Nanotubes, Carbon Nanostruct,* 11**,** 79-87.

227. Yoon, S. J., Park, J. E., Yang, J.-H. & Park, J.W. 2002. OxyR regulon controls lipid peroxidation-mediated oxidative stress in *Escherichia coli*. *J Bio Mol Biol.,* 35**,** 297-301.

228. Yuan, G., Joshua P, S. & Holden, P. A. 2011. Evidence for negative effects of TiO2 and ZnO nanoparticles on soil bacterial communities. *Environ. Sci. Technol.,* 45**,** 1659–1664.

229. Xiao.Z., Levy-Nissenbaum, E., Alexis, F., Lupták, A., Teply, B. A., Chan, J. M., Shi, J., Digga, E., Cheng, J., Langer, R. & Farokhzad, O. C. 2012. Engineering of targeted nanoparticles for cancer therapy using internalizing aptamers isolated by cell-uptake selection. *ACS Nano,* 6**,** 696-704.

230. Zevenhuizen, L. 1997. Succinoglycan and galactoglucan. *Carbohydrate Polymer,* 33**,** 139-147.

231. Zhang, Y., Chen, D., Smith, M. A., Zhang, B. & Pan, X. 2012. Selection of reliable reference genes in *Caenorhabditis elegans* for analysis of nanotoxicity. *PLoS ONE 7(3): e31849. doi:10.1371/journal.pone.0031849*.

232. Zhao, B., He, Y. Y., Chignell, C. F., Yin, J. J., Andley, U. & Roberts, J. E. 2009. Difference in phototoxicity of cyclodextrin complexed fullerene [(gamma-CyD)2/C60] and its aggregated derivatives toward human lens epithelial cells. *Chem Res Toxicol,* 22**,** 660-7.

233. Zylicz, M., LeBowitz, J. H., McMacken, R. & Georgopoulos,C.1983 The dnaK protein of *Escherichia coli* possesses an ATPase and autophosphorylating activity and is essential in an in vitro DNA replication system. *Proc Natl Acad Sci U S A. ,* 80(21)**,** 6431–6435.

Chapter 2

Silver nanoparticle toxicity to bacteria occurs *via* multiple mechanisms

Abstract

Predicting the impact of silver nanoparticles in the natural environment is currently a subject of great interest but is constrained by inadequate understanding of the factors that control bioavailability of silver from the nanoparticles. In this work the mechanism of silver nanotoxicity has been investigated by using mutant strains of *Escherichia coli* lacking specific protective mechanisms. In order to assess the impact of ions like chlorides that are present in natural waters, the effect of medium composition on the silver nanotoxicity has also been investigated. Deletion mutant strains lacking silver ion efflux systems show increased sensitivity to silver nanoparticle toxicity. Furthermore, the speciation of silver from nanoparticles was studied by developing a bioreporter strain responsive to silver ions. The biosensor did not respond to silver nanoparticles even at levels, which lead to a significant reduction in cell viability. Deletion mutant strains lacking major resistance mechanisms against oxidative stress also show increased sensitivity to silver nanoparticles, while enzyme supplementation helps to restore cell viability; this is consistent with oxidative stress being an important mechanism for nanoparticle toxicity. These observations suggest multiple mechanisms for silver nanoparticle toxicity, with the formation of soluble ions being arguably the most important.

2.1 Introduction

Engineered metal based nanoparticles (NPs) such as silver, zinc oxide and titanium dioxide are toxic to bacteria and other microorganisms as a result of their enhanced reactivity arising from their small size (Nel et al., 2006, Huang et al., 2008). In addition to the chemical properties of nanoparticles, variables including the presence of capping agents, shape of nanoparticles, oxidation state and pH have been shown to affect nanoparticle toxicity (Auffan et al., 2008, French et al., 2009, Lankoff et al., 2012). Recent studies indicate that oxidative stress and metal ion dissolution play an important role in nanoparticle toxicity (Carlson et al., 2008, Gajjar et al., 2009, Jin et al., 2010, Horie et al., 2011, Xiu et al., 2011), which may also involve membrane damage and protein oxidation (Sondi and Sondi, 2004, Lyon and Alvarez, 2005, Choi and Hu, 2008, Dimkpa et al., 2011, Napierska et al., 2012). While all these findings contribute significantly to the existing knowledge about the toxic potential of nanoparticles, the overall picture remains ambiguous. Firstly, there is a strong possibility that two or more of the toxicity mechanisms mentioned above operate collectively to produce a net impact. Secondly, the extent and nature of the damage also varies with the type of nanomaterial and exposure conditions. Thirdly, extrapolating observed impacts from laboratory experiments to the natural environment needs to consider the chemical complexities of the environment. For instance, the presence of ions such as chlorides and phosphates and variation in pH can influence the net impact of nanoparticles by altering the solubility of ions. Thus, the outcome of controlled laboratory experiments as a basis to understanding the effect of nanoparticles in the environment requires further research under environmentally relevant conditions that may modify nanoparticle bioavailability.

Toxicity studies so far have largely employed cell viability assays, with oxidative stress being detected using fluorescent probes that at times provide unreliable data (Patsoukis et al., 2005). However, microarray studies conducted on *Escherichia coli* using silver and polystyrene nanoparticles indicate that multiple genetic pathways are up-regulated on exposure to nanoparticles (Gou et al., 2010, Ivask et al., 2012). Systematic investigation of the interaction of bacteria with engineered nanoparticles requires an overview of the stress responsive and metal ion responsive genes in the bacteria under study. This could provide better insight into the toxicity mechanisms.

Escherichia coli is a model bacterium with well-understood stress resistance mechanisms. All of the non-essential genes in *E. coli* have been individually mutated, and mutant strains are available from the KEIO collection (Baba et al., 2006). Furthermore, bioreporter strains can be developed in which known stress-responsive promoters are linked to reporter genes. This can help to detect induction of different stress responses by a particular analyte; in this case, silver nanoparticles. This offers a powerful system for investigating the cellular effects of nanoparticle exposure. *E. coli* strains mutated in different stress-involved proteins together with a silver ion responsive biosensor have been used to investigate the toxic effects of silver nanoparticles on *E. coli*.

Since urban freshwater bodies are the first receptors of nanoparticle discharges and always contain some chloride from road run-off (Kaushal et al., 2005, Novotny et al., 2008), it is important to consider the impact of silver speciation on nanoparticle toxicity in such media (Chinnapongse et al., 2011). Nanoparticle exposure studies were conducted in a medium which contains chloride at concentrations in the range found in urban freshwater and upper estuarine bodies. Based on recent predictions

that ionic silver will precipitate as silver chloride in freshwaters (Levard et al., 2012); it was hypothesised that mechanisms besides ionic silver could also contribute to nanoparticle toxicity. The hypothesis was tested using mutant strains lacking ion efflux genes, as well as a silver ion responsive biosensor, an approach that is critical in order to develop a realistic model of the true impact of nanoparticles in aquatic environments.

2.2. Materials and Methods

2.2.1 Strains and plasmids

Bacterial strains used in these experiments are listed in Table 2-1. Deletion strains were obtained from the KEIO collection *via* the Yale Genetic Stock Centre (Baba et al., 2006). The triple deletion strain LE106, lacking *katG*, *katE* and *ahpF*, was kindly provided by Prof. James Imlay, University of Iowa (Seaver and Imlay, 2004). Copper is taken up as divalent ions (Cu^{+2}) but reduced to Cu^{+1} by copper reductase and then removed by shuttle pump. *copA* produces a P type ATP'ase pump that drives out excess copper ions (monovalent) from the cytoplasm (Rensing, 2000). The biosensor responsive to silver ions was developed by cloning the promoter of *copA* in BioBrick RFC10 format (Knight, 2003, Norville et al., 2010) in vector pSB1C3 (Registry of Standard Biological Parts). The following primer sequences were designed to amplify the promoter of *copA* and sourced from Sigma Aldrich:

5'-CCTT**GAATTC**GCGGCCGCT**TCTAGA**GTGAAATTGGGTGTAAGC-3'

5'-AAGGCTGCA**GCGGCCGC**T**ACTAGT**ACTGTGATAAAGGTTAAACC-3'

A reporter gene, Enhanced Yellow Fluorescent Protein (EYFP, BioBrick BBa_E0040), was then inserted downstream of the promoter to generate the final reporter construct. The biosensor was designated pSB1C3-P*copA_Yfp*.

2.2.2 Chemicals

Chemicals for the growth medium (Minimal medium), catalase, and silver nanoparticles were obtained from Sigma-Aldrich. LIVE-DEAD cell viability kit was procured from Invitrogen. PBS (phosphate buffered saline) was made by adding 8 g/L NaCl, 0.2 g/L KCl and 1.44 g/L Na_2HPO_4 in a litre of deionized water. The pH was adjusted to 7.4 and the solution sterilized by autoclaving. Catalase (Cat.number C1345) (5 mg/ml) was suspended in PBS and added to the cultures to achieve a final concentration of 100 units per ml culture. Oxidative stress sensitive dye, *p*-aminophenyl fluorescein (APF) was obtained from Sigma-Aldrich and was added to cells pre-treated with silver nanoparticles as per the manufacturer's instructions.

Bacterial strain	**Genotype**	**Details**
MG1655		Wild type *E .coli*, parent strain of LE106.
LE106		Triple deletion mutant strain *ΔkatG*/Δ *katE*/Δ*ahpF*
BW25113		Parent strain of KEIO strains.
JW0473-3	*ΔcopA767::kan*	Deletion of copper efflux pump
JW0476-1	*ΔcueR770::kan*	Deletion of regulator of *copA*
JW0564-1	*ΔcusA784::kan*	Deletion of cation transporter
JW0563-2	*ΔcusB783::kan*	Deletion of copper/silver efflux membrane fusion protein
JW0562-1	*ΔcusF782::kan*	Deletion of copper/silver efflux system protein
JW0560-1	*ΔcusR780::kan*	Deletion of DNA binding transcriptional activator of *cusABF*
JW3914-1	*ΔkatG729::kan*	Deletion of catalase
JW1721-1	*ΔkatE731::kan*	Deletion of catalase
JW3879-1	*ΔsodA768::kan*	Deletion of superoxide dismutase A
JW1648-1	*ΔsodB734::kan*	Deletion of superoxide dismutase B
JW0005-1	*ΔyaaA 726::kan*	Deletion of peroxidase
JW0422-1	*ΔcyoA789::kan*	Deletion of cytochrome bo terminal oxidase subunit
JW0421-1	*ΔcyoB788::kan*	Deletion of component of cytochrome bo terminal oxidase
JW0723-2	*ΔcydB782::kan*	Deletion of cytochrome *bd*-I terminal oxidase subunit
JW0912-1	*ompF746(del)::kan*	Deletion of outer membrane protein, OmpF
JW2203-1	*ompC768(del)::kan*	Deletion of outer membrane protein, OmpC

Table 2-1:Bacterial strains used for the study have been shown. Δ represents deletion of the following genes: copper and silver ions efflux (*copA, cueR, cusB, cusA cusF* and *cusR*). For oxidative stress mitigation (*sodA, sodB, sodC, katG, katE, yaaA*). Porin formation (*ompC and ompF*). The genes that express to form subunits of cytochrome oxidase (*cyoA, cyoB and cydB*) have been selected for this study.

2.2.3 Growth conditions and assays

The impact of silver nanoparticles was investigated by developing a medium that contained chloride ions in the range found in urban freshwater bodies (0-1000 mg/L). M9 medium, made by diluting a 4x stock solution containing 64 g/L $Na_2HPO_4.7H_2O$, 15g/L KH_2PO4, 1.24 g/L NH_4SO4 and 2.5 g/L NaCl, conveniently satisfies this requirement. The diluted medium was further supplemented with 0.1 mM calcium chloride, 10 mM magnesium sulphate, 2 g/L Casamino acids, 1 mM thiamine hydrochloride and 0.4% w/v glycerol as a carbon source. Control tests for silver chloride precipitation were conducted by using M9 medium modified by replacing sodium chloride with sodium nitrate and ammonium chloride with ammonium sulphate at equivalent molar concentrations.

Plasmids based on pSB1C3 were maintained by addition of chloramphenicol (40 μg/ml). Cultures were grown at 37˚C with shaking at 150 rpm. Cell viability was assessed by serial dilution, and cultures were plated on L-agar. Luminescence based ATP assays were performed using the luminescence module of a multimode reader (BS040271 Turner Biosystems). Fluorescence of APF assays and specific bioreporter strains was measured using the same instrument with the green fluorescence module. ATP assay was performed using the Bactiter Glo Kit from Promega.

2.2.4 Nanoparticle source and characterization

A 10 nm sodium citrate stabilized silver nanoparticle dispersion at 20 mg/L concentration was obtained from Sigma-Aldrich (Catalogue no. 730785). Size characterization was carried out by Dynamic Light Scattering (DLS) using a Zeta Pals 90 sub-micron analyser (Brookhaven Instruments Corporation Holtsville, NY,

USA).The samples were sonicated (230V, 50 Hz) for 5 minutes prior to use. The data were collected in triplicate at a temperature of 25^{o}C (Fabrega, 2009).

The extent of metal dissolution from the nanoparticle surface was determined after suspending known amounts (7 mg/L) of nanoparticles in (a) deionized water, (b) M9 medium and (c) modified M9 medium made by replacing all chlorides with sulphates at the same concentration as described above. These samples were incubated with rotary shaking (200 rpm) at 37ºC for 2 hours, the same time as the exposure tests. The supernatant was recovered by centrifugation at 3000 g using a centrifugal filter (3000 MWCO, Millipore) for 60 minutes at 10^{o}C. It was acidified by addition of 2% (v/v) nitric acid and analysed using ICP-OES (Optima 5300DV, Perkin Elmer) (Singh and Ramarao, 2012). Solutions of silver nitrate (4 mg/L ionic silver equivalent) were incubated in parallel to check recovery of dissolved silver. These concentrations were chosen as these were in range of concentrations of silver np and silver ions used for exposure assays.

2.2.5 Nanoparticle and other stress exposure experiments

For KEIO mutant strains, bacteria were grown overnight in minimal medium with kanamycin (50µg/ml) to prevent contamination. The optical density at 600 nm (OD_{600}) was adjusted to 0.2 by diluting with fresh medium. Nanoparticles were added to final concentrations of 5.5 and 7 mg/L of silver nanoparticles (a range that compromised cell viability of the deletion mutant strains). The cultures were incubated at 37ºC for 120 minutes on a rotary shaker (150 rpm) in the dark. For ionic toxicity studies, the procedure was the same except that silver (ionic) was added at final concentrations of 3.5 and 8.5 mg/L silver nitrate (equivalent to 2 and 5.4 mg/L

equivalent ionic silver respectively). Viability and luminescence assays were conducted as described above. For one set of experiments, modified M9 medium was made by replacing chlorides with sulphates as described above. This experiment was conducted to investigate possible changes in toxicity caused by alteration of the medium composition. The data analysis was initially conducted by student t-test. Further to this, ANOVA followed by Tukey's posthoc Honestly Significance Difference (HSD) test on treatment means was also done. These results have been shown in the appendix.

2.3. Results

2.3.1 Speciation of ionic silver in the exposure medium and impact on cell viability

Prior to exposure studies, nanoparticles were characterised for size distribution and dissolved silver, the latter being operationally defined as that fraction in filtrate from centrifugal filtration using 3000 MWCO Amicon filters (Raghupati et al., 2011). Particle size analysis shows that the nanoparticles maintained their nominal size when dispersed in de-ionised water (9+/-2nm) and in M9 medium (12+/-3nm). The dissolution of silver nanoparticles was investigated by incubating 7 mg/L nanoparticles for 2 hours (equivalent to exposure time) in deionized water, M9 medium and modified M9 medium in which chloride was replaced by sulphate and nitrate. After ultrafiltration, silver in the filtrate averaged 0.09 mg/L (8.5×10^{-7} mol/L) in deionised water, 0.014 mg/L (1.34×10^{-7} mol/L) in M9 and 0.056 mg/L (5.2×10^{-7} mol/L) in M9 without chloride. By comparison, incubation of 4 mg/L

$AgNO_3$ showed 0.12 mg/L (~1.1 x 10^{-6} mol/L) dissolved silver in M9 and 0.09 mg/L(8.5 x 10^{-7} mol/L) in M9 without chloride.

Preliminary tests were carried out on viability of three strains of *E. coli*, including control strain BW25113 and two deletion mutants lacking in ionic efflux genes for copper/silver (*ΔcueR* and *ΔcusF*) .The exposure assay produced statistically similar effect ($p>0.05$) for both deletion strains at 5.4 mg/L total silver exposure in chloride-free and standard M9 medium prepared by replacing chlorides with sulphates and nitrate (Figure 2-1a and 2-1b). As expected, reduction in cell viability correlates with an increase in initial silver concentration (Figure 1b). These results imply either, (i) that particulate forms of Ag (either as $AgCl_2$ or $AgCl_2^{3-}$) are also toxic, albeit slightly less so than ionic silver, or (ii) the presence of ionic silver in sufficient quantities to compromise cell viability. It has been shown earlier that nanoparticle-free silver concentrations in the range measured in this study can still compromise viability of bacterial biofilms by as much as 20%, whereas concentrations around 0.1 mg/L as measured for the silver nitrate suspensions can result in almost 80% biofilm death (Wirth et al., 2012). These concentration ranges are likely to be even more toxic to the planktonic cultures used in this study, although Xiu et al (2011) also reported about 20% reduction in viability for planktonic *E. coli* when exposed to both chloride-free Ag^+ ions in 0.1mg/L chloride at the Ag^+ concentrations (0.1mg/L) detected in the suspensions.

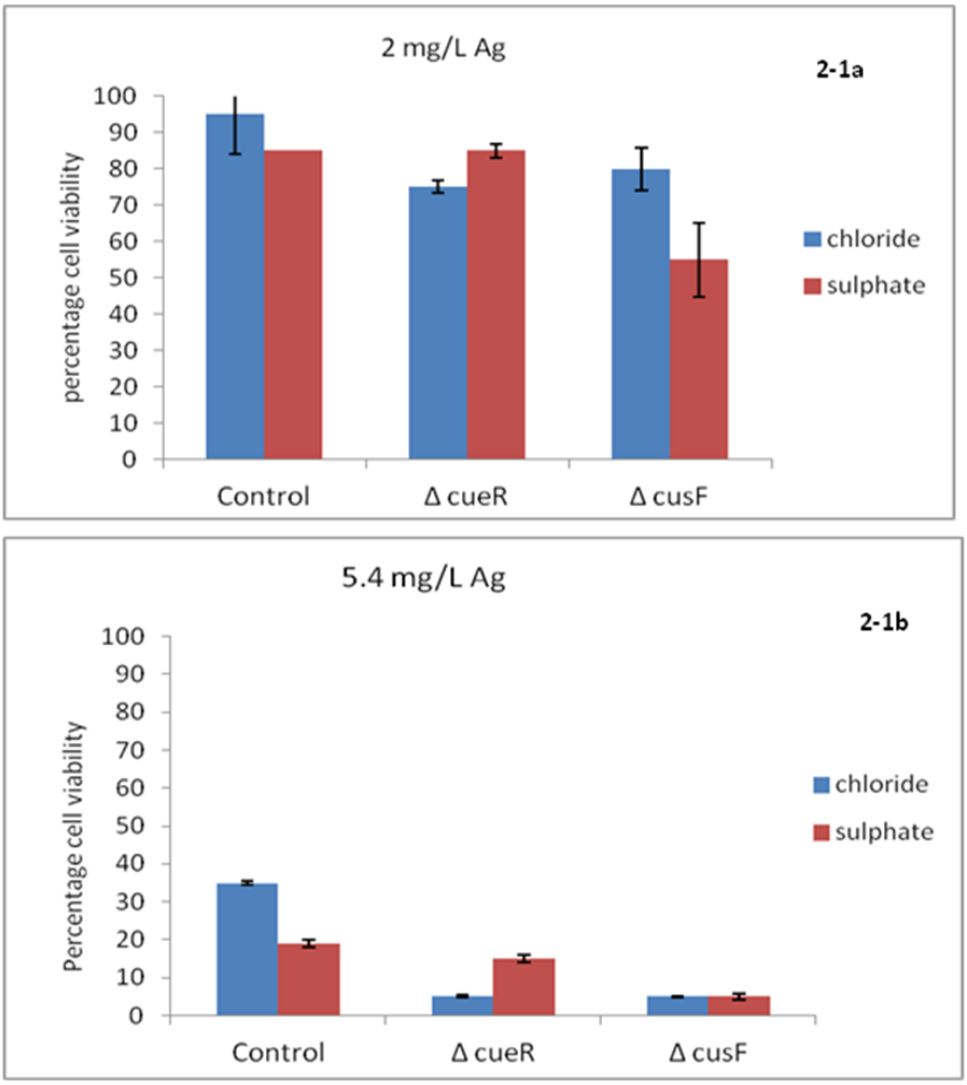

Figure 2-1a and 2-1b: effect of medium composition on the ionic speciation and cell viability. Y axis represents the percentage survival for each strain, normalized to control samples. Control strain is BW25113, Δ cueR is deletion strain for copper regulatory gene and Δ CusF is deletion strain lacking efflux pump for copper/silver ions.

2.3.2 Sensitivity of ion efflux deletion mutants points to silver ion-mediated damage

E. coli and related bacteria possess multiple mechanisms for detoxification of heavy metals such as copper and silver. These include substrate specific efflux pumps and binding proteins (Li et al., 1997, Petersen and Moller, 2000, Outten et al.2000, Loftin et al., 2005). KEIO mutant strains lacking a selection of these genes (Table 2-1) were tested for sensitivity to silver nanoparticles (Figure 2-2a, 2-2b) and ionic silver (Figure 2-3a and 2-3b). In the silver nanoparticle exposure studies, Δ*copA* and Δ*cusA* showed sensitivity to silver nanoparticles at 5.5 mg/L (t test $p<0.05$) whereas *ΔcusF* and *ΔcusB* demonstrated the greatest decrease in cell viability at 7 mg/L. The deletion mutant Δ*cusR* was least sensitive amongst these strains; at 5.5 mg/L concentration it did not show a statistically significant drop in cell viability ($p=0.09$). This suggests that efflux of silver ions is controlled by a network of genes and ionic silver plays an important role in toxicity associated with silver nanoparticles. As expected based on earlier results (Figure 2-1b), mutant strains also showed increased susceptibility to silver ions relative to control in both chloride and sulphate based M9 medium.

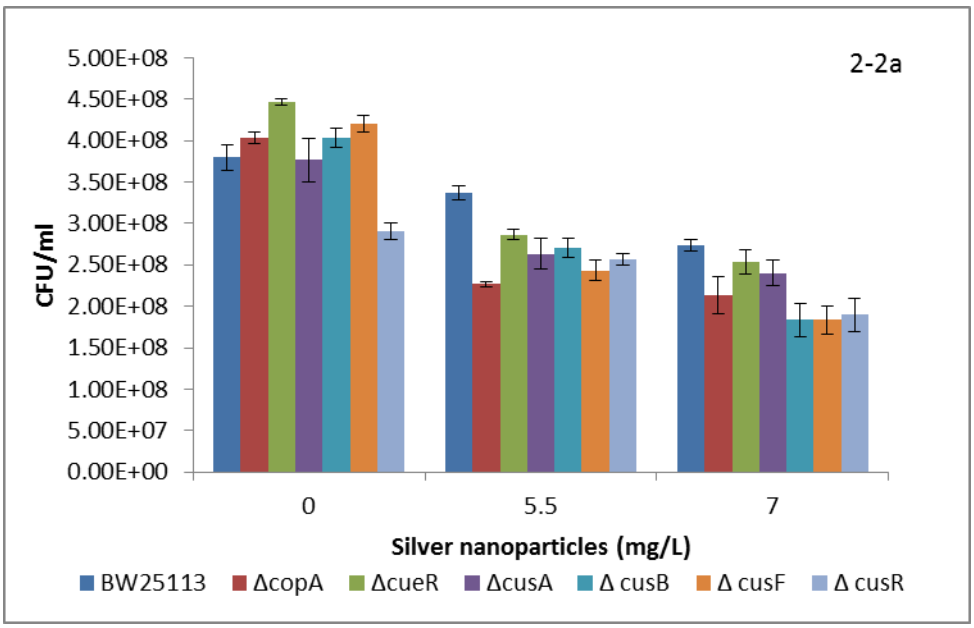

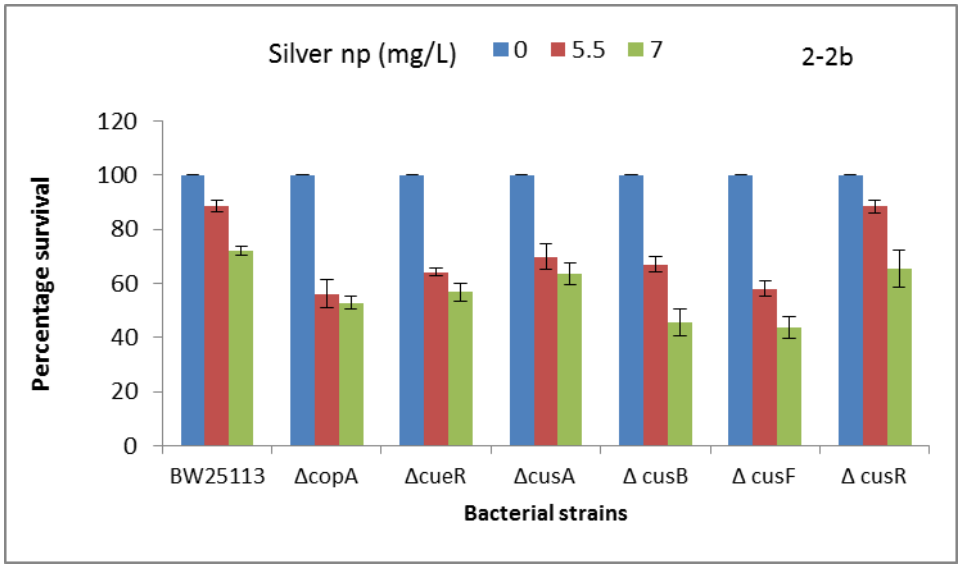

Figure 2-2a and 2-2b: Nanoparticle exposure assay using deletion mutants for copper/silver ion efflux mechanism. The mutants show a greater sensitivity to silver nanoparticles thus lower cell viability than control strain, BW25113

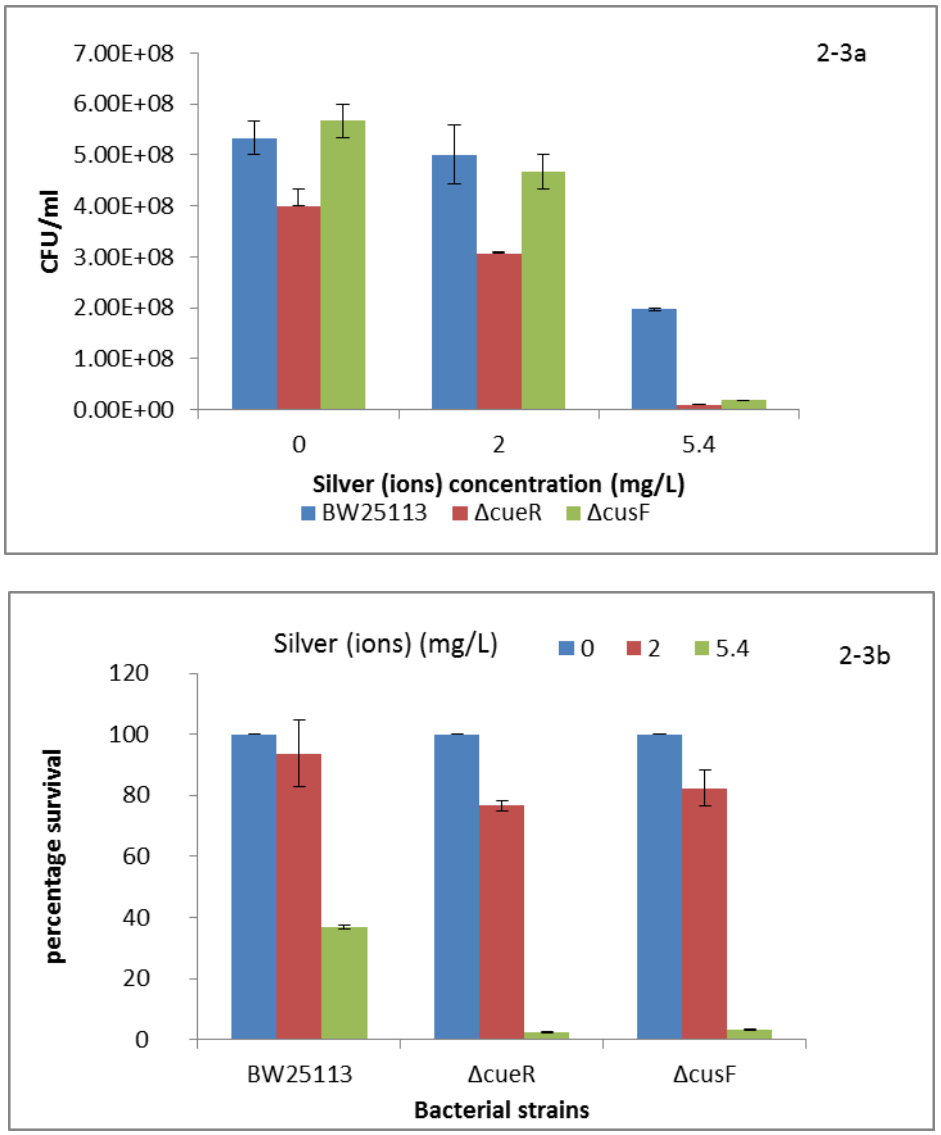

Figure 2-3a and 2-3b: Effect of silver nitrate on cell viability of deletion strains, ΔcueR and Δ cusF. The cell viability of these strains is compromised more than the control strain BW25113, with increasing concentration of silver nitrate.

Strains deficient in porins have also been reported to show greater resistance to toxic ions and to acid stress, presumably by excluding toxic ions and molecules from the periplasm (Forst et al., 1988, Li et al., 1997, Kaeriyama et al., 2006, Sharma et al., 2009, Desai and Miller, 2010, Bekhit et al., 2011, Radzig et al., 2012). In the

exposure assays, cells deficient in *ompC*, but not *ompF* showed enhanced resistance to silver nanoparticles, based upon CFU data (Figure 2-4a). *ΔompC* showed higher cell viability at 7 mg/L than the control strain ($p=0.04$). The control strain shows a statistically significant drop in cell viability ($p<0.05$) at each nanoparticle concentration, however, the *ΔompC* did not register a significant drop in cell viability ($p=0.3$) at 7 mg/L. The porin deficient strains also showed a higher resistance to silver ions in the range of 0.6-1.3 mg/L (Figure 2-4c, 2-5) whereas the control strain, BW25113, showed a consistent drop in cell viability with increase in silver nitrate concentration ($p<0.05$ for each condition). Both mutant strains did not register a statistically significant drop in cell numbers ($p=0.1$ for *ΔompC* and $p=0.4$ for *ΔompF* at 1.3 mg/L). However, at a higher concentration of silver nitrate these strains were found to be more sensitive to ionic silver than the parent strain (Figure 2-4b). LIVE/DEAD staining (Figure 2-5) also confirmed the enhanced resistance to ionic silver toxicity at low concentrations for these porin-deficient strains.

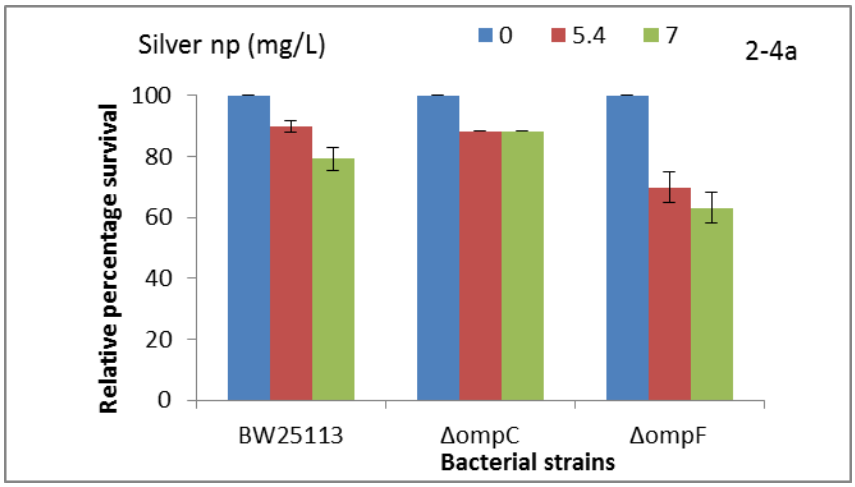

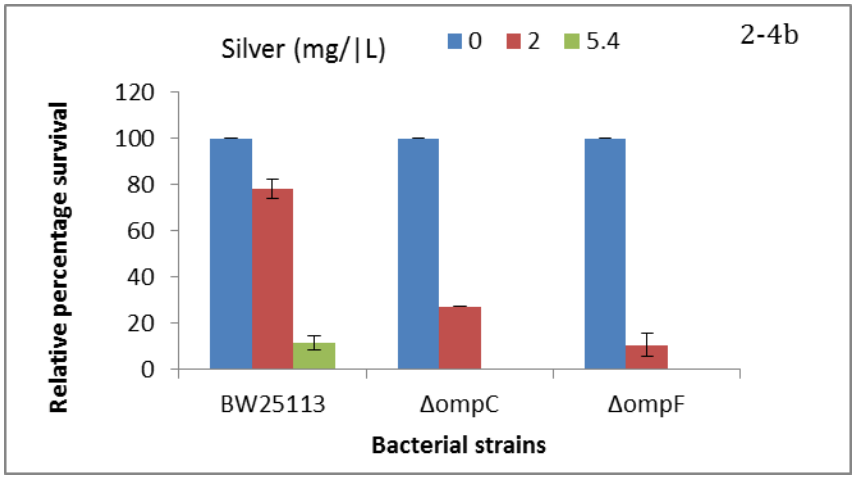

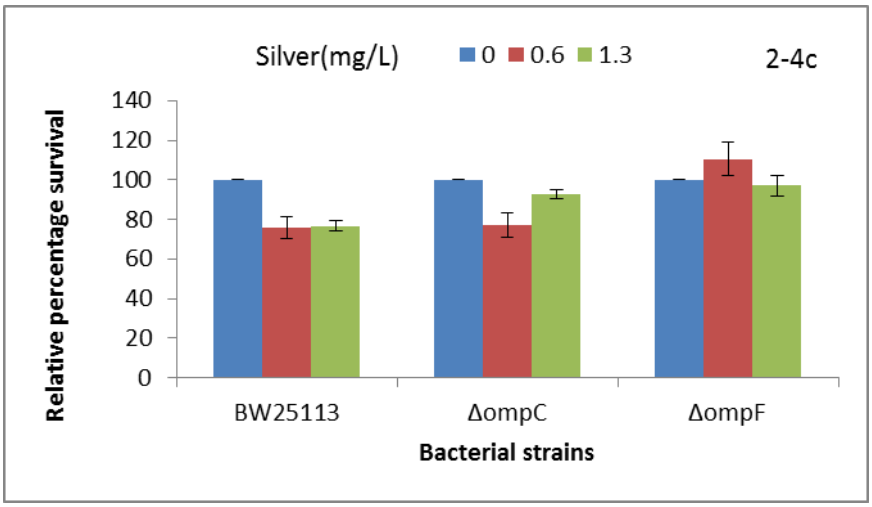

Figure 2-4: Effect of silver nanoparticles (2-4a) and silver ions (2-4b, 2-4c) on the deletion strains for porins. The error bars are small hence not visible in figure 2-4 a, b.

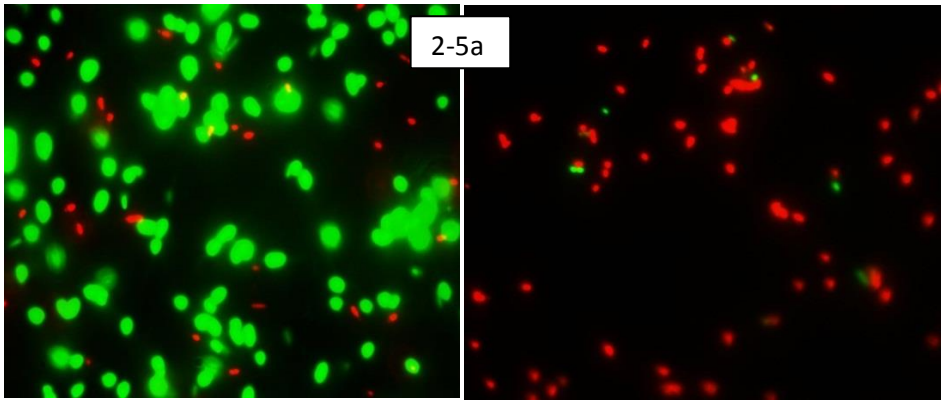

BW25113 at 0 and 1 mg/L silver ions

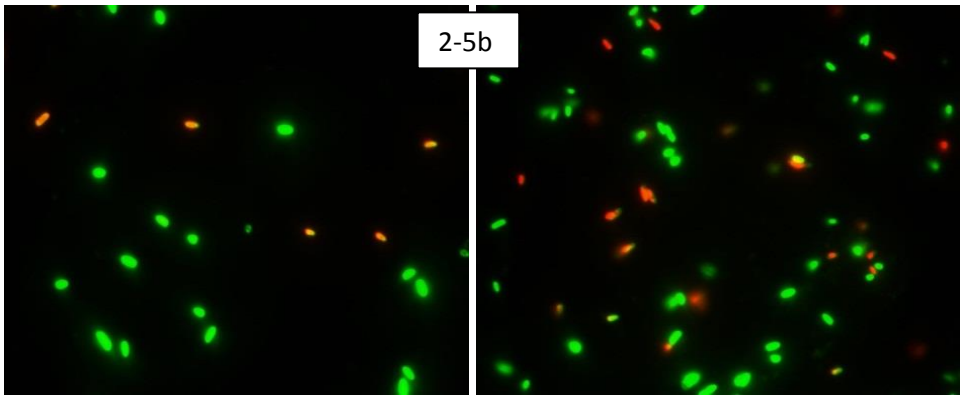

ΔompC: 0 and 1 mg/L silver ions

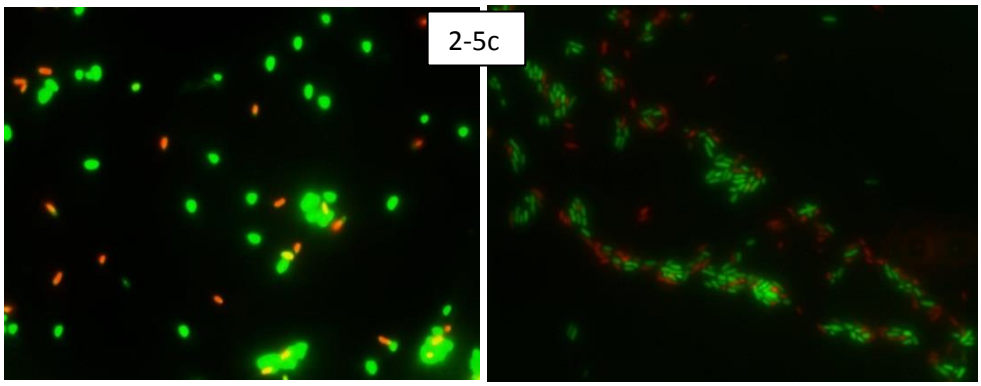

Δ ompF: 0 and 1 mg/L silver ions

Figure 2-5a, b, c: LIVE DEAD stain images for porin deletion mutants exposed to silver ions (Bars= 10µm). Porin deficient strains, Δ ompC and Δ ompF show more live cells (green coloured) than the control strain BW25113 when exposed to silver nitrate.

2.3.3 Silver ion biosensor suggests additional nanoparticle toxicity mechanisms

Silver nanoparticle exposure assays using the KEIO control strain and ion efflux deletion mutants suggested that silver ions are involved in nanoparticle toxicity at the concentration range found in exposure media. In order to gain further insight into ionic silver involvement in nanoparticle toxicity, a bioreporter that responds to ionic silver was developed. The biosensor (pSB1C3-PcopA_Yfp) was constructed by using the CueR regulated promoter of *copA* in *E. coli*. CueR is a transcriptional activator of *copA*, which encodes a copper efflux pump (Petersen and Moller, 2000). This gene also plays an important role in regulating intracellular levels of silver ions (Loftin et al., 2005). Preliminary characterization of the construct was carried out by using copper sulphate and addition of copper sulphate solution to the liquid culture resulted in significant increase in fluorescence as shown in Figure 2-6a. Addition of silver nitrate and silver nanoparticles produced a change in fluorescence of cells as shown in Figure 2-6c and 2-6d respectively. Further, the cells were induced by ionic silver in the range of 0.5-2 mg/L (Figure 2-7a and 2-7b) in minimal medium.

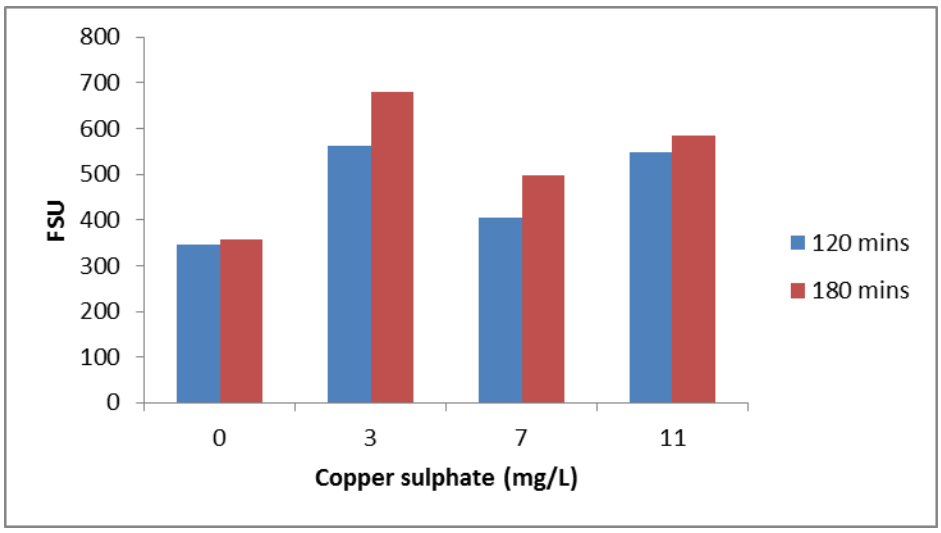

Figure 2-6a: Induction of biosensor, P*copA_Yfp* with copper sulphate. Addition of copper sulphate (copper ions induce the promoter, P*copA*) results in expression of Eyfp.

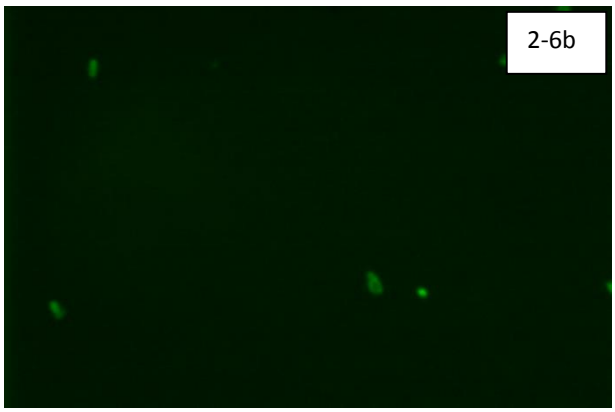

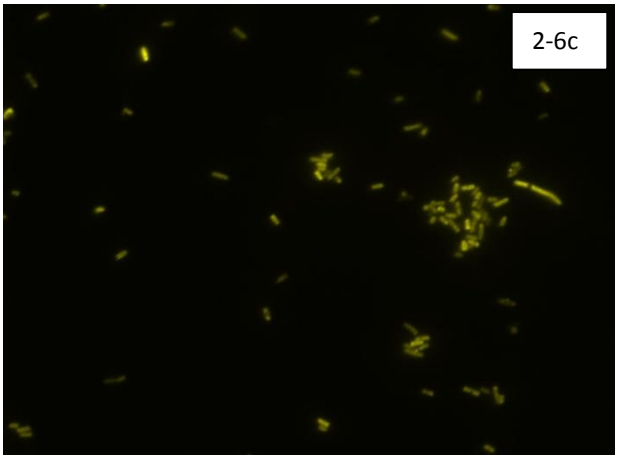

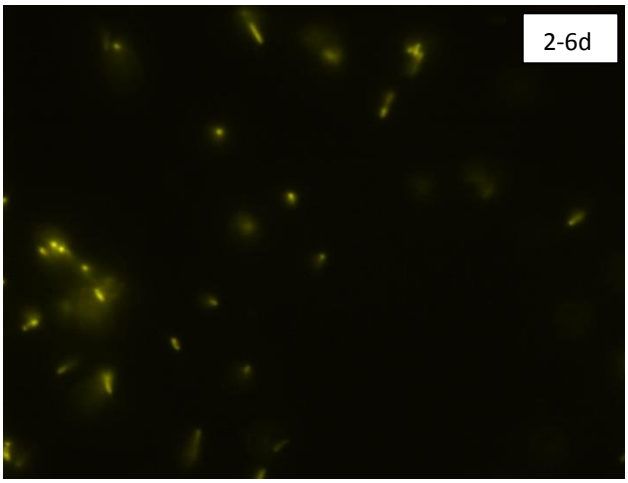

Figure 2-6 Fluorescence of biosensor exposed to silver ions: 2-6b is control sample that shows basal level of fluorescence that increases in presence of ionic silver (Fig. 2-6c) and nanoparticles (Fig 2-6d). Image scale is 10 μm

Figure 2-7a shows that fluorescence (FSU) increases with increasing concentration of ionic silver in the range 0.3-1.6 mg/L, after which it starts to decline. This trend is consistent with the biosensor responding by induction with silver ions, but with fluorescence declining when ionic silver reaches toxic concentrations. When the biosensor was tested with silver nanoparticles, there was no significant induction (Fig. 2-7c, 2-7d), with fluorescence values similar to those for control samples without dissolved silver, suggesting that there was insufficient ionic silver in the cytoplasm to induce the biosensor. The low ionic silver is consistent with the speciation measurements (Figure 2-14) and in tests; using supernatants to induce the biosensor following three-hour incubation of nanoparticles in the medium (Figure 2-8). Both the ICP measurements and lack of induction of biosensor cells suggest that the rate of ionic dissolution from the nanoparticle surface was quite low.

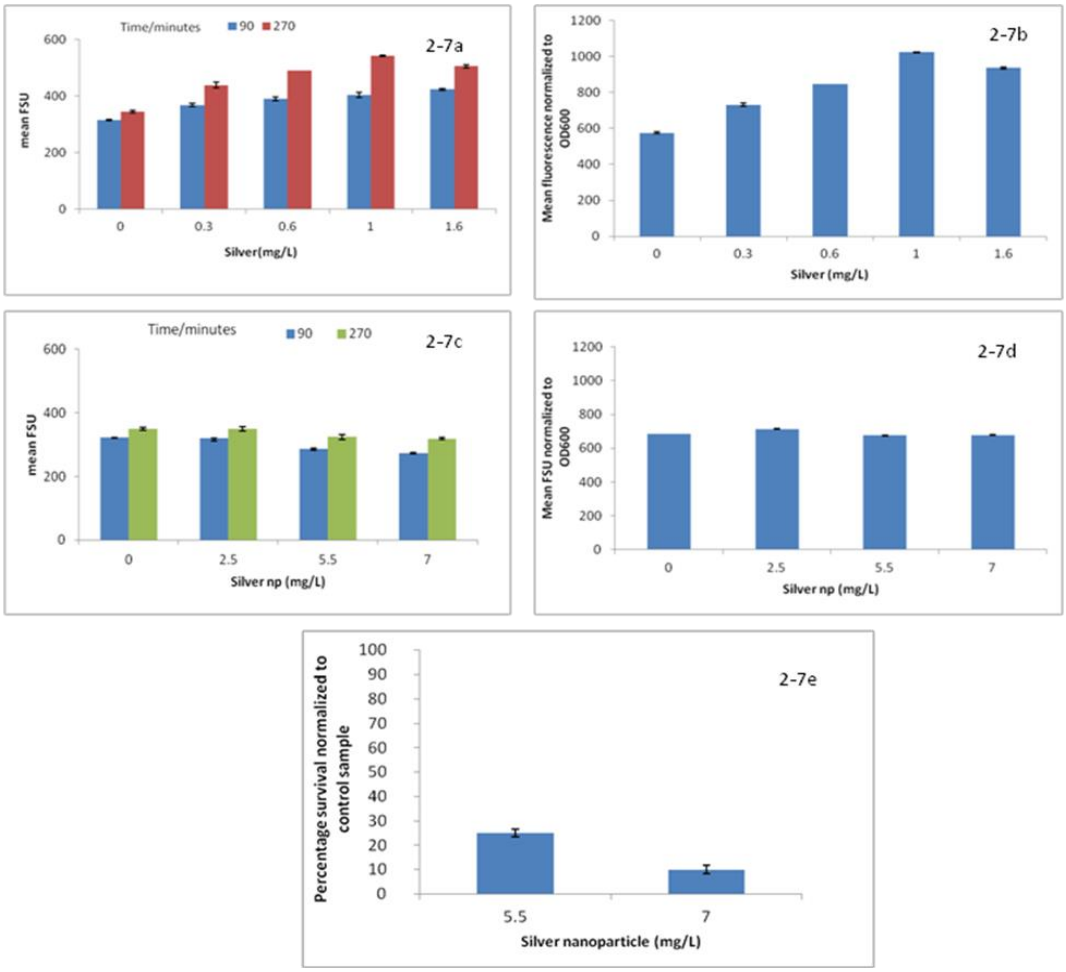

Figure 2-7: Fluorescence units (FSU) measured on biosensor exposed to silver ions (2-7a, b) and silver nanoparticles (2-7c, d). Figure 2-7e shows the relative cell survival normalized to sample without any silver nanoparticles. Figure 2-7b, 2-7d and 2-7e are plotted at time point 270 minutes. The error bars represent the standard error, n=3.

However, the cell viability test conducted after exposure to silver nanoparticles showed a significant drop in cell survival as shown in Figure 2-7e. This suggests that nanoparticles produce toxicity by more than one mechanism.

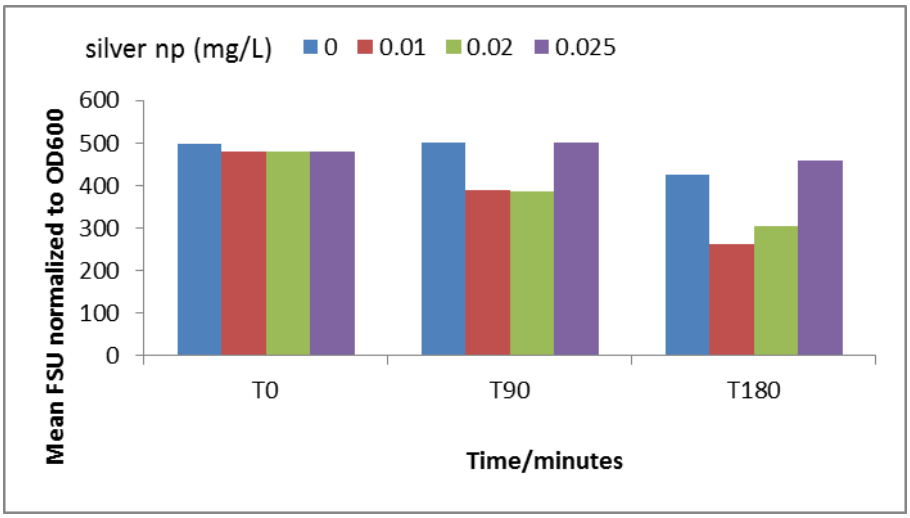

Figure 2-8: Biosensor cells exposed to centrifuged medium with suspended silver nanoparticles. The assay was not done in replicates hence no error bars.

2.3.4 Mutants lacking oxidative stress protective genes show sensitivity to silver nanoparticles

Numerous studies have reported that oxidative stress plays a major role in nanoparticle toxicity (Choi and Hu, 2008, Carlson et al., 2008., Auffan et al., 2008., Dimkpa et al., 2011., Napierska et al., 2012). To determine whether this mechanism can be detected at the genetic level, *E. coli* strains with mutations in important oxidative-stress resistance components of the *oxyR* and *soxR* regulons were tested (Table 2-1). Results (Figure 2-9) showed that these strains were more susceptible to nanoparticle toxicity compared to the control strain. Furthermore, some of these strains were sensitive to silver ions (0-5.4 mg/L) with ionic silver reducing viability by about the same level as a twofold higher concentration of silver in nanoparticulate form (Figure 2-9c).

E. coli strain LE106, with three major peroxidases, *katG*, *katE* and *ahpF*, deleted (Seaver and Imlay, 2004), also showed an enhanced susceptibility to silver

nanoparticles (Figure 2-10a, b) as compared to the wild type parent strain MG1655. Besides the cell viability assay this strain demonstrated a higher level of oxidative stress as detected by the dye para aminophenyl fluorescein (APF) in Figure 2-10c on exposure to silver NP. These results are consistent with other reports that oxidative stress is one of the major mechanisms of nanoparticle toxicity.

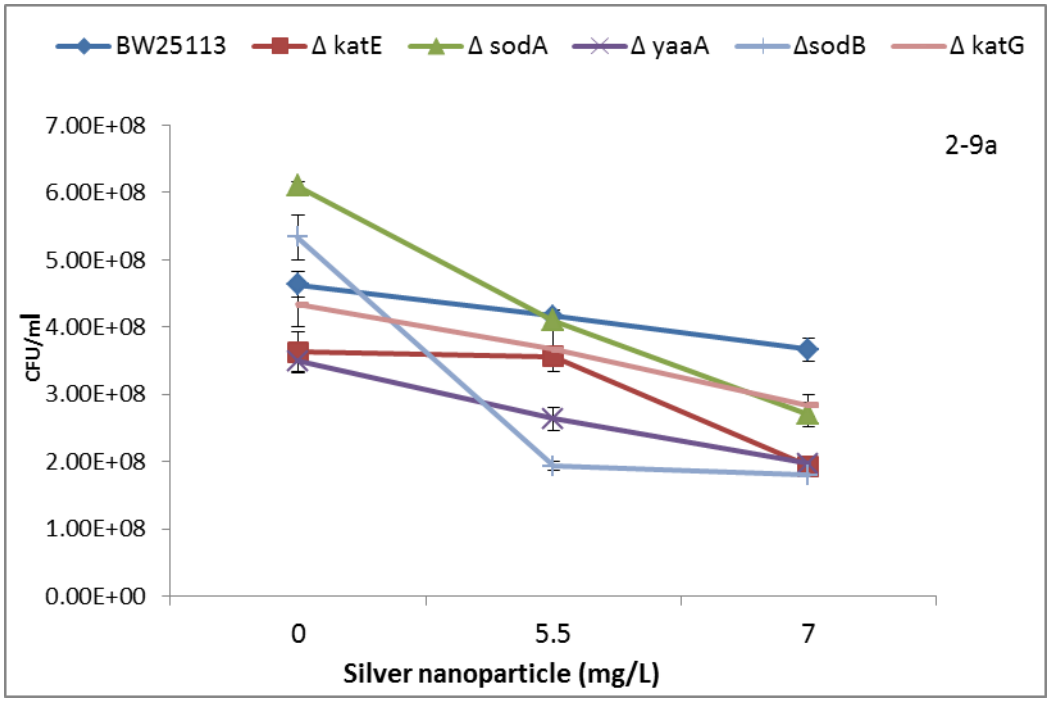

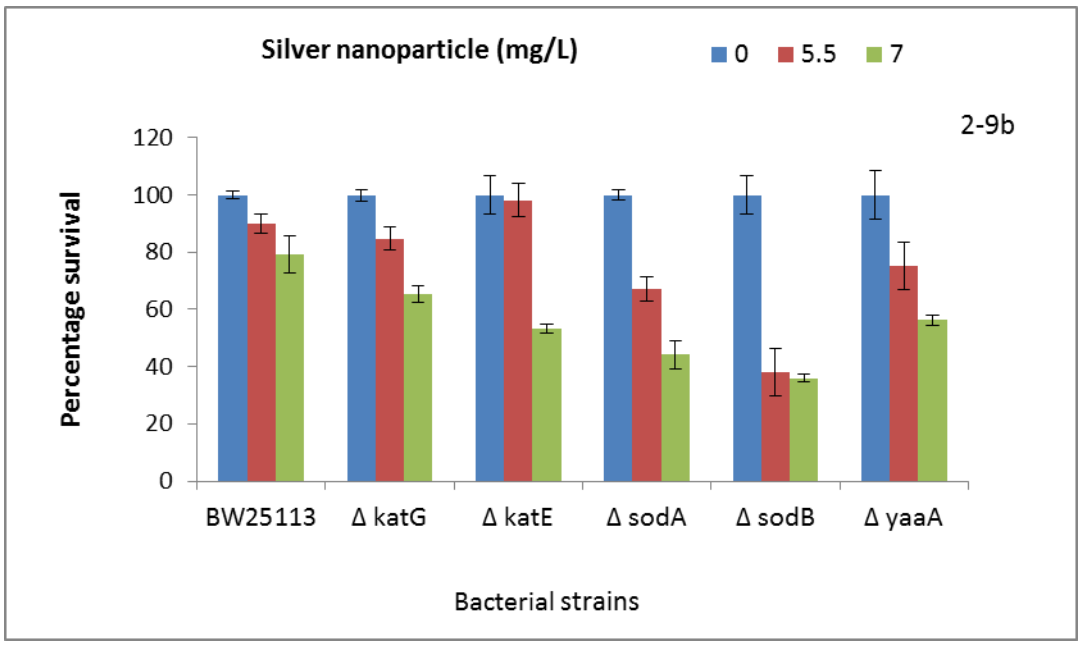

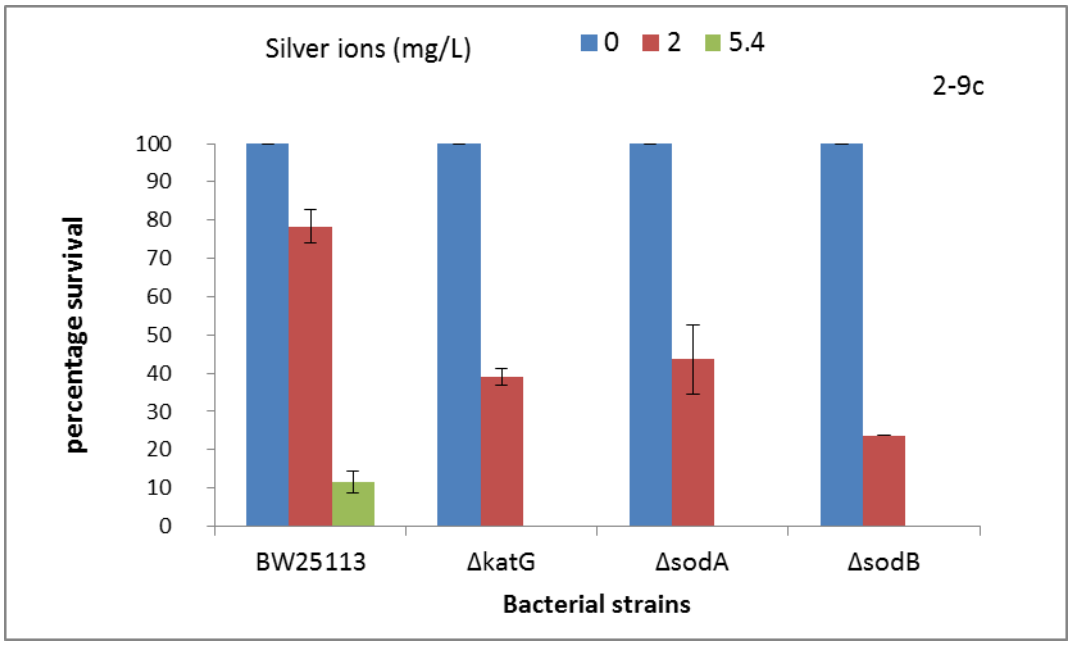

Figure 2-9a, b (silver nanoparticle) and 2-9c (silver nitrate) exposure assay for oxidative stress deletion mutants for catalase (*katG* and *katE*), superoxide dismutase (*sod A, B, C*) and peroxidase (*yaaA*) (n=3 and error bars represent the standard errors)

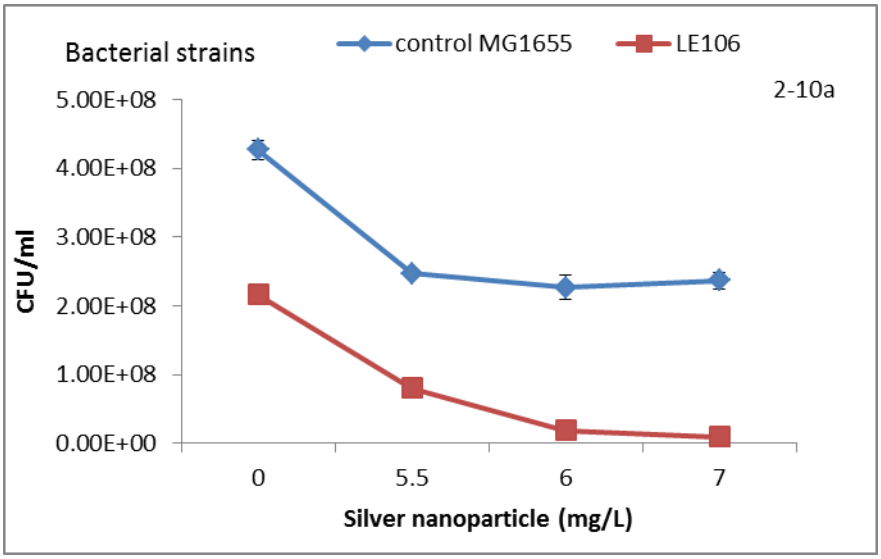

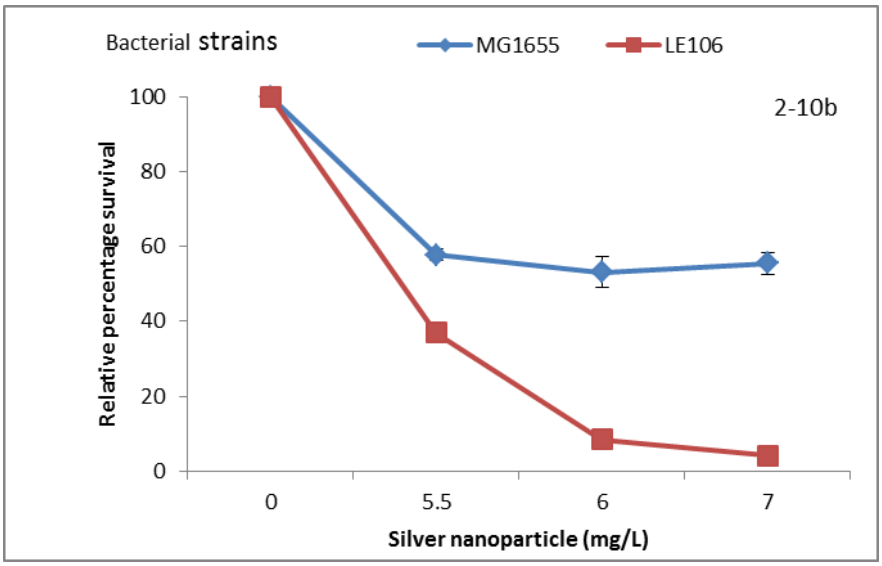

Figure 2-10: 2-10a, b: cell viability assay for triple deletion strain LE106 against silver nanoparticles.

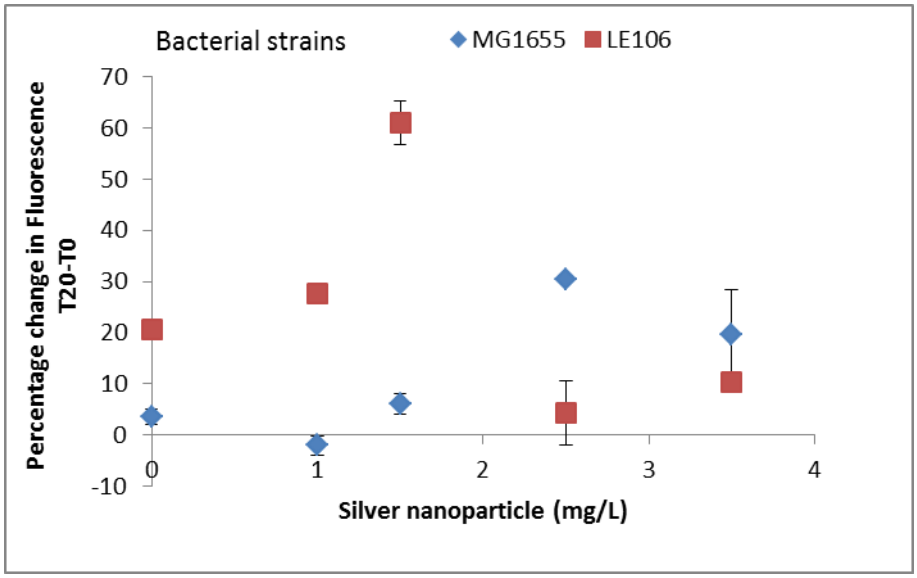

2-10c: Detection of oxidative stress by APF dye. The y- axis shows the change in fluorescence level after 20 minutes of addition of dye to nanoparticles exposed cells

Aerobic respiration in *E. coli* requires the cytochrome oxidase genes encoded by the *cyo* (cytochrome bo) and *cyd* (cytochrome bd) operons. It has been reported that *cyoA*, encoding a subunit of terminal oxidase cytochrome bo, is upregulated on exposure to silver nanoparticles (Gou et al., 2010). In the assays, *cyoA* and *cyoB* mutants showed increased sensitivity to nanoparticles (Figure 2-11). This may reflect a specific effect, or may be due to reduced energy availability in such mutant strains. The deletion of *cydB* had little or no significant impact on cell viability.

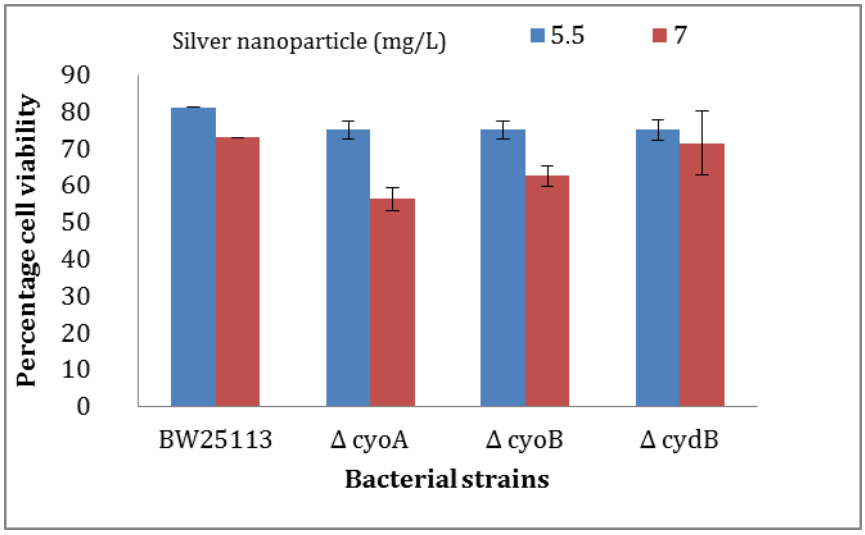

Figure 2-11: Exposure assay for deletion mutants for cytochrome oxidase against silver nanoparticles

To further investigate the role of oxidative stress, the impact of catalase in nanoparticle exposure experiments was investigated. Catalase is an enzyme produced by living organism including bacteria as a protective response against oxidative stress (Storz et al., 1990). This enzyme helps to degrade hydrogen peroxide into water and oxygen. Catalase (180 U/ml final concentrations) was added during the nanoparticle exposure study. The cell viability was determined by colony counts (CFU) and the Bactiter Glo cell viability assay, which measures ATP levels. The addition of catalase led to an increase in cell viability as assessed by ATP levels (Figure 2-12a) and CFU data (Figure 2-12 b). The cell viability test also showed a similar trend, the samples with catalase showing a higher cell number than the ones with only nanoparticles. This effect was much more pronounced in the mutant strains ($p=0.03$ and $p=0.01$ for Δ*katG* and Δ*katE* respectively at 7 mg/L silver nanoparticle concentration) than the control (parent) strain, BW25113. The parent strain showed a

marginal but statistically insignificant increase in survival on addition of catalase (Figure 2-12.b).

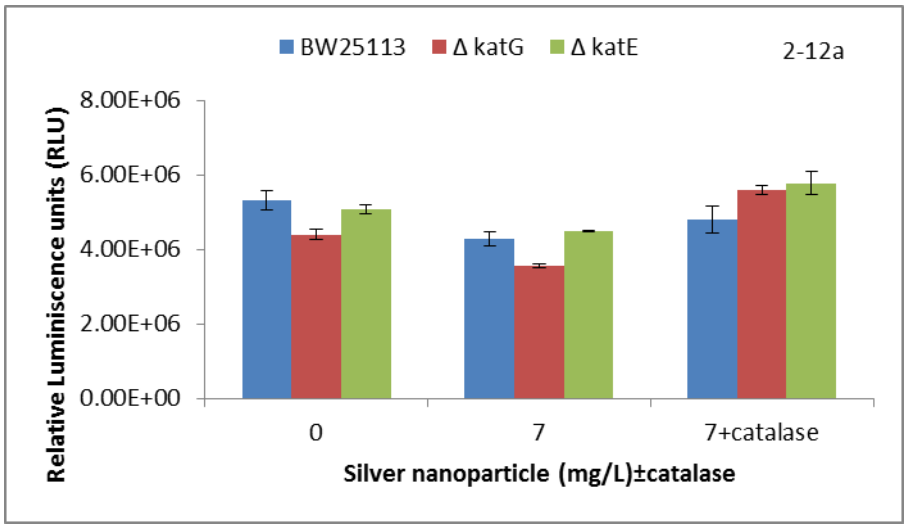

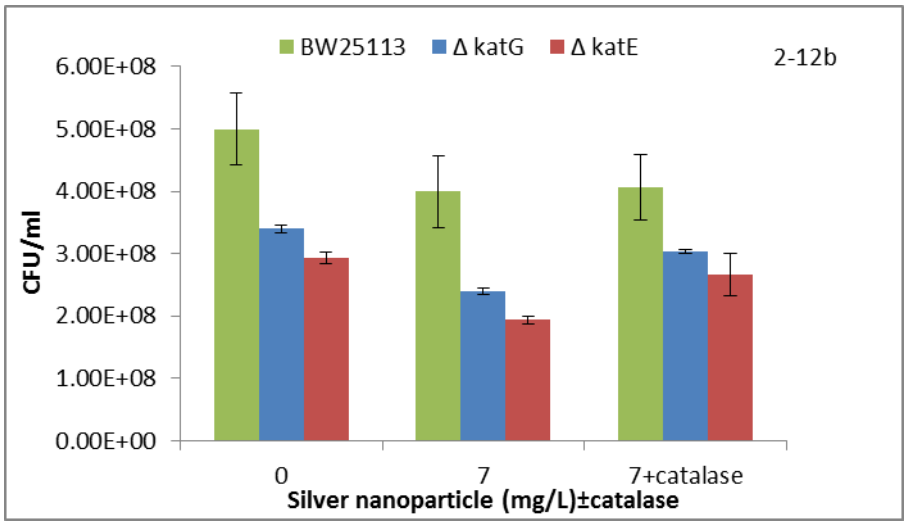

Figure 2-12: Protective effect of addition of catalase to deletion mutants on exposure to silver np. 2-12a: cell viability determination by Bactiter kit (y-axis shows the change in luminescence) 2-12b: cell viability assay for same experiment

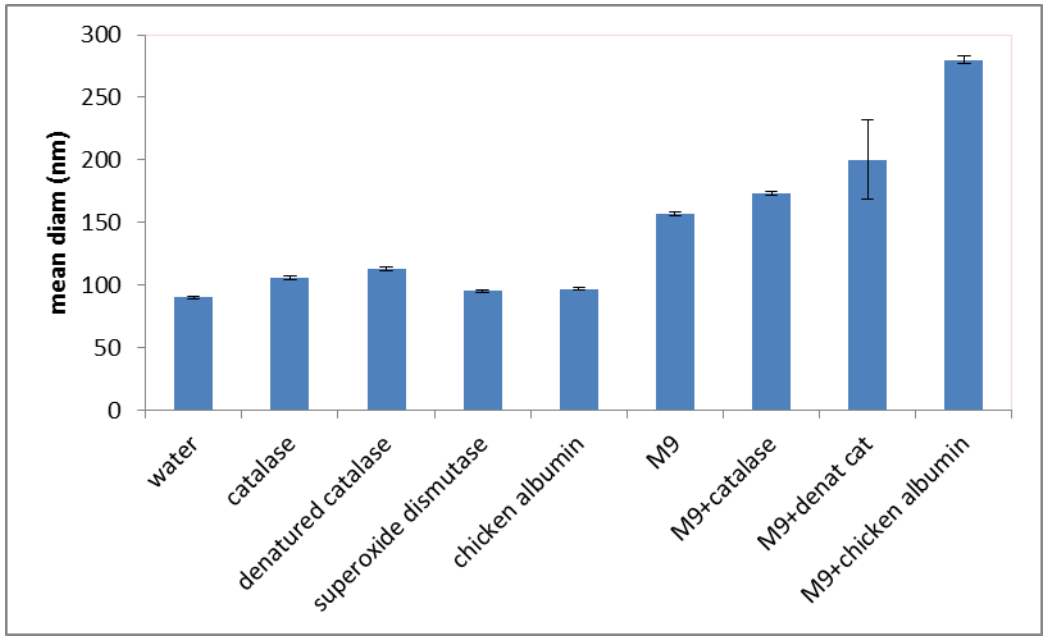

Figure 2-13: Size characterization of silver nanoparticles under different conditions. The 10 nm diam silver nanoparticles were not available hence this assay was conducted using 100 nm (mean diam) sodium citrate stabilized silver np's.

To confirm that these results were due to enzymatic activity of catalase, the experiment was repeated using heat-denatured catalase, and an inactive control protein (ovalbumin 90 μg/ml). Due to unavailability of 10 nm Ag np, 100 nm silver np's were used in this experiment. It was observed that addition of albumin and heat denatured catalase also produced a significant increase in cell viability but only at a higher concentration of these additives (data not shown). The nanoparticle stability was subsequently tested in the presence of catalase and albumin, and it was found that addition of these proteins at concentrations greater than 80 μg/ml led to increase in average diameter of silver nanoparticles (Figure 2-13). The presence of catalase at the concentration used in the cell viability assay did not produce such aggregation.

2.4 Discussion

2.4.1 Nanoparticles and associated ionic damage

Although silver nanoparticles have been shown to be toxic to bacteria, recent studies demonstrate that dissolution of silver ions from the nanoparticulate surface is the major factor contributing to toxicity (Sondi and Sondi, 2004, Morones et al., 2005, (Fabrega et al., 2009, Jin et al., 2010, Sheng and Liu, 2011, Levard et al., 2012). In the current study, this possibility was investigated by making use of two types of deletion mutant strains of *E. coli*.

E. coli has an inbuilt mechanism to detoxify metal ions of copper and silver by switching on responsive efflux pumps (Belliveau et al., 1987, Outten et al., 2000, Petersen and Moller, 2000, Stoyanov et al., 2001). Mutant strains deficient in genes whose products either have a regulatory function or form the subunits of the efflux pumps were selected. These strains showed a higher sensitivity to both silver nanoparticles and silver ions than the control strain (Figure 2-2). Some variation was observed amongst the strains; however, these findings suggest that intracellular silver ions play a role in silver nanoparticle toxicity.

Some bacteria have been shown to be resistant to silver toxicity when porins are absent in their cell walls (Li et al., 1997). Porins are hydrophilic channels present on the surface of cell membranes and play an important role in maintaining osmolarity, nutrient uptake and movement of ions (Hancock, 1987, Hofnung, 1995). The role of porins with respect to silver nanotoxicity was investigated. It was observed that porin deficient strains showed a smaller decrease in cell viability on being exposed to silver nanoparticles than the control strain (Figure 2-4a). These strains were also found to be resistant to ionic silver up to 1.5 mg/L above which they were very

sensitive (Figure 2-4c). It has been reported in other works that deletion mutants of *E.coli* without porins show significant resistance to silver nanotoxicity (Radzig et al., 2012). Similarly, Li et al. (1997) have also shown that bacterial strains resistant to silver have reduced porin levels, but that laboratory strains of *E. coli* lacking porins did not show increased resistance to silver. These discrepancies may be due to differences in the choice of growth medium, exposure periods and the bacterial strains employed.

Both OmpC and OmpF are important outer membrane porins, but the level of expression is dependent on environmental conditions such as temperature and most importantly the osmolarity of the medium (Forst et al., 1988). These results indicate that porin is only one of the channels of transport and that silver nanotoxicity cannot be explained purely on this basis. It has been shown in other works that ionic silver uptake also occurs by active sites responsible for copper uptake (Ghandour, 1988). In this condition with no copper ions in the vicinity, silver ions might as well be using these routes. It also suggests that ionic toxicity is one important but not the sole mechanism by which silver nanoparticles produce toxicity. Under the growth conditions used in this study, it is possible/likely that OmpC is the major porin present, and that OmpF is not expressed, explaining the lack of effect of OmpF deletion. Thus both porin and ion efflux deletion mutants strongly point to nanoparticle toxicity being mediated partially by ionic silver, which must therefore be bioavailable.

2.4.2 Bioavailability of ionic silver from nanoparticulate silver

The silver responsive biosensor was developed to determine whether silver ions were released from nanoparticles in sufficient levels in the cytoplasm to account for the toxicity observed. However, the exposure studies using the biosensor produced some contradictory results; fluorescence measurements showed that the biosensor responded as expected to ionic silver (Figure 2-7b) but did not show response to silver nanoparticles, even at levels where cell viability was significantly affected (Figure 2-7e). These observations might be reconciled by reference to speciation of dissolved silver or to other toxicity mechanisms.

Nanoparticle dissolution experiments in the absence of cells showed that a maximum of 0.09 mg/L (<2% of total) of silver added as nanoparticles was in the form of dissolved silver in de-ionised water. The concentration decreased to 0.014 mg/L (1.34×10^{-7} mol/kg) in M9 medium. Similarly, only 0.12 mg/L (1.1×10^{-6} mol/kg or 3% of the added ionic silver remained in solution in M9. These results are consistent with precipitation of silver chloride in M9 medium, and are confirmed by equilibrium speciation modelling using Geochemists' Workbench, which predicts AgCl solid as the thermodynamically stable phase (Figure 2-14) when the range of concentration of total Ag is equilibrated with M9 medium. Furthermore, speciation of the residual dissolved silver after precipitation of the AgCl predicts that less than 1% (~8×10^{-9} mol/L) exists as a tetra-aqua cation (Figure 2-15), with the rest being neutral AgCl (~29%), $AgCl^{2}$- (~68%) and $AgCl_3^{2}$- (~2%) complexes.

The concentrations measured in the nanoparticle-water suspensions and $AgNO_3$-M9 incubations are similar to levels over which up to 80% loss in viability has been

reported in biofilms by Lowry etal., 2012. When nanoparticles are suspended in M9 medium, however, dissolved Ag^+ in the cytoplasm is too low to induce fluorescence in the biosensor, yet sufficiently bioavailable to cause loss of viability, as suggested by deletion mutants. This suggests that as well as ionic silver, complexed silver species such as $AgCl_2^-$ (aq) act as a continual slow source of ionic silver to bacteria *via* thermodynamic equilibration between the bulk solution and the cell surface, consistent with the Biotic Ligand Model (Cremazi et al.,2013). In turn, any uptake by cells will drive a constant and steady flux from nanoparticles. Alternatively, it is possible that ions could be forming inside cells once silver nanoparticles are internalized as shown in an earlier study (Joshi et al., 2012). It can be argued that silver nanoparticles either attached to the cell wall or were transported into the periplasm. Similarly, silver nanoparticles transported inside the periplasm can further furnish more silver ions that could lead to higher toxicity in porin deletion mutants as observed in this study. Once inside the cell, the nanoparticles could have formed ions to produce this observed induction. Lastly, release of silver ions could have triggered a chain of other events like membrane disruption, leakage of cytoplasm, DNA damage and oxidative stress that could account for observed toxicity (Figure 2-7e) without appreciable increase in total fluorescence. Overall, this situation will automatically reduce the number of viable cells and net fluorescence will either drop or stay constant.

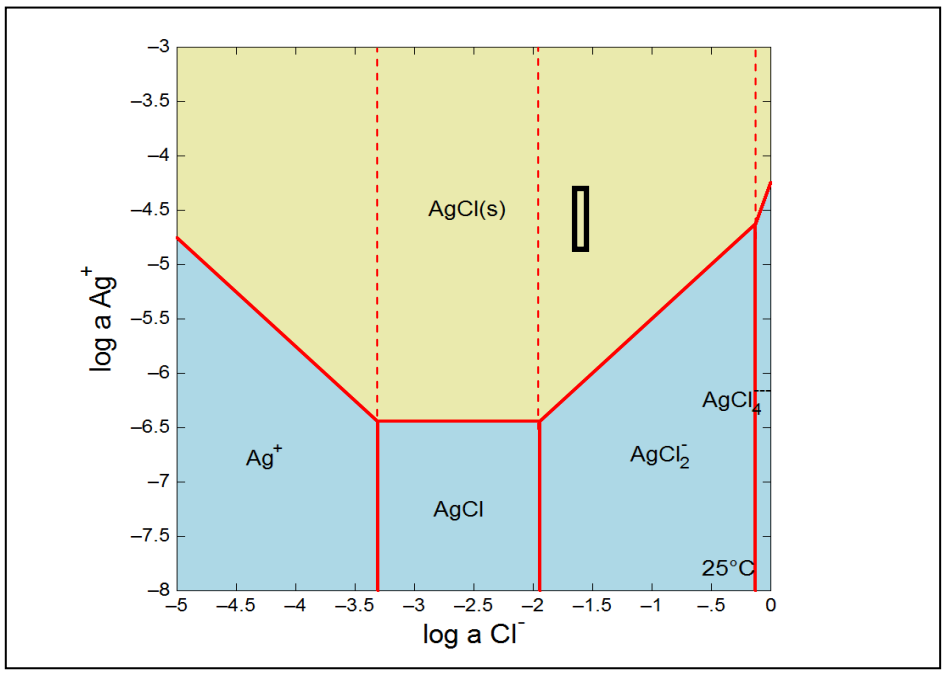

Figure 2-14: Log activity diagram depicting predominant species in the Ag-Cl system modelled using Geochemists' Workbench v7 Act2 code using thermodynamic parameters from the Thermo database, with the solubility constant for AgCl replaced by the value from the MINTEQ database. The "bar" represents the range of total Ag added to exposure experiments.

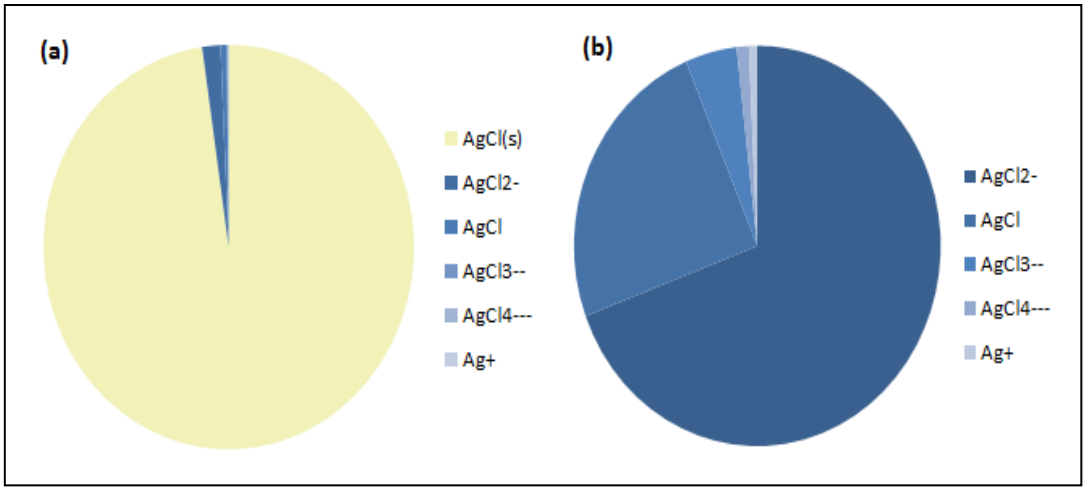

Figure 2-15a:Distribution of dissolved and precipitated species in the system modelled using the Geochemists' Workbench v7 React code for 7mg/L total Ag equilibrated in M9 growth medium. 2-15b Distribution of residual aqueous species after AgCl precipitation. Tetra-aqua cationic silver represents less than 1% of the total dissolved silver.

2.4.3 Nanoparticles and oxidative stress

In this study, silver nanoparticles have been shown to cause oxidative stress in bacteria, consistent with previous studies (Park et al., 2009, Jin et al., 2010, , He et al., 2012). Ivask et al. (2012) report similar findings; deletion mutants in genes of the *soxR* and *oxyR* regulons were sensitive towards nanotoxicity. In this study, the deletion mutant for *sodB* was found to be most susceptible to silver ions and silver nanoparticles. If we compare this observation with other reports, regardless of the type of metal nanoparticle involved, *sod* deletion strains were found to be highly sensitive to metal nanoparticles. For instance, the deletion mutants of *sodA* and s*odM* for *Staphylococcus aureus* were highly sensitive to zinc oxide nanoparticles (Raghupathi et al., 2011).

The fact that deletion mutants for peroxidase (Figure 2-9a) show a higher survival than those for superoxide dismutase suggests that superoxide radicals could be one of the major reactive oxygen species being formed during exposure to silver nanoparticles. The degree of aeration during nanoparticle exposure can also influence the extent of oxidative stress damage (Inoue et al., 2002). It is expected that the deletion mutants will show lesser growth and viability compared to control strains in aerobic environments, which promote nanoparticle oxidation (Xiu et al., 2011). If the response of strain LE106 is analysed in this light, it is found to be less viable than the control strain even in absence of nanoparticles. In the presence of silver nanoparticles it becomes highly sensitive and shows a sharp increase in fluorescence on addition of APF (Figure 2-10c). Furthermore, the oxidative stress deletion mutants in general have a higher concentration of unresolved free radicals and these could be indirectly involved in producing a chain reaction promoting rapid

dissolution of silver from the nanoparticle surface. A recent study (He et al., 2012) has demonstrated that the presence of peroxide in cells promotes the dissolution of silver ions and generation of superoxide in the cells. This process is pH dependent and sets up a chain reaction leading to a higher toxicity. This observation is in agreement with other studies that prove the potential role of silver nanoparticles in production of oxidative stress (Choi and Hu, 2008, Dimkpa et al., 2011, Park et al., 2009, He et al., 2012). Enzyme supplementation with catalase while exposing strains Δ*katG* and Δ*katE* to nanoparticles helped to restore cell viability. The addition of albumin also produced a similar protective effect, though the hydrodynamic diameter of silver nanoparticles increased in the presence of albumin or heat denatured catalase and this could partially explain reduced toxicity.

It could be argued that silver ions (from np) interact with sulfhydryl residues present on the cysteine molecules (present in) catalase. But catalase especially, bovine liver catalase used here has been reported to have 4 cysteine per 60 kda subunits (Sevinc et al, 1995). In this process certainly some silver ions could thus become less bioavailable. The fact that the addition of catalase brings about a greater increase in cell viability for catalase deficient strains however suggests that this cannot be the sole reason in fact, it suggests that hydrogen peroxide or peroxide like species might be forming due to nanoparticle (NP) exposure and exogenous addition of catalase acts in two ways (1) by decomposing free radicals and (2) by promoting aggregation of nanoparticles. Amongst the mutants of cytochrome oxidase, Δ*cyoA* was most sensitive (Figure 2-11); the varying response could be partially due to the exposure conditions. In *E. coli, cyoA* is expressed under high oxygen conditions while cytochrome bd is expressed in micro aerobic conditions (Cotter et al., 1990, Fu et al.,

1991). This may explain why the deletion of cytochrome bd did not affect cell viability during nanoparticle exposure.

2.4.4 Environmental implications for silver nanotoxicity

Recent studies have focussed on resolving the exact mechanism by which silver nanotoxicity to bacteria operates and predominantly conclude that toxicity occurs via nanoparticles releasing ionic silver. The implications of this mechanism are that in most natural environments, particularly those likely to be first level receptors of nanoparticle release (freshwaters, urban ponds etc), the presence of chloride coupled with the predicted precipitation of AgCl in such media will ameliorate silver nanotoxicity. This study confirmed that ionic silver was an important toxicity mechanism even in chloride-containing media, suggesting that chloride waters offer no protection to nanotoxicity by this mechanism.

The speciation model in this study indicates that soluble dichloride of silver could well act as a source of silver ions, which contribute to toxicity (Levard, 2011). Just as important, the use of deletion mutants for oxidative stress genes suggests that oxidative stress is also important and that some of this is directly linked to nanoparticles rather than ionic silver. Overall, it suggests that silver nanoparticles are likely to harm environmental bacteria even at the low concentrations of ionic silver in chloride-containing natural waters.

Significantly, speciation in natural waters will not be as straightforward as measured/predicted here for chloride-containing waters given the presence of other ligands, redox state and/or residence time of the nanoparticles. In particular, Ag_2S is predicted to form under reducing conditions, while the presence of organic

compounds containing thiol functional groups will drive speciation towards formation of stable organic ligands that can render Ag^{+} non-bioavailable (Levard et al., 2012).

Clearly, more work is required to constrain the different environmental variables that influence the bioavailability and toxicity of metal nanoparticles. The speciation of ions released from nanoparticles has been further investigated by developing microcosms and discussed in chapter five.

References:

1. Auffan, M. l., Ahouak, W., Rose, J. r., Roncato, M.-A., Chanéac, C., Waite, D. T., Mason, A., Woicik, J. C., Wiesner, M. R. & Bottero, J.-Y. 2008. Relation between the redox state of Iron-based nanoparticles and their cytotoxicity toward *Escherichia coli. Environ. Sci & Technol,* 42**,** 6730-6735.

2. Baba, T., Ara, T., Hasegawa, M., Takai, Y., Okumura, Y., Baba, M., Datsenko, K. A., Tomita, M., Wanner, B. L. & Mori, H. 2006. The construction of systematic in-frame, single-gene knockout mutant collection in *Escherichia coli* K-12. *Mol.Syst.Biol*.

3. Bekhit, A., Fukamachi, T., Saito, H. & Kobayashi, H. 2011. The role of OmpC and OmpF in acidic resistance in *Escherichia coli*. *Biol Pharm Bull.*. 34**,** 330-4.

4. Belliveau, B. H., Starodub, M. E., Cotter, C. & Trevors, J. T. 1987. Metal resistance and accumulation in bacteria. *Biotechnology Advances,* 5**,** 101-127.

5. Bethke, C. M. 1996. Geochemical reaction modeling, concepts and applications. *Oxford University Press, New York.*

6. Carlson, C., Hussain, S. M., Schrand, A. M., K. Braydich-Stolle, L., Hess, K. L., Jones, R. L. & Schlager, J. J. 2008. Unique cellular interaction of silver nanoparticles: size-dependent generation of reactive oxygen species. *J.Phys.Chem.B,* 112**,** 13608-13619.

7. Chinnapongse, S. L., MacCuspie, R. I. & Hackley, V. A. 2011. Persistence of singly dispersed silver nanoparticles in natural freshwaters, synthetic seawater, and simulated estuarine waters. *Sci Total Environ.,* 409**,** 2443-2450.

8. Choi, O. & Hu, Z. 2008. Size Dependent and Reactive Oxygen Species Related Nanosilver Toxicity to Nitrifying Bacteria. *Environ. Sci & Technol.,* 42**,** 4583-4588.

9. Cotter, P. A., Chepuri, V., Gennis, R. B. & Gunsalus, R. P. 1990. Cytochrome o (cyoABCDE) and d (cydAB) oxidase gene expression in *Escherichia coli* is regulated by oxygen, pH, and the fnr gene product. *J. Bacteriol,* 172(11)**,** 6333-8.

10. Cremazy A, Campbell P, Fortin F 2013 The biotic ligand model can successfully predict the uptake of a trivalent ion by a unicellular alga below pH 6.50 but not above: possible role of hydroxo-species. *Environ Sci Technol*. **47** 2408–15.

11. Desai, K. K. & Miller, B. G. 2010. Recruitment of Genes and Enzymes conferring resistance to the nonnantural toxicn Bromoacetate. *Proc. Natl.Acad.Sci,* 107**,** 17968-17973.

12. Dimkpa, C., Calder, A., Gajjar, P., Merugu, S., Huang, W., Britt, D., McLean, J., Johnson, W. & Anderson, A. J. 2011. Interaction of silver nanoparticles with an environmentally beneficial bacterium, *Pseudomonas chlororaphis*. *J.Hazard.Mater,* Volume 188**,** 428-435.

13. Fabrega , J., Shona, R., Fawcett, S., Renshaw, J. C. & Lead, J. R. 2009. Silver nanoparticle impact on bacterial growth: effect of pH, concentration, and organic matter. *Environ. Sci. Technol.,* 43(19)**,** 7285-90.

14. Forst, S., Delgado, J., Ramakrishnan, G. & Inoyue, M. 1988a. Regulation of OmpC and OmpF expression in *E.coli* in the absence of envz. *J. Bacteriol.,* 170**,** 5080-5085.

15. Forst, S., Delgado, J., Ramakrishnan, G. & Inoyue, M. 1988b. Regulation of ompC and ompF expression in *Escherichia coli* in the absence of envZ. *J.Bacteriol.,* 170**,** 5080-5085.

16. French, R. A., Jacobson, A. R., Kim, B., Isley, S. L., Penn, R. L. & Baveye, P. C. 2009. Influence of ionic strength, pH, and cation Valence on aggregation kinetics of titanium dioxide nanoparticles. *Environ. Sci Technol.,* 43**,** 1354-1359.

17. Fu, H., Luchi, S. & LIn, E. C. 1991. The requirement of ArcA and Fnr for peak expression of the cyd operon in *Escherichia coli* under microaerobic conditions. *M o l 6 Gen Genet,* 226**,** 209-213.

18. Gajjar, P., Pettee, B., Britt, D., Huang, W., Johnson, W. & Anderson, A. 2009. Antimicrobial activities of commercial nanoparticles against an environmental soil microbe, *Pseudomonas putida* KT2440. *J. Biol.Eng.,* 3**,** 1611-1754.

19. Gou, N., Onnis-Hayden, A. & Gu, A. Z. 2010. Mechanistic toxicity assessment of nanomaterials by whole-cell-array stress genes expression analysis. *Environ. Sci. Technol.,* 44**,** 5964–5970.

20. Hancock, R. E. W. 1987. Role of porins in outer membrane permeability. *J.Bacteriol.,* 27**,** 929-933.

21. He, D., Garg, S. & Waite, T. D. 2012. H2O2-mediated oxidation of zero-valent silver and resultant interactions among silver nanoparticles, silver ions, and reactive oxygen species. *Langmuir,* 28(27)**,** 10266-75.

22. Hofnung, M. 1995. An intelligent channel (and more). *Science,* 267(5197)**,** 473-4.

23. Horie, M., Kato, H., Fujita, K., Endoh, S. & Iwahashi, H. 2011. In vitro evaluation of cellular response induced by manufactured nanoparticles. *Chemical Res.Toxicol.,* 25**,** 605-619.

24. Huang, Z., Zheng, X., Yan, D., Yin, G., Liao, X., Kang, Y., Yao, Y., Huang, D. & Hao, B. 2008. Toxicological Effect of ZnO Nanoparticles based on bacteria. *Langmuir,* 24**,** 4140-4144.

25. Inoue, Y., Hoshino, M., Takahashi, H., Noguchi, T., Murata, T., Kanzaki, Y., Hamashima, H. & Sasatsu, M. 2002. Bactericidal activity of Ag-zeolite mediated by reactive oxygen species under aerated conditions. *J Inorg Biochem,* 30**,** 37-42.

26. Ivask, A., Suarez, E., Patel, T., Boren, D., Ji, Z., Holden, P., Telesca, D., Damoiseaux, R., Bradley, K. A. & Godwin, H. 2012. Genome-wide bacterial toxicity screening uncovers the mechanisms of toxicity of a cationic polystyrene nanomaterial. *Environ. Sci. Technol.,* 46**,** 2398–2405.

27. Jin, X., Li, M., Wang, J., MarambioJones, C., Peng, F., Huang, X., Damoiseaux, R. & Hoek, E. M. V. 2010. High-Throughput screening of silver nanoparticle stability and bacterial inactivation in aquatic media: influence of specific ions. *Environ. Sci Technol.,* 44**,** 7321-7328.

28. Joshi, N., Ngwenya, B. & French, C. E. 2012. Enhanced resistance to nanoparticle toxicity is conferred by overproduction of extracellular polymeric substances. *J. Hazard. Mater.,* 241–242**,** 363-370.

29. Kaeriyama, M., Machida, K., Kitakaze, A., Wang H, L. Q., Fukamachi, T., Saito, H. & Kobayashi, H. 2006. OmpC and OmpF are required for growth under hyperosmotic stress above pH 8 in *Escherichia coli*. *Lett Appl Microbiol.,* 42(3)**,** 195-201.

30. Kaushal, S. S., Groffman, P. S., Likens, G. E., Belt, K. T., Stack, W. P., Kelly, V. R., Band, L. E. & Fisher, G. T. 2005. Increased salinization of fresh water in the northeastern United States. *Proc Natl Acad Sci,* 102(38)**,** 13517–13520.

31. Kittleson, J., Loftin, I., Hausrath, A., Engelhardt, K., Rensing, C. & McEvoy, M. 2006. Periplasmic metal-resistance protein CusF exhibits high affinity and specificity for both CuI and AgI. *Biochem.,* 45**,** 11096-02.

32. Knight, T. 2003. Idempotent Vector Design for Standard Assembly of Biobricks, . *mit.edu/handle/1721.1/21168 1–11*.

33. Lankoff, A., Sandberg, W., Wegierek-Ciuk, A., Lisowska, H., Refsnes, M., Sartowska, B., Schwarze, P., Meczynska-Wielgosz , S., Wojewodzka, M. & Kruszewski, M. 2012. The effect of agglomeration state of silver and titanium dioxide nanoparticles on cellular response of HepG2, A549 and THP-1 cells. *Toxicol. Lett.,* 208**,** 197-213.

34. Levard, C., Hotze, E. M., Lowry, G. V. & Brown, G. E. 2012. Environmental transformations of silver nanoparticles: impact on stability and toxicity. *Environ. Sci.Technol.,* 46**,** 6900-6914.

35. Li, H., Nikaido, H. & Williams, K. E. 1997. Silver-resistant mutants of *Escherichia coli* display active efflux of Ag+ and are deficient in porins. *J Bacteriol.* , 179(19)**,** 6127–6132.

36. Loftin, I., Franke, S., Roberts, S. A., Weichsel, A., Heroux, A., Montfort, W. R., Rensing, C. & McEvoy, M. M. 2005. A novel copper-binding fold for the periplasmic copper resistance protein CusF. *Biochemistry,* 44**,** 10533-40.

37. Lyon, D. & Alvarez, P. J. 2005. Fullerene water suspension (nC60) exerts antibacterial effects via ROS-independent protein oxidation. *Environ. Sci.Technol.,* 42**,** 8127-8132.

38. Morones, J. R., Elechiguerra, J., Camacho, A., Holt, K., Kouri, J., Ramrez, J. T. & Yacaman, J. 2005. Bactericidal impact of silver nanoparticles. *Nanotechnology,* 16**,** 2346-2353

39. Munson, G., Lam, D. L., Outten, F. W. & O'Halloran, T. V. 2000. Identification of a copper-responsive two-component system on the chromosome of *Escherichia coli* K-12. *J Bacteriol.,* 182(20)**,** 5864-71.

40. Napierska, D., Rabolli, V., Thomassen, L. C. J., Dinsdale, D., Princen, C., Gonzalez, L., Poels, K. L. C., Kirsch-Volders, M., Lison, D., Martens, J. A. & Hoet, P. H. 2012. Oxidative stress induced by pure and iron-doped amorphous silica nanoparticles in subtoxic conditions. *Chem. Res Toxicol*.

41. Nel, A., Xia, T., Madler, L. & Li, N. 2006. Toxic potential of materials at the nanolevel. *Science,* 311**,** 622-627.

42. Norville, J., Derda, R., Gupta, S., Drinkwater, K., Belcher, A., Leschziner, A. & Knight, T. J. 2010. Introduction of customized inserts for streamlined assembly and optimization of BioBrick synthetic genetic circuits. *4***,** 17.

43. Novotny, E. V., Murphy, D. & Stefan, H. G. 2008. Increase of urban lake salinity by road deicing salt. *Sci Total Environ.,* 406**,** 131-144.

44. Outten, F., Hale, J. & O'Halloran, T. V. 2000. Transcriptional activation of an Escherichia coli copper efflux regulon by the chromosomal MerR homologue, cueR. *J. Biol. Chem.,* 275**,** 310424-9.

45. Park, H. J., Kim, J. Y., Kim, J., Lee, J. H., Hahn, J. S., Gu, M. B. & Yoon, J. 2009. Silver-ion-mediated reactive oxygen species generation affecting bactericidal activity. *Water Res.,* 43(4)**,** 1027-32.

46. Patsoukis N, Papapostolou I & CD., G. 2005. nterference of non-specific peroxidases in the fluorescence detection of superoxide radical by

hydroethidine oxidation: a new assay for H2O2. *Anal Bioanal Chem.,* 381(5)**,** 1065-72.

47. Petersen, C. & Moller, L. B. 2000. Control of copper homeostasis in *Escherichia coli* by a P-type ATPase, CopA, and a MerR-like transcriptional activator, CopR. *Gene,* 261**,** 289-298.

48. Radzig, M. A., Nadtochenko, V. A., Koksharova, O. A., Kiwi, J., Lipasova, V. A. & Khmel, I. A. 2012. Antibacterial effects of silver nanoparticles on Gram-negative bacteria: Influence on the growth and biofilms formation, mechanisms of action. *Colloids and Surfaces B: Biointerfaces*.

49. Raghupathi, K. R., Koodali, R. T. & Manna, A. C. 2011. Size-Dependent Bacterial Growth Inhibition and Mechanism of Antibacterial Activity of Zinc Oxide Nanoparticles. *Langmuir,* 27**,** 4020-4028.

50. Registry http://partsregistry.org/Catalog.

51. Rensing, C., Fan, B., Sharma, R., Mitra, B. & Rosen, B. P. 2000a. CopA: An *Escherichia coli* Cu(I)-translocating P-type ATPase. *Proc Natl Acad Sci,* 97(2)**,** 652-656.

52. Rensing, C., Fan, B., Sharma, R., Mitra, B. & Rosen, B. P. 2000b. Escherichia coli mechanisms of copper homeostasis in a changing environment. *Proc. Natl. Acad. Sci. U. S. A.,* 94**,** 652-656.

53. Seaver, L. A. & Imlay, J. A. 2004. Are Respiratory Enzymes the Primary Sources of Intracellular Hydrogen Peroxide? *J. Biol. Chem.,* 279**,** 48742-48750.

54. Sevinc, M., Ens,W., Lowern, P.C. 1995. The Cysteines of Catalase HPII of *Escherichia coli,* including Cys438 which is blocked, do not have a catalytic role. E J Biochem., 230., 127-132.

55. Sharma, O., Dastensko, K. A., Ess, S. C., Zhalnina, M. V., Wanner, B. L. & Cramer, W. A. 2009. Genome wide screens: novel mechanism in colicin import and cytotoxicity. *Mol.Microbiol.,* 73**,** 571-585.

56. Sheng, Z. & Liu, Y. 2011. Effects of silver nanoparticles on wastewater biofilms. *Water Res.***,** 879-2448 (Electronic).

57. Singh, R. P. & Ramarao, P. 2012. Cellular uptake, intracellular trafficking and cytotoxicity of silver nanoparticles. *Toxicol. Lett.,* 213(2)**,** 249-59.

58. Sondi, I. & Sondi, B. S. 2004. Silver nanoparticles as antimicrobial agent: a case study on *E. coli* as a model for Gram-negative bacteria. *J.Colloid. Interphase Sci.,* 275**,** 177-182.

59. Storz, G., Tartaglia, L. A. & Ames, B. N. 1990. The OxyR regulon. *Antonie Van Leeuwenhoek,* 58(3)**,** 157-161.

60. Stoyanov, J. V., Hobman, J. L. & Brown, N. L. 2001. CueR (YbbI) of Escherichia coli is a MerR family regulator controlling expression of the copper exporter CopA. *Mol Microbiol. ,* 39**,** 502-11.

61. Wirth, S. M., Lowry, G. V. & Tilton, R. D. 2012. Natural organic matter alters biofilm tolerance to silver nanoparticles and dissolved silver. *Env. Sci.Technol.,* 46**,** 12687-96.

62. Xiu, Z.-M., Ma, J. & Alvarez, P. J. J. 2011. Differential effect of common ligands and molecular oxygen on antimicrobial activity of silver nanoparticles versus silver ions. *Environ. Sci Technol.,* 45**,** 9003-9008.

Chapter 3

Development of bioreporters to investigate the mechanism of silver nanotoxicity

Abstract

The mechanism of toxicity of engineered metal and metal oxide nanoparticles is debatable. Recent studies indicate that ions play an important role in the nanotoxicity and that environmental factors can influence this process significantly through controlling rate of ionic dissolution. However, conditions that do not promote rapid dissolution of ions have also been shown to cause toxicity to bacteria. This observation indicates that the nanoparticulate form and mechanisms other than ions contribute to observed toxicity. This chapter aims to investigate the potential role of nanoparticles in generating reactive oxygen species in bacteria. Synthetic biology tools have been used for (1) developing biosensors that respond to known stress agents and (2) generating overexpression strains to produce enzymes that mediate a protective response during oxidative stress. They do not conclusively identify the nature of nanotoxicity but provide further useful indications that silver nanotoxicity operates by multiple pathways.

3.1 Introduction

Nanoparticles have unique properties such as small size, high reactivity and a large surface area; all these make them a suitable candidate for many applications with respect to material sciences (Nel et al., 2006, Xia et al., 2008). Recent developments include their extensive usage in various applications including the food industry, electronics and medicine (Maynard and Michelson, 2006, Wiesner et al., 2006). Nevertheless, there is a growing concern about the potential toxicity these nanoparticles could produce and their adverse impact, that has been demonstrated in a large number of studies including bacteria (Huang et al., 2008, Hu et al., 2009), mammalian systems (Lam et al., 2004, Kenichiro et al., 2008) and invertebrates (Heinlaana et al., 2008, Roh et al., 2009). In case of microorganisms, like bacteria these findings suggest that engineered nanoparticles produce toxicity by two major mechanisms, one being production of oxidative stress (Choi and Hu, 2008, Xia et al., 2008) and the other by damage to the cell membrane, an effect usually associated with ions (Sondi, 2004).

All the above mentioned studies rely largely on cell viability tests or use of probes that detect reactive oxygen species, and sometimes provide unreliable results (Patsoukis et al., 2005). However, the impact of nanoparticles needs to be studied at the cellular and genetic level in order to understand their mode of action. Nanotoxicity can be investigated in a systematic manner by development of stress responsive biosensors as sensitive tools for environmental monitoring. Oxidative stress detecting biosensors have been found to be responsive against known stress inducing agents (Belkin et al., 1996, Lee et al., 2003). For instance, Mitchell (2004) developed a dual stress response biosensor using promoters of two oxidative stress

responsive genes of *E. coli*, *katG* and *recA*. By integrating each of them with *lux* they found them to be quite sensitive towards hydroxyl radical forming chemicals. Similarly, Michan et al. (1999) have shown that genes belonging to the OxyR regulon detect peroxide and show a significant induction varying from five to eight fold depending on the growth conditions and gene.

In order to investigate nanotoxicity three types of biosensors have been used so far. First, the biosensors that show effect of toxicity by demonstrating a drop in a measurable signal such as fluorescence or luminescence. For instance, Gajjar et al. (2009) investigated the toxicity of silver (Ag), copper oxide (CuO) and zinc oxide (ZnO) nanoparticles by transforming a soil bacterium *Pseudomonas putida* KT2440 with a *lux* plasmid. This biosensor showed a rapid drop in fluorescence activity with increasing concentration of Ag and CuO nanoparticles. In another work (Dams et al., 2011), a *lux*-based biosensor was developed by integrating a copy of *luxCDABE* in natural isolate of *Pseudomonas putida* BS566. The magnitude of toxicity was detected by measuring the change in luminescence value of samples exposed to various forms of silver (silver nanoparticles and ionic silver), and exposure studies revealed that nanoparticulate silver was the most toxic form.

In the second category are biosensors designed to investigate the nature of toxicity. These usually have a promoter specific to known inducer/stress fused to a reporter gene. Thus in theory, if the nanoparticle under study induces the promoter, this increases the detectable signal. This can indirectly point to the nature of toxicity depending on the promoter used. For instance, Gou et al. (2010) developed a library of genes fused to *gfp* and demonstrated that silver and titanium dioxide nanoparticles produce a global SOS response in *E. coli*. The exposure to nanoparticulate silver led

to upregulation of many genes related to inner membrane and transport systems like *emrE, cmr* and *fsr* indicating that oxidative stress and membrane damage were two main modes of toxicity.

Recently, Bondarenko et al (2012) developed three kinds of biosensors one that detects hydrogen peroxide (*lux* integrated to *katG* in chromosome); second biosensor had the *recA* fused to *lux* in a plasmid and third consisted of *copA* integrated to *lux.* Exposure to copper oxide nanoparticles induced all three types of biosensors. This showed that formation of reactive oxygen species, DNA damage and role of ionic copper; all three are instrumental in total toxicity of CuO nanoparticles.

In the third category, is the whole cell biosensor integrated on chips. This biosensor produced a change in capacitance as detectable signal. For instance, Quereshi et al. (2012) developed a chip based biosensor where *E. coli* integrated on a capacitive base could respond to the toxicity produced by gold nanoparticles. This biosensor showed a greater change in capacitance when exposed to small size (5nm diam) gold nanoparticles. This response was primarily due to changes in membrane potential as nanoparticles produce damage to cell membranes. Secondly, metal dissolution studies using FTIR (Fourier transformed infrared spectroscopy) revealed significant drop in amide levels (conformational changes in proteins) and an asymmetric stretching of phopho diester and phospholipid bonding (cell membrane associated). All these cause adverse impact on cell viability.

This work aims to develop whole cell biosensors to identify the nature of silver nanotoxicity; firstly, by developing biosensors to determine whether nanoparticles cause oxidative stress; secondly, to explore the possibility that the

overexpression of oxidative stress responsive genes can help to minimize nanotoxicity. This approach was used to consolidate further evidence of the role of reactive oxygen species (chapter 2) as a major mechanism of silver nanotoxicity.

E. coli produces two types of peroxidases, hydroperoxidase1 (encoded by *katG*) and hydroperoxidase 2 (encoded by *katE*) (Imlay, 2003). KatG is responsible for the majority of catalase activity and mediates disproportionation of hydrogen peroxide into water and oxygen. Similarly, there are three superoxide dismutase enzymes: Mn-Sod (encoded by *sodA*), Fe-Sod (by *sodB*) and Cu-Zn (coded by *sodC*). Both of these enzymes help to carry out the superoxide dismutation reaction (Liochev et al., 1999). In addition, there are other proteins that play an important role in environmental stress conditions like starvation, metal/acid stress and high temperature (Boor, 2006). There is an overlap in expression of certain genes in stress conditions, including the acid stress and oxidative stress genes. DNA binding protein from starved cells (Dps) is one such protein that has been shown to play an important role in alleviating oxidative stress, nutritional deprivation and more recently the stress caused by high copper concentrations (Ishikawa et al., 2003, Bellapadrona et al., 2010). In stress conditions, Dps binds non-specifically to the genome and forms a nucleoprotein complex, which protects the chromosomal DNA (Ishikawa et al., 2003). It is worth mentioning that conditions like heat shock, acid stress and oxidative stress produce damage by accelerating the process of protein misfolding (Cabiscol et al., 1999). Therefore, the mode of nanotoxicity was also investigated by overexpression of membrane chaperone prefoldin, from a thermophilic archaeon *Pyrococcus horikoshii*, in *E. coli*. Prefoldin has been shown to protect against solvent tolerance and associated stress (Okochi et al., 2008). It was hypothesized that the

overexpression of the above discussed proteins will alleviate nanotoxicity and indirectly provide clues about the nature of silver nanotoxicity. For this purpose, an overexpression library has been developed wherein *E. coli* has been modified to overexpress diverse proteins including KatG, SodA, Dps and Prefoldin.

3.2. Materials and Methods

3.2.1 Primers and plasmids used for the study

The biosensors and overexpression strains were developed by cloning the genes of interest using the vectors (Table 3-1) from the Registry of Biological parts in RFC10 format (Knight, 2003, Norville et al., 2010).

In order to develop biosensor and overexpression strains the following genes were selected:

- *katG*: encodes HP1 catalase (hydroperoxidase 1 to degrade hydrogen peroxide)
- *sodA, sodB* and *sodC:* encode superoxide dismutase, for dismutation of superoxide into oxygen and hydrogen.
- *gorA*: encodes, glutathione oxidoreductase which sustains levels of reduced glutathione during oxidative stress.
- *recA*: encodes RecA which is important for DNA repair and maintenance. The primers used to amplify these genes are listed in table 3-2a and 3-2b.

Vector	Features	BioBrick ID
pSB1A2	High copy number, ampicillin resistance marker (2079 bp)	pSB1A2-Bba_J33207
pSB1C3	High copy number, chloramphenicol marker (2070 bp)	pSB1C3-BBa_J04450
pSB4C5	Low copy number, chloramphenicol resistance marker	pSB4C5-BBa_J04450
pSB4K5	Low copy number kanamycin resistance marker	pSB4K5-BBa_J04450
pSB4K5	Low copy kanamycin resistance marker with *lux* operon under pBAD	pSB4K5-BBa_K325909

Table 3-1: Plasmids used for the study

Gene	Sequence	Tm (^{o}C)
katG f	5’ TCTGAATTCCTTCTAGAGTAGAGGGGAGCACAT TGATG 3’	76.4
kat G r	5’ ATCCTGCAGCTACTAGTATTACAGCAGGTCGAA	76.6
kat G mut f	5’ TAGCAAATTAGATTACTACGGC 3’	56.9
kat G mut r	5’ AATTCTTTGCGGTAGTCAAAGTCC 3’	65.2
sodA f	TCTGAATTCCTTCTAGAGCCGACAATACTGGAG ATGGA	76.6
sodA r	ATCCTGCAGCTACTAGTTTTATTTTTTCGACAAT ACTGGAGATGAA	78.3
sodB f	TCTGAATTCCTTCTAGAGGAGAGTAGCAATGTC ATTCG	75.2
sod B r	GCTACTAGTATTATGCAGCGATTTTTCGCTACA AATTCCC	76.1
sodC f	TCTGAATTCCTTCTAGAGAACGGAGGTCCTATG AAAC	74.5
sodC r	ATCCTGCAGCTACTAGTATTACTTAATTACACC ACAGGCATAGC	74.2
gorA f	TCTGAATTCCTTCTAGAGATAAGGACTTTGTCA TGAC	73.2
gorA r	ATCCTGCAGCTACTAGTATTAACGCATTGTCAC GAACTC	75.7
ahpF f	TCGAGATCTGCAGGAGATAAACATGCTCGAC	75.7
ahpF r	GCTACTAGTATTATGCAGTTTTGGTGCGAATC	69.7
*ahp*F mut f	GTTCGAAACCTATTACTCG	57.9
ahpF mut r	TCAAAATCACCGTCAATATGGC	65.5

Table 3-2a: Primer sequences generated to develop overexpression strains (Tm is melting temperature of the oligonucleotides calculated by software provided on Sigma Aldrich website)

Primer	Sequence	Restriction site	Tm (^{o}C)
P *recA* f1	5'-TCTGAATTCCTTCTAGAGCTACTGCGTATGCATTG 3'	EcoR1, Xba1	75.9
P *recA* r1	5'-ATCCTGCAGCTACTAGTACGGATAGTCAATATGTTCTG -3'	Spe1 Pst1	72.2
P *gorA* f1	5'-TCTGAATTCCTTCTAGAGGGCATGATTGTGATTAACCC -3'	EcoR1 Xba1	76.9
P *gor A* r1	5'-ATCCTGCAGCTACTAGTATATCGTTGATTACCGCGATTG -3'	Pst1 Spe1	76.2

Table 3-2b Primer sequences generated to develop oxidative stress responsive biosensors

3.2.2 Growth medium and exposure conditions used for the study

3.2.2.1 Growth medium recipe

Bacterial cultures were prepared in two media, M9 supplemented medium and Luria Bertani (LB) broth as required, and the recipes of these media are as follows:

Luria Bertani medium: 10g/L tryptone, 5 g/L NaCl and 5 g/L yeast extract.

M9 minimal medium (Sambrook et al., 1989): The recipe for 4X stock is 64 g/L $Na_2HPO_4.7H_2O$, 15g/L KH_2PO4, 5 g/L NH_4Cl, 2.5 g/L NaCl. This was diluted four fold in deionized water and further supplemented with 2 g/L Casamino acids, 1 mM thiamine hydrochloride and 0.4% w/v glycerol as a carbon source. Plasmids based on

pSB1C3 were maintained by addition of chloramphenicol (40 µg/ml). The constructs developed using pSB1A2 were maintained by using ampicillin (100 µg/ml of culture). Cultures were grown at 37˚C at 150 rpm on a rotary shaker.

3.2.2.2 Exposure conditions

LB was used as a growth and exposure medium for the experiments involving ethidium bromide, UV radiation and hydrogen peroxide as it does not interfere with the toxicity studies as such. However, M9 minimal medium was chosen for nanoparticle exposure study for two reasons: (a) to minimize background fluorescence as LB showed a high fluorescence value on its own and (b) to reduce aggregation of silver nanoparticles (Li et al., 2011). The bacteria were inoculated and grown overnight at 37˚C on a rotary shaker at 150 rpm. For exposure studies, the optical density of the culture (600 nm) was adjusted to 0.2 by dilution with fresh medium and then silver nanoparticles were added or stress induction was performed.

3.2.3 Molecular biology techniques used to develop bioreporters and overexpression strains

PCR was carried out for DNA amplification and screening colonies. KOD hot start DNA polymerase (Novagen) was used to amplify the genes to develop biosensors and overexpression strains. The reaction mixture was obtained from Novagen and prepared according to the manufacturer's protocol. A PTC 200 DNA thermal cycler was used. The cloning was carried out by using the BioBrick vectors

as described above in RFC10 format. Forbidden restriction sites (EcoR1, Xba1, spe1 and Pst1) were removed by site directed mutagenesis.

Plasmid DNA isolation: Plasmid DNA was prepared by alkaline lysis (Sambrook et. al. 1989).

DNA purification: DNA was purified from the gel by adsorbing it on silica beads using the protocol based on the US Bioclean (US Biochemical Corporation).

Sequencing of the DNA: The sequencing was done by SBS sequencing service at the School of Biological Sciences, University of Edinburgh.

Preparing and using the competent *E. coli* cells: Competent cells were prepared by the method of Chung et al. (1989).

Gel electrophoresis: Agarose gel electrophoresis was performed in 0.8% agarose gel according to the manufacturer's protocol. Bio Rad minisub cell GT tank was used for the purpose.

3.2.4 Overexpression strains and bioreporters

3.2.4.1 Development of overexpression strains of *E. coli* for oxidative stress protection

The overexpression strains were developed by cloning genes of the OxyR and SoxR regulon *katG, sodA* and *sodB* in plasmid pSB1C3 followed by the addition of BioBrick BBa_J33207 (P*lac+lacZ'*) upstream of the coding sequence. Overexpression was achieved by addition of Isopropyl β-D-1-thiogalactopyranoside (IPTG) (90 μg/ml) to the cultures. Bioreporters were also developed by co-transforming these strains with compatible plasmid pSB4K5/BBa_K325909, which has the *lux* operon and is induced by arabinose.

The strains JM109/pPhPFD and JM109/pDps and data for solvent stress were provided by Eugene Fletcher (School of Biological Sciences, University of Edinburgh).

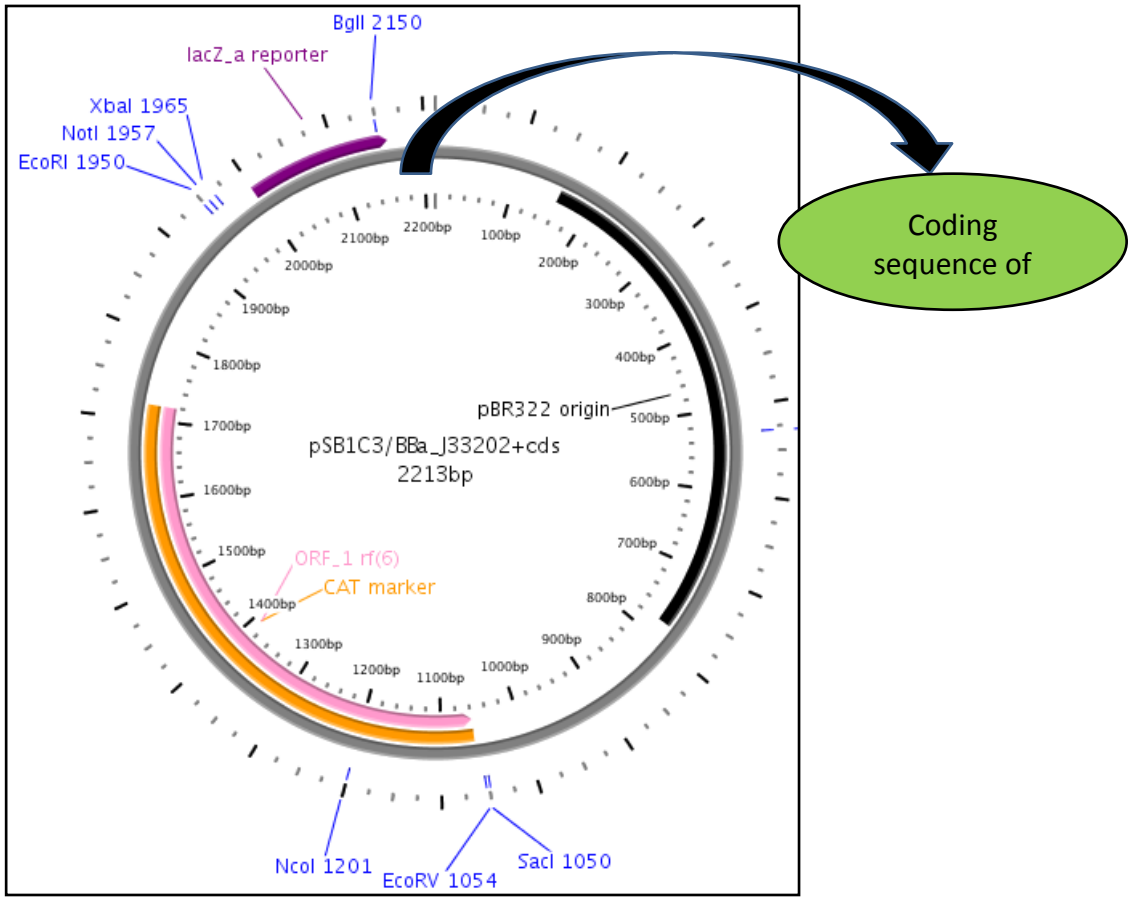

Figure 3-1: Vector assembly used to design overexpression strains

3.2.4.2 Development of oxidative stress responsive biosensors

Oxidative stress responsive biosensors were developed by fusing the promoters of the genes *recA* and *gorA* to reporter green fluorescent protein (GFP) or red fluorescent protein (mCherry). Two reporter genes were tested in order to select

for the optimum signals on induction. The assembly was made by using plasmid pSB1A2 as shown in Figure 3-1.

3.2.5 Exposure assays for developed strains

3.2.5.1 Growth and exposure conditions for overexpression strains

The strains developed for the study are illustrated in table 3-3. Characterization of these strains was carried out by exposure to inducers like ethidium bromide, hydrogen peroxide and later silver nanoparticles. The cells were grown in M9 medium (recipe described above) and the next day diluted to an OD600 of 0.1 with fresh medium and antibiotic and grown for about 3 hours on a shaker at 37^{o}C and then induced with IPTG. After three hours, the OD600 was readjusted to 0.2 and the cells were treated with silver nanoparticles. The cell viability was determined by two methods: by using the Bactiter glo kit (Promega) and by co-transforming these strains with a *lux* plasmid, pSB4K5-BBa_K325909. This resulted in overexpression strains with an additional feature/parameter to use as bioreporters. The purpose behind developing bioreporters was to make use of the fact that only live cells exhibit luminescence and it decreases in conditions that inhibit metabolism. Therefore, the impact of nanoparticles could be tested in two ways, by determining the cell viability of the samples (CFU/ml) and by measuring the luminescence of the samples. The strains were initially induced with arabinose and then exposed to silver nanoparticles. The luminescence was measured by luminometer (BS040271 Turner Biosystems). All samples were in triplicate and checked for reproducibility by using statistical analysis (student t-Test wherever applicable).

3.2.5.2 Growth and exposure conditions for oxidative stress responsive biosensors

An overnight culture of the biosensor cells was grown at 37^{o}C and next day diluted with fresh medium. It was grown for two hours (OD 600 of 0.2). The cells were induced with ethidium bromide in the range of 0.32 μM to 0.6 μM. Fluorescence was measured using a Turner Biosystem single cell fluorometer.

GFP (green fluorescent protein) based biosensors were initially developed and tested. Primary characterization of the biosensor cells showed a high background fluorescence value (the fluorescence value for P*recA+gfp* (uninduced) sample was 18090 FSU at time zero in LB and 18665 in M9 medium). It was therefore decided that RFP (red fluorescent protein) based biosensors could perhaps function better. The rationale was that RFP possibly enables using longer wavelengths for both stimulation and emission and that could reduce the background fluorescence. The excitation/emission range for GFP is 395/509 nm whereas for mCherry, it is 587/610 nm. mCherry also has a longer maturation time and is more photo stable than GFP which is prone to auto bleach (Beers and Sizer, 1952).

This also demonstrated the benefits of designing parts as individual BioBricks, which provides flexibility while adding or replacing parts, as in this case the reporter gene could be changed easily.

3.2.6 Chemicals and assays

Catalase (catalogue number C1345) was used to prepare standards to monitor peroxidase activity of strain JM109/pKatG. It was sourced from Sigma Aldrich and suspended in PBS (5 mg/ml) and added to the cultures to achieve a final

concentration of 100 units per ml of bacterial culture. In order to determine cell viability by alternate methods, ATP assay was performed using the Bactiter Glo Kit from Promega (catalogue number G8233). Cell viability was assessed by serial dilution and plating on L-agar. Luminescence of non-specific reporter strains and ATP assays were measured using the luminescence module of the multimode reader (BS040271 Turner Biosystems). Fluorescence of specific bioreporter strains was measured using the same instrument with the Green fluorescence module.

3.2.7 Nanoparticle source and characterization

10 nm silver nanoparticle dispersion at 20 mg/L concentration was obtained from Sigma-Aldrich (catalogue number 730785). Size characterization was carried out by Dynamic light scattering (DLS) using a ZETAPALS 90 submicron analyser. (Brookhaven Instruments Corporation Holtsville, NY, USA). The samples were sonicated prior to use. The data were collected in triplicate at 25^{o}C.

The extent of metal dissolution from the nanoparticle surface was determined by ICP-OES. The silver nanoparticles were suspended in M9 supplemented medium and incubated on a shaker (200 rpm) at 37ºC for two hours. The supernatant was recovered by centrifugation at 3000g and filtered using an Amicon filter (3000 MWCO) for one hour at 16^{o}C. It was acidified by 2% (v/v) nitric acid and used for ICP-OES analysis (Singh and Ramarao, 2012).

3.2.8 Characterization of overexpression strains

The overexpression strains for catalase, prefoldin and Dps, were characterized by measuring the growth kinetics and then tested for their response

against known stress inducers like peroxide and organic solvents. The following induction tests were done on developed strains:

3.2.8.1. Catalase assay

The catalase overexpressing strain JM109/pKatG was characterized by catalase assay and exposure study using hydrogen peroxide. The absorbance assay (Stern, 1937, Beers and Sizer, 1952) was used. Cells were grown overnight in LB. The next day the culture was diluted with fresh medium and grown for 2 hours to OD600 of 0.4 and then induced for 2 hours with IPTG (90 μg/ml). Cells were sonicated with brief pulses of 5 seconds separated by an interval of 30 seconds (total 4 pulses). The lysate was used for catalase assay. All the solutions were made in 1mM potassium phosphate buffer adjusted to a pH of 7-7.5 with 1M KOH. This buffer was cooled and then used to make a 0.03% w/w H_2O_2 solution. Catalase standards (100, 25 and 6 units/ml stocks) were prepared in the same buffer. Hydrogen peroxide has an absorption peak at 240 nm and the extinction coefficient is 43.6 $M^{-1}cm^{-1}$ at 240 nm (Nobles and Gibson, 1970). The buffer was used as a blank, and then absorbance of peroxide was adjusted to 0.5. Catalase activity was determined by measuring the rate of decrease in absorbance at 240 nm and the time taken was recorded to calculate the enzyme activity per ml of culture.

3.2.8.2 Hydrogen peroxide assay

The developed strain JM109/pKatG was tested against hydrogen peroxide. The induction and exposure method was as described in section 3.2.5.1 earlier. A final concentration of 0.75-2.5 mM peroxide was used per ml of cell culture at an

OD600 of 0.2. The cell viability was determined using the Bactiter ATP kit and the percentage change in relative luminescence (RLU) was calculated by normalizing the values to control samples without peroxide. Furthermore, the protective response of catalase was determined by a disc diffusion assay. The method of Ishikawa *et al* (2003) was optimised. The induced cells were spread on a LB agar plate containing chloramphenicol (40 μg/ml) and IPTG (90 μg/ml), at OD600 of 0.1 and then a sterile filter paper was soaked in hydrogen peroxide (0.2 mM final concentration in agar plate) and placed at the centre of plate. The plates were incubated at 37^{o}C and the following day the zone of exclusion was measured for each of the samples. All assays were performed in duplicate.

3.3 Results

3.3.1 Overexpression strains for production of proteins protecting against oxidative stress were developed.

The strains to overproduce proteins like catalase, superoxide dismutase and peroxidase were constructed (Table 3-3). Growth kinetic studies of these strains with and without induction with IPTG were done. It was observed that the induced samples of all the strains exhibited a lower growth rate than the uninduced samples (Figure 3-2). The probable reason could be that overexpression of the proteins was creating a metabolic burden.

Bacterial strain	**Genotype**	**Source**
E. coli JM109/pKatG	Overexpress catalase	This work
E. coli JM109/pSodA	Overexpress superoxide dismutase A	This work
E. coli JM109/pSodB	Overexpress superoxide dismutase B	This work
E. coli JM109/pSodC	Overexpress superoxide dismutase C	This work
E .coli JM109/pGorA	Overexpress glutathione oxidoreductase	This work
E. coli JM109/pDps	Overexpresses "DNA protection during starvation" protein	E. Fletcher
E. coli JM109/pPrefoldin	Overexpress prefoldin	E. Fletcher
recA mutant host strain *E. coli* (JM109) with *recA* assembly	pSB1A2 with promoter of *recA* fused to gfp/mCherry	This work
recA mutant host strain *E. coli* (JM109) with *gorA* assembly	pSB1A2 with promoter of *gorA* fused to gfp/ mCherry	This work
Wild type *E. coli* MG1655 with *recA* assembly	pSB1A2 with promoter of *recA* fused to gfp/mCherry	This work
Wild type *E.coli* MG1655 with *gorA* assembly	pSB1A2 with promoter of *gorA* fused to gfp or mCherry	This work
E.coli.JM109pPrefoldin/DPS+ pSB4K5_BBa_K325909	Lux biosensor developed by adding pSB4K5/BBa_K325909	E. Fletcher

Table 3-3: Strains overexpressing catalase (KatG, KatE), superoxide dismutase (SodA, B, and C), prefoldin and DNA binding protein (Dps) have been used. Two strains of *E. coli* (JM109 and K12) have been used to develop biosensors

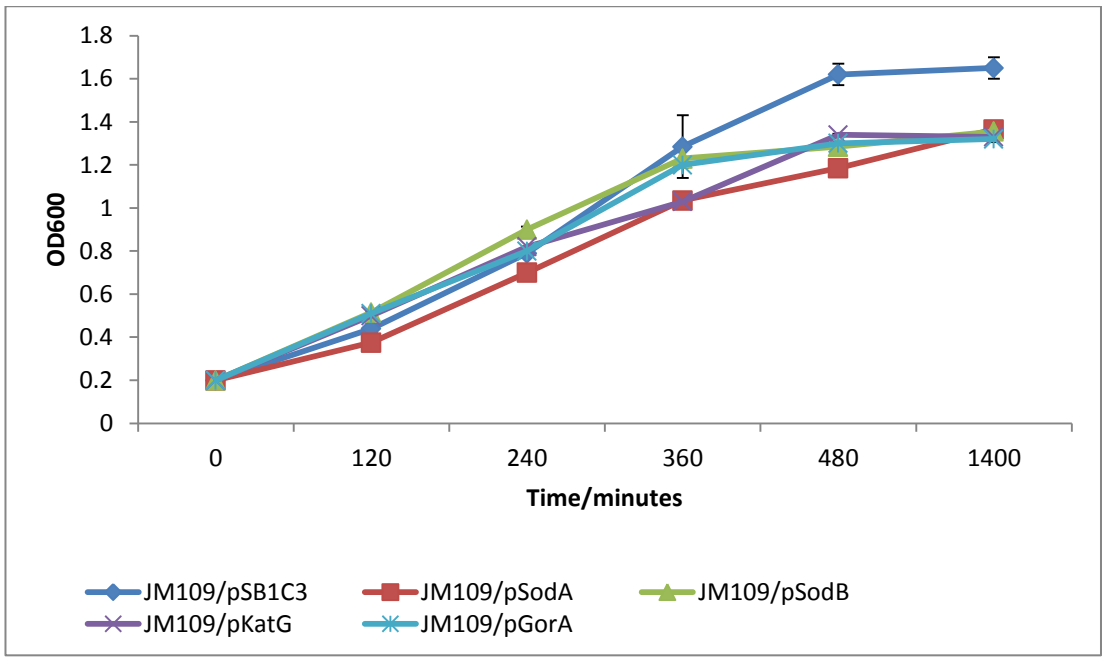

Figure 3-2a: Growth curve of overexpression strains without induction with IPTG

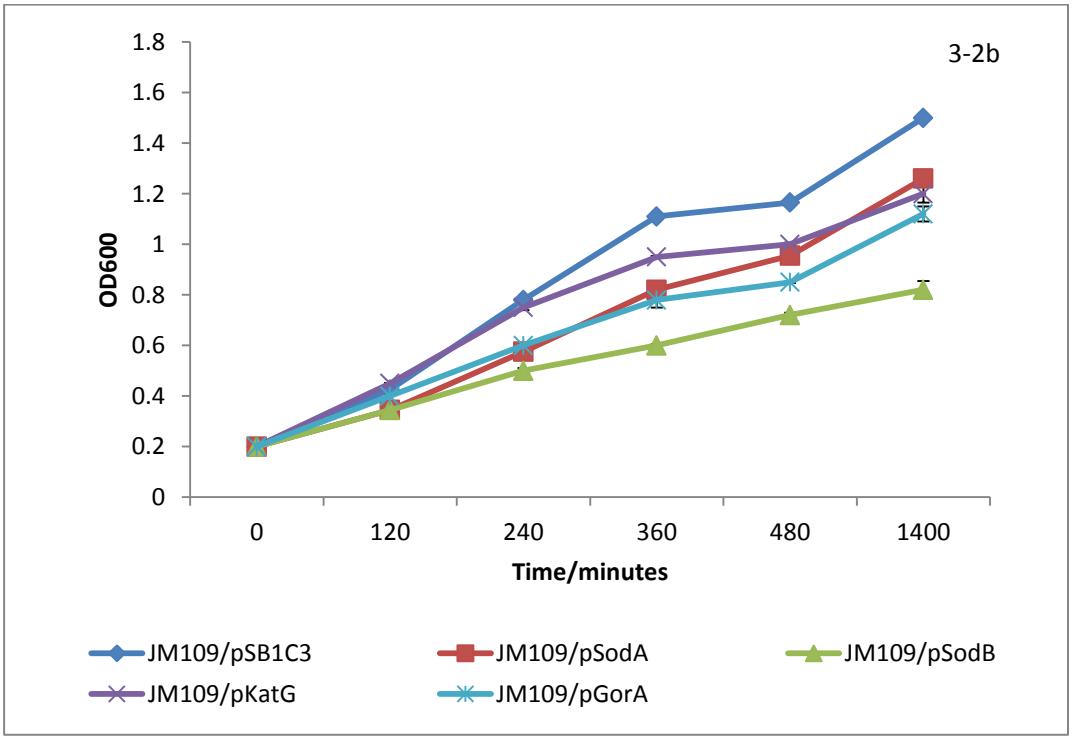

Figure 3-2b: Growth curve after induction with IPTG

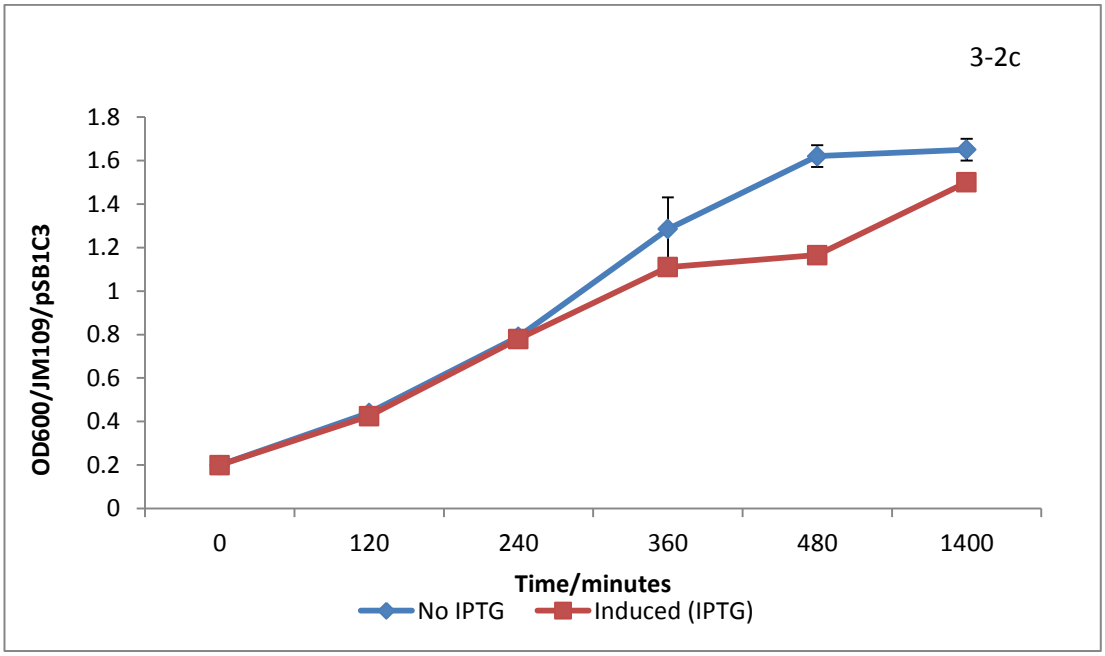

Figure 3-2c: Comparison of growth kinetics for JM109/pSB1C3

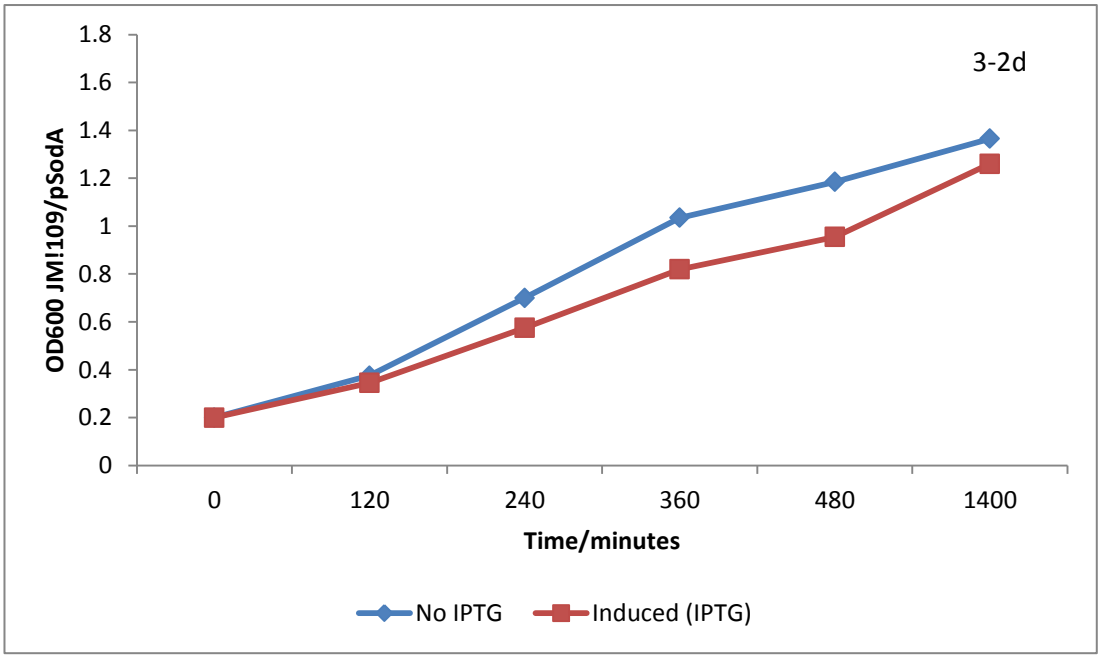

Figure 3-2d: Comparison of growth kinetics for JM109/pSodA

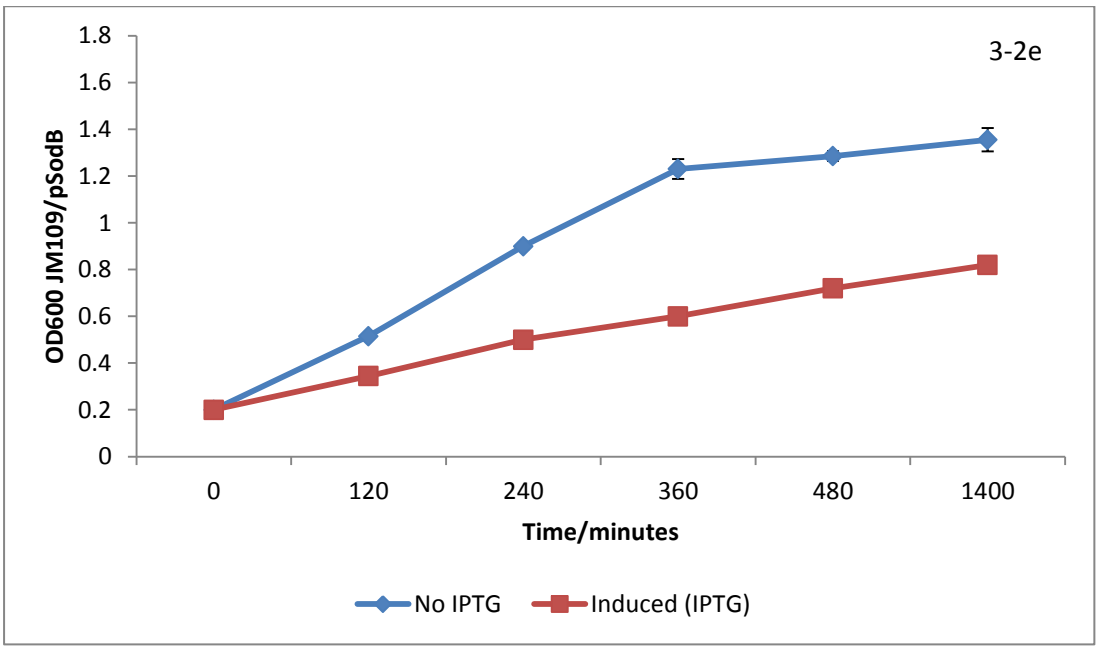

Figure 3-2e: Comparison of growth kinetics for JM109/pSodB

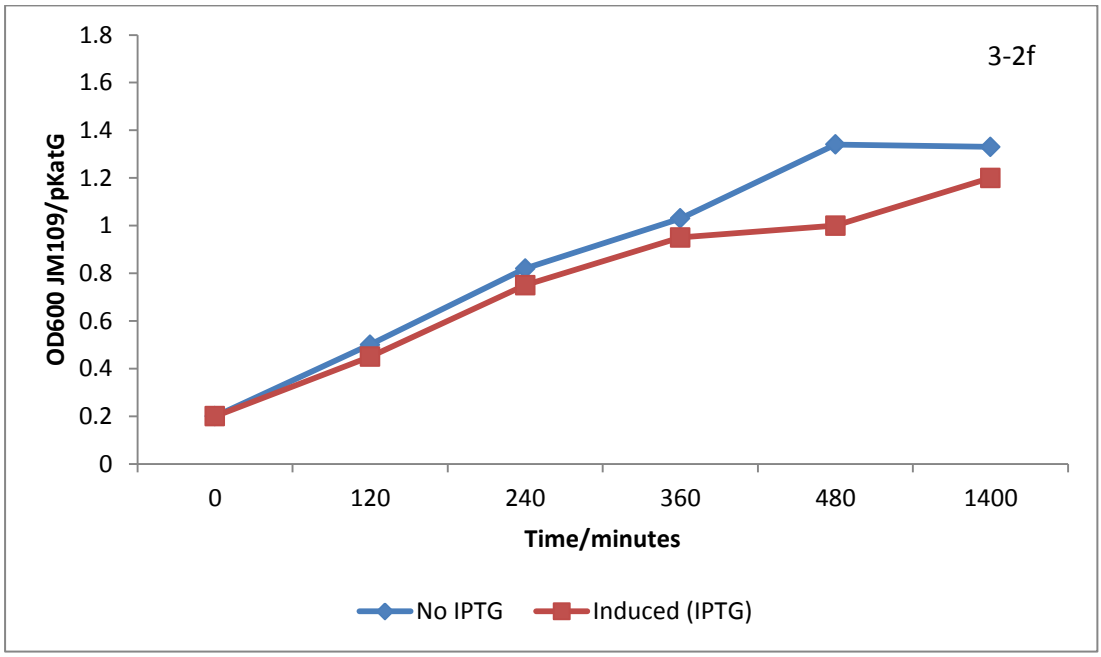

Figure 3-2f: Comparison of growth kinetics for JM109/pKatG

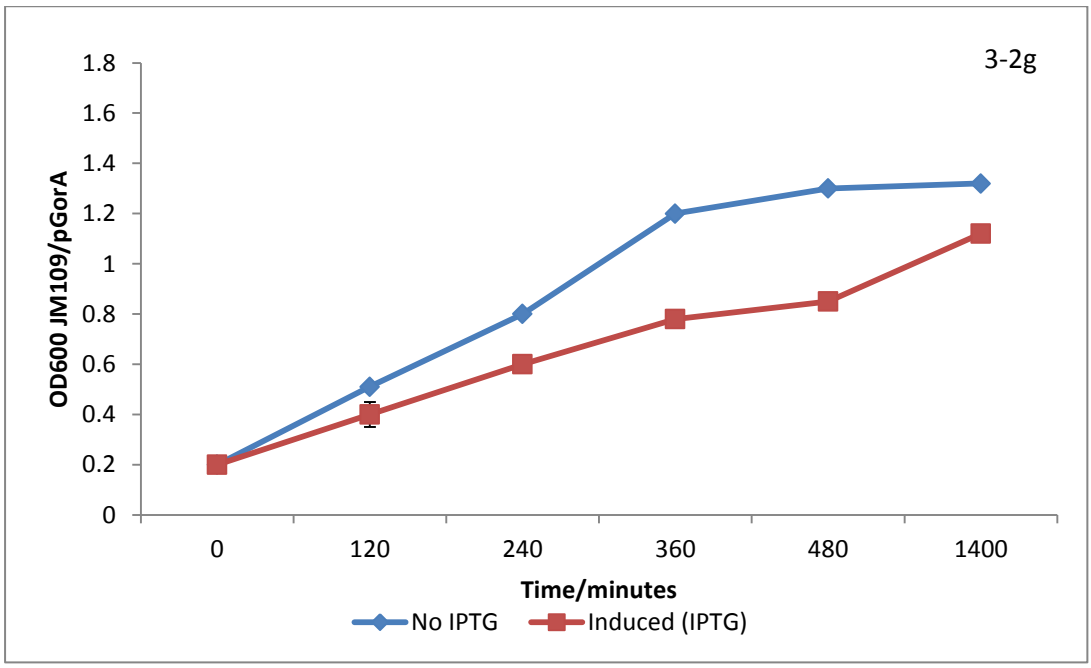

Figure 3-2g: Comparison of growth kinetics for JM109/pGorA

3.3.2 A catalase overexpressing strain was developed and shows resistance to hydrogen peroxide

Catalase overproducing strain JM109/pkatG was initially tested for catalase activity as described previously (section 3.2.8.1). The overexpression strain JM109/pKatG showed about five times higher enzyme activity than the control strain (5 units/ml catalase production approximately). Disc diffusion assay using hydrogen peroxide absorbed on a sterile filter paper also showed a reduced zone of exclusion for this strain (Figure 3-3).

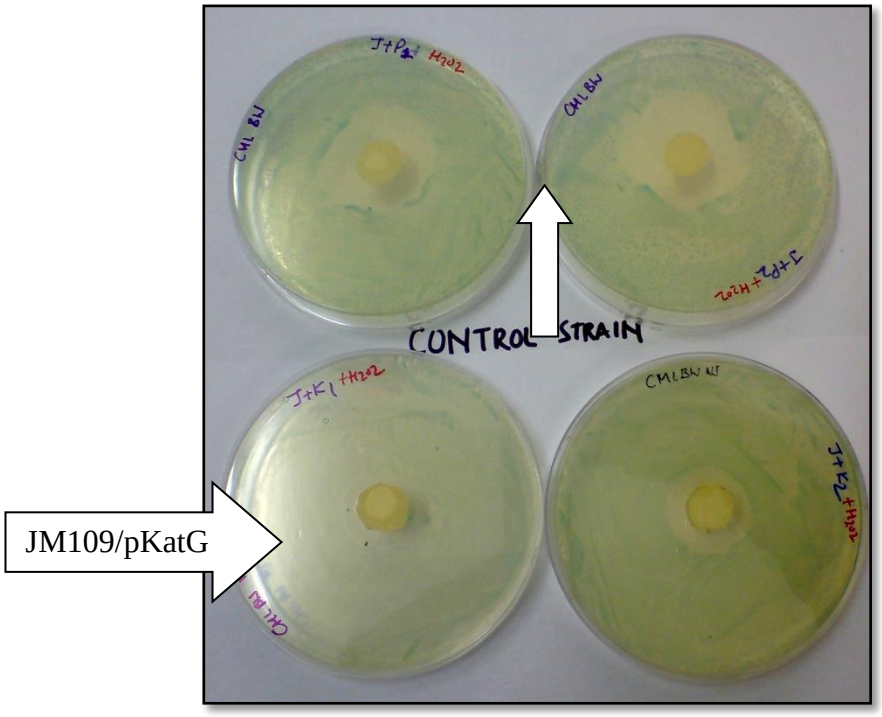

Figure 3-3: Disc diffusion assay for catalase overexpressing strain. The two plates in bottom panel have the catalase overexpressing strain, JM109/p KatG, while plates in the top panel are the vector control strain, JM109/ pSB1C3.

This strain was also tested against hydrogen peroxide and the cell viability was determined by using Bactiter Glo kit as shown in Figure 3-4a and 3-4b. The samples exposed to hydrogen peroxide were spread on L-agar plates and it was observed that catalase overproducing strain showed lower cell cultivability than the control strain (Figure 3-5). This is an important observation also recorded with other overexpression strains. Presumably, the overexpression of certain genes might be detrimental to cell viability and culturability. These genes are usually up regulated in oxidative stress conditions and overexpression of certain proteins can affect the cell growth kinetics. This can explain to some extent the reduced growth rate of cells expressing catalase.

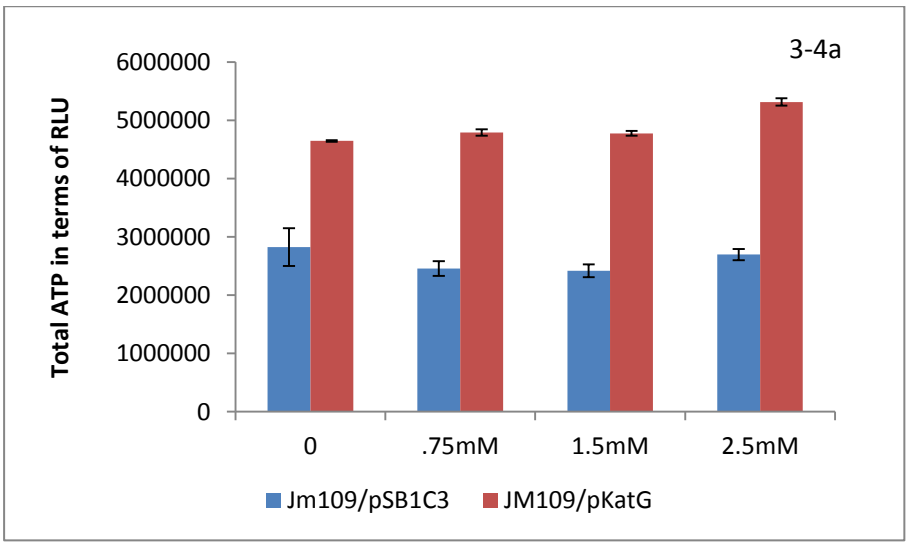

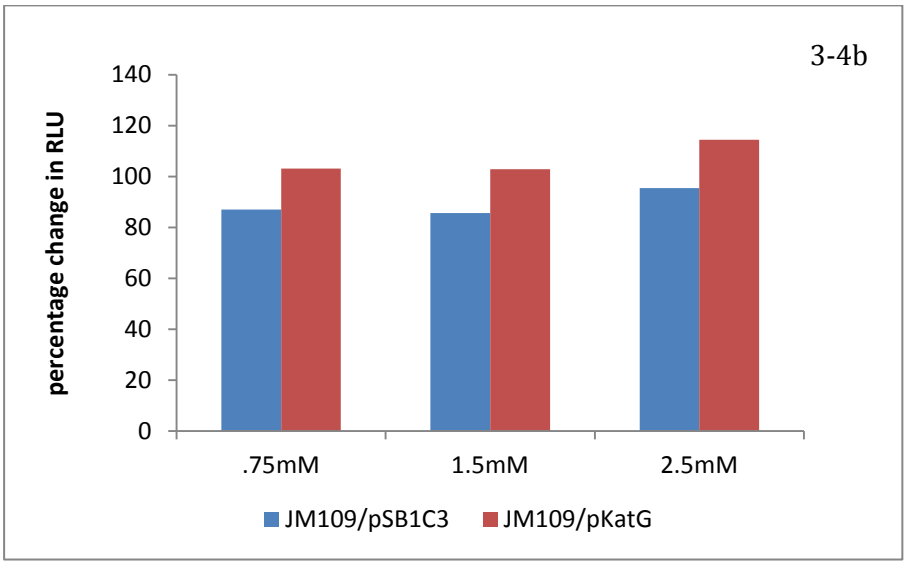

Figure 3-4a and 3-4b: Hydrogen peroxide exposure assay using Bactiter kit. JM109/pSB1C3 (control strain), JM109/pKatG is catalase producing strain

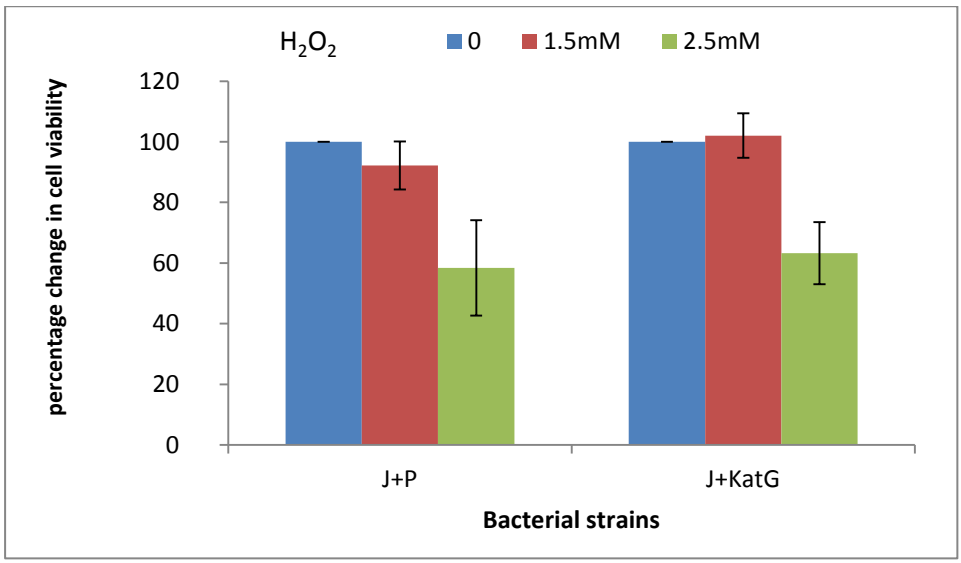

Figure 3-5: Cell viability of catalase overexpressing strain after exposure to hydrogen peroxide. X axis represents the bacterial strains and y axis shows the percentage change in cell viability normalized to controls of each of the strains.

3.3.2.1 Response of catalase overproducing strain to silver nanoparticles

Exposure to increasing concentration of silver nanoparticles demonstrated that this strain did not show a significant resistance to silver nanotoxicity as shown in Figure 3-6. The strain JM109/pKatG did not show higher cell viability and it was difficult to draw a significant conclusion from this observation. The fact that it showed a poorer growth than the control strain raises questions about the choice of this strategy to investigate silver nanotoxicity. This observation is in agreement with other experiments conducted using the overexpression strains.

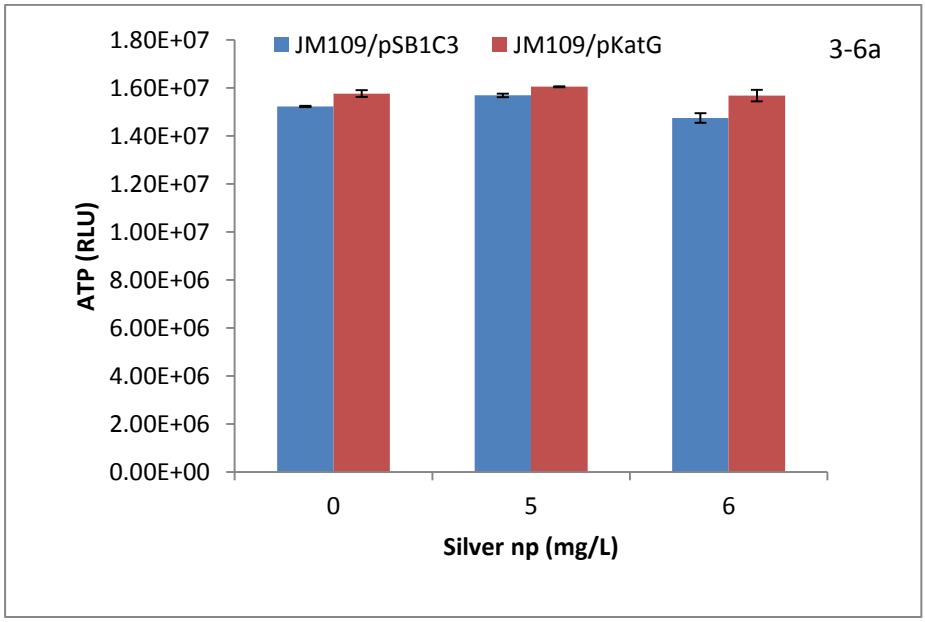

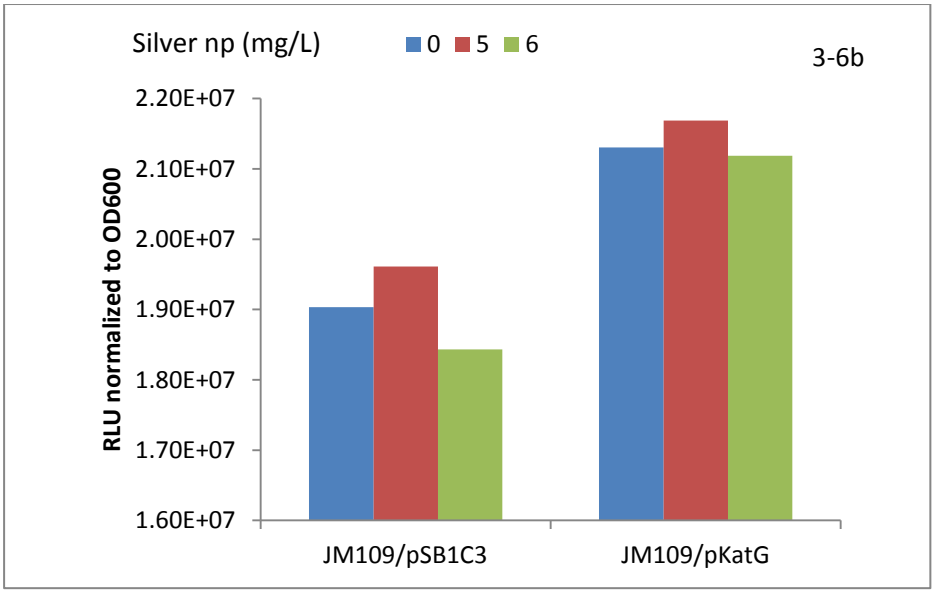

Figure 3-6a and 3-6b: Response of JM109/pKatG against silver nanoparticles, cell viability measured by bactiter kit. Y-axis shows relative luminescence units and x- axis the bacterial strain.

3.3.3 Response of strains JM109/pSodA and JM109/pGorA to silver nanoparticles

The superoxide dismutase overproducing strain (JM109/pSodA) showed poor growth even without addition of any toxins. On exposure to silver nanoparticles, it showed a sharp drop in cell viability in contrast to the control strain, JM109/pSB1C3, which showed a consistent drop in percentage survival (Figure 3-7b). The GorA overproducing strain, JM109/pGorA showed low cell culturability, however it did show a marginal increase in cell number on addition of silver nanoparticles (Figure 3-7b). It was difficult to draw a conclusion from this experiment, although this assay was reproducible.

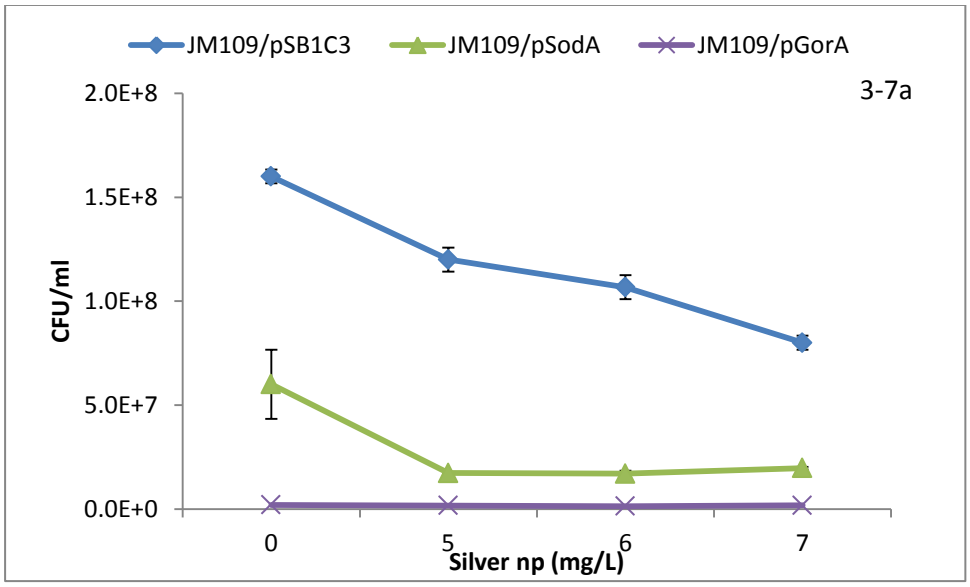

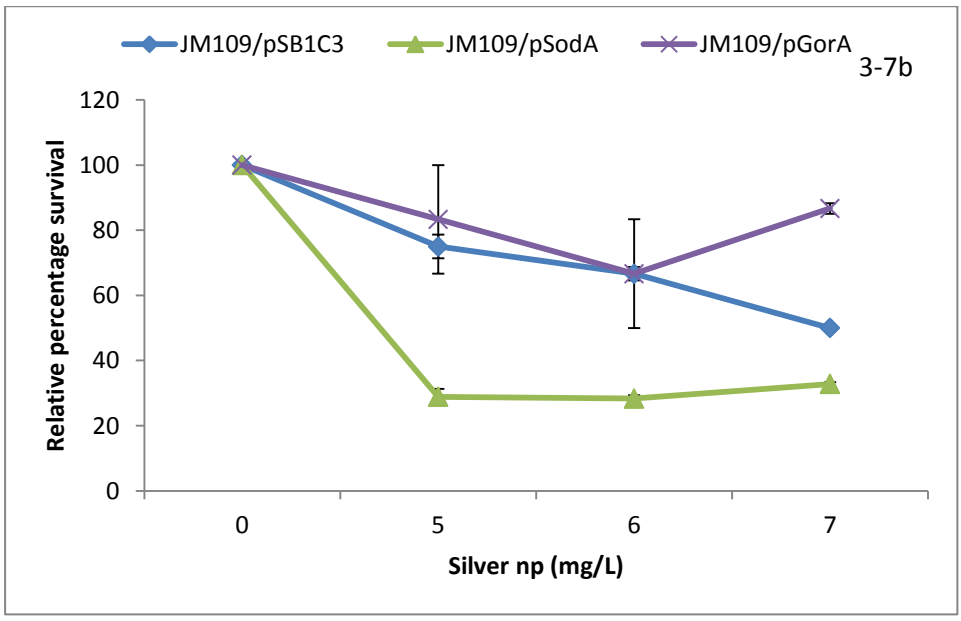

Figure 3-7a and 3-7b: Response of overexpression strains to silver nanoparticles

3.3.4 Characterization of the prefoldin and Dps overexpressing strains

One objective of the research was to identify the nature of stress produced by silver nanoparticles; it was a reasonable approach to test certain strains that overproduce enzymes synthesized by microorganisms in stress conditions. This was an attempt to investigate the impact of nanoparticles by exposing strains specially modified to produce proteins associated with protective response in bacteria. The strains overexpressing prefoldin and DNA binding protein (Dps) were initially tested for their response towards organic solvents like ethanol and butanol as a primary characterization of the strains by E. Fletcher and were subsequently used in this project. The growth and exposure methods are described earlier in experiments. Ethanol (4%) and butanol (0.5% v/v) were selected as toxic agents as they have been

shown to affect cell membrane integrity. The cell viability for this assay was determined at time 0 and at the end of the experiment (24 hours incubation period).

It was observed that at the end of the exposure period the overexpression strains, JM109/pPhPFD and JM109/pDps exhibited a variable response towards the organic solvents. The prefoldin overexpressing strain was found to be resistant to both ethanol and butanol (Figure 3-8) whereas, the Dps producing strain was more resistant towards ethanol (Figure 3-8a).

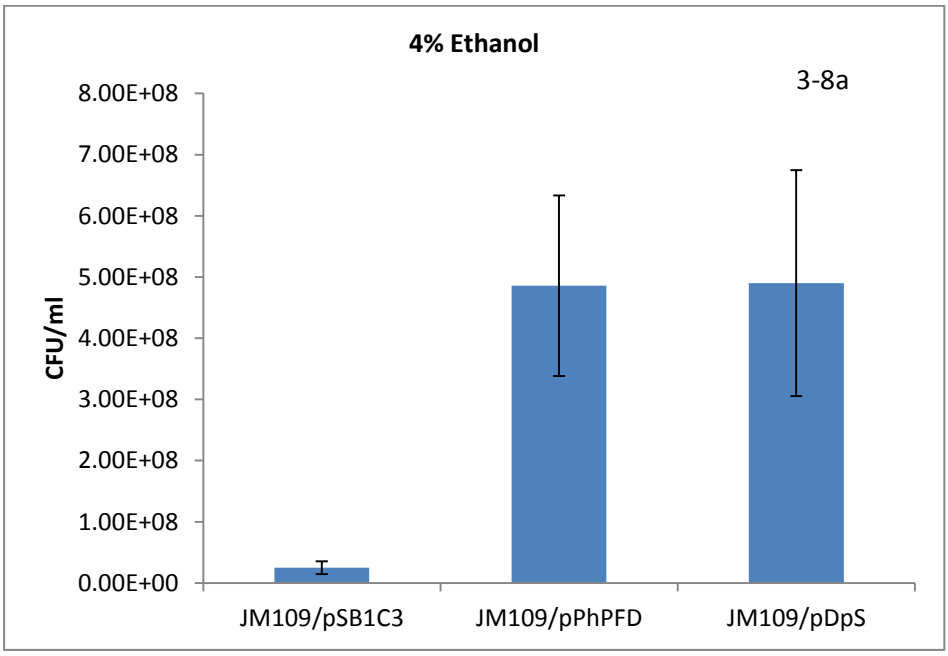

Figure 3-8a: **Cell viability of two strains after 24hours exposure to 4% ethanol**

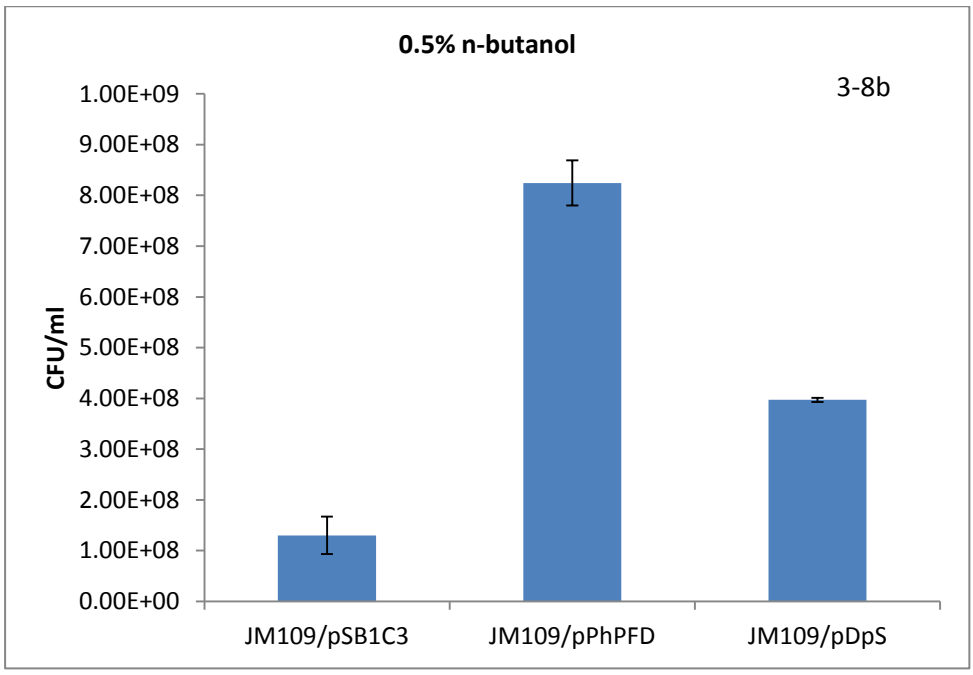

Figure 3-8b: Cell viability of two strains after 24hours exposure to 0.5% butanol (E.Fletcher's unpublished data).

Bioreporters were developed by co-transforming these two strains with *lux* plasmid pSB4K5/BBa_K325909 (details in section 3.2.5.1) and the cell viability was then measured in terms of change in luminescence after exposure to ethanol and butanol. It was seen that these strains also showed a similar response to both the solvents. Prefoldin overexpression helped to minimize solvent toxicity for both butanol and ethanol (Figure 3-9). However, the Dps overexpressing strain was found to be more susceptible to butanol as shown in Figure 3-9b.

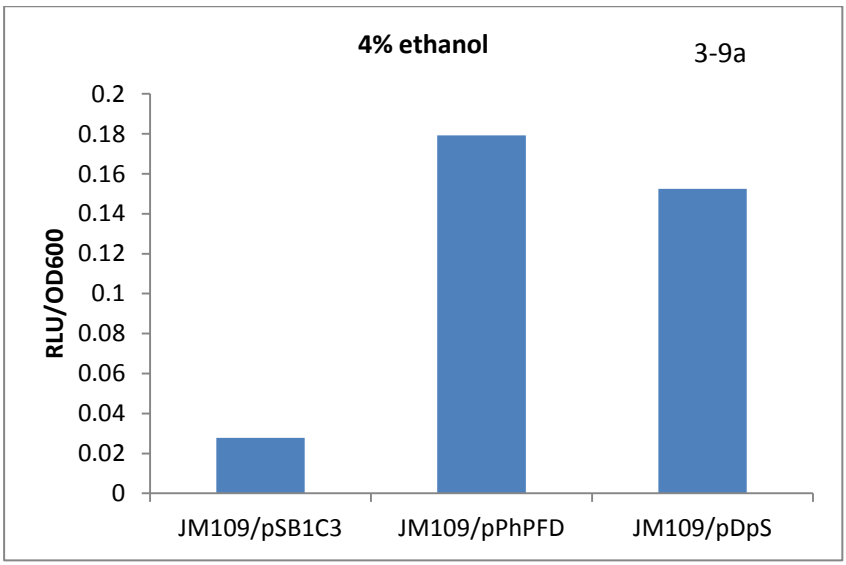

Figure 3-9a: Response of Bioreporters to 4%ethanol

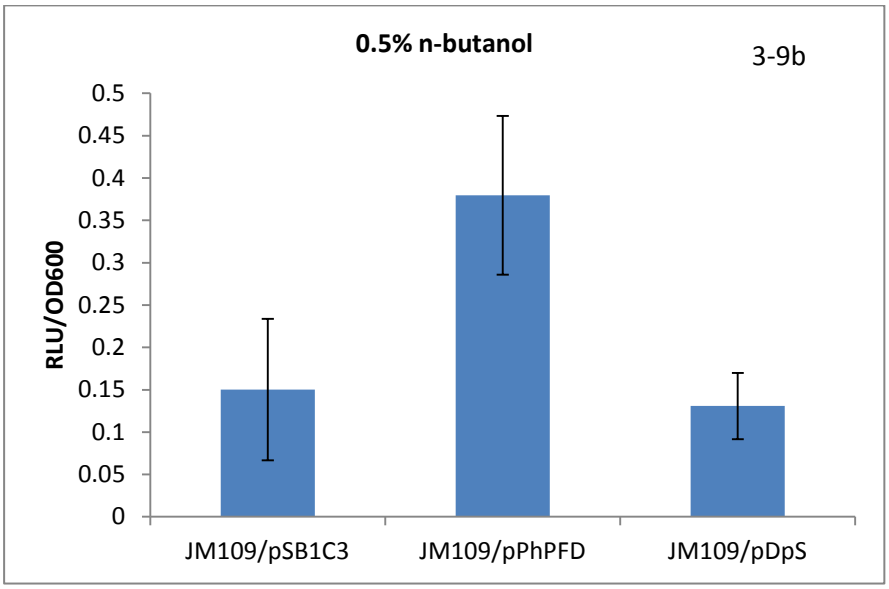

Figure 3-9.b: Response of Bioreporters to 0.5% n-butanol

3.3.4.1 Production of DNA binding protein, Dps protects against silver nanotoxicity

The two strains JM109/p PhPFD and JM109/pDps were tested (details provided in the methods section) and found to be resistant to silver nanotoxicity.

Besides the ATP assay, co-transformation of these strains with pSB4K5/BBa_K325909 (a plasmid with *lux* operon) also helped to detect if they showed any resistance towards silver nanotoxicity (Figure 3-10). The overexpression strains registered a lower drop in luminescence on addition of silver nanoparticles than the control strain JM019/pSB1C3 as shown in Figure 3-10a and 3-10b. These treated samples were used to check the cell viability. It was observed that the control strain showed a consistent drop in cell number but the Dps overproducing strain showed resistance towards silver nanotoxicity (Figure 3-10c).

The data was analyzed by student t-Test and the p values determined. The control strain JM109/pSB1C3 showed drop of 25% in cell viability at 5 mg/L ($p=0.03$) but at 6 mg/L it shows a greater reduction in cell numbers in comparison to DpS overexpressing strain. JM109/pDps initially showed a drop in survival at 5 mg/L ($p=0.03$) but between 5 and 6 mg/L silver np, it showed statistically insignificant reduction ($p=0.4$). JM019/pPhPFD showed a statistically significant reduction at both concentrations.

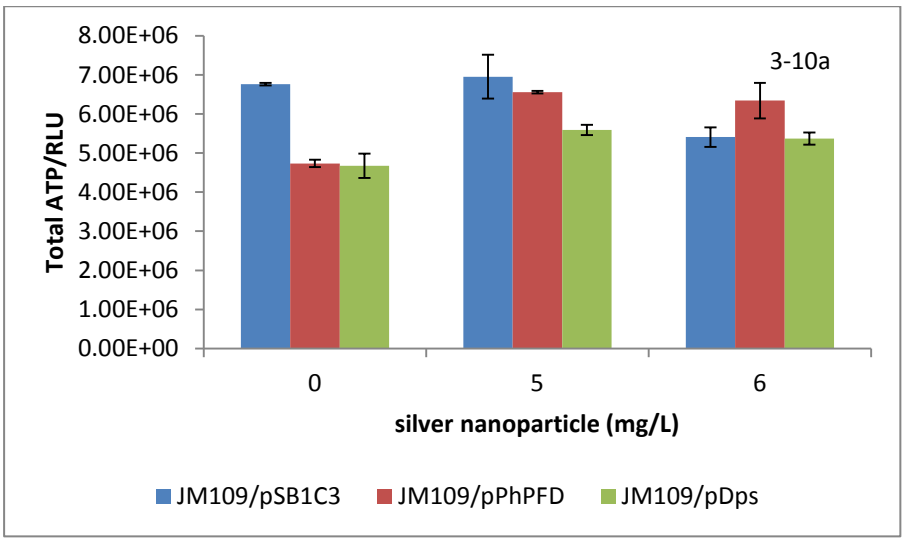

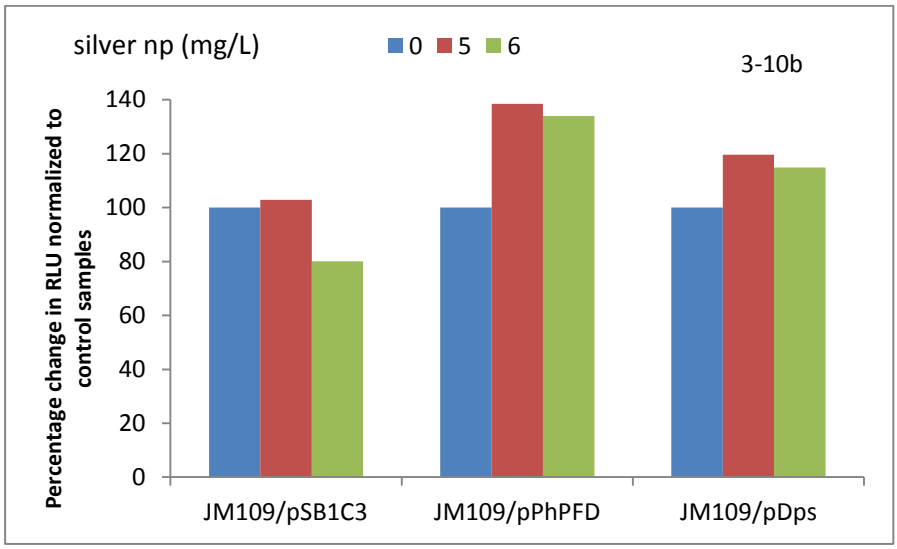

Figure 3-10a and 3-10b: cell viability test using ATP kit

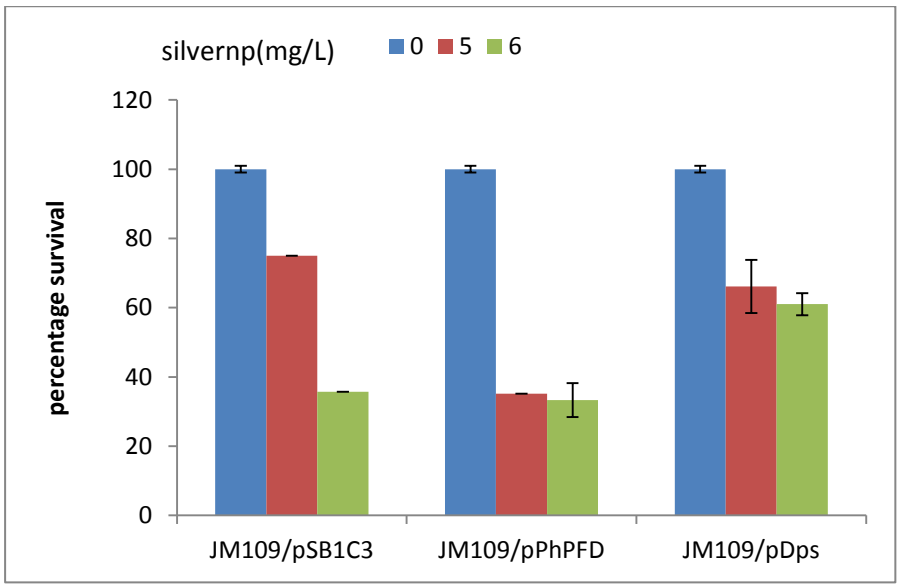

Figure 3-10c Cell viability normalized to the control samples

3.3.5 Development of oxidative stress responsive biosensors

Oxidative stress responsive biosensors were developed by cloning the promoters of *recA* and *gorA* genes of *E. coli* and adding a reporter gene (*mCherry gfp*) downstream, the details have been discussed in method section 3.2.5.2. These biosensors were characterized and tested against known stress inducers like ethidium bromide (for P*recA*) and hydrogen peroxide (for P*gorA*) respectively. Ethidium bromide (0-0.6 μM) was used for initial characterization of biosensors. Since the lab strain of *E. coli*, JM109, is *recA* deficient, the wild type strain, *E. coli*/MG1655 was also transformed with the biosensor plasmids, pSB1A2_P*recA*+*mCherry* (RFP) and pSB1A2_P*gorA*+*mCherry* (RFP). The biosensors were tested against known inducers UV radiation, hydrogen peroxide and ethidium bromide to check their sensitivity levels prior to being used in nanoparticle exposure studies.

3.3.5.1 Impact of UV exposure on the Biosensor activity

UV radiations are specific inducers for *recA*. The cells were grown in LB and next day diluted to an OD600 of 0.1 and grown further for 2 hours (37^{o}C on a rotary shaker). After adjusting the OD600 to 0.2, approximately 15 ml of culture was poured into a petri dish and exposed to UV radiation (254 nm) for a period of three minutes. Plates were wrapped in foil and left in the dark for thirty minutes in order to avoid photo reactivation/photolyase repair activity. The fluorescence reading was recorded for two time points: T0, before the start of the UV exposure and T30 (thirty minutes after recovery). Figure 3-11 shows the T30 reading. No such induction was seen in the biosensor with *gorA* promoter. The biosensor P*recA+gfp* (MG1655) showed an appreciable increase in fluorescence, thereby demonstrating that the constructed biosensor, *PrecA+gfp* was responsive and active.

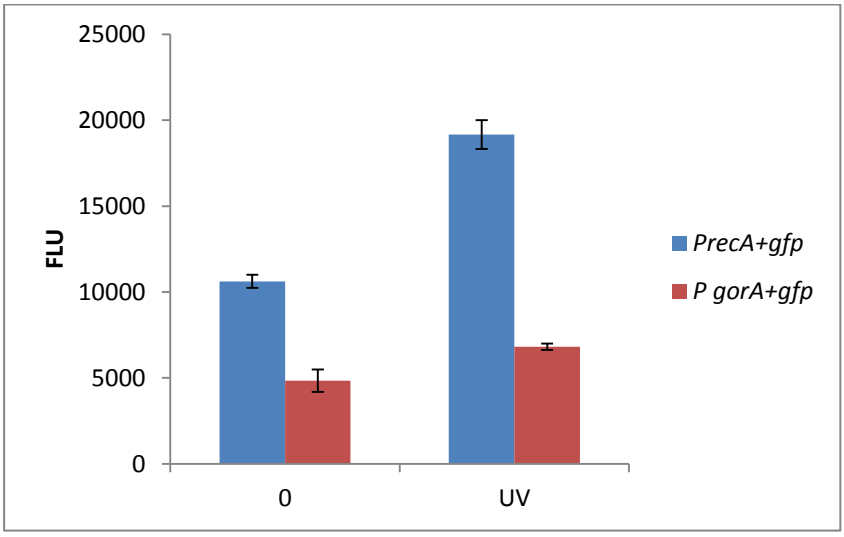

Figure 3-11: Impact of UV radiations on the biosensor activity

3.3.5.2 Impact of addition of hydrogen peroxide

The cells were exposed to hydrogen peroxide (2 and 4.4 mM) and the fluorescence was recorded after two time intervals, 15 minutes and 30 minutes.

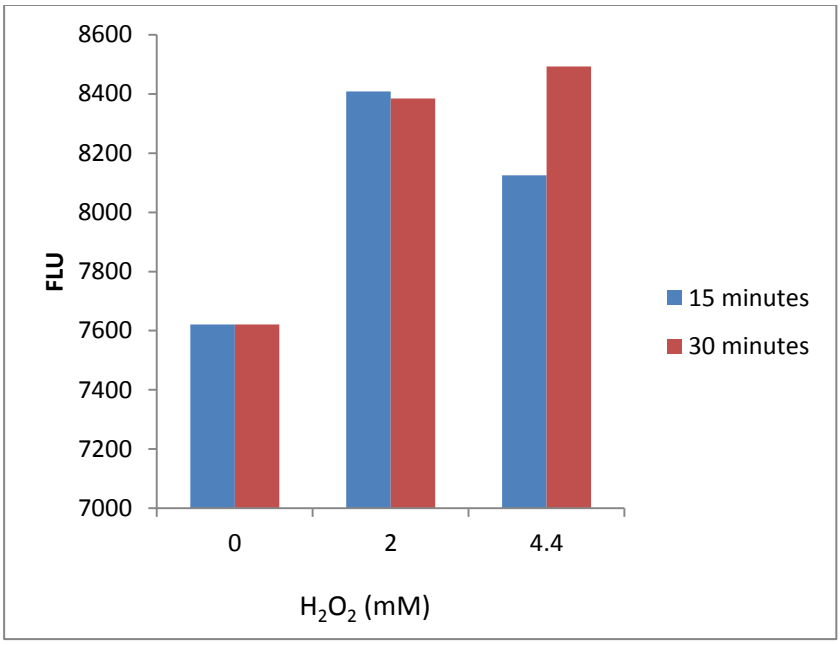

Figure 3-12: Response of P*gorA*+*gfp* against hydrogen peroxide

The biosensor P*gorA*+*gfp* showed an overall increase in fluorescence after 30 minutes (Figure 3-12). The subsequent assays were conducted using mCherry (RFP) based biosensors. The fluorescence of M9 was also measured and subtracted from the final reading. Strain MG1655 was used as the host cells since it showed a better response to ethidium bromide.

3.3.5.3 Response of biosensors to ethidium bromide

The wild type *E. coli* (MG1655) carrying the biosensor pSB1A2/P*recA*+mCherry showed an increase in fluorescence on the addition of

ethidium bromide. There was also an increase observed in the controls without ethidium bromide but it was not statistically significant. The biosensor with *recA* promoter showed a maximum increase after 1.5 hours (Figure 3-13a) whereas the one with *gorA* promoter responded better after longer exposure duration of 15 hours (Figure 3-13b). The statistical analysis using student t-Test showed that a significant change in fluorescence was shown by the biosensor P*recA*+mcherry at 0.32 μM (p=.01) ethidium bromide whereas P*gorA*+mcherry did not show significant response towards ethidium bromide.

A similar experiment was conducted on the *E. coli*/JM109 cells and the biosensor P*recA*+mCherry showed a significant increase in fluorescence at 0.32-0.48 μM ethidium bromide concentration (Figure 3-14a) ($p<0.05$ at 0.32, 0.48 and 0.6 μM ethidium bromide). At the end of fifteen hours of incubation, significant differences were observed (Table 3-4). Means of the control and the induced samples were used to determine p values, with values <0.05 signifying statistical differences in the response to induction. The biosensor P*gorA*+mCherry showed a statistically significant increase in fluorescence at 0.48 and between 0.32 and 0.6 μM ethidium bromide concentration (p=0.005 and 0.008 respectively).

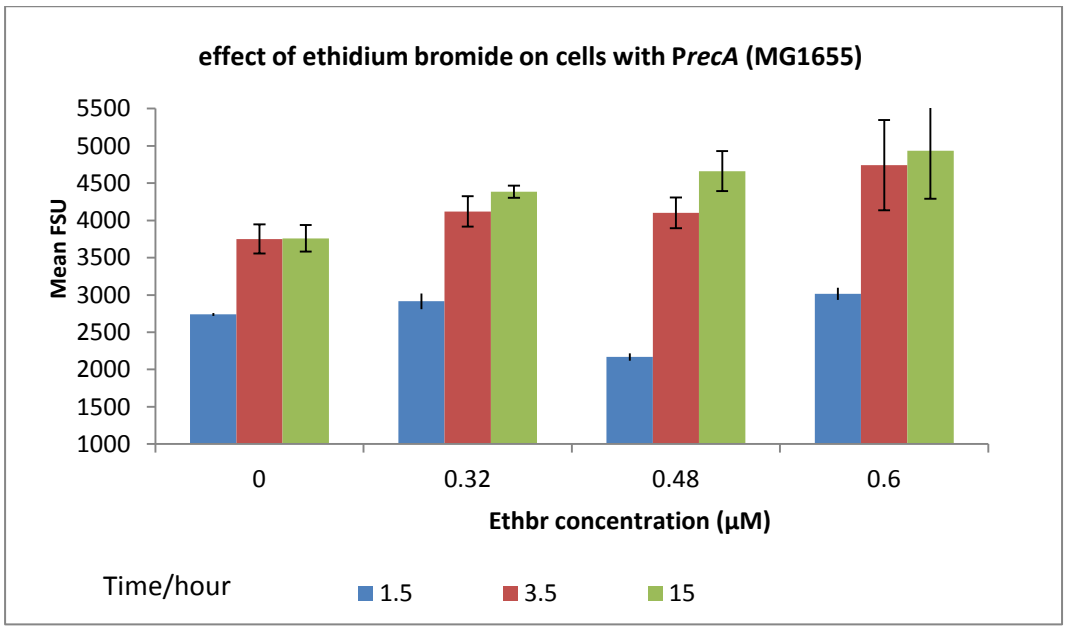

Figure 3-13a: The response of biosensors against ethidium bromide

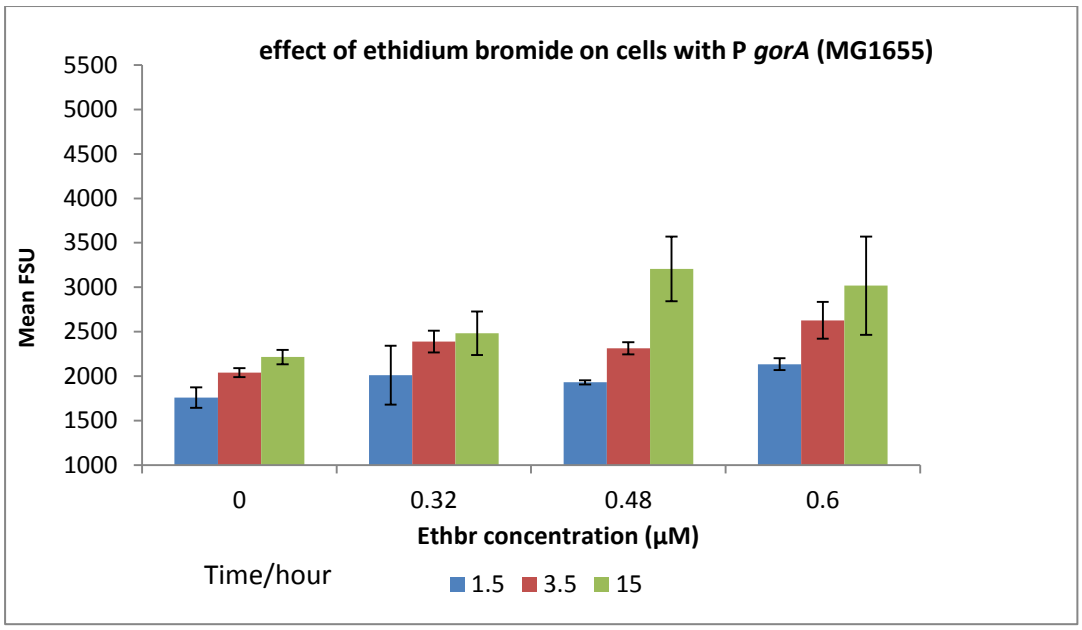

Figure 3-13b Strain specific response of the biosensors in *E. coli*/MG1655

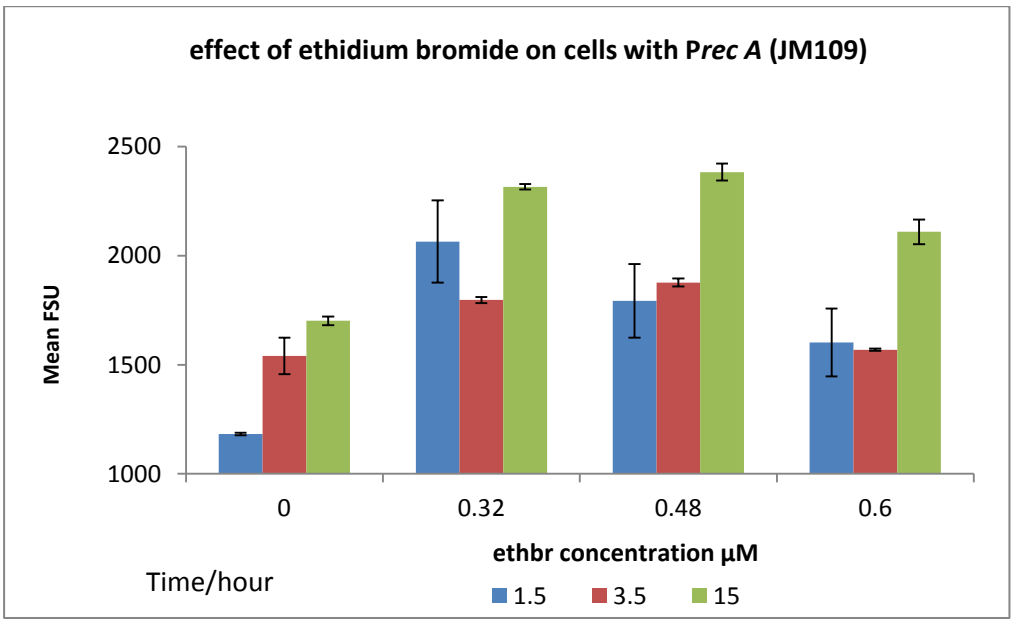

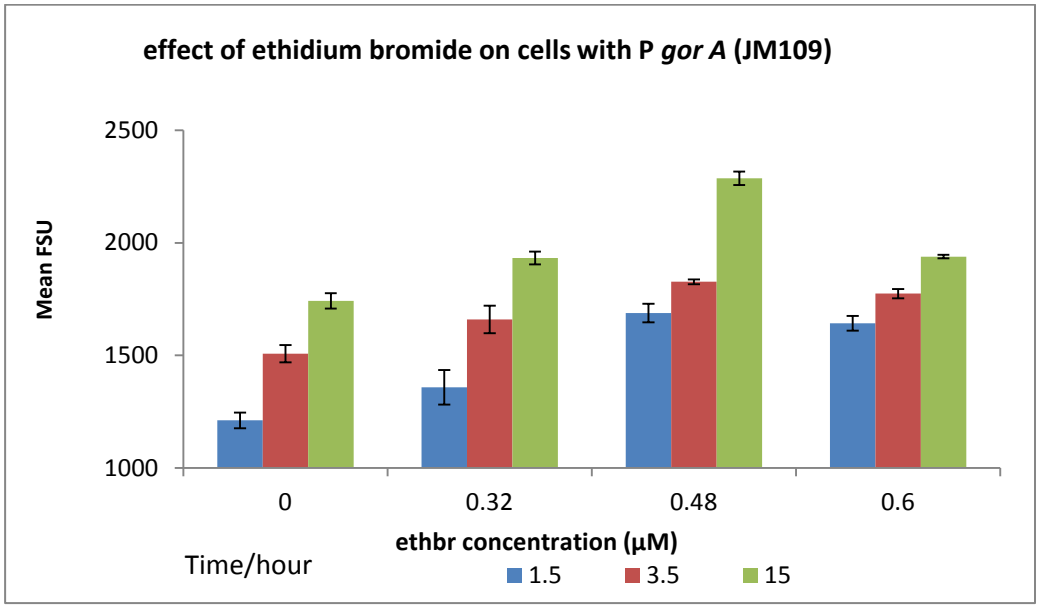

Figure 3-14a and 3-14b: JM109 used as host strain for ethidium bromide exposure

The t- test indicates that there is a significant difference in the *p* values of the control and the induced samples at the end of fifteen hours of incubation. When the *p* values of the induced samples were compared amongst themselves (Table 3-4 and 3-5), no

significant changes were observed except for JM109 cells in concentration range of 0.32μM and 0.6 μM. The OD_{600} of the sample show a consistent increase from time zero to fifteen hours in all the samples below 0.48μM ethidium bromide while in case of the samples with 0.6 μM concentration a drop in OD600 was seen. This could possibly be due to the toxicity of ethidium bromide. This observation is supported by the *p* values obtained for 0.6 μM ethidium bromide concentration. It was therefore decided to use MG1655 rather than JM109 in subsequent studies.

Sample	**Ethidium bromide concentration (μM)**	***p*-value**
P*recA*+mCherry	0 and 0.32	0.10
	0 and 0.48	0.01
	0.32 and 0.6	0.48
	0 and 0.6	0.13
	0.32 and 0.48	0.45
P*gorA*+mCherry		*p*-value
	0 and 0.32	0.28
	0 and 0.48	0.10
	0.32 and 0.6	0.5
	0 and 0.6	0.26
	0.32 and 0.48	0.27

Table 3-4: Statistical analysis for the response of biosensor, strain MG1655

Sample	Ethidium bromide concentration (µM)	p-value
P*recA*+mCherry	0 and 0.32	0.04
	0 and 0.48	0.75
	0.32 and 0.6	0.049
	0 and 0.6	0.06
	0.32 and 0.48	0.53
P*gorA*+mCherry		*p*-value
	0 and 0.32	0.155
	0 and 0.48	0.005
	0.32 and 0.6	0.08
	0 and 0.6	0.16
	0.32 and 0.48	0.18

Table 3-5: Statistical analysis for the response of biosensors, strain JM109

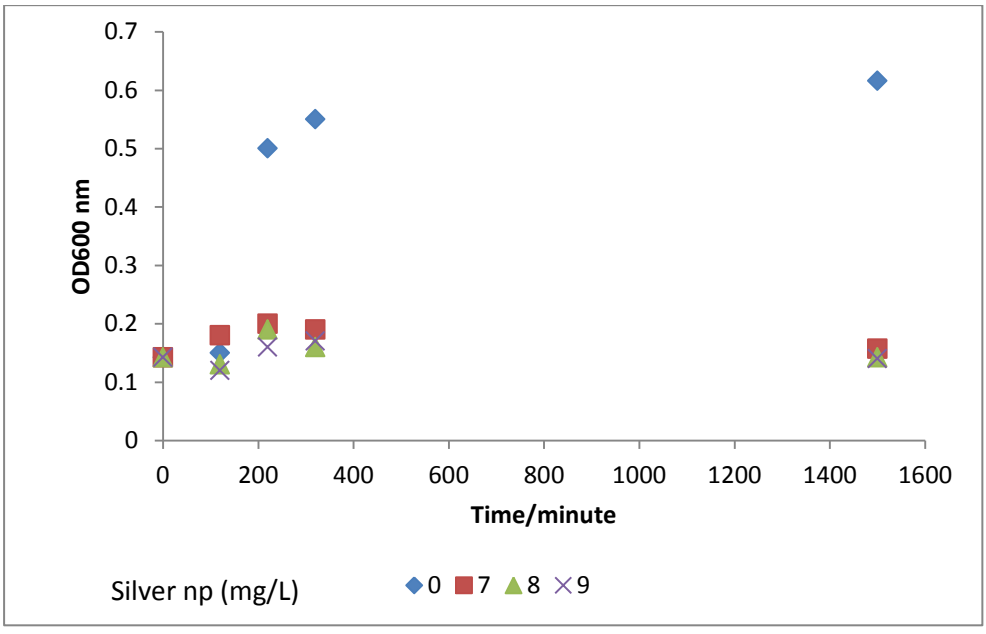

Figure 3-15: Growth kinetics of P*recA*+mCherry against silver nanoparticles (mg/L)

3.3.5.4 Response of biosensors to silver nanoparticles

These biosensors were tested with silver nanoparticles. Silver nanoparticles in the range of 0-20 mg/L were used for a total volume of 5 ml for each sample.

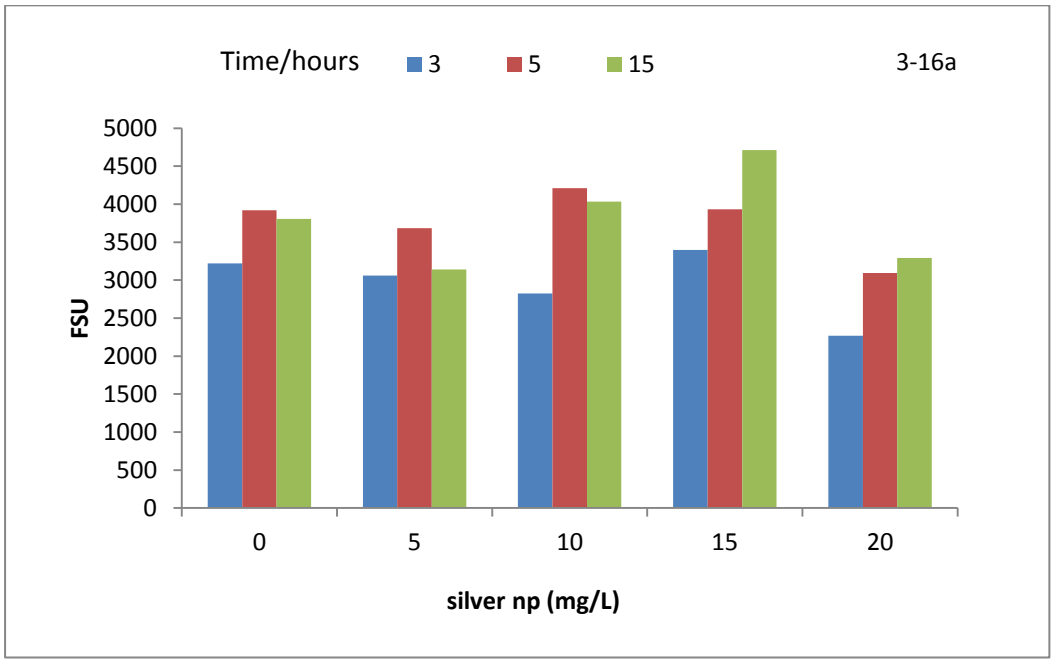

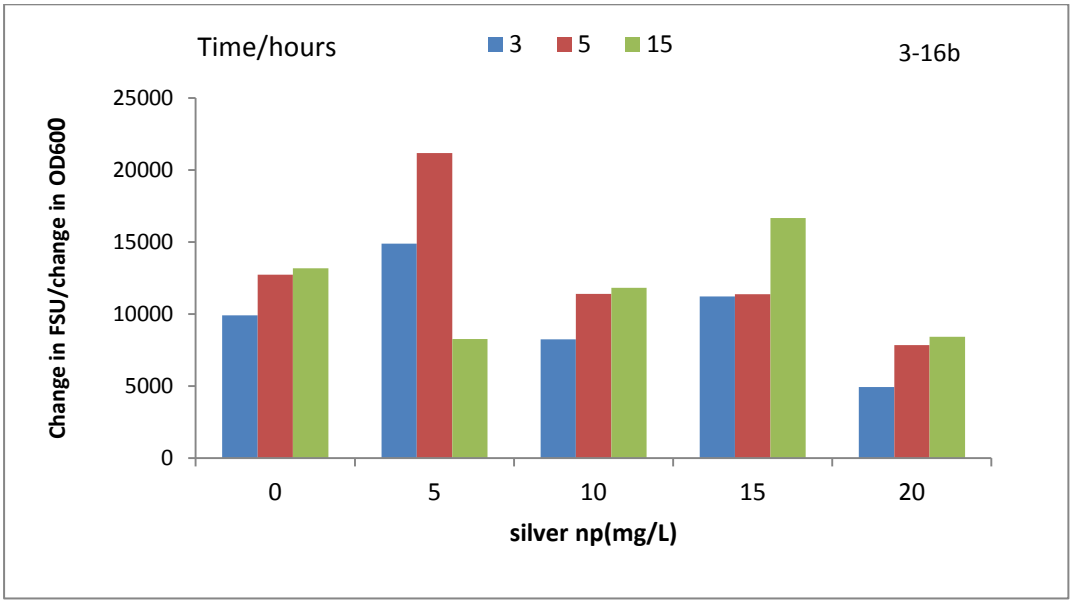

Figure 3-16a and 3-16b: P*recA+mcherry* (MG1655) exposed to silver nanoparticles

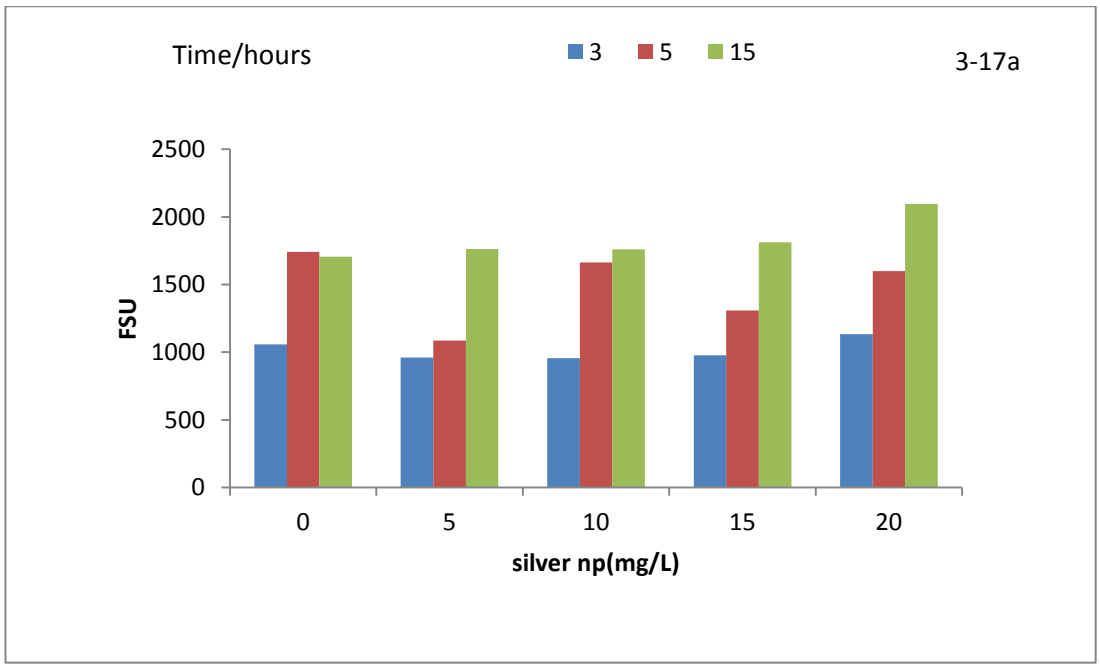

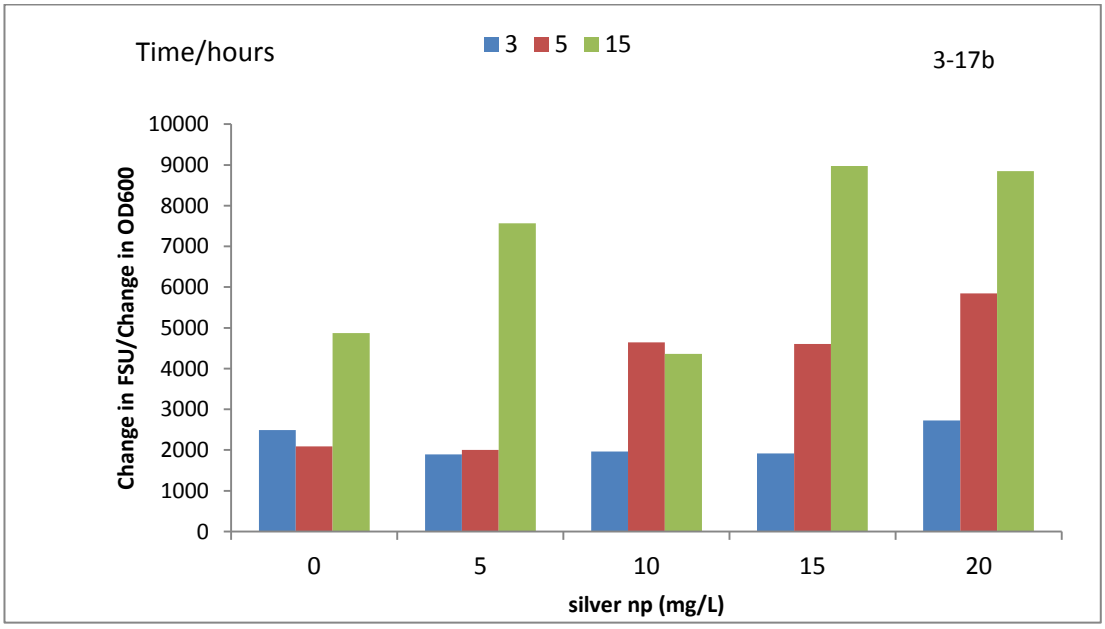

Figure 3-17a and 3-17b P*gorA+mcherry* (MG1655) exposed to silver nanoparticles

The concentration of nanoparticles was sufficient to affect the growth of the cells (Figure 3-15). Since the fluorescence values obtained from fluorometer were (relative) and not absolute, these were normalized to the optical density of the cell culture at that time point, in order to estimate the amount of mCherry (protein)

produced per cell. This helped to assess the activity of promoter with respect to exposure time. The change in fluorescence was normalized to the change in OD 600 for three time intervals: 3 hours, 5 hours and 15 hours respectively (Figure 3-16b and 3-17b). The biosensor with *recA* promoter shows a response to silver nanoparticles at 5ppm only after five hours. Overall, there is an appreciable difference between 0 and 20 ppm for three time points ($p=0.02$).

The fluorescence increases for each treatment after 15 hours. The biosensor with *gorA* promoter does not show any induction in the first 5 hours and it is only after fifteen hours that an increase in fluorescence is observed (Figure 3-16b). This suggests that peroxide mediated damage may not be the primary mechanism of silver nanotoxicity. The biosensor cells were exposed to low concentration of silver nanoparticles (0-4.5 mg/L) to ensure cell induction without compromising their viability.

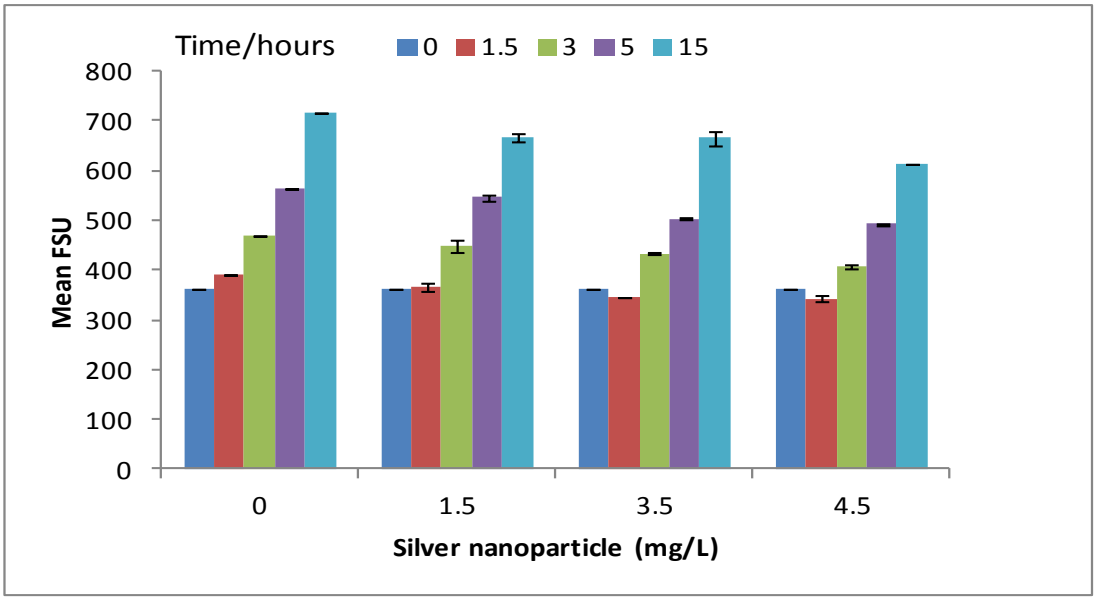

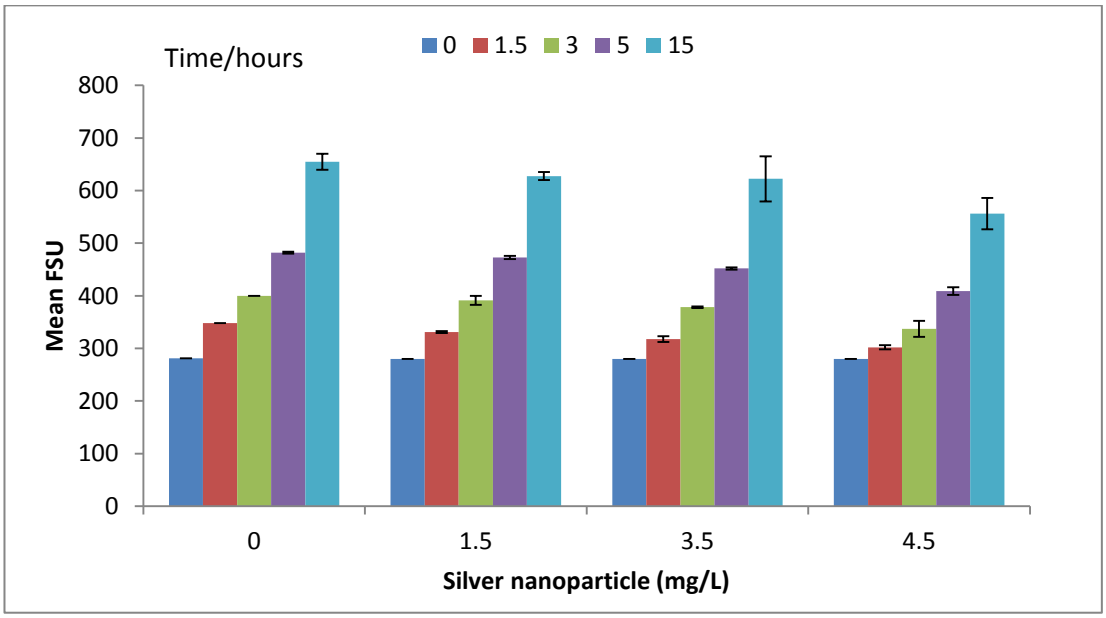

Figure 3-18a and Figure 3-18b: P*recA*+*mcherry* and P*gorA*+*mcherry* (MG1655) exposed to lower Ag NP concentrations

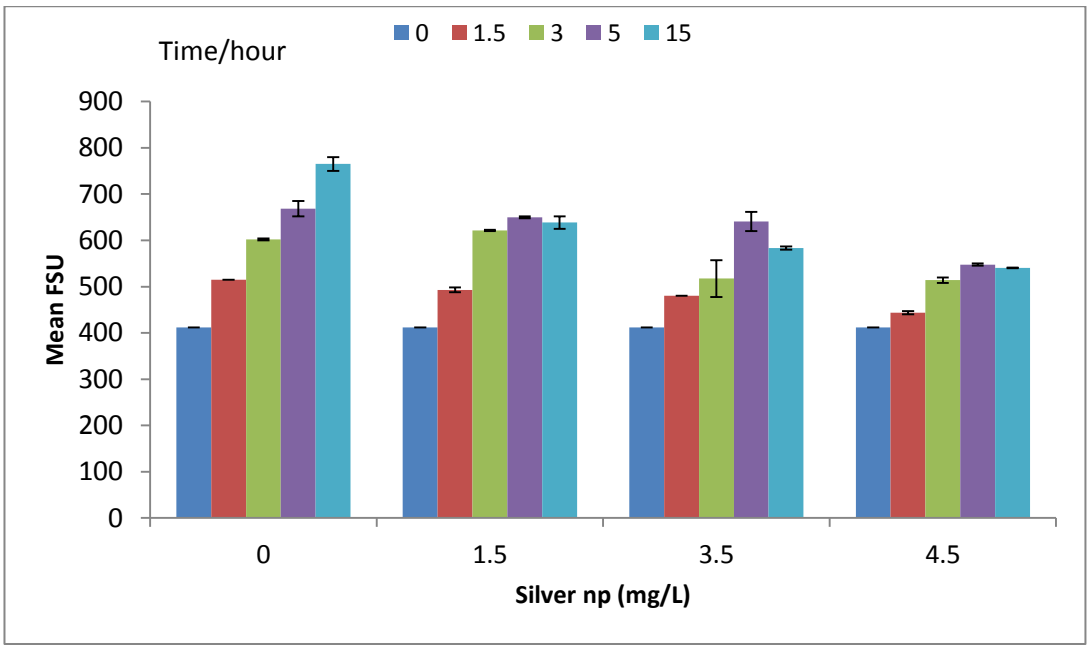

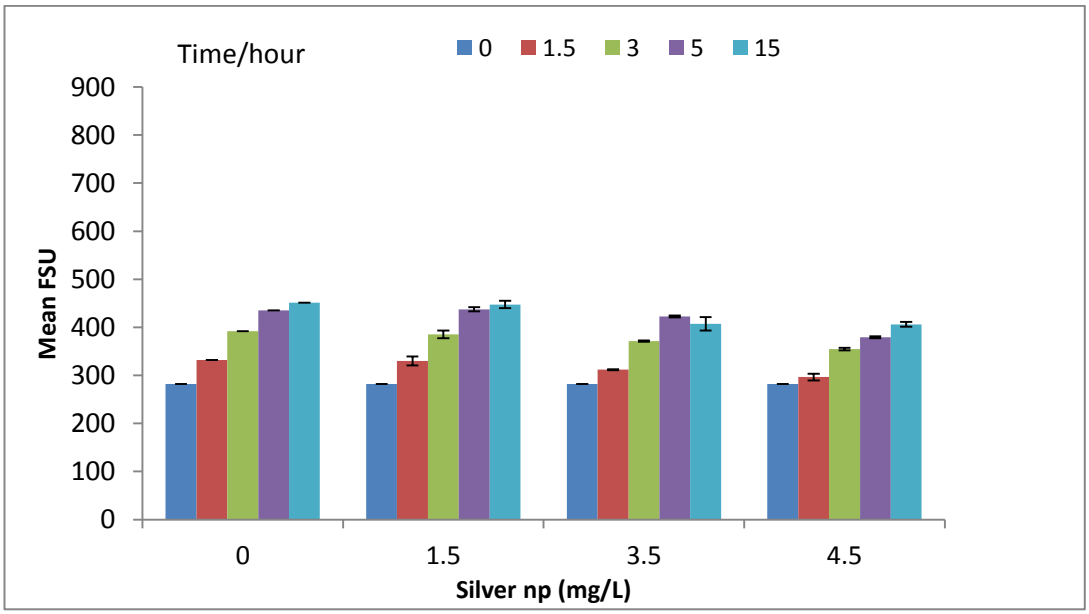

Figure 3-19a and Figure 3-19b: P*recA*+*mcherry* and P*gorA*+*mcherry* (JM109) exposed to lower Ag NP concentrations

It was observed that at low concentration of silver nanoparticles, the biosensors did not show appreciable increase in fluorescence, and the uninduced samples showed an increase in fluorescence as shown in Figure 3-18 and 3-19 resepectively.

This also suggests that either concentration below 5 mg/L was not sufficient to unduce reponse or the addition of nanoparticles resulted in toxicity due to multiple pathways.

3.4 Discussion

3.4.1 Overexpression strains and oxidative stress

The overexpression strategy needs to be optimized. It was seen that the overexpression strains JM109/pSodA and JM109/pSodB did not grow appreciably relative to the control strain, so determining the cell viability, is perhaps not the most suitable strategy to check the response of these strains. A closer examination of the percentage survival reveals that although JM109/pSodA and JM109/pDps exhibit low cell growth, the cell numbers stayed more or less constant on addition of silver nanoparticles (Figure 3-7b and Figure 3-10c). The ATP assays show that these constructs show better cell survival.

The slow growth rate of cells is an indirect evidence of resistance mechanism of cells against antibiotics and external stress etc. (Eng et al., 1991). Thus it can be inferred that overexpression of *sodA* is in fact mediating a protective response against silver nanotoxicity by making cells grow slower which leads to resistance. Over expression of proteins can also delay cell growth and shift the growth kinetics, so better analytical techniques like reverse transcription polymerase chain reaction (RT-PCR) can help to quantify the target genes and provide a better diagnostic method (Mo,

2012). Techniques like microscopy, LIVE DEAD staining and flow cytometer analysis might help to investigate silver nanotoxicity. Overexpression strategy can be further modified to include the regulatory genes, and not just the enzymes that resolve specific free radicals assuming that the exact nature of silver nanotoxicity is yet not established. For instance, overexpression of CpdA has been shown to decrease the cellular cAMP (cyclic adenosine monophosphate, used for intracellular signal transduction in bacteria) levels and it imparts resistance against HOCl and H_2O_2 in *E. coli* (Hall et al., 2012). Such proteins should be selected and modified strains expressing these should be used for silver nanoparticle exposure assays. If these strains exhibit increase in cellular ATP levels or a better cell viability in exposure assays, it can help to indirectly infer that silver nanoparticles produce oxidative stress. Preliminary work on developing more strains has been conducted and some genes cloned for this purpose. There strains developed as a part of this project will be submitted to the Registry of Standard Biological Parts and can be used by other researchers working on toxicity and stress responses in bacteria.

3.4.2 Biosensors and oxidative stress

The growth kinetic study conducted on *E. coli* shows a significant drop in OD600 at higher nanoparticle concentration (Figure 3-15). The increase in fluorescence activity of biosensor (Figure 3-16a) at low doses of silver nanoparticles (5 mg/L) is primarily a response towards induction and the possibility of hormesis can therefore be ruled out, since an increase in fluorescence is not observed in the other biosensor, P *gorA+mCherry* at all (Figure 3-17a and 3-17b).

Based on the recorded fluorescence and growth patterns it becomes quite clear that the biosensors are not strongly responding towards silver nanoparticles, though some induction is observed in the preliminary stages. There could be a number of reasons for this. Firstly, it is not necessary that *recA* or *gorA* are specifically induced by silver nanoparticles. Oxidative stress is a broad term that involves a wide range of reactive oxygen species (ROS). There is a possibility that ROS forming as a result of nanotoxicity are diffused, that is more than one type is forming. Since promoters used to construct biosensor cells are specific in nature, they are not significantly induced on addition of nanoparticles. Furthermore, the cell viability is compromised on exposure to silver nanoparticles and this can indirectly affect the signal response (as observed in preceding chapter and figure 3-15).

For example, the biosensors developed by adding the promoters of *sodA* and *katG* to the *luxCDABE* operon by Gou et al.(2010), show differences in signal strength when induced with specific chemical inducers. Therefore, it is clear that not all systems will respond effectively to silver nanoparticles as well, which has a complex mechanism of toxicity.

Secondly, half-life of ROS is very small, with hydrogen peroxide having a half-life of 1 ms and hydroxyl radical 1 μs (Stern, 1937) and this can also influence the biosensor sensitivity. This fact coupled with the nature of experimental design involving long incubation periods, can dilute the signal strength and the response of biosensors.

The nature of oxidative stress produced by silver nanoparticles is still not clear. Park et al (2009) showed that biosensors constituted by combining *sodA* with *lacZ* were induced by silver nanoparticles whereas the ones with *katG* promoter did not

show *lacZ* activity. It largely points to the fact that silver nanoparticles could be promoting the formation of superoxide radicals while peroxide levels could still be low and might not be the primary radical at all. This can also explain the inactivity of P*gorA*+mCherry designed in this study and lack of protection to cells by overexpression of catalase by the strain *E. coli* JM109/pKatG. In contrast, He et al. (2012) used an electric model to demonstrate that the presence of hydrogen peroxide in cells exposed to silver nanoparticles promotes the formation of ionic silver and superoxide anions. This indicates that some peroxide levels existing in cells can contribute synergistically to formation of reactive oxygen species in cells exposed to silver nanoparticles.

Since the mechanism of silver nanotoxicity has been investigated with many experimental designs, it is difficult to predict the exact nature of stress or form conclusions. It has also been shown by Gou (2010) that adding nanoparticles induces a global SOS response in bacteria thereby implying that no single gene, but a network of genes are activated and protein expression could be diverted in favour of all these genes. In this situation, it becomes quite difficult to exactly identify the nature of stress involved. It would be more useful if more biosensors with different combinations of genes were tested rather than relying on two constructs.

Since the biosensor cells show a high background activity, it would be quite useful to transfer these constructs into a low copy number plasmid that could perhaps minimize the high fluorescence values. A more flexible approach is required while designing biosensors where a combination of reporter genes like *lacZ* and *xylE* might provide a better quantitative signal to monitor the biosensor activity. Furthermore, advanced methods like extensive microarray techniques and real time sequencing

methods can perhaps serve as better tools to identify the genes involved in the process.

References:

1. Auffan, M. l., Achouak, W., Rose, J. r., Roncato, M.-A., Chanéac, C., Waite, D. T., Mason, A., Woicik, J. C., Wiesner, M. R. & Bottero, J. 2008. Relation between the redox state of iron-based nanoparticles and their cytotoxicity toward *Escherichia coli. Environ Sci Technol.,* 42**,** 6730-6735.

2. Beers, R. F. J. & Sizer, I. W., 133-140 1952. *J. Biol. Chem.,* 195**,** 133-140.

3. Belkin, S., Smulsk, D. R., Vollmer, A. C., Vandyk, T. K. & Larossa, R. A. 1996. Oxidative stress detection with *Escherichia coli* harboring a katG9::lux fusion. *Appl Env. Microbio.,* 62**,** 2252–2256.

4. Bellapadrona, G., Ardini, M., Ceci, P., Stefanini, S. & Chiancone, E. 2010. Dps proteins prevent Fenton-mediated oxidative damage by trapping hydroxyl radicals within the protein shell. *Free Radic Biol Med. ,* 48(2)**,** 292-297.

5. Bondarenko, O., Ivask, A., Käkinen, A. & Kahru, A. 2012. Sub-toxic effects of CuO nanoparticles on bacteria: kinetics, role of Cu ions and possible mechanisms of action. *Environ. Pollut.,* 169**,** 81-90.

6. Boor, J. K. 2006. Bacterial stress responses: what doesn't kill them can make them stronger. *PLoS ONE,* 4**,** 23.

7. Cabiscol, E., Tamarit, J. & Ros, J. 1999. Oxidative stress in bacteria and protein damage by reactive oxygen species. *Int. Journ Microbiol.,* 3**,** 3-8.

8. Carlson, C., Hussain, S. M., Schrand, A. M., K. Braydich-Stolle, L., Hess, K. L., Jones, R. L. & Schlager, J. J. 2008. Unique cellular interaction of silver nanoparticles: size-dependent generation of reactive oxygen species. *J. Physic. Chem. B,* 112**,** 13608-13619.

9. Choi, O. & Hu, Z. 2008. Size dependent and reactive oxygen species related nanosilver toxicity to nitrifying bacteria. *Environ. Sci. Technol.,* 42**,** 4583-4588.

10. Chung, C.T., Niemela, S.L., Miller,R.H. 1989. One step preparation of competent *E. coli*: transformation and storage of bacterial cells in the same solution. *Proc.Natl.Acad.Sci.,* 86(7), 2172-2175.

11. Dams , R., Biswas, A., Olesiejuk, A., Fernandes, T. & Christofi, N. 2011. Silver nanotoxicity using a light-emitting biosensor *Pseudomonas putida* isolated from a wastewater treatment plant. *J. Hazard. Mater.,* 195**,** 68-72.

12. Eng, R. H., Padberg, F. T., Smith, S. M., Tan, E. N. & Cherubin, C. E. 1991. Bactericidal effects of antibiotics on slowly growing and nongrowing bacteria. *Antimicrob Agents Chemother.,* 35**,** 1824–1828.

13. Gajjar, P., Pettee, B., Britt, D., Huang, W., Johnson, W. & Anderson, A. 2009. Antimicrobial activities of commercial nanoparticles against an environmental soil microbe, *Pseudomonas putida* KT2440. *J Biol. Eng.,* 3**,** 9.

14. Gou, Na.,Hayden, A.H.,Gu, A.Z.2010. Mechanistic Toxicity Assessment of Nanomaterials by Whole-Cell-Array Stress Genes Expression Analysis. Environ. Sci.Technol.,44.,5964-5970.

15. Hall, S. R., Hnilova, M., Grosh, C., Fong, H., Baneyx, F., Schwartz, D., Sarikaya, M., Tamerler, C. & Traxler, B. 2012. Engineered *Escherichia coli* silver-binding periplasmic protein that promotes silver tolerance. *Applied Env. Microbio.***,** doi:10.1128/AEM.06823-11

16. He, D., Garg, S. & Waite, T. D. 2012. H_2O_2-mediated oxidation of zero-valent silver and resultant interactions among silver nanoparticles, silver ions, and reactive oxygen species. *Langmuir,* 28(27)**,** 10266-75.

17. Heinlaana, M., Ivaska, A., Blinovaa, I., Dubourguier, H.-C. & Kahru, A. 2008. Toxicity of nanosized and bulk ZnO, CuO and TiO2 to bacteria *Vibrio fischeri* and crustaceans *Daphnia magna* and *Thamnocephalus platyurus*. *Chemosphere,* 71**,** 1308–1316.

18. Hetrick, E. M., Shin, J. H., Stasko, N. A., Johnson, C. B., Wespe, D. A., Holmuhamedov, E. & Schoenfisch, M. H. 2008. Bactericidal efficacy of nitric oxide-releasing silica nanoparticles. *ACS Nano,* 2**,** 235-246.

19. Hu, X., Cook, S., Wang, P. & Hwang, H. M. 2009. In vitro evaluation of cytotoxicity of engineered metal oxide nanoparticles. *Sci.Total Environ.,* 407**,** 3070-3072.

20. Huang, Z., Zheng, X., Yan, D., Yin, G., Liao, X., Kang, Y., Yao, Y., Huang, D. & Hao, B. 2008. Toxicological effect of ZnO nanoparticles based on bacteria. *Langmuir,* 24**,** 4140-4144.

21. Imlay, J. A. 2003. Pathways of oxidative damage. *Annu Rev Microbiol.* , 57**,** 395-418.

22. Ishikawa, T., Mizunoe, Y., Kawabata, S., Takade, A., Harada, M., Wai, S. N. & Yoshida, S. 2003. The iron binding protein Dps confers hydrogen peroxide resistance to *Campylobacter jejuni*. *J Bacteriol.,* 158(3)**,** 1010-1017.

23. Kamat, J. P., Devasagayama, T. P. A., Priyadarsini, K. I. & Mohan, H. 2000. Reactive oxygen species mediated membrane damage induced by fullerene derivatives and its possible biological implications. *Toxicol.,* 155**,** 55-61.

24. Kenichiro, I., Hirohisa, T., Koike, E., Yanagisawa, R., Sakurai, M., Tasaka, S., Ishizaka, A. & Shimada, A. 2008. Effects of pulmonary exposure to carbon nanotubes on lung and systemic inflammation with coagulatory disturbance induced by lipopolysaccharide in mice. *Exp Biol Med* 233**,** 1583-1590.

25. Knight, T. 2003. Idempotent Vector Design for Standard Assembly of Biobricks, . *mit.edu/handle/1721.1/21168 1–11.*

26. Lam, C., James, J. T., McCluskey, R. & Hunter, R. L. 2004. Pulmonary toxicity of single-wall carbon nanotubes in mice 7 and 90 days after intratracheal instillation. *Toxicol. Sci.,* 77**,** 126-134.

27. Lee, H. J. & Gu, M. B. 2003. Construction of a *sodA::luxCDABE* fusion *Escherichia coli*: comparison with a *katG* fusion strain through their responses to oxidative stresses. *Appl Microbiol Biotechnol.,* 60**,** 577–580.

28. Liochev, S. I., Benov, L., Touati, D. & Fridovich, I. 1999. Induction of the soxRS regulon of *Escherichia coli* by Superoxide. *J Biol. Chem.,* 274**,** 9479-9481.

29. Li,M., Zhu, L., Lin, D. 2011. Toxicity of ZnO nanoparticles to *Escherichia coli:* mechanism and the influence of medium components. *Environ. Sci.Technol.,* 45**,** 1977-1983.

30. Maynard, A. & Michelson, E. 2006. The nanotechnology consumer productsinventory. Washington, DC: Project on emerging nanotechnologies, Woodrow Wilson International Center for Scholars.*Available from:<http://nanotechproject.org/44>; March 2006 [accessed 12.09.2009]*.

31. Michan,C., Manchado.,M.,Dorado, G.,Puyeo,C.1999. In vivo transcription of the *Escherichia coli* oxyR regulon as a function of growth phase and in response to oxidative stress. *J.Bacteriol*. 181, 2759-2764.

32. Mitchell, R.J&GU, M.B.2004. Construction and characterization of novel dual stress-responsive bacterial biosensors. *Biosensors Bioelectron*. 19(9), 977-85.

33. Mo Y, Wan R, Zhang Q.2012. Application of reverse transcription-PCR and real-time PCR in nanotoxicity research.Methods Mol.Biol.926, 99-112.

34. Nel, A., Xia, T., Mädler, L. & Li, N. 2006. Toxic potential of materials at the nanolevel. *Science,* 311**,** 622-627.

35. Nobles, R. & Gibson, Q. H. 1970. The reaction of ferrous horse radish peroxidase with hydrogen peroxide. *J.Biol.Chem.***,** 2409-13.

36. Norville, J., Derda, R., Gupta, S., Drinkwater, K., Belcher, A., Leschziner, A. & Knight, T. J. 2010. Introduction of customized inserts for streamlined assembly and optimization of BioBrick synthetic genetic circuits. *4***,** 17.

37. Okochi, M., Kanie, K., Kurimoto, M., Yohda, M. & Honda, H. 2008. Overexpression of prefoldin from the hyperthermophilic archaeum *Pyrococcus horikoshii* OT3 endowed *Escherichia coli* with organic solvent tolerance. *Appl Microbiol Biotechnol. ,* 79(3)**,** 443-449.

38. Outten, F., Hale, J. & O'Halloran, T. V. 2000. Transcriptional activation of an *Escherichia coli* copper efflux regulon by the chromosomal MerR homologue, cueR. *J. Biol. Chem.*, 275**,** 310424-9.

39. Patsoukis, N., Papapostolou, I. & Georgiou, C. D. 2005. Interference of non-specific peroxidases in the fluorescence detection of superoxide radical by hydroethidine oxidation: a new assay for H2O2. *Anal Bioanal Chem.*, 381(5)**,** 1065-72.

40. Plasmapper http://wishart.biology.ualberta.ca/PlasMapper [accessed on 21/2/2013].

41. Qureshi, A., Gurbuz, Y. & Niazi, H. 2012. Capacitive biosensor for nanotoxicity detection. *Procedia Engineering* 47**,** 1331 – 1333.

42. Roh, J., Sim, S. J., Yi, J., Park, K., Chung, K. H., Ryu, D.-y. & Choi, J. 2009. Ecotoxicity of silver nanoparticles on the soil nematode *Caenorhabditis elegans* using functional ecotoxicogenomics. *Environ. Sci Technol.*, 43**,** 3933-3940.

43. Sambrook, J., Fritsch, E. F. & Maniatis, T. 1989. Molecular Cloning 2nd Ed. 3**,** p. A.3

44. Singh, R. P. & Ramarao, P. 2012. Cellular uptake, intracellular trafficking and cytotoxicity of silver nanoparticles. *Toxicol. Lett.*, 213(2)**,** 249-59.

45. Sondi, I. & Sondi, B. S. 2004. Silver nanoparticles as antimicrobial agent: a case study on *E. coli* as a model for Gram-negative bacteria. *J.Colloid. Interphase Sci.*, 275**,** 177-182.

46. Stern, K. G. 1937. *J Biol. Chem.* 121**,** 561-572.

47. Wiesner, M., Lowry, G., Alvarez, P., Dionysiou, D. & Biswas, P. 2006. Assessing the risks of manufactured nanomaterials. *Environ Sci Technol.* , 40(14)**,** 4336-45.

48. Xia, T., Kovochich, M., Brant, J., Hotze, M., Sempf, J., Oberley, T., Sioutas, C., Yeh, J. I., Wiesner, M. R. & Nel, A. E. 2006. Comparison of the abilities of ambient and manufactured nanoparticles to induce cellular toxicity according to an oxidative stress paradigm. *Nano Letters*, 6**,** 1794-1807.

49. Xia, T., Kovochich, M., Liong, M., Mädler, L., Gilbert, B., Shi, H., Yeh, J. I., Zink, J. I. & Nel, A. E. 2008. Comparison of the mechanism of toxicity of zinc oxide and cerium oxide nanoparticles based on dissolution and oxidative stress properties. *ACS Nano*, 2**,** 2121-2134.

Chapter 4

Enhanced resistance to nanoparticle toxicity is conferred by overproduction of extracellular polymeric substances.

This chapter has been published as a paper as "***Enhanced resistance to nanoparticle toxicity is conferred by overproduction of extracellular polymeric substances";*** *Journal of Hazardous Materials vol. 241-242, p363-370.*The paper is reproduced here with additional data/figures.

Abstract

The increasing production and use of engineered nanoparticles, coupled with their demonstrated toxicity to different organisms, demands the development of a systematic understanding of how nanoparticle toxicity depends on important environmental parameters as well as surface properties of both cells and nanomaterials. In order to investigate if production of extracellular polymeric substances (EPS) protects bacteria against silver nanotoxicity, in vitro toxicity tests were conducted using strains of *Escherichia coli* engineered to over-express EPS production. It was observed that the production of the extracellular polymeric substance, colanic acid by engineered *E. coli* protects the bacteria against silver nanoparticle toxicity. Moreover, exogenous addition of EPS to a control strain results in an increase in cell viability, as does the addition of commercial EPS polymer analogue xanthan. Furthermore, an EPS producing strain of *Sinorhizobium meliloti* shows higher survival upon exposure to silver nanoparticles than the parent strain. Transmission electron microscopy (TEM) observations showed that EPS traps the

nanoparticles outside the cells and reduces the exposed surface area of cells to incoming nanoparticles by inducing cell aggregation. Nanoparticle size characterization in the presence of EPS and xanthan indicated a marked tendency towards aggregation. Both are likely effective mechanisms for reducing nanoparticle toxicity in the natural environment.

4.1. Introduction

Due to their small size, composition and reactivity, engineered nanoparticles are widely used in a variety of applications, including sunscreens, clothes and advanced targeted drug delivery for cancer treatments (Nowack and Bucheli, 2007). Whereas their unique physicochemical properties account for their versatile uses, the very same features raise considerable concern about their possible impact on the environment. As a result many studies have investigated the possible impact of engineered nanoparticles, including carbon nanotubes, metal and metal oxide nanoparticles on human cell lines, yeasts, bacteria and aquatic organisms (Adams et al., 2006, Hu et al., 2009, Kasmets et al., 2009, Scown et al., 2010). Silver (Ag) nanoparticles have been reported to be toxic to many bacteria including *Escherichia coli, Pseudomonas chlororaphis,* and *Pseudomonas putida* (Sondi and Sondi, 2004, Choi and Hu, 2008a, Fabrega et al., 2009, Gajjar et al., 2009, Dimkpa et al., 2011a). Suggested causes of nanoparticle toxicity include death *via* injury to cells, membrane damage (Sondi and Sondi, 2004, Choi and Hu, 2008a, Fabrega et al., 2009, Gajjar et al., 2009) and oxidative stress promoted by the formation of reactive oxygen species (ROS)(Xia et al., 2008, Choi and Hu, 2008b).

The objective of these studies is to be able to predict the behavior and impact of engineered nanoparticles on organisms in the natural environment. However, this goal is not attainable without taking into consideration environmental variables such as pH, presence of dissolved salts, shape of nanoparticles, type of organic matter and type of medium under study (Morones et al., 2005, Pal et al., 2007, Auffan et al., 2008, Fabrega et al., 2009, Jin et al., 2010, Li et al., 2011a, Lowry et al., 2012). The dynamic interaction with environmental variables can lead to changes in, and loss of

properties associated with reactivity and toxicity of the nanoparticles. Moreover, intrinsic properties of the nanoparticles themselves, including surface charge and coatings, can have a significant impact on their reactivity. As a result, recent studies on microbe-nanoparticle interactions have begun to systematically examine these aspects. For instance, it was found that the toxicity of silver nanoparticles was dependent on the surface charge of these particles and that capping agents like citrate and organic compounds like humic acid can reduce the toxicity of silver nanoparticles (Fabrega et al., 2009, El Badawy et al., 2011).

Surface properties of bacteria could also play an important role in influencing the net toxicity of nanoparticles. For instance, the toxicity of a metal nanoparticle like silver could be different for gram positive and gram negative bacteria based on differences in cell wall characteristics. Amato et al. (2011) have shown that the minimum inhibitory concentration values (MIC) of glutathione capped silver nanoparticles are different for *Staphylococcus aurous* and *E. coli*, 180 and 15 μg/ml respectively.

Bacteria are known to secrete exopolysaccharides (EPS), particularly while growing in a biofilm mode (Allison et al., 1998, Moreau et al., 2007, Flemming and Wingender, 2010). EPS could play an important role in controlling the toxicity of nanoparticles in the environment, (Liu et al., 2007, Battin et al., 2009, Dimkpa et al., 2011b). For example, it has been shown that bacteria exposed to nanoparticles in the biofilm mode and planktonic mode show different behavior, with bacteria in planktonic mode being more vulnerable to nanoparticle toxicity. In another study by Jian et al. (2011), bacteria covered with EPS showed a lower inactivation rate in the

presence of titanium oxide (TiO_2) nanoparticles. The addition of EPS to *Pseudomonas chlororaphis* eliminated silver nanoparticle toxicity at lower concentrations of nanoparticles (Dimkpa et al., 2011b).

Most of this work has hypothesized that EPS acts as a physical barrier or interacts with nanoparticles and competes with cell surfaces thereby reducing their bioavailability and toxicity. In order to demonstrate this, EPS was removed from the cells by the mechanical means such as cation exchange resins or glass beads. All these methods can affect the metabolic state of bacteria (Hong and Brown, 2009). Secondly, the process of EPS extraction by using resins, ethanol precipitation or sonication produces quite variable outcomes with some loss in cell viability (Gong et al., 2009). This can interfere indirectly with the nanoparticle toxicity results, particularly those that rely on cell viability testing. In order to investigate further the potential protective role of EPS, a strain of *Escherichia coli* that could produce an excess colanic acid, an extracellular polysaccharide was developed. Colanic acid is produced by most strains of *E. coli* and plays an important role in its protection against desiccation, osmotic and oxidative stress (Wehland and Bernhard, 1999, Chen et al., 2004, Flemming and Wingender, 2010). An environmental isolate of *Sinorhizobium meliloti* and its EPS overproducing mutants were tested and the impact of xanthan as a biopolymer analogue of EPS was also investigated. This combination of tests helped to pose and investigate the following hypotheses: (i) EPS and associated biopolymers will alter the behaviour of nanoparticles and influence their toxicity by promoting their aggregation under natural conditions; (ii) such a mechanism will also extend to protection of non-EPS producing cells growing in co-culture with EPS-producing strains.

4.2 Materials and Methods

4.2.1 Bacterial strains and plasmids used for the study

In order to investigate the protective role of EPS on the impact of silver nanoparticles *E. coli* (JM109) and *Sinorhizobium meliloti* were used (Meade et al., 1982, Doherty et al., 1988, Reuber and Walker, 1993). Three strains of *Sinorhizobium meliloti*, a nitrogen fixing, and hence environmentally significant bacterium, were used to explore the environmental relevance of our findings. Exopolysachharides produced by bacteria protect them against many environmental stress conditions such as heat shock, desiccation, starvation and oxidative stress (Flemming and Wingender, 2010). The biosynthesis of high molecular weight EPS (type 1) is one of the key mechanisms that operates in stress conditions in many bacteria like *E. coli*, *Salmonella typhi* and *Pantoea stewartii* (Allison et al., 1998). This process is controlled by the Rcs regulatory network (Rcs stands for regulation of capsular polysaccharides), Majdalani and Gottesman, 2005. The RcsAB complex plays an important role in colanic acid biosynthesis. *E. coli* was genetically modified to overproduce capsular polysaccharide, colanic acid by overexpressing RcsA, which has been shown to act as a positive regulator of the *cps* operon in *E. coli* (Beloin et al., 2008) and shown to activate its own expression (Stout et al., 1991, Ebel and Trempy, 1999, Wehland and Bernhard, 1999). The primer sequences for the promoter and coding sequence of the *rcsA* gene were designed and sourced from Sigma Aldrich, UK. Table 4-1 shows all the bacterial strains and plasmids used for this study.

4.2.2 Chemicals and reagents used

The salts to prepare growth medium were sourced from Fisher Scientific, UK. The primers and antibiotics were sourced from Sigma Aldrich. KOD hot start DNA polymerase (Invitrogen) was used for PCR reactions to clone the promoter and coding sequence of *rcsA.* All the restriction enzymes and antibiotics were sourced from Melford. Bactiter Glo Kit was sourced from Promega

4.2.3 Medium and growth conditions

For *E. coli,* exposure studies were carried out in minimal medium supplemented with salts and a carbon source. The recipe for 4X stock solution of Minimal medium (64 g/L $Na_2HPO_4.7H_2O$, 15g/L KH_2PO_4, 5 g/L NH_4Cl, and 2.5 g/L NaCl) was diluted four times with deionized water. It was then supplemented with 0.2 % (w/v) Casamino acids, 1 mM thiamine hydrochloride and 0.4% w/v glycerol as a carbon source Ampicillin (100 µg/ml) was used to maintain plasmids when required in *E. coli.* Cultures were incubated at 37^{o}C for *E. coli* on a rotary shaker at 250 rpm.

For *Sinorhizobium meliloti,* M9 medium (recipe as above) supplemented with 2.5 mM calcium chloride and 2.5 mM magnesium sulphate was used. Streptomycin (500 µg/ml) was added to the cultures of mutant strains. These were incubated at 30^{o}C on a rotary shaker at 200 rpm.

Bacterial strains	Genotype/characteristics	Source
1. *E.coli*		
E.coli JM109/pRcsA2	Lab strain used to contruct mucoid strain	This work
E.coli/JM109/pEdinbrick1	Vector control strain	(Registry of Standard Biological parts).
E.coli JW3077-1	*yhaK725*(del)::kan	(Baba et al., 2006)
2.*Sinorhizobium meliloti*		
Rm1021	Rm1021 is parent strain	(Doherty, 1988 and Reuber, 1993)
Rm7096	Rm1021 *exoS*::Tn5 EPS overproducing strain	(Wehland,M;1999)
Rm7210	Rm1021 *exoY*:: Tn5 Lacks EPS production	(Doherty, 1988 and Reuber, 1993)
Plasmids		
pEdinbrick1	Cloning vector	(Registry of Standard Biological parts)
p RcsA2	Construct designed to form colanic acid producing strain	This work

Table 4-1: List of Bacterial strains and plasmids used for the study

4.2.4 Construction of a colanic acid over producing strain of *E. coli* and colanic acid analysis

To develop the colanic acid overproducing strain, *rcsA* was overexpressed in *E. coli.* Primers for promoter and the coding sequence of *rcsA* were designed in a standard BioBrick format RFC10 as defined by the Registry of Standard Biological parts. The promoter of *rcsA* and corresponding coding sequence were amplified using KOD

polymerase (recipe below in Table 4-2) and PTC 200 DNA Engine Thermocycler (Biorad).

Reagents	**Volume in µl**
Sterile water	32
10 X Reaction Buffer	5
25 mM MgS04	3
Forward primer (10pmol/ul)	1.5
Reverse primer (10pmol/ul)	1.5
2 mM dNTP mix	5
Template (cell suspension/plasmid DNA)	1-2
KOD hot start DNA polymerase	1

Table 4-2: Reaction mixture used for DNA amplification (final volume 50µl)

The following primers were designed: Forward primer with BioBrick prefix: TCTgaattcgcggccgcttctaga gAAGCTCACTCACATATCGCAA and reverse primer ctgcagcggccgctactagta TTAGCGCATGTTGACAA. The plasmids pSB1A2 and BioBrick BBa_J33207 were sourced from the Registry of Standard Biological Parts. The generated Bio Brick P_{rcsA}+*rcsA* was cloned in pSB1A2 to generate pRcsA1 and then Bba_J33207 (*lac* promoter) was inserted upstream to generate pRcsA2 (Figure 4-1). It was induced with IPTG (90 µg/ml) to achieve overexpression of *rcsA*.

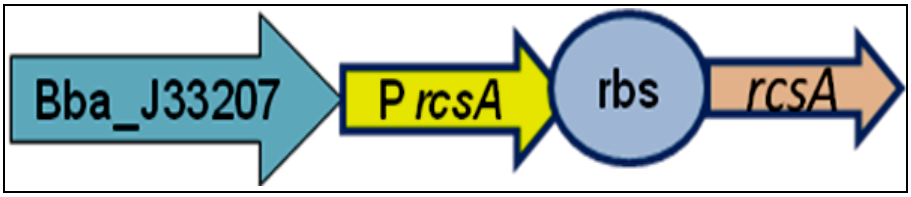

Figure 4-1: Schematic depiction of the BioBrick assembly designed for colanic acid overproducing strain *E.coli*/JM109/pRcsA2

4.2.4.1 Analysis of the EPS recovered from the developed strain, pRscA2/JM109

Quantification of total carbohydrate (EPS) produced by colanic acid overproducing strain *E.coli*/JM109/pRcsA2 was accomplished by anthrone sulphuric acid assay by the method of Obadia et al. (2007). The cells were scraped from an LB Agar plate (approx. 30-40 mg) and suspended in 1 ml of water by vortexing the samples briefly. The cell concentration was determined by measuring the OD600 of this sample. In order to inactivate any EPS degrading enzymes, these samples were boiled in a water bath for 10 minutes and then cooled for 1 hour before the start of the experiment. The same procedure was used for the cells recovered from the control strain JM109/pEdinbrick. These samples were centrifuged at 16000 g for 10 minutes and the supernatants collected. For this assay, 2% w/v of anthrone was dissolved in concentrated sulphuric acid. Each sample (including standards) required 1 ml of this reagent so it was prepared fresh every time. Approximately 0.4 ml of diluted supernatant was mixed with 1 ml of this reagent in a fume hood. The test tubes were placed in ice and the absorbance of samples was measured at 620 nm

using distilled water as a blank. Total carbohydrate was determined using a glucose standard prepared in the same way (2, 10, 50,100 μg/ml) and final values were normalized to corresponding OD600 values of the bacterial suspensions.

4.2.4.2 Fucose assay to determine the presence of colanic acid in the EPS recovered from pRscA2/JM109 and the control strain pEdinbrick1/JM109

Total EPS and colanic acid recovery from *E. coli* JM109/pRcsA2 was carried out as described by Obadia et al. (2007). When a class of sugar reacts with sulphuric acid and cysteine it forms a product, the stability of which is dependent on the concentration of sulphuric acid (Dische and Shettles, 1951). With the addition of water, the product so formed tends to degrade, and at a similar concentration of acid, every sugar will form a product that is characteristic of that sugar. This assay relies on initially measuring the content of the product when sulphuric acid and cysteine hydrochloride are added and then subsequently measuring their rate of degradation on addition of water. The culture was made in M9 supplemented medium, the next day centrifuged, and the supernatant was used to recover EPS by ethanol precipitation. Cold ethanol was added (3:1 v/v) to the supernatant and it was incubated at 4^{o}C to facilitate the precipitation of EPS. It was centrifuged at 13500 g for 30 minutes at 4^{o}C. The resulting pellet was dissolved in deionized water and dialyzed for 48 hours using a Floatalyzer G2 column (10 kDa MWCO). The recovered samples were lyophilized and used for fucose assays. Approximately 10-50 μl of colanic acid preparation was added to 1 ml mixture of sulphuric acid and water (6:1 v/v). This mixture was heated at 100^{o}C / for 20 minutes and cooled to

room temperature. The absorbance was measured at 396 nm and 427 nm before and after addition of 100 µl of 10M cysteine hydrochloride to these samples. A negative control of glucose in sterile water was used for the assay.

Two sets of readings were recorded to minimize the interference produced by other components of biological origin that have been shown to cross react with sulphuric acid to produce a brown coloration. The difference between these two readings helped determine the actual value of reaction and it was then correlated to fucose standards (5-100 µg/ ml) and water was used as blank (Sutherland, 1969).

4.2.5 Nanoparticles source, sample preparation, characterization and speciation analysis

Silver nanoparticles of 100 nm diameter were obtained from Sigma Aldrich, UK (Catalog no. 576832). In order to prepare a silver dispersion (100 nm), the method of Fabrega et al. (2009) was used. A stock suspension of silver nanoparticles was prepared by adding 1 gm of silver nano powder to 250 ml deionized water along with 0.25 mM sodium citrate as a stabilizer. The resultant suspension was sonicated (230 V, 50 Hz) for 30 minutes for four days and then silver nanoparticle dispersion was recovered by gravity separation. The final concentration of silver in the sample was determined in triplicate using ICP-OES and was found to be 70 mg/L. 10 nm silver nanoparticle dispersion (20 mg/L) was sourced from Sigma Aldrich, UK (Catalog no. 730785).

Size characterization of silver nanoparticles was carried out in the presence of deionized water and growth media (Luria Bertani or minimal medium) with or without EPS or an EPS analogue (xanthan). Both 10 nm and 100 nm silver

dispersions were used. A median concentration of 100 mg/L was used for xanthan as a substitute for EPS and 9 mg/L of glucose equivalent of the EPS preparation recovered from JM109/pRcsA2 was used. Particle size distribution was analyzed by Dynamic Light Scattering (DLS) using a Zeta PALS 90 Plus submicron size analyzer (Brookhaven Instruments Corporation Holtsville, NY, USA). The samples were sonicated for 5 minutes prior to use. The data were collected in triplicate at a temperature of 25ºC.

In order to determine the extent of ion dissolution/speciation for the exposure period chosen for experiments (120 minutes), a background study was conducted. The nanoparticles were suspended in M9 supplemented medium and incubated on a shaker at 200 rpm. Suspensions were centrifuged at 22000 g for 60 minutes at 4ºC. The supernatant was acidified with 2% nitric acid and total silver concentration was determined by ICP-OES analysis. Samples for each of the concentration were in duplicate, and there was no change in pH during this treatment.

4.2.6 Nanoparticle exposure and viability study

Bacteria were grown overnight in minimal medium (described above) with suitable antibiotics. The next day these samples were diluted with fresh medium to an OD600 of 0.2 and the exposure experiments were then carried out. All experiments were conducted using 10 nm silver nanoparticles, except for the experiment investigating the effects of nanoparticle size on toxicity, where 100 nm silver nanoparticles were also used. The nanoparticle treated samples were incubated in the dark for 120 minutes on a rotary shaker at 37ºC for *E. coli* and *S. meliloti*. Cell viability was tested by determining colony forming units (CFU/ml) following serial

dilution. An incubation temperature of 37ºC was used for *E. coli* grown on LB-agar plates. For *Sinorhizobium meliloti*, LB agar supplemented with 2.5 mM magnesium sulphate and calcium chloride was used and incubated at 30ºC.

A Bactiter-Glo microbial cell viability kit (Promega Catalog no.G8230) was used to determine the number of viable cells in bacterial cultures based on the quantification of ATP content (in terms of luminescence values) after exposure to silver nanoparticles. The exposure method was as described above and the kit was used as per the manufacturer's protocol. The luminescence was determined by using a Modulus single tube multimode reader (BS040271 Turner Biosystems). The possible interference by silver nanoparticles and the background noise was assessed and the final luminescence (relative luminescence value/RLU) was obtained after deducting the background.

The potential role of EPS produced by one strain of bacteria on the other strain was also tested. The EPS recovered from *E. coli* JM109/pRcsA2 culture was used to test protection of non mucoid cells against nanoparticle toxicity. A different strain of *E. coli* BW25113*ΔyhaK* strain was used to investigate if the EPS produced by one strain can provide cross protection to another. 6.5 mg/L final silver nanoparticles concentration (10 nm diameter silver nanoparticles) was used. The method was as described above. An EPS preparation 2 µl (9 mg/L of glucose equivalent) was added per ml of bacterial culture.

In order to study the impact of xanthan on cell viability a xanthan suspension in water (100 mg/L) was used (50 µl per ml of culture) with silver nanoparticles of 10 nm diameter. All the experiments were conducted in triplicate and also conducted at different time intervals to ensure the reproducibility of the data. The data analysis

was done using Excel 2007 and Student's t test was used to determine the statistical significance of the data.

4.2.7 Microscopy and image analysis

A Phillips CM120 Transmission Electron Microscope (FEI UK Ltd, Cambridge, England) operated at 80 kV was used to study the fate and spatial distribution of Ag nanoparticles in/around bacteria. The bacterial samples, both the control strain and the EPS overproducing strain of *E. coli*, were exposed to silver nanoparticles as described above and then used for sample preparation for TEM imaging. Representative images were taken on a Gatan Orius CCD camera (Gatan UK, Oxon, England). Sample preparation for TEM was conducted according to the method of Bechtel and Bulla (1976). The cells were exposed to silver nanoparticles (as discussed earlier) and later centrifuged. They were then washed three times with 0.01 M PBS treated with 4% glutaraldehyde and trapped in 2% water-agar. Thin sections of agar were made and washed with cold PBS four times and fixed with osmium tetra oxide. The samples were incubated overnight in 0.5% uranyl acetate and then dehydrated by a series of graded acetone washes and fixed on spur resin. Thin sections were then examined under TEM.

4.3. Results

4.3.1a A colanic acid overexpressing strain was successfully constructed.

A colanic acid overproducing strain of *E. coli,* JM109/pRcsA2 was developed and characterized. This strain showed enhanced mucoidy and glossy texture when

grown on LB agar plates supplemented with IPTG and ampicillin as shown in Figure 4-2.

Figure 4-2: Left panel shows the mucoid cells of *E .coli* JM109/pRcsA2 and the control strain is on the right side

These samples were tested for total carbohydrate production and presence of colanic acid based on fucose content (Sutherland, 1969). The total carbohydrate content of JM109/pRscSA2 strain was found to be about five times higher than that of the control strain JM109/pEdinbrick1 (Figure 4-3), and the colanic acid content of JM109/pRcsA2 was fourteen times greater than that of the control strain.

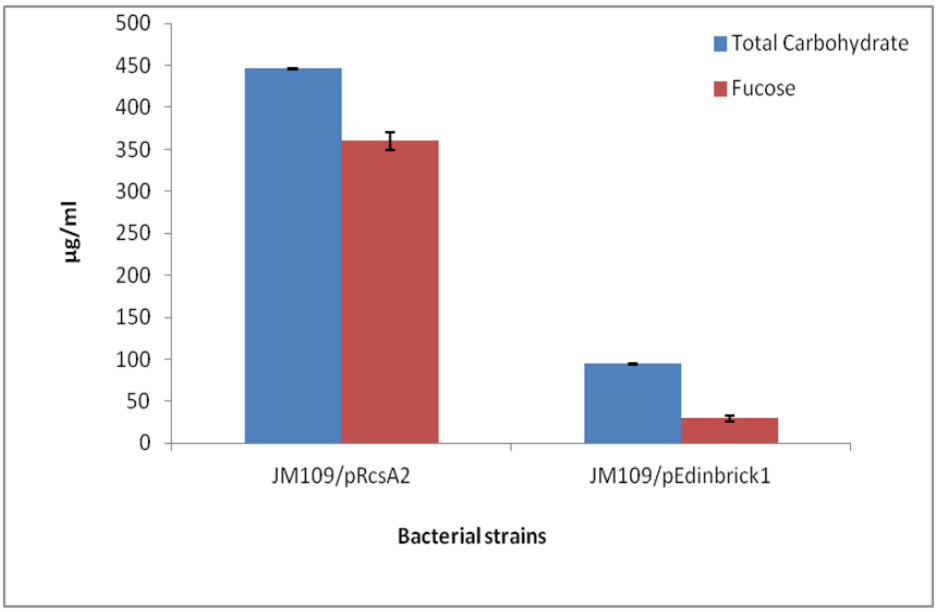

Figure 4-3: Quantification of total EPS and Fucose for JM109/pRcsA2 (mucoid) and JM109/pEdinbrick1 (control) strain

4.3.1 b Preliminary investigation of the growth kinetics of the mucoid strain, E. *coli* JM109/pRcsA2

The developed strain *E.coli*/pRcsA2 and the control strain were tested using silver nanoparticles (10nm diameter) and the growth patterns were studied. It was observed that both strains showed a similar trend but the growth rates varied (Figure 4-4). The control strain is sensitive to increase in nanoparticle concentration, whereas the growth rate of *E. coli* JM109/pRcsA2 is statistically unaffected by increasing silver nanoparticle concentration, at least between the range of 5.5 and 9.2 mg/L tested here. In order to confirm this, the OD values at 360 minutes for each nanoparticle concentration were normalized to samples without nanoparticles for

each strain in order to account for the difference in natural growth rate. The normalized OD values decrease much more sharply for the JM109/pEdinbrick1 strain (Figure 4-4c), confirming a higher dose-sensitivity than JM109/pRcsA2. This experiment was repeated but unfortunately, there were no experimental replicates to confirm the observation.

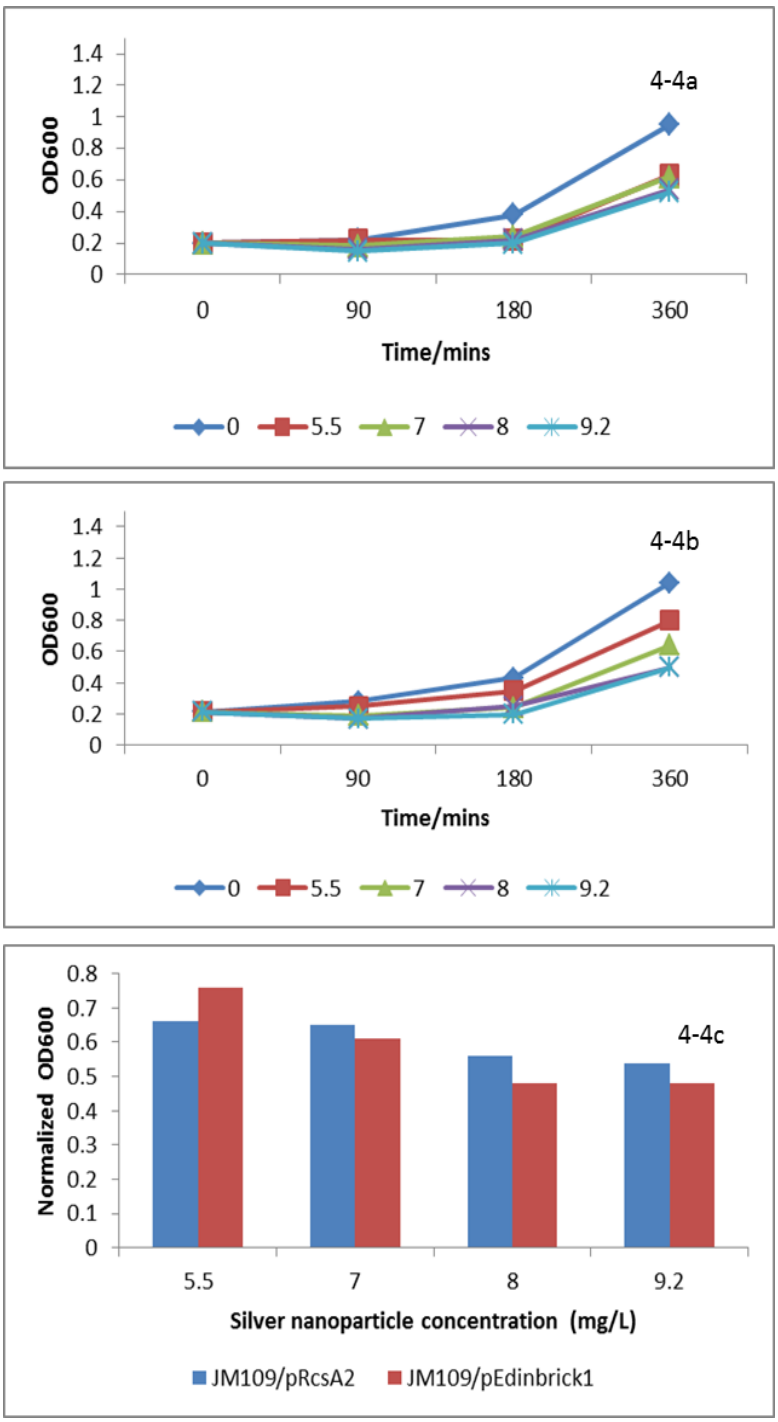

Figure 4-4: (a) JM109/pRcsA2 (mucoid) and Fig. 4-4b, JM109/pEdinbrick1 (control). In Fig. 4-4c, the OD600 values at time = 360 minutes for the different nanoparticle concentrations (mg/L) normalized to the control samples.

4.3.2. *E. coli* JM109 pRcsA2 shows better survival upon exposure to nanoparticles

The response of JM109/pRcsA2 towards nanoparticles was investigated by exposing the cells to both 100 nm and 10 nm silver nanoparticles at the same concentration of 6 mg/L. This experiment provided an insight into the protective role of EPS and at the same time, the effect of grain size on the toxic potential of nanoparticles. It was found that the EPS overproducing strain JM109/pRcsA2 showed higher cell viability than the control strain JM109/pEdinbrick1. The marginal increase in CFU/ml for JM109/pRcsA2 at 100 nm exposure is not statistically significant relative to controls without nanoparticles (Figure 4-5) For the 10 nm exposure condition, there was a statistically significant decrease in cell growth between controls and nanoparticle-treated samples between the strains (p=0.02) as shown in Figure 4-5. In addition, this experiment shows that the 10 nm Ag nanoparticles were more toxic than the 100 nm (p=0.02). This observation has been reported in other studies too (Choi, 2008a, b, Carlson e al., 2008). Similarly, JM109/pEdinbrick1 shows a higher drop in cell viability when exposed to 10 nm particles (p=0.01) than JM109/pRcsA2.

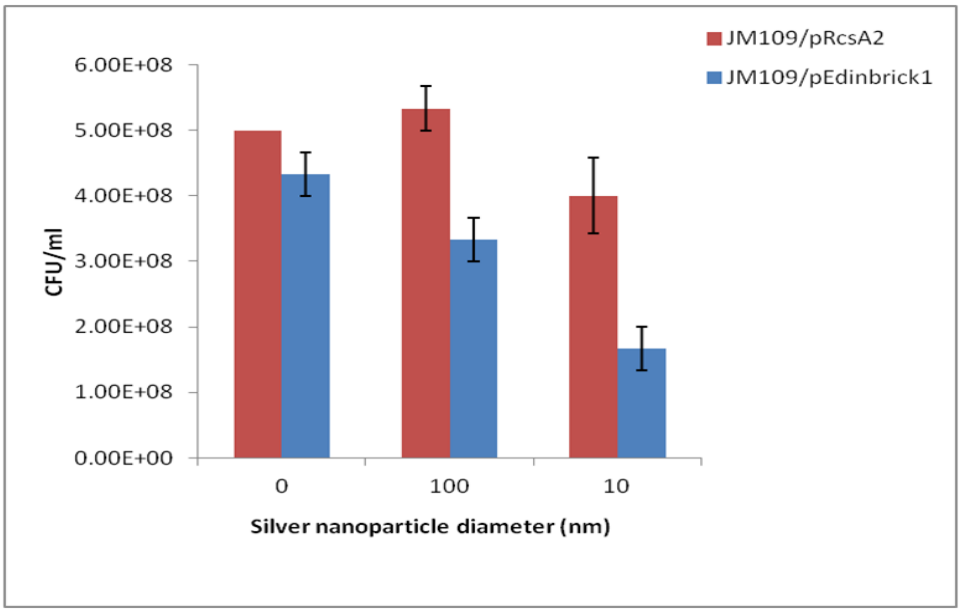

Figure 4-5: Cell viability test at 100 and 10 nm silver nanoparticle exposure

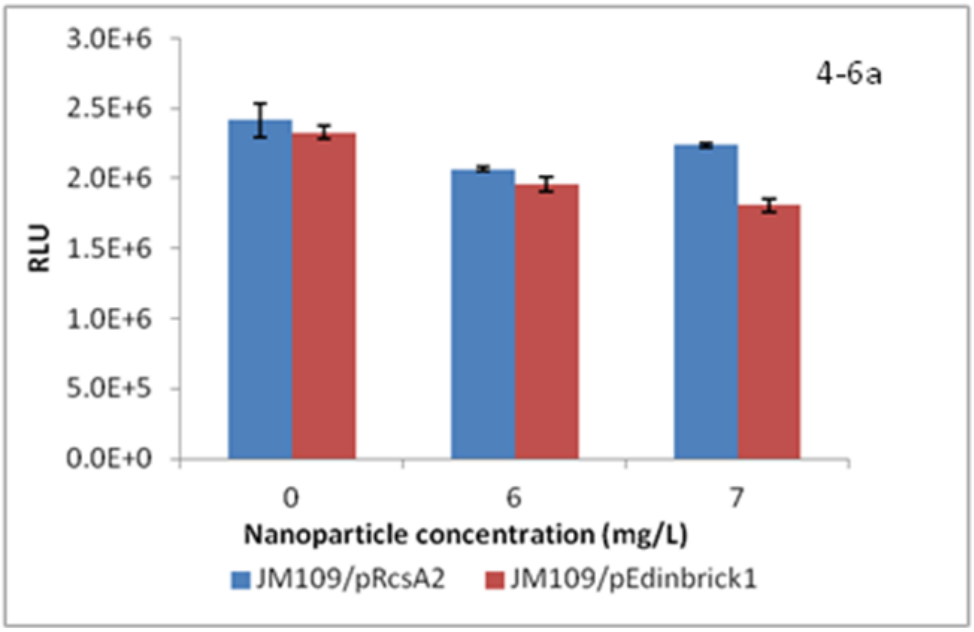

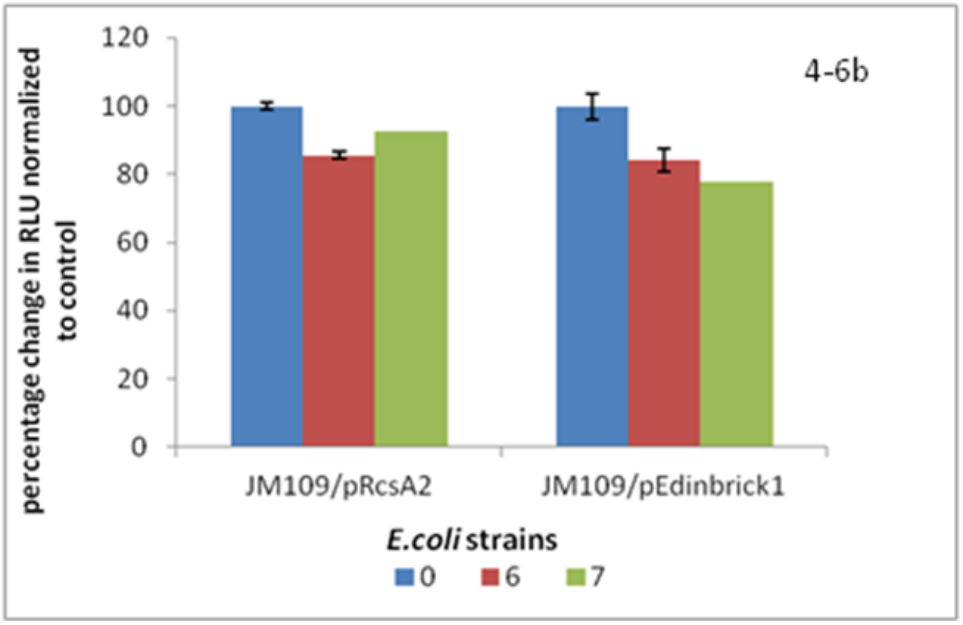

Figure 4-6a and 4-6b: Cell viability of JM109/pRcsA2 and JM109/pEdinbrick1 at 6 and 7 mg/L silver nanoparticle concentration (10 nm diameter) using Bactiter glo kit. Y-axis represents the (a) luminescence units (RLU) for each of the strains and (b) RLU normalized to control samples for each of the strains.

The Bactiter microbial cell viability kit was used to determine the cell viability in another experiment where both strains were exposed to 10 nm silver nanoparticles. The control strain showed a decrease in luminescence (Relative luminescence units/RLU) while the mucoid strain JM109/pRcsA2 shows a marginal change (statistically insignificant), indicative of the fact that it shows slight resistance towards nanoparticle toxicity (Figure 4-6b).

4.3.3 Rm7096, a succinoglycan overproducing strain of *Sinorhizobium meliloti* shows better survival than the parent strain Rm1021 and non EPS producing mutant strain Rm7210

The impact of silver nanoparticles on the *S. meliloti* parent strain RM1021 which produces EPS (Type 1 succinoglycan) was compared with two mutant forms: Rm7096, an EPS overproducing strain, and Rm7210 which does not produce any EPS (Doherty et al., 1988, Yao et al., 2004, Reuber and Walker, 1993, Zhang et al., 2008, Meade et al., 1982). Figure 4-7a and 7b respectively show the microscopic images where EPS has been effectively stained by the dye calcofluor in two strains, exoS (EPS overeproducing strain) and RM1021 (the parent strain). The EPS overproducing mutant Rm7096 strain showed maximum cell viability at all three different silver nanoparticle concentrations (Figures 4-7c and 4-7d) compared with the mutant strain Rm7210. Rm7210 shows similar survival to the parent strain at 7 mg/L and 8.2 mg/L silver nanoparticle concentrations bars =10μm.

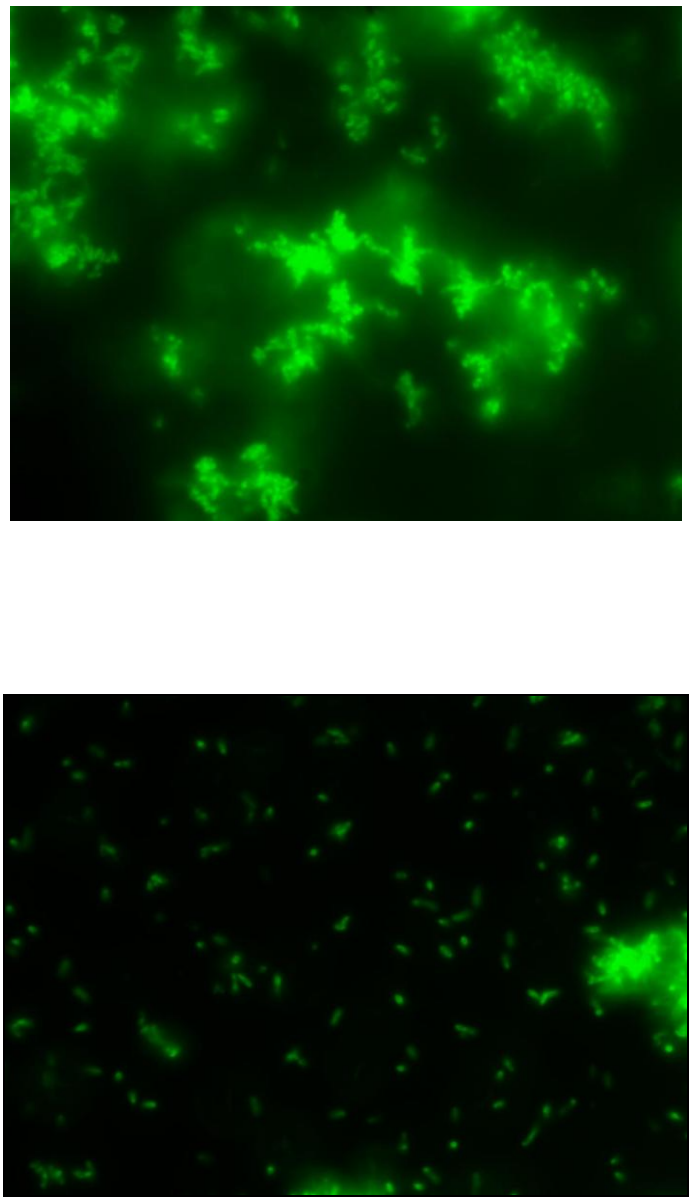

Figure 4-7a: Calcofluor stained samples of *S.meliloti* (a) Rm7096 and (b) Rm1021, parent strain (bars=10 μm). Phase contrast microscopy of cells showing distribution of succinoglycan stained by calcofluor and imaged by fluorescent microscopy

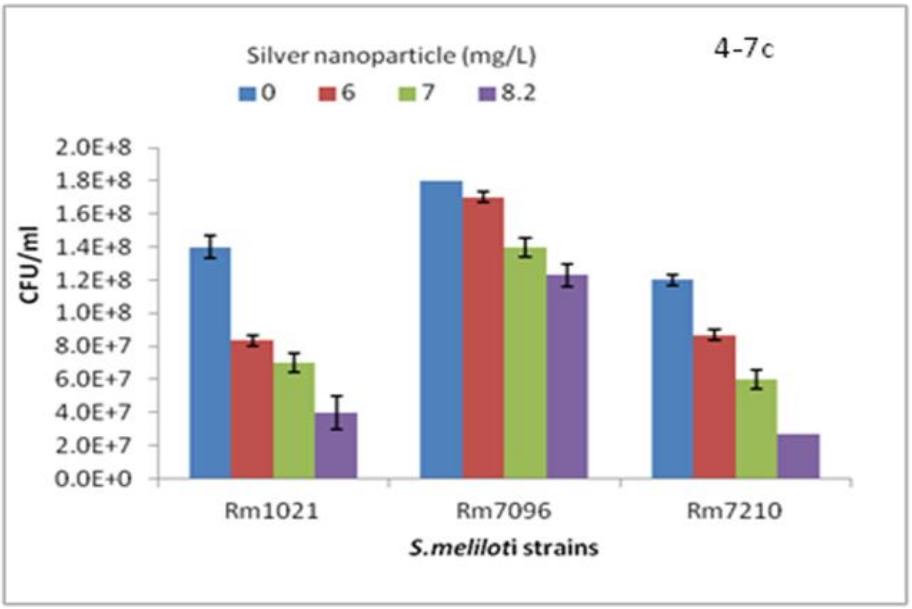

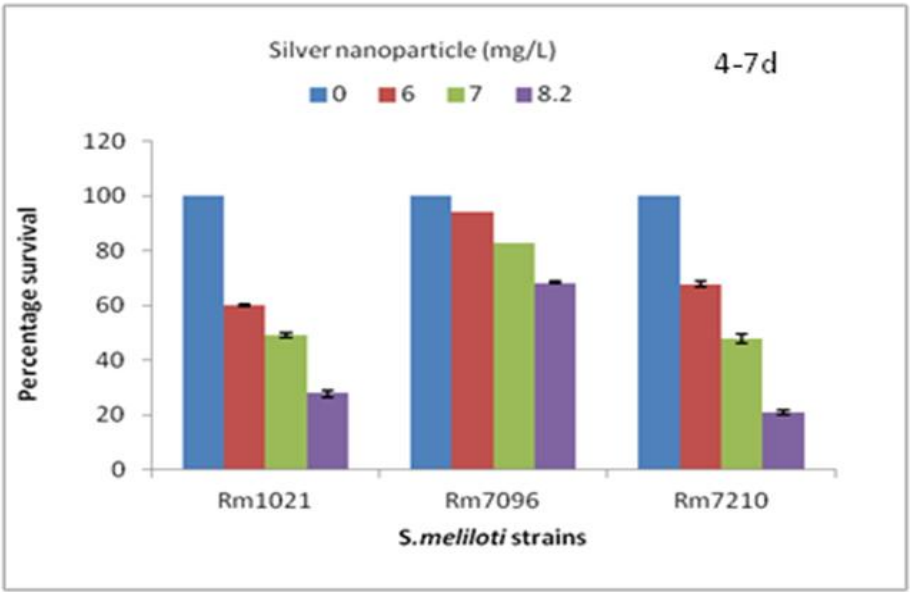

Figure 4-7c and 4-7d: Silver nanoparticle exposure study using mutant strains of *S.meliloti*. The EPS producing strain Rm7096 shows higher cell viability than the parent strain, Rm1021 and non eps producing strain Rm7210

4.3.4 Speciation of silver from silver nanoparticles

ICP analysis indicated that a small fraction of dissolved silver was being released into the medium in a 2 hour exposure period (accounting for 0.27 mg/L or 4.5% of initial concentration of silver nanoparticle dispersion added to the medium). Exposure of cells to the equivalent 0.27 mg/L silver nitrate solutions does not lead to an appreciable drop in cell count (Figure 4-8); suggesting that release of silver ions from nanoparticle surface cannot alone explain all the toxicity observations.

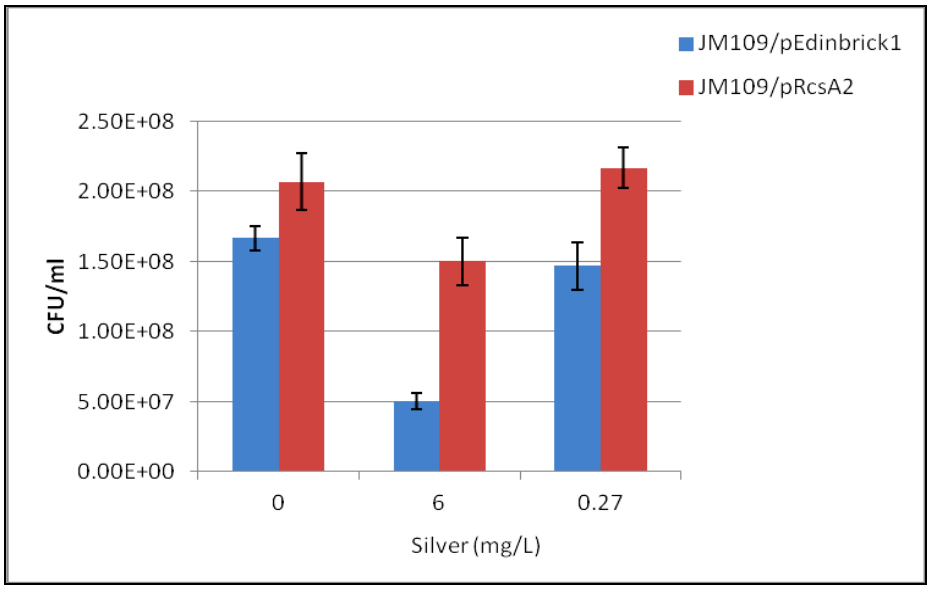

Figure 4-8: **Comparison of toxicity impact of silver nanoparticles (10 nm diameter) vs. residual ionic silver on *E. coli.* Based on the ICP-OES analysis the toxicity of ionic silver released in the exposure medium (0.27 mg/L) has been compared to the silver nanoparticles (6 mg/L).**

This supports the hypothesis that the loss in cell viability was primarily due to the nanoparticles that could have entered the cells rather than just ionic silver

released into the medium. However, the impact of silver ions cannot be totally negated because media used for exposure studies also contained chloride, which potentially led to precipitation of AgCl (Dimkpa et al., 2011b, Calder et al., 2012), thereby reducing total bio-available ionic silver. To fully account for this removal requires determining the relative rates of silver nanoparticle dissolution and silver chloride precipitation in order to demonstrate whether the residence time of silver ions in the medium is long enough to make it bioavailable. While this was beyond the scope of this study, the concentration of Ag^{+} ions in equilibrium with 0.0343 mol/L total chloride in the medium could be calculated based on the solubility product constant of 1.77×10^{-10} mol^2L^{-2} for AgCl (Levard et al., 2012). Using the extended Debye-Huckel equation for activity correction (and ignoring organic compounds in the ionic strength calculation) yields an equilibrium ionic silver concentration of about 5.15×10^{-9} mol/L or 5.56×10^{-4} mg/L. This is several magnitudes lower than the average 0.3mg/L we can detect, suggesting that some of the silver detected is probably still nanoparticulate. The probable presence of silver nanoparticles in the supernatant was also implied by residual absorbance at 400nm using a UV-Visible spectrometer. Together, these analyses suggest that most of the Ag^{+} ions are precipitated out of the media and hence that all/most of the toxicity we see is due to nanoparticles. Perhaps the separation method used, adapted from is not as effective as suggested. This is an important observation regarding the protective role of extracellular polymeric substance (EPS) to nanoparticle toxicity since ionic silver may well diffuse through the EPS barrier. This method was further optimized and the dissolution rate of silver ions from nanoparticlulate surface was done by using ulttrafiltration and centrifugation by using amicon filters (3000MWCO) (Singh

and Ramarao, 2012). This method showed low concentration of ionic silver in the supernanatant thereby suggesting that the procedure used earlier was not efficient for effective seperation of nanoparticles and ions.

4.3.5 EPS and Xanthan protect non-EPS containing cells against nanoparticle toxicity

Further nanoparticle exposure experiments were carried out with addition of the well-characterized polymer xanthan to investigate whether it can play a protective role against nanoparticle toxicity, using the control strain JM109/pEdinbrick1, which does not produce a significant level of colanic acid. The cell viability was higher when xanthan was added during exposure (Figure 4-9). For each silver nanoparticle concentration, the addition of xanthan results in better growth in terms of CFU (Figure 4-9a) and survival percentage (Figure 4-9b). A similar protective response was also observed when EPS purified from JM109/pRcsA2 was added to another strain of *E. coli*, BW25113*/Δyhak,* which also produces minimal levels of polysaccharides (Figure 4-10a and 4-10b). The result was statistically significant (p=0.03).

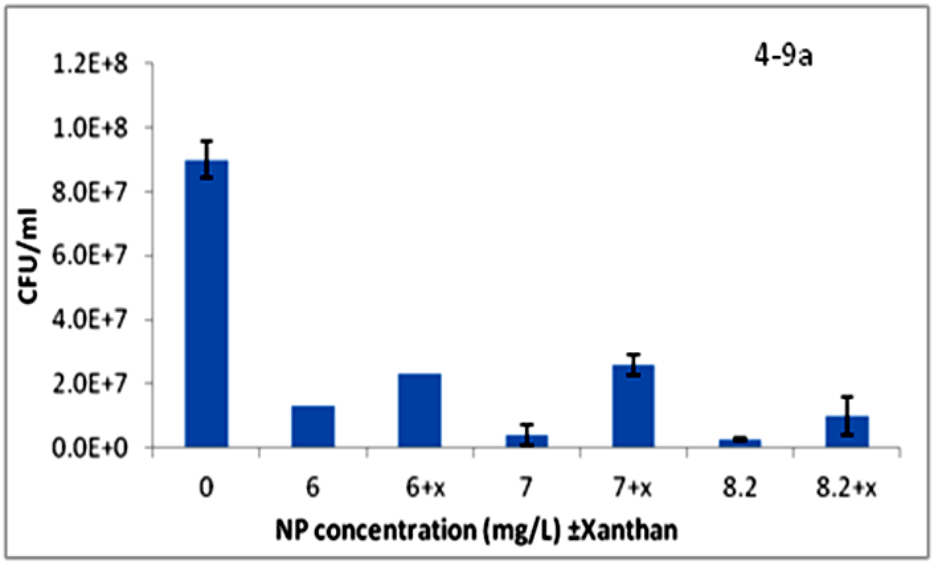

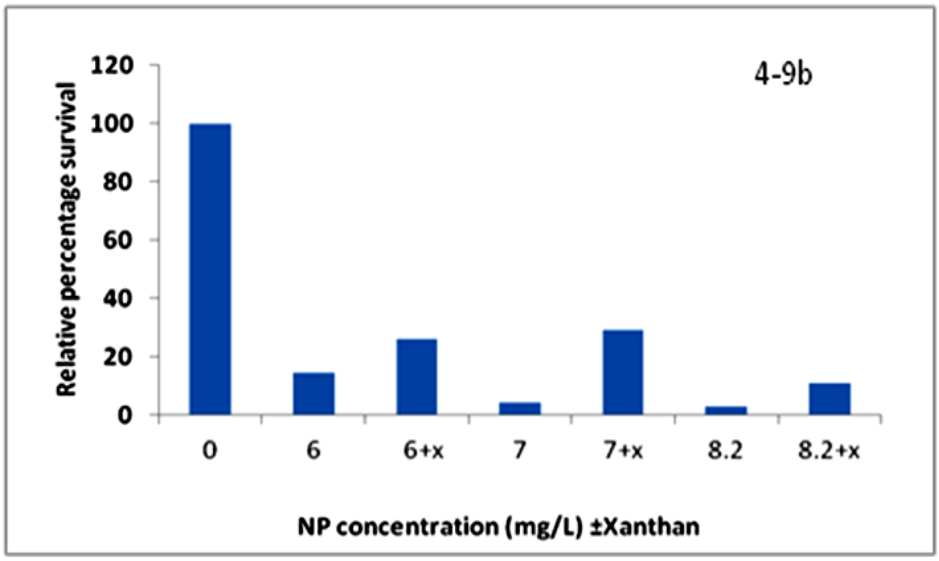

Figure 4-9a and 4-9b: Addition of xanthan to cell culture provides protection against silver nanotoxicity. The y axis (4-9b) shows relative percentage survival normalized to controls without nanoparticles.

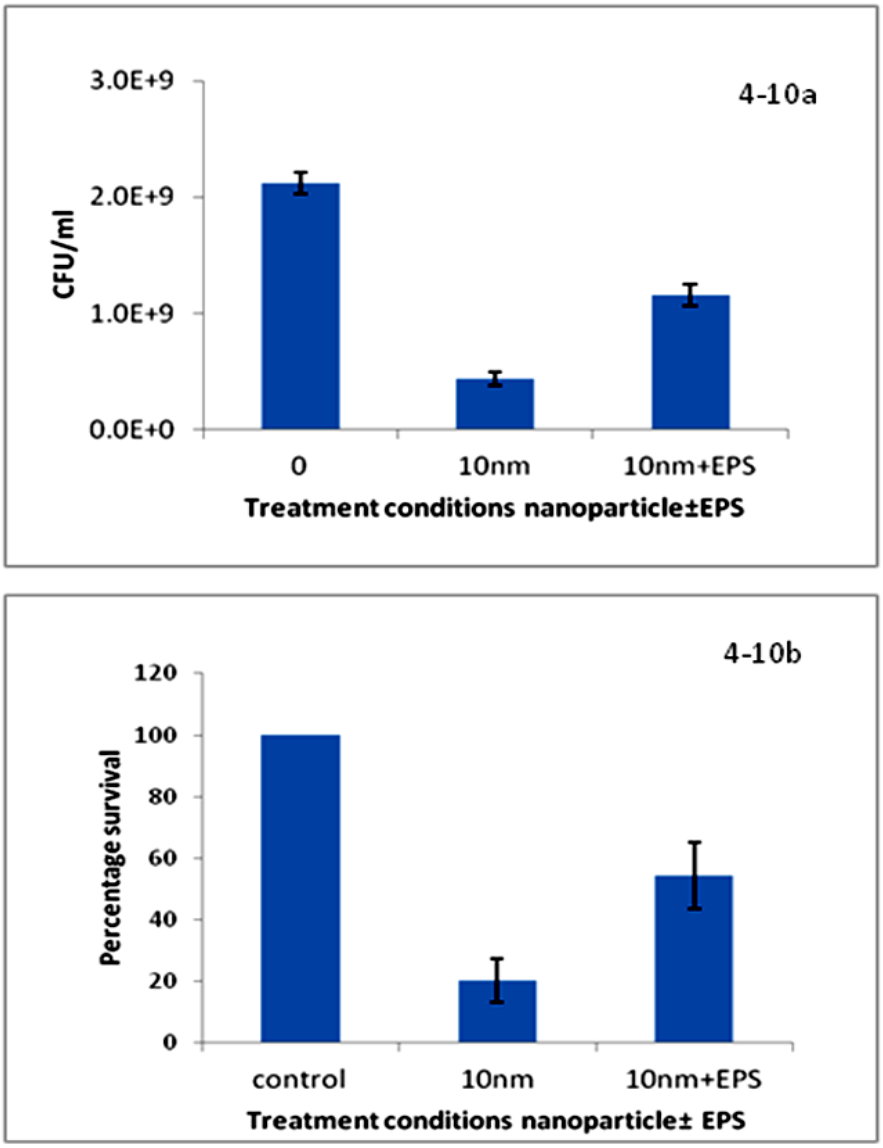

Figure 4-10a and 4-10 b: Protective effect of EPS isolated from *E.coli*/JM109/pRscA2 on *E.coli*/Δ yhaK

4.3.6. TEM analysis shows silver nanoparticle invasion of JM109/pEdinbrick1 control cells

In order to study the fate of nanoparticles and their spatial relationship to cells, TEM was performed on samples of JM109/pRcsA2 and control strain

JM109/pEdinbrick1 exposed to 7 mg/L silver nanoparticles (10 nm). Figure 4-11 compares sections of the two strains when exposed to nanoparticles. After exposure to silver nanoparticles, JM109/pEdinbrick1 cells show diffuse cell membranes, with the occasional dark spots representing silver nanoparticles inside cells (Figure 4-11a). Nanoparticles outside cells appear to have been washed away during preparation and mounting in the case of the control strain (Figure 4-11b); however, the EPS released by the JM109/pRcsA2 seems to have trapped much of the nanoparticulate silver in the matrix as seen in Figure 4-11c. Secondly, JM109/pRcsA2 cells show a marked tendency towards clumping/aggregation, with the nanoparticles trapped on/outside a relatively intact membrane (Figure 4-11c), while cells of the control strain do not show this.

4.3.7. Polysaccharide increases the hydrodynamic diameter of silver nanoparticles

Particle size analysis shows that both sets of nanoparticles used in this study (10 nm and 100 nm diameter) maintained their nominal sizes when dispersed in water and M9 medium (Figures 4-12a and 4-12b). Moreover, no change in size was evident when polysaccharides were added to nanoparticles dispersed in water. However, addition of polysaccharides to nanoparticle suspensions in M9 medium had a significant effect, particularly on the 10 nm nanoparticle dispersion where measured particle sizes more than doubled, while 100 nm nanoparticles increased their apparent size by 20%. The nanoparticles also show a greater aggregation depending on the length of time they were left suspended in the medium.

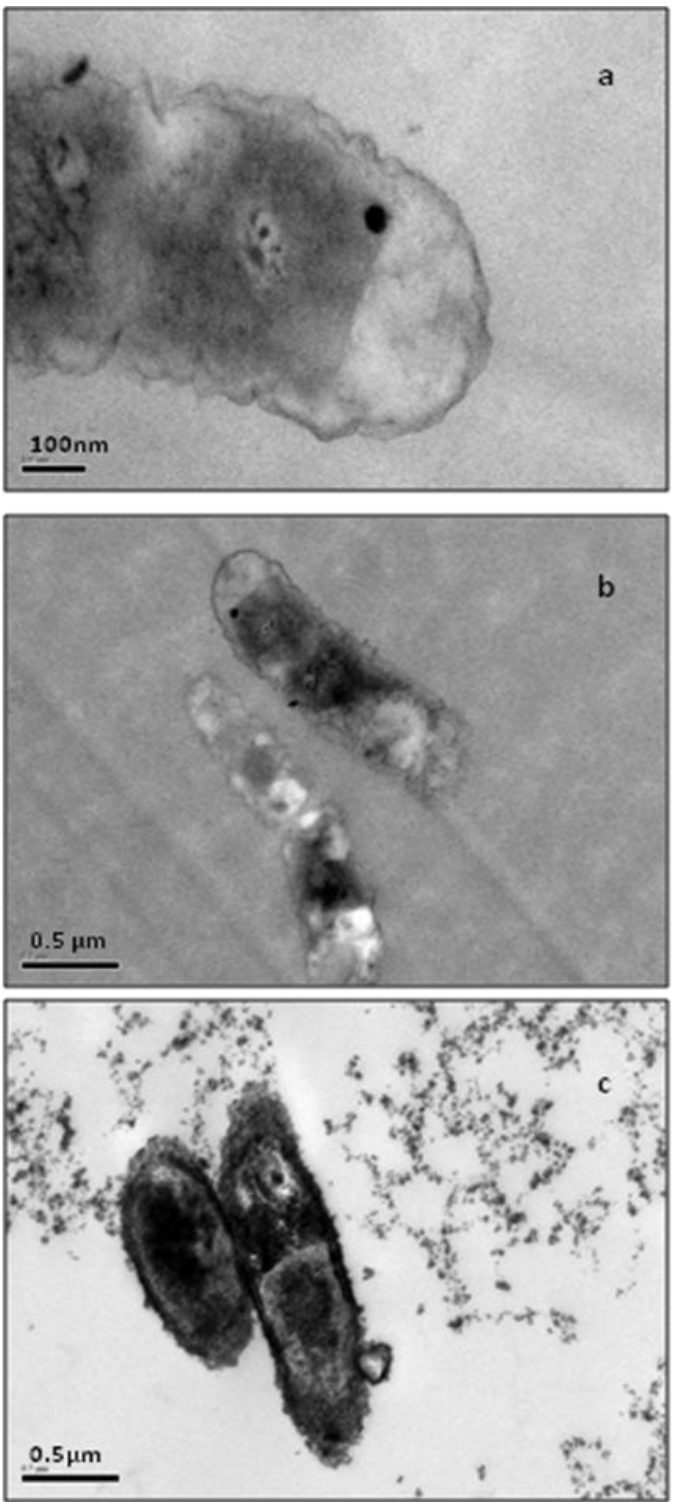

Figure 4-11: TEM images of *E. coli* exposed to silver nanoparticles: comparison between *E.coli*/pRcsA2 (4-11c) and *E.coli*/pEdinbrick1 (4-11a, b). The EPS producing strain, JM109/pRcsA2 (Figure c) shows aggregations and attached nanoparticles on the surface.

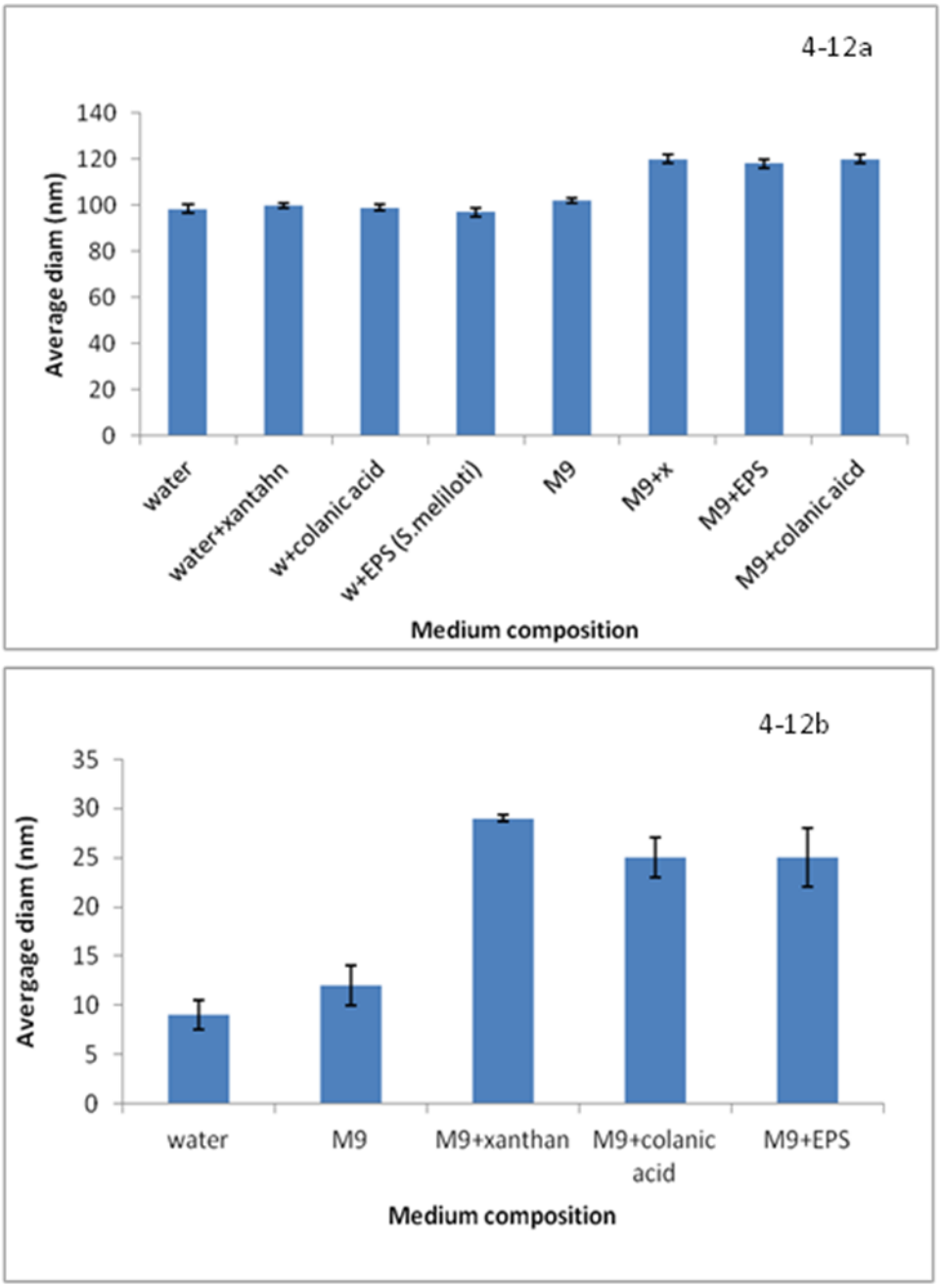

Figure 4-12a and 4-12 b Presence of ions and EPS/xanthan promotes aggregation of silver nanoparticles. 100 nm AgNP (Figure 4-12a) and 10 nm silver dispersion (Figure 4-12b) have been used for characterization study

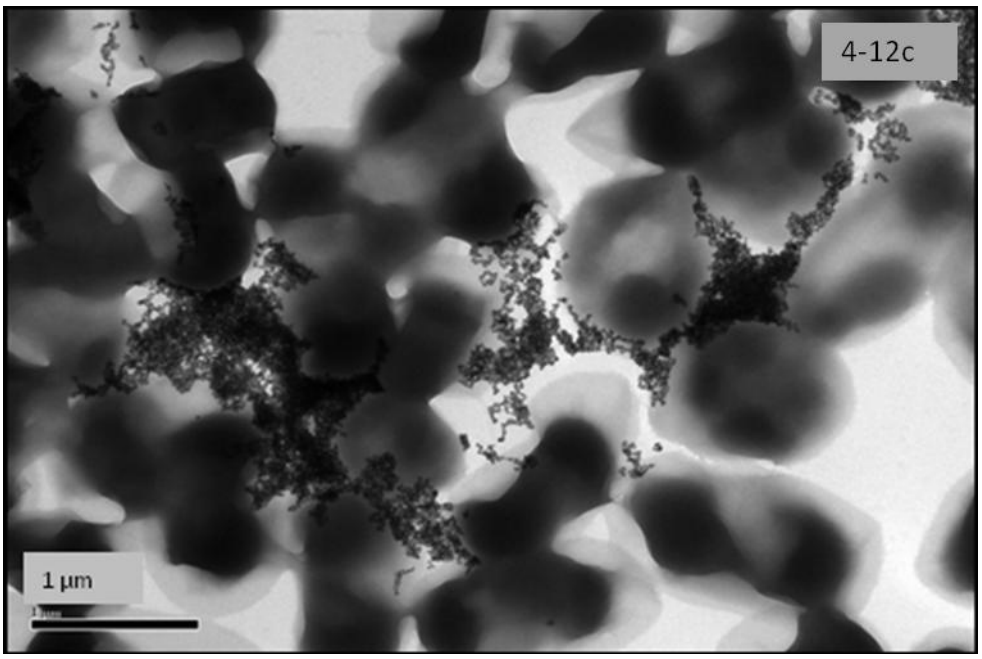

Figure 4-12c: SEM of silver nanoparticles exhibiting aggregation between the cells suspended in LB medium (Bars= 1 µm).

4.4. Discussion

4.4.1 EPS encapsulates the cells and reduces exposed surface area

EPS production by microbial cells serves a number of different functions including stabilization and protection of the biofilm structure through increasing resistance to dehydration and biocides, facilitating adhesion to surfaces (Omoike and Chorover, 2004, Perry et al., 2005, Omoike and Chorover, 2006) and promoting cell aggregation and biofilm accumulation (Cammarota and Sant anna, 1998). The protective role of EPS against different biocides, including metals, is well established. These results are therefore consistent with the few recent studies in the literature (Liu et al., 2007, Battin et al., 2009, Dimkpa et al., 2011b, Dimkpa et al.,

2011a). What remain unclear are the mechanisms by which EPS mediates cell survival. Most previous studies have demonstrated the protective role of EPS either by comparing toxicity of nanoparticles between planktonic cells (which produce less EPS) and biofilms (Fabrega et al., 2009) or by extracting the EPS using physicochemical methods (Dimkpa et al., 2011b). However, planktonic and biofilm cells have other physiological differences which may affect the results, and use of physical methods to remove EPS can in itself compromise cell viability or result in partial removal of EPS. JM109/pRcsA2 produces EPS and had a higher percentage survival than the control strain when exposed to silver nanoparticles of two different sizes, 100 and 10 nm diameter (Figure 4-5). This observation clearly supports the fact that EPS protects the cells against nanoparticle toxicity. A statistically significant difference between the samples of both strains of *E.coli* was observed (p=0.0002) at 6 mg/L silver (10 nm diameter). One possible reason is that EPS encapsulates the bacteria and provides a protective layer against incoming nanoparticles, which is consistent with the microscopic observations in Figure 4-12c. Moreover, EPS has been shown to be an efficient adsorbent for all nanoparticles, but especially for silver nanoparticles (Kiser et al., 2010, Khan et al., 2011b). By keeping nanoparticles distant from the cells, EPS may also act as a protective barrier by localising reactive oxygen species (ROS) away from cells. It is well known that ROS have very short lifetimes, about 3 nanoseconds (Liu et al., 2007, Battin et al., 2009) and are only effective if produced close to or inside the cell membrane.

4.4.2. EPS reduces toxicity by inducing aggregation of silver nanoparticles

Based on TEM observations, it was hypothesized that EPS may also protect cells by inducing aggregation of nanoparticles in the liquid (Lankoff et al., 2012) thus reducing both their solubility and propensity to penetrate cell walls (Limbach et al., 2005). In order to test this hypothesis, the hydrodynamic diameter of the silver nanoparticles was measured in different media, comparing the mean particle size between suspensions with and without EPS isolated from *E. coli* and *S. meliloti*, and by using the synthetic EPS analogue xanthan. The results supported the hypothesis, showing a statistically significant increase in hydrodynamic diameter in the presence of EPS and xanthan (Figure 4-12 b), but only when nanoparticles were dispersed in minimal medium. Moreau et al. (2007) have also shown that extracellular proteins of microbial origin have the potential to induce aggregation of metal sulphide nanoparticles.

EPS and xanthan also caused silver nanoparticle aggregation when sodium citrate stabilized silver nanoparticles (10 nm) were used in a similar experimental set. Aggregation was not observed when EPS or xanthan were added to nanoparticle suspensions in water. By contrast, Khan et al. (2011a) reported significant aggregation of silver nanoparticles after 4 hours of dispersion in water, which decreased with increasing concentration of EPS extracted from *Bacillus pumilus.* These differences may reflect differences in the composition and hence charge characteristics of the EPS. For example, Dimkpa et al. (2011b) showed that EPS consisting of neutral sugars did not significantly affect the zeta potential of silver nanoparticles, although particle size data was not reported.

Intuitively, colloidal stabilisation of nanoparticle suspensions should lead to increased toxicity (Valodkar et al., 2010). However, surface coatings can also reduce toxicity of silver nanoparticles by reducing oxidative dissolution of nanoparticles, which is now considered to be an important mechanism for increasing bioavailability of ionic silver (Navarro et al., 2008). The effects of EPS are therefore likely to be complex; however, the observed aggregation in the presence of EPS/xanthan, coupled with higher survival of cells in the presence of these macromolecules, suggests that EPS-induced nanoparticle aggregation is an important protective mechanism in this study.

4.4.3 Environmental Implications

An outstanding question to be addressed by *in vitro* toxicity findings is whether they have environmental relevance given the tendency for nanoparticles to aggregate under natural environmental conditions and the possible transformations such as oxidation, dissolution and biotransformation that could happen in the environment. The fact that only a fraction of silver ions were released in the medium suggests that the primary toxicity was due to the silver nanoparticles that could either be disrupting the cell membrane or releasing ionic silver in the cytoplasm following nanoparticle invasion. The finding that silver nanoparticles aggregate in the presence of EPS, and consequently display reduced toxicity in this and other studies (Battin et al., 2009, Fabrega et al., 2009, Jiang et al., 2011, Li et al., 2011b), has important implications for the environment where bacteria occur in the form of biofilms consisting of consortia of microbes. These results suggest that adding xanthan or extracted EPS to cultures that do not produce EPS leads to some degree of co-protection, at lower

concentrations of nanoparticles, by influencing nanoparticle size and stability. However, studies have also shown that when mixed culture biofilms are exposed to nanoparticles, some of the strains show better survival than others, leading to shifts in community composition (Battin et al., 2009, Li et al., 2011b). It is therefore not possible to extrapolate observed EPS co-protection effects on monoculture studies directly to the natural environment. One accepted source of differential susceptibility to toxins is growth rate; wherein cells that grow slowly appear to show better survival (Allison et al., 1998, Moreau et al., 2007). *E. coli* JM109/pRcsA2 shows a slightly lower growth rate relative to the control strain, which is associated with enhanced protection from nanoparticles (Figure 4-4a). Thus, the slower growth rate may be due to EPS overexpressing cells diverting effort into EPS synthesis rather than being due to susceptibility to added nanoparticles.

Finally, it should be noted that many studies are consistent with EPS acting as a physical barrier that traps nanoparticles and prevents entry into cells. Moreover, some studies have demonstrated that components of EPS often lead to aggregation of nanoparticles (Moreau et al., 2007), with consequent reduction in mobility of nanoparticles, while others report enhanced stability of nanoparticles in the presence of EPS (Khan et al., 2011a). These discrepancies likely reflect the diversity of EPS composition, and suggest that the effects of EPS may not be amenable to generalisations.

This work demonstrated that silver nanoparticles were toxic to bacteria and the presence of EPS does reduce the toxicity levels.

References:

1. Adams, L. K., Lyon, D. Y. & Alvarez, P. J. J. 2006. Comparative eco-toxicity of nanoscale TiO2, SiO2, and ZnO water suspensions. *Water Research,* 40**,** 3527-3532.

2. Allison, D. G., Sutherland, I. & et.al), e. A. M. 1998. In biofilm communities: order from chaos? *Bioline Cardiff***,** 381-387.

3. Amato, E., Diaz-Fernandez, Y. A., Taglietti, A., Pallavicini, P., Pasotti, L., Cucca, L., Milanese, C., Grisoli, P., Dacarro, C., Fernandez-Hechavarria, J. M. & Necchi, V. 2011. Synthesis, characterization and antibacterial activity against Gram positive and Gram negative bacteria of biomimetically coated silver nanoparticles. *Langmuir,* 27**,** 9163-9173.

4. Auffan, M., Achouak, W. R. J., Roncato, M., Chaneac, C., Waite, D., Masion, A., Woicik, J., Wiesner, M. R. & Bottero, J. Y. 2008. Relation between the redox state of iron-based nanoparticles and their cytotoxicity toward *Escherichia coli*. *Environ. Sci. Technol.,* 42**,** 6730-6735.

5. Battin , T., Frank, V. D., Weilhartner, A., Ottofuelling, S. & Hofmann, T. 2009. Nanostructured TiO2: transport behavior and effects on aquatic microbial communities under environmental conditions. *Environ. Sci. Technol.,* 43**,** 8098-8104.

6. Beloin, C., Roux, A. & Ghigo, J. 2008. Escherichia coli biofilms. *Curr Top Microbiol Immunol. ,* 322**,** 249-89.

7. Calder, A., Dimkpa, C., McLean, J., Britt, D., Johnson, W. & Anderson, A. 2012 Soil components mitigate the antimicrobial effects of silver nanoparticles towards a beneficial soil bacterium, *Pseudomonas chlororaphis* O6. *Sci Total Environ.,* 429**,** 215-22.

8. Cammarota, M. C. & Sant anna, G. L. 1998. Metabolic blocking of exopolysaccharide sysnthesis: effects on microbial adhesion and biofilm accumulation. *Biotechnol. Lett.,* 20**,** 1-4.

9. Chen, J., Lee, S. M. & Mao, Y. 2004. Protective effect of exopolysaccharide colanic acid of *Escherichia coli* O157:H7 to osmotic and oxidative stress. *International Journal of Food microbiology,* 3**,** 281-286.

10. Choi, O. & Hu, Z. 2008a. Size dependent and reactive oxygen species related nanosilver toxicity to nitrifying bacteria. *Environ. Sci. Technol.,* 42**,** 4583-4588.

11. Choi, O. & Hu, Z. 2008b. Size Dependent and Reactive Oxygen Species Related Nanosilver Toxicity to Nitrifying Bacteria. *Environ. Sci Technol,* 42**,** 4583-4588.

12. Dimkpa, C., Calder, A., Britt, D., McLean, J. E. & Anderson, A. 2011a. Responses of a soil bacterium, *Pseudomonas chlororaphis* O6 to commercial metal oxide nanoparticles compared with responses to metal ions. *Environ Pollut.,* 159**,** 1749-56.

13. Dimkpa, C., Calder, A., Gajjar, P., Merugu, S., Huang, W., Britt, D., McLean, J., Johnson, W. & Anderson, A. J. 2011b. Interaction of silver nanoparticles with an environmentally beneficial bacterium, *Pseudomonas chlororaphis*. *J.Hazard.Mater,* Volume 188**,** 428-435.

14. Doherty, D., Leigh, J. A., Glazebrook, J. & Walker, G. C. 1988. *Rhizobium meliloti* mutants that overproduce the *R. meliloti* acidic calcofluor-binding exopolysaccharide. *J Bacteriol.,* 170(9)**,** 4249-4256.

15. Ebel, W. & Trempy, J. E. 1999. *Escherichia col*i RcsA, a positive activator of colanic acid capsular polysaccharide synthesis, functions To activate its own expression. *J Bacteriol.,* 181(2)**,** 577-584.

16. El Badawy, A., Silva, R. G., Morris, B., Scheckel, K. G., Suidan, M. & Tolaymat, T. M. 2011. Surface charge-dependent toxicity of silver nanoparticles. *Environ. Sci. Technol.,* 45**,** 283-287.

17. Fabrega, J., Renshaw, J. C. & Lead, J. R. 2009. Interactions of Silver Nanoparticles with *Pseudomonas putida* Biofilms. *Environ Sci Technol.,* 43**,** 9004-9009.

18. Fabrega , J., Shona, R., Fawcett, S., Renshaw, J. C. & Lead, J. R. 2009. Silver nanoparticle impact on bacterial growth: effect of pH, concentration, and organic matter. *Environ. Sci. Technol.,* 43(19)**,** 7285-90.

19. Flemming, H. & Wingender, J. 2010. The biofilm matrix. *Nature Reviews,* 8**,** 623-633.

20. Gajjar, P., Pettee, B., Britt, D., Huang, W., Johnson, W. & Anderson, A. 2009. Antimicrobial activities of commercial nanoparticles against an environmental soil microbe, *Pseudomonas putida* KT2440. *J Biol.Eng.,* 3**,** 1611-1754.

21. Gong, A. S., Bolster, C. H., Benavides, M. & Walker, S. L. 2009. Extraction and Analysis of Extracellular Polymeric Substances:Comparison of methods and Extracellular Polymeric Substance Levels in Salmonella pullorum SA 1685. *Environ Eng Sci,* 26**,** 1523-1532.

22. Hong, Y. & Brown, D. G. 2009. Variation in bacterial ATP level and proton motive force due to adhesion to a solid surface. *Appl Environ Microbiol. ,* 75**,** 2346–2353.

23. Hu, X., Cook, S., Wang, P. & Hwang, H. M. 2009. In vitro evaluation of cytotoxicity of engineered metal oxide nanoparticles. *Sci.Total Environ.,* 407**,** 3070-3072.

24. Jiang, G., Shen, Z., Niu, J., Bao, Y., Chen, J. & He, T. 2011. Toxicological assessment of TiO2 nanoparticles by recombinant *Escherichia coli* bacteria. *J. Env. Monit.,* 13**,** 42-48.

25. Jin, X., Li, M., Wang, J., MarambioJones, C., Peng, F., Huang, X., Damoiseaux, R. & Hoek, E. M. V. 2010. High-Throughput screening of silver nanoparticle stability and bacterial inactivation in aquatic media: influence of specific ions. *Environ Sci Technol,* 44**,** 7321-7328.

26. Kasmets, K., Ivask, A., Dubourgier, H. & Kahru, A. 2009. Toxicity of nanoparticles TiO2,ZnO,SiO2 to yeast *Saccharomyces cerevisiae*. *Toxicity invitro,* 23**,** 1116-1122.

27. Khan, S., Mukherjee, A. & Chandrasekaran, N. 2011a. Silver nanoparticles tolerant bacteria from sewage environment. *J. Environ. Sci,* 23(2)**,** 346-352.

28. Khan, S. S., Mukherjee, A. & Chandrasekaran, N. 2011b. Impact of exopolysaccharides on the stability of silver nanoparticles in water. *Water Res.,* 45**,** 5184-5190.

29. Kiser, M. A., Ryu, H., Jang, H., Hristovski, K. & Westerhoff, P. 2010. Biosorption of nanoparticles to heterotrophic wastewater biomass. *Water Res.,* 42**,** 4104-4114.

30. Lankoff, A., Sandberg, W., Wegierek-Ciuk, A., Lisowska, H., Refsnes, M., Sartowska, B., Schwarze, P., Meczynska-Wielgosz , S., Wojewodzka, M. & Kruszewski, M. 2012. The effect of agglomeration state of silver and titanium dioxide nanoparticles on cellular response of HepG2, A549 and THP-1 cells. *Toxicol. Lett.,* 208**,** 197-213.

31. Levard, C., Hotze, E. M., Lowry, G. V. & Brown, G. E. 2012. Environmental Transformations of Silver Nanoparticles: Impact on Stability and Toxicity. *Environ. Sci.Technol.,* 46**,** 6900-6914.

32. Li, M., Noriega-Trevino, Eugenia, M., Nino-Martinez, N., Marambio-Jones, C., Wang, J., Damoiseaux, R., Ruiz, F. & Hoek, E. M. V. 2011a. Synergistic Bactericidal Activity of Ag-TiO2 Nanoparticles in Both Light and Dark Conditions. *Environ Sci Technol.,* 45**,** 8989-8995.

33. Li, M., Zhu, L. & Lin, D. 2011b. Toxicity of ZnO nanoparticles to *Escherichia coli*: mechanism and the influence of medium components. *Environ. Sci.Technol.,* 45**,** 1977-1983.

34. Limbach, L., Y.Li, R.Grass, Brunner, T. J., Hintermann, M., M.Muller, Gunther, D. & Stark, W. 2005. Cerium oxide nanoparticle uptake in human lung fibroblasts: effects of particle size, agglomeration and diffusion at low concentrations. *Environ. Sci.Technol.,* 39**,** 9370-9376.

35. Liu, Y., Li, J., Qiu, X. & Burda, C. 2007. Bactericidal activity of nitrogen-doped metal oxide nanocatalysts and the influence of bacterial extracellular polymeric substances (EPS). *J Photochem Photobiol. A: Chem,* 190**,** 94-100.

36. Lowry, G. V., Gregory, K. B., Apte, S. C. & Lead, J. R. 2012. Transformations of Nanomaterials in the Environment. *Environ. Sci.Technol.,* dx.doi.org/10.1021/es300839e.

37. Majdalani, N. & Gottesman, S. 2005. The Rcs phosphorelay: A Complex Signal Transduction System. *Annual Review of Microbiology,* 59**,** 379-405.

38. Meade, H., Long, S. R., Ruvkun, G. B., Brown, S. E. & Ausubel, F. M. 1982. Physical and genetic characterization of symbiotic and auxotrophic mutants of *Rhizobium meliloti* induced by transposon Tn5 mutagenesis. *J Bacteriol.,* 149(1)**,** 114-122.

39. Moreau, J., Weber, P., Michael, C., Martin, M., Gilbert, B., Hutcheon, I. & Banfield, J. F. 2007. Extracellular proteins limit the dispersal of biogenic nanoparticles. *Science,* 316**,** 1600-1603.

40. Morones, J. R., Elechiguerra, J., Camacho, A., Holt, K., Kouri, J., Ramrez, J. T. & Yacaman, J. 2005. Bactericidal impact of silver nanoparticles. *Nanotechnology,* 16**,** 2346-2353

41. Navarro, E., Piccapietra, F., Wagner, B., Marconi, F., Marconi, F., Kaegi, R., Odzak, N., Sigg, L. & Behra, R. 2008. Toxicity of silver nanoparticles to *Chlamydomonas reinhardtii*. *Environ. Sci. Technol.,* 42**,** 8959-8964.

42. Nowack, B. & Bucheli, T. D. 2007. Occurrence, behavior and effects of nanoparticles in the environment. *Environ. Pollut. ,* 150**,** 5-22.

43. Omoike, A. & Chorover, J. 2004. Spectroscopic study of extracellular polymeric substances from *Bacillus subtilis*: aqueous chemistry and adsorption effects. *Biomacromolecules,* 5**,** 1219-1230.

44. Omoike, A. & Chorover, J. 2006. adsorption of geothite to extracellular polymeric substances from *Bacillus subtilis*. *Geochem.Cosmochim.Acta,* 70**,** 827-838.

45. Pal, S., Tak, Y. & Song, J. M. 2007. Does the antibacterial activity of silver nanoparticles depend on the shape of the nanoparticle? A study of the Gram-negative bacterium *Escherichia coli*. *Appl. Environ. microbiol.,* 73**,** 1712-1720.

46. Perry , T., Klepac, C., Zhang, X. V., McNamara, C. J., Polz, M. F., Martin, S. T., Berk, N. & Mitchell, R. 2005. Binding of harvested bacterial exopolymers to the surface of calcite. *Environ. Sci.Technol.,* 39**,** 8770-8775.

47. Reuber, T. & Walker, G. C. 1993. Biosynthesis of succinoglycan, a symbiotically important exopolysaccharide of *Rhizobium meliloti*. *Cell,* 74(2)**,** 269-280.

48. Scown, T. M., Santos, M. E., Eduarda, M., Johnston, B. D., Gaiser, B., Baalousha, M., Mitov, S., Lead, J. R., Stone, V., Fernandes, T. F., Jepson, M., Aerle, R. & Tyler, C. R. 2010. Effects of aqueous exposure to silver nanoparticles of different sizes in rainbow trout. *Toxicol. Sci.,* 115(2)**,** 521-534.

49. Singh, R. P. & Ramarao, P. 2012. Cellular uptake, intracellular trafficking and cytotoxicity of silver nanoparticles. *Toxicol. Lett.,* 213(2)**,** 249-59.

50. Sondi, I. & Sondi, B. S. 2004. Silver nanoparticles as antimicrobial agent: a case study on *E. coli* as a model for Gram-negative bacteria. *J.Colloid. Interphase Sci.,* 275**,** 177-182.

51. Stout, V., Torres-Cabassa, A., Maurizi, M. R., Gutnick, D. & Gottesman, S. 1991. RcsA, an unstable positive regulator of capsular polysaccharide synthesis. *J Bacteriol.,* 173**,** 1738-1747.

52. Sutherland, I. 1969. Structural Studies on Colanic Acid, the Common Exopolysaccharide found in the Enterobacteriaceae, by Partial Acid Hydrolysis. *J.Biol.Chem.,* 115**,** 935-945.

53. Valodkar, M., Bhadoria, A., Pohnerkar, J., Mohan, M. & Thakore, S. 2010. Morphology and antibacterial activity of carbohydrate-stabilized silver nanoparticles. *Carbohydrate Res.,* 345**,** 1766-1773.

54. Wehland, M. & Bernhard, F. 1999. The RcsAB box. Characterization of a new operator essential for the regulation of exopolysaccharide biosynthesis in enteric bacteria. *J.Biol.Chem.,* 275**,** 7013-7020.

55. Xia, T., Kovochich, M., Liong, M., Mädler, L., Gilbert, B., Shi, H., Yeh, J. I., Zink, J. I. & Nel, A. E. 2008. Comparison of the Mechanism of Toxicity of Zinc Oxide and Cerium Oxide Nanoparticles Based on Dissolution and Oxidative Stress Properties. *ACS Nano,* 2**,** 2121-2134.

56. Yao, S., Luo, L., Har, K. J., Becker, A., Ruberg, S., Yu, G. Q., Zhu , J. B. & Cheng, H. P. 2004. *Sinorhizobium meliloti* ExoR and ExoS proteins regulate both succinoglycan and flagellum production. *J Bacteriol.,* 186(18)**,** 6042-6049.

57. Zhang, X., Garcia-Contreras, R. & Wood, T. K. 2008. *Escherichia coli* transcription factor YncC (McbR) regulates colanic acid and biofilm formation by repressing expression of periplasmic protein YbiM (McbA). *The ISME,* 2**,** 615-631.

Chapter 5

Rapid transformation of silver and zinc oxide nanoparticles amended into sediments from an urban pond.

Abstract

In vitro studies have shown that metal and metal oxide nanoparticles are toxic to living organisms through production of ions and reactive oxygen species. However, correlating these findings to the natural environment remains challenging. In this study, freshwater sediment microcosms amended with uncapped silver and zinc oxide nanoparticles were analysed for changes in speciation using X-ray absorption spectroscopy. Linear combination fitting of the XANES spectra showed that the nanoparticles were rapidly transformed to sulfides under this treatment, with higher transformation rates for Ag nanoparticles compared to ZnO nanoparticles. Analysis of bacterial diversity using DNA fingerprinting revealed that sulfate reducing bacteria were successfully stimulated but overall microbial community composition was marginally affected, and only at nanoparticle concentrations above 500µg/g sediment, with slightly different community compositions between silver and zinc oxide treatments. Assuming that such speciation changes reduce toxicity, these results suggest that presence of ligands such as sulphide at low concentrations can promote transformation of nanoparticles into insoluble forms, offering an important strategy for reducing nanotoxicity in the environment.

5.1 Introduction

Engineered nanoparticles are being used in many industrial applications (Nel et al., 2006). Thus, it is inevitable that they will find their way into the environment, especially terrestrial and aquatic systems. This creates possibilities of their interaction with the biota in the environment. Therefore, it is important to investigate the toxicity of nanoparticles in a wider context rather than deriving conclusions purely based on in vitro experiments, which often employ pure cultures of bacteria or a plant dosed with high concentrations of a known nanoparticle. These assays, which are conducted in, defined medium help to establish short-term toxicity impacts. These findings (Liu et al., 2007, Huang et al., 2008, Dimkpa et al., 2011), suggest that nanoparticles cause toxicity by DNA damage, injury to cell membrane and oxidative stress (Morones et al., 2005, Kasemets et al., 2009, Park et al., 2009, Li et al., 2011, He et al., 2012). However, these studies provide little information on the net impact of nanoparticles on biota at ecosystem level. There are significant gaps in our current information that makes it difficult to correlate the laboratory findings to the environment where a great degree of heterogeneity exists. For instance, metal nanoparticles like silver, zinc oxide and titanium dioxide have been shown to be very toxic to bacteria (Sondi and Sondi, 2004, Battin et al., 2009, Gajjar et al., 2009, Li et al., 2011). The impact has been attributed to metal ion dissolution and generation of reactive oxygen species (He et al., 2012, Xiu et al., 2012). However, these observations cannot be directly applied to natural systems where sediment has an established presence of dissolved organic matter, humic acid and ligands such as chloride (Fabrega et al., 2009) that could precipitate silver being released from surface of nanoparticles (Levard et al., 2012). Similarly, any water body, for instance

a pond in an urban setting, could have dissolved ions like chloride to precipitate silver that could be released from surface of nanoparticles (Levard et al., 2012).

Such observations have therefore prompted research on the impact of engineered nanoparticles on the natural microbial community present in terrestrial and aquatic habitats (Das et al., 2012, Tong et al, 2012). Terrestrial ecosystem, such as soil comprises of a complex network of abiotic (soil, ions) and biotic (plants, microorganisms) components that interact and drive many physical and chemical processes. A microcosm is an attempt to simplify and mimic an ecosystem in order to investigate the specific issues like nutrient cycling or impact studies (Verhoef, 1996). Microcosms serve as an ideal tool to conduct research on the possible impacts of nanoparticles on a mixed bacterial community under controlled conditions. This experimental design can help simulate a micro environment and the findings could be more useful to predict long term impact of nanoparticles in the environment. The DNA content derived from nanoparticle amended columns can help identify the microbial community and any changes in their composition following treatment. Recent studies conducted in the field of ecotoxicology using the above methods have provided a valuable insight into this subject (Ma et al., 2009, Yuan et al., 2011, Bone et al., 2012). Although most variables are controlled in a microcosm, some element of variability still exists in the experimental design, but it can be argued that real environment is not devoid of such a features too (Becker et al., 2006).

Microcosm studies using engineered nanoparticles done to date are contradictory in their findings and conclusions. On one hand some studies show that nanoparticles do not bring about a drastic impact on microbial community composition, while others report some impact on bacterial communities. For

instance, Tong et al. (2007) demonstrated that exposure to fullerene produced little effect on bacterial population and community structure. However, they later reported that non-functionalized single wall carbon nanotubes can suppress the metabolic activity of bacterial community within a microcosm (Nagy et al., 2011). Bradford et al. (2011) used estuarine sediments to develop microcosms amended with silver nanoparticles. It was observed that most of the silver nanoparticles migrated to the solid phase (an observation found in the current study too) and there was no net impact on the microbial community composition.

Similarly, a study by Muhling et al. (2009) showed that presence of silver nanoparticle in microcosms (made by using estuarine water) had no effect on the microbial community composition. Most of the silver nanoparticles were in top 3 mm of microcosm and the bacteria isolated from these zones did not show any resistance to heavy metals. In contrast to above studies, Ge et al. (2011) found that sediment communities exposed to varying concentrations of zinc oxide and titanium dioxide nanoparticles produced a variable response on bacterial community. Zinc oxide was found to be more toxic than TiO_2 and led to a greater drop in bacterial diversity. Similarly, Rousk et al. (2012) used soil microcosms and found that ZnO nanoparticles were more toxic than the copper oxide nanoparticles. The toxicity mechanism in most of these studies was due to formation of metal ions from the nanoparticles rather than the direct interaction or movement of engineered nanoparticles inside the cells. The exposure studies using Fullerene (C60) have produced some variable results. Application of fullerene led to a reduction of certain bacterial communities only (Kanaly et al., 2011) in contrast to studies discussed above that produced a global reduction in community composition. Similarly, Das et

al. (2009) used bacterial communities from fresh water and found that single exposure to silver nanoparticles did produce changes in the community composition.

Bone et al. (2012) demonstrated that sediment-water microcosms dosed with silver nanoparticles showed a differential behaviour depending on whether plants were also present. Dissolved organic matter released from plants effectively complexed the ionic silver. The microcosms with sediment-water matrix showed that most of the ionic silver occurred as silver sulphide. This study suggests that nanoparticles are prone to transformation and the presence of biogenic matter will contribute significantly to this process.

In this chapter, the potential biotransformation of silver nanoparticles was studied by using sediments from an urban eutrophic pond rich in organic matter. Sulphate levels were scaled up to promote growth of sulphate reducing bacteria that could mediate biotransformation of nanoparticles into sulphides, consistent with previous report. This experimental design was developed in order to address the question of whether presence of sulphide/sulphate can promote rapid transformation of nanoparticles in the environment. XAS analysis showed that nanoparticle amendments to sediment microcosms under conditions relevant to freshwater urban ponds resulted in transformations of metal nanoparticles into metal sulfides, which occur within a few hours of adding nanoparticles to the sediment, possibly driven by natural ambient levels of reactive sulphide in the sediment, due to naturally high organic content of these sediments.

5.2 Materials and Methods

5.2.1 Chemicals and reagents

Silver (100 nm diameter) and ZnO nanoparticles (40 nm diam), zinc sulfide nanoparticles (NP) were obtained from Sigma Aldrich. The bulk salts of silver sulphide, silver sulphate, silver oxide, calcium sulphate, calcium carbonate and cellulose were sourced from Sigma Aldrich and Fisher Scientific, UK. Primers and TA cloning kit were sourced from Sigma. The Ultrapure soil DNA kit was sourced from Cambio Ltd. Gel loading buffer was made with bromophenol blue and xylene cyanol both sourced from Fisher Scientific. Ammonium persulfate and TEMED were sourced from Sigma Aldrich. The reagents to cast gel and gel electrophoresis are as follows: agarose, EDTA, Tris buffer, urea, sodium hydroxide, silver nitrate from Sigma Aldrich, UK. Glacial acetic acid, ethanol, formaldehyde, formamide, acrylamide solution (N.N'-methylene bisacrylamide) solutions were procured from Fisher Scientific.

5.2.2 Development of microcosms

Sediment and water were collected from Blackford pond, within the metropolitan city of Edinburgh, Scotland (Figure 5-1). The organic debris, plant residual matter were removed by wet sieving the sediment and collecting the fraction below 5 mm. The sediment was supplemented with calcium carbonate (a source of pH buffer) and calcium sulphate (as source of sulphur) and cellulose (a carbon source).

Figure 5-1: Blackford Pond: a model for understanding nanoparticle (NP) behaviour in urban water bodies likely to be first receptors for NP discharge.

Nanoparticles were added in the range from 100 to1000 ppm (220 mg/kg -690 mg/kg dry soil equivalent). To 400 g lake sediment about 10 g of cellulose, 2 g of calcium carbonate and 20 g calcium sulphate were added. After homogenizing the mixture, this supplemented sediment was added to Falcon tubes (approximately 20 g) and packed with a glass rod to avoid any air bubbles. The sediment was then topped with 20 ml water collected from the same site and then mixed thoroughly. After mixing, silver and zinc oxide nanopowders were added to the columns and further mixed thoroughly.

Silver nanopowder (100 nm diameter)	**Weight of nanoparticles added to columns each with 40 ml slurry**
A100 mg/L	3.99 mg (220 mg/kg dry soil equivalent)
A 200 mg/L	7.9 mg (438 mg/kg)
A 500 mg/L	19.8 mg (526 mg/Kg)
A 1000 mg/L	40 mg (670 mg/kg)
Zinc oxide nanopowder	
Z 100	3.9 mg (220mg/kg soil)
Z 200	7.8 mg (438 mg/kg soil)
Z 500	19.8 mg (526 mg/kg soil)

Table 5-1a: Nanoparticle concentration used for columns as mg/kg dry soil)

Each sample was prepared in triplicate and there was a set of controls without any nanoparticles. Another set of controls was also prepared with nanoparticles added (T0) and the samples autoclaved (to assess the speciation of added nanoparticles at the start of experiment). This assembly was incubated in light conditions at 26^{o}C for a period of three months to facilitate the formation of a stratified nutrient cycling system and formation of a redox zonation.

5.2.3 Analytical techniques used to investigate the dynamics of nanoparticles in the microcosms

The microcosms were used as model small-scale environment to assess the impact of the nanoparticles on the bacterial community composition and at the same time to investigate changes in the speciation and fate of the nanoparticles. In order to

understand these processes two approaches were employed; (a) **speciation of nanoparticles by** Xray absorption fine structured spectroscopy (XAFS) analysis to investigate if nanoparticles had been transformed to different compounds (b) **molecular biology techniques** to extract the DNA from sediment and assess the bacterial community composition in microcosms.

5.2.3.1 X-ray absorption spectroscopy analysis

The speciation of nanoparticles was studied by using Extended Xray absorption spectroscopy at Beamline B18 at the Synchrotron facility at Diamond, UK.

The experimental set up of the beam line consisted of a source of high-powered x-rays produced from the storage ring. This beam further passes through an optical setup consisting of collimating mirrors to condition the spectral contents as required for analysis (Jiang, 2002). Finally, it is focussed on the samples to be analysed. The samples (0.5 mm thickness approximately) were kept on static flat perspex sample holder. The beam size was 200x250 μm; the sample was aligned about 55^{o} to the beam and a fluorescence detector placed perpendicular to the beam (Figure 5-2a). A Si (311) monochromator and a 9-element Ge solid-state detector were used. The standards were analysed in transmission mode and samples in fluorescence mode. The data for both x-ray absorption near edge (XANES) and fine structure (XAFS) was collected. The spectra was then analysed by Six-pack and Athena software packages according to the standard procedure (Ravel and Newwille, 2005). The spectra recovered after background subtraction and normalization (pre edge and post edge corrections) were fitted to various K ranges depending on the XAF quality.

Normalized μ (E) spectra of all the standards and the samples were then modelled using linear combination fitting (LCF) based on several standards analysed before samples. This helped to determine the species present in the samples of interest (Gondikas et al., 2012).

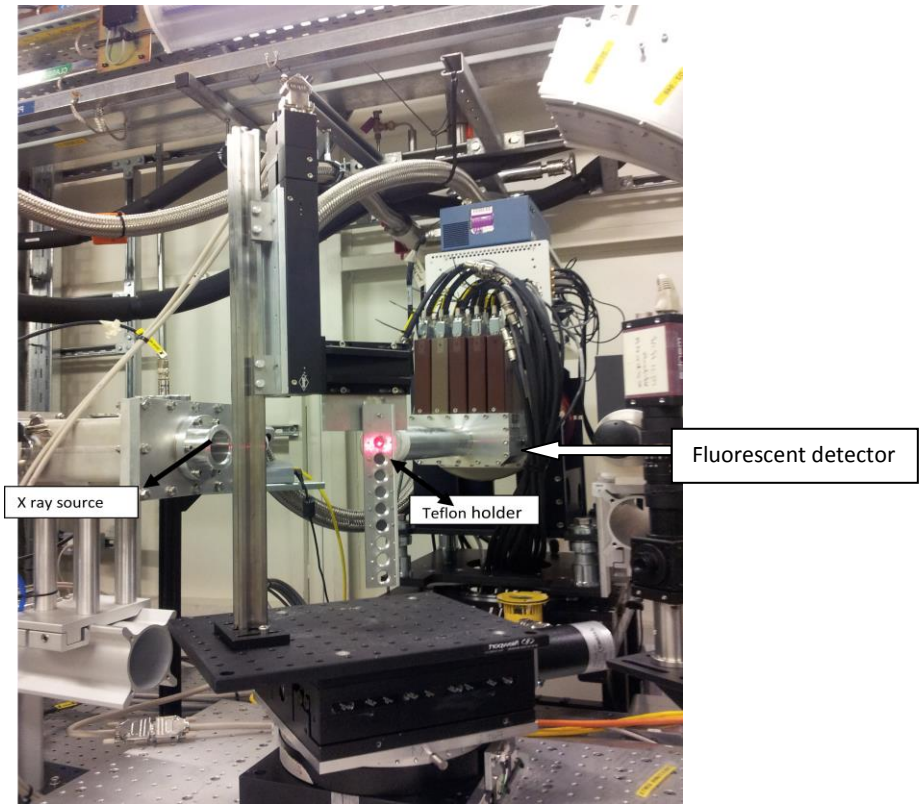

Figure 5-2a: The experimental setup at the Beam B18, synchrotron facility

For the analysis, the sediment samples were freeze- dried. The standards were homogenized and pellets were made by adding cellulose powder. The sediment samples were used without adding cellulose. The following standards were used for silver speciation analysis: silver nanoparticles, silver sulphide, silver chloride, silver

sulphate and silver oxide. As for zinc analysis, zinc oxide nanoparticles, zinc carbonate and zinc sulphides were used.

Besides the dosed microcosms, a few controls (time zero and sterilized time 0) were prepared in the same way for silver 500/1000/ZnO 500 T0. Columns with silver (500 and 1000 mg/L), ZnO (500 mg/L) were sectioned as top, bottom and bulk (mixed) and analysed separately.

5.2.3.2 Molecular Biology techniques

5.2.3.2.1 Community DNA extraction and PCR techniques

The changes in community composition and the presence of sulphate reducing bacteria were determined by DNA extraction and DNA finger printing. Bacterial 16S rRNA genes contain the hyper variable regions (up to 9, V1-V9) that show significant differences between bacterial species and are thus used in diagnostic analysis and determination of variations in bacterial community compositions (Van de Peer et al., 1996).

PCR for the total bacterial community analysis

This process comprises of initially, extracting the DNA from the bulk sediment (0.3 gm) and using it as a template to amplifying the DNA corresponding to 16S rRNA complementary to positions 19-38 and 1581-1541 in the *Escherichia coli* sequence as previously described (Fedorovich et al., 2009) and is approximately 1.5 kb in size. It is then followed by amplification of a smaller region specifically between 341 and 534 on 16 s DNA (that also adds a GC clamp in this process) and is about 250 bp.

GC clamp binds to the conserved DNA sequence flanking the variable region and helps to amplify it.

PCR for the dsrB gene:

Sulphate reducing bacteria (SRB) play an important role in the precipitation of toxic metals through conversion of sulphate to sulphides. The SRB's have a dsr gene that encodes the dissimilatory sulphite reductase, an important enzyme. The DGGE based determination of the SRB's in the microcosms was conducted by using the specific primers developed earlier**.**

A single step PCR was done for the dsrB analysis (Geets et al., 2006) and DSRp2060F (contains a GC clamp) and DSR4R reverse primer (Wagner, 1998) was used. These primers amplify a 350 bp sequence in dsrB gene. Primer sequences and PCR conditions for both amplifications are described in Table 5-1b.

The Cambio UltraClean soil DNA kit was used to extract genomic DNA according to manufacturer's protocol. Both, the water samples and soil (1 gm) was collected from microcosm for total community DNA extraction The PCR reactions were set up in PCR6 Vertical Laminar Airflow Cabinet (Labcaire Systems Ltd.). Negative controls containing no added DNA template were used. Extracted DNA was stored at -20^{o}C. The PCR reaction was carried out in total volume of 50µl reaction mixture using one µl DNA as template according to the manufacturer's protocol. The PCR sprint thermocylcer from Thermo Electron Corporation was used.

Target	Primer	Positions[1]	Sequence 5'-3'	PCR Round	Thermal Cycling Conditions	Reference
Bacteria (16S rRNA genes), DGGE	BactF	8-27	AGAGTTTGATCCTGGCTCAG	1	94 °C for 5 min; followed by 30 cycles of 94 °C for 1 min, 55 °C for 1 min, 72 °C for 3 min; followed by 72 °C for 7 min.	Fernández *et al*., 1998
	BactR	1541-1522	AAGGAGGTGATCCAGCCGCA	1		
	341F-GC	341-357	CGCCCGCCGCGCCCCGCGCCCGTCCCGCCGCCCCCGCCCGCCTACGGGAGGCAGCAG	2	95 °C for 5 min; followed by 28 cycles of 94 °C for 1 min, 64 °C for 1 min, 72 °C for 1 min 30 s; followed by 72 °C for 10 min.	Muyzer *et al*., 1993
	534R	534-518	ATTACCGCGGCTGCTGG	2		
Sulphate reducers (*dsrB*), DGGE	DSRp2060F-GC	420-440	CGCCCGCCGCGCCCCGCGCCCGGCCCGCCGCCCCCGCCCCAACATCGTYCAYACCCAGGG	1	94 °C for 4 min; followed by 35 cycles of 94 °C for 1 min, 55 °C for 1 min, 72 °C for 1 min; followed by 72 °C for 10 min.	Geets *et al*., 2006
	DSR4R	797-781	GTGTAGCAGTTACCGCA	1		

Table 5-1b: Primer sequence and PCR amplification programs used and the underlined sequences correspond to the GC-clamp (Muyzer *et al*., 1993).

5.2.3.2.2. Denaturing gel electrophoresis

The community structure was analysed by denaturing gradient gel electrophoresis (DGGE). The principle behind this technique is that under application of an electric potential and a denaturant gradient, DNA molecules migrate preferentially based on their composition. In order to do so the gel matrix is made up of polyacrylamide containing an increasing concentration gradient of urea and formamide (30/70% for DGGE of normal samples and 40/80% for dsrB) and the samples are run beside an assortment of 16 s clones from various sources as a marker (Figure 5-2b).

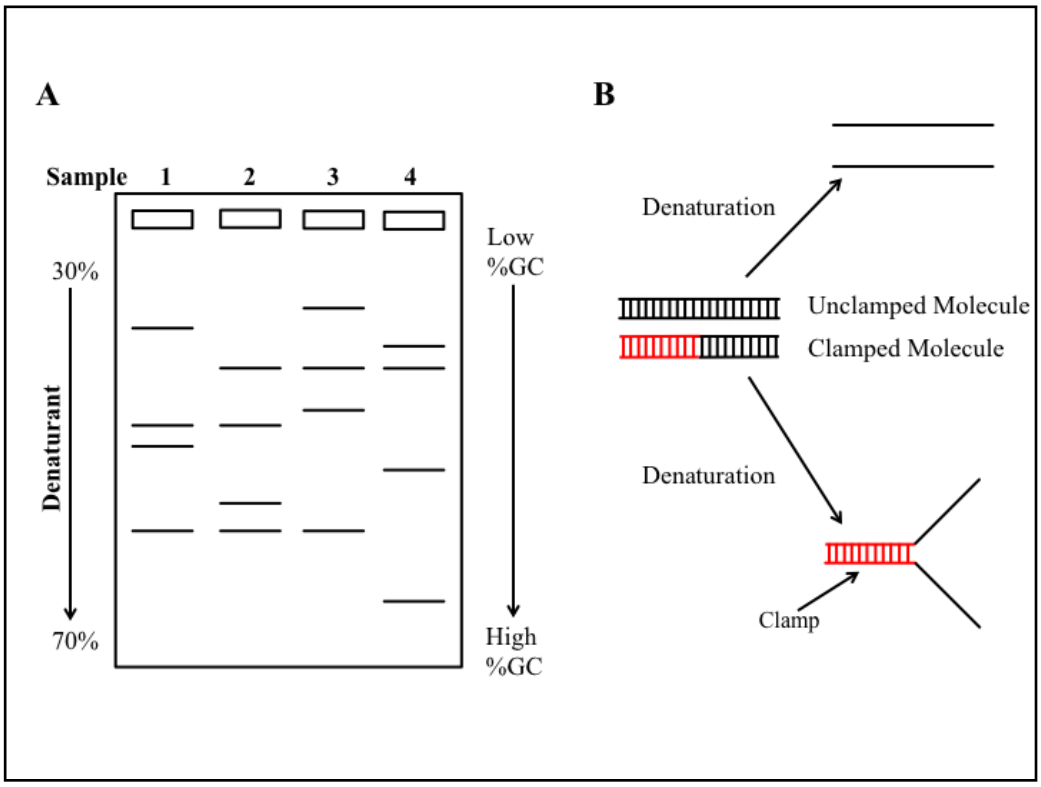

Figure 5-2b: Mechanism of DNA strand separation in DGGE (Strathdee &Free, 2012)

During electrophoresis, the double stranded DNA moves through the gel and denatures based on the GC content. So different DNA molecules based on their composition denature and develop a pattern specific to their composition. The DNA samples that are run on these gels have a GC clamp attached to them by PCR amplification using specific primers. The moment melting of strands reaches the clamp the migration of DNA stops at that point on the gel and it exhibits a specific band pattern on the gel matrix. This band pattern is subsequently analysed by Bionumerics and Primer 6 (software).

Gel preparation:

Gel gradient for a DGGE is either 30-70% (for total community composition) or a 40-80% for dsrB depending on the requirement. The gel preparation requires developing gradient solutions, plug, main gel and the stacker.

a. **Two gradient solutions were prepared, one designated as 0% and the other 80%:**

Recipe per 100 ml of 0% stock consists of 2 ml 50X TAE solution and 27 ml 30% acrylamide solution, it was made to 100 ml with deionized water. High gradient solution was made by mixing 33.6 g urea, 32 ml formamide, 2 ml 50X TAE solution and 27 ml acrylamide solution. This mix was made up to 100 ml with deionized water. Both the solutions were wrapped in foil and stored at 4^{o}C (Strathdee and Free, 2012).

APS solution: a 10 % ammonium persulpahte solution was made by dissolving 100 mg APS in one ml of water and stored at 4^{o}C.

Plug: 1 ml 0% DGGE solution and Gel: A 30% and 70% gel mix is made by using the two stocks of gradient solutions the stacker is made up of a 0% DGGE solution only.

b. Gel preparation requires following apparatus:

DGGE gel apparatus includes glass plates, spacers, clamps, casting stand, tank with a stirrer and heater (Biorad D Code systems). The gel is poured between two glass plates on a Gel Bond PAG film with the hydrophilic side sandwiched (Lornza Corp.) in between. The assembly of the glass sandwich is mounted on a stand. Before the gel is prepared, a plug is added. The plug is made of 0% DGGE gradient solution. The gradient mix solution for gel is prepared by mixing the two gradients in an electrically stirred mixer and poured to set on hydrophilic film (gel bond PAG film). Once the gel is poured, water-saturated butanol is added to it and later it is removed and top layer is rinsed. The wells are placed and stacker is then poured. About 10 ml DNA sample is mixed with dye and loaded in the wells. The gel is run for 16 hours under 75 mV in a linear 30-70% gradient. The gel assembly is shown in Figure 5-2c.

c. Gel staining: This process is sequential and initially gel is rinsed in a fixer solution, followed by silver nitrate stain developer and finally in the fixer solution (200 ml) again. It is analysed under a scanner. Fixer solution is made of (2.5ml) glacial acetic acid, ethanol (50 ml) and final volume made up to 500 ml with deionized water. Staining solution has 300 mg silver nitrate dissolved in the fixer

solution. Developing solution comprises of formaldehyde (2.7 ml) and 6 gms of sodium hydroxide dissolved in a final volume of 200 ml deionized water.

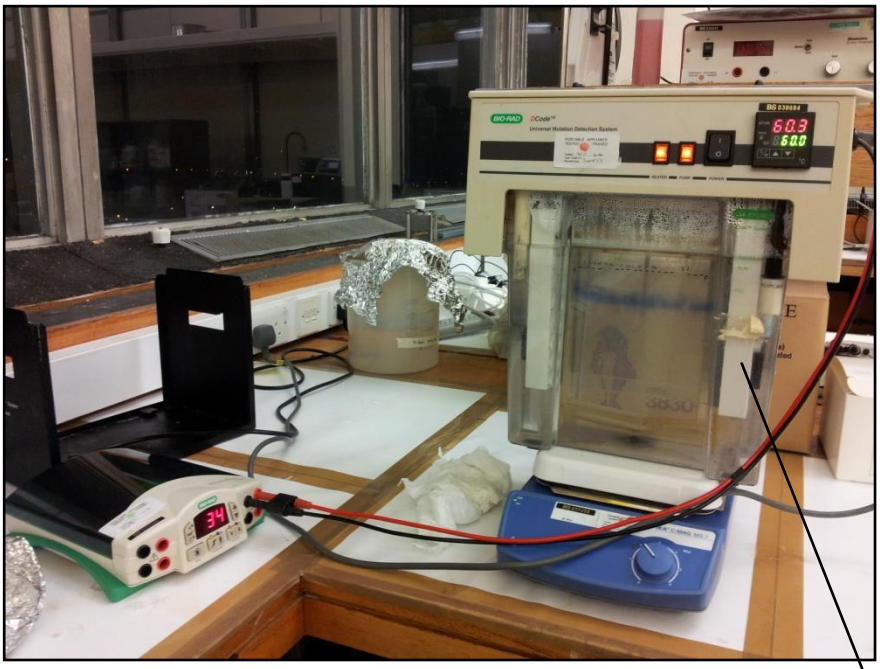

Figure 5-2c: DGGE gel set up

d. DGGE finger print analysis:

The DGGE gel images were scanned and analysed by using Bionumerics (version 6) software. This software initially normalizes the band intensity by analysis of the gel image obtained after DGGE. It uses the marker lane as the reference for the quantification purposes and creates a band intensity pattern. This data is further analysed by Primer 6 version 6.1.12. Primer 6 analyses the similarity between the gel bands and for this, it generates a Bray-Curtis similarity matrix following square-root transformation to avoid domination by the most abundant species. In order to depict

this in a two dimensional space, Nonparametric Multi-Dimensional Scaling (NMDS) plots are then generated from the Bray-Curtis similarity matrix (Clarke and Warwick, 2001). This analysis is based on position of objects in a Euclidean space and comparing their pair wise similarity index (Son et al., 2011). This processes the data to generate a plot that show the sample relatedness in two-dimensional spaces.

5.3 Results

5.3.1 Microcosms develop stratification

The sediment microcosms usually develop stratification based on well-known metabolic pathways, the top layers exhibit green zones (photosynthetic bacteria), and the middle regions with chemosynthetic bacteria followed by dark anoxic zones Brock, 2011). The sediment microcosms developed as a part of this study also exhibited zonations but these were not distinctly clear (Figure 5-3a and 5-3b) therefore, sediment samples were extracted from these microcosms, homogenised and air-dried on petri dishes. Notable changes in the colour were observed across the concentration gradient (mg/L) of nanoparticles added as shown in Figures 5-3a and 5-3b. The increasing concentration of nanoparticles resulted in reduction of photosynthesizing organisms as seen by gradual reduction of green zone in columns.

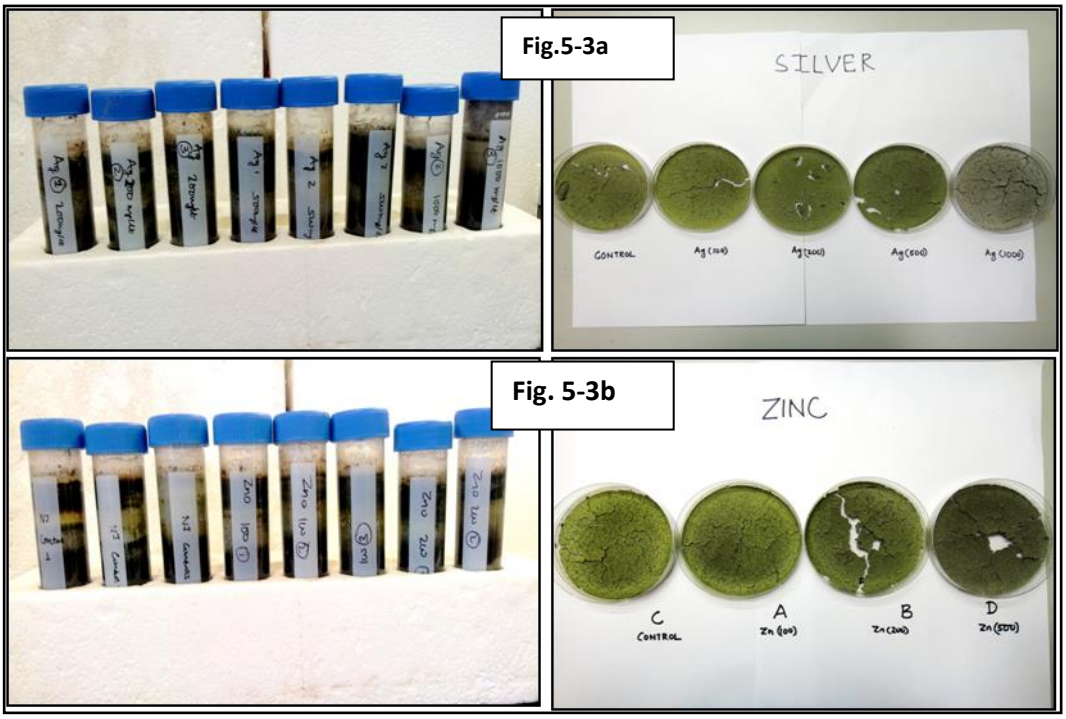

Figures 5-3a and 5-3b: Columns amended with silver and ZnO nanoparticles

5.3.2 X-ray absorption spectroscopy of sediments derived from microcosms

Metal speciation studies were conducted using Ag K- edge X- ray absorption spectroscopy. Linear combination fitting of XANES data for sediments samples was performed by fitting a mixture of reference standards including silver nanoparticles, silver sulphide, silver oxide, silver chloride, zinc sulphate and zinc sulphide (respectively). The percentage error and relative proportion of each standard within amended samples is determined by using least square fitting method. The fits with lowest R factor and chi values have been used and illustrated in the tables 5-2 and 5-3 respectively.

5.3.2.1 Silver speciation analysis

Plots of the XANES and k weighted EXAFS analysis (Ag K edge 25514 eV) of the sediment from the microcosm samples with silver nanoparticles are shown in Figure 5-4a and 5-4 b (500 ppm) and Figure 5-4 c and 5-4d for 1000 ppm. In both cases, samples with silver nanoparticle amendments exhibit a spectral resemblance to the silver sulphide standard, irrespective of position of extraction from the microcosm, be it top layer, bottom or bulk.

A significant finding is that even at the time zero; samples show peaks that match closely with samples incubated for three months. This is an important observation as it indicates that added silver nanoparticles have undergone rapid transformation (predominantly) into silver sulphide even before incubation.

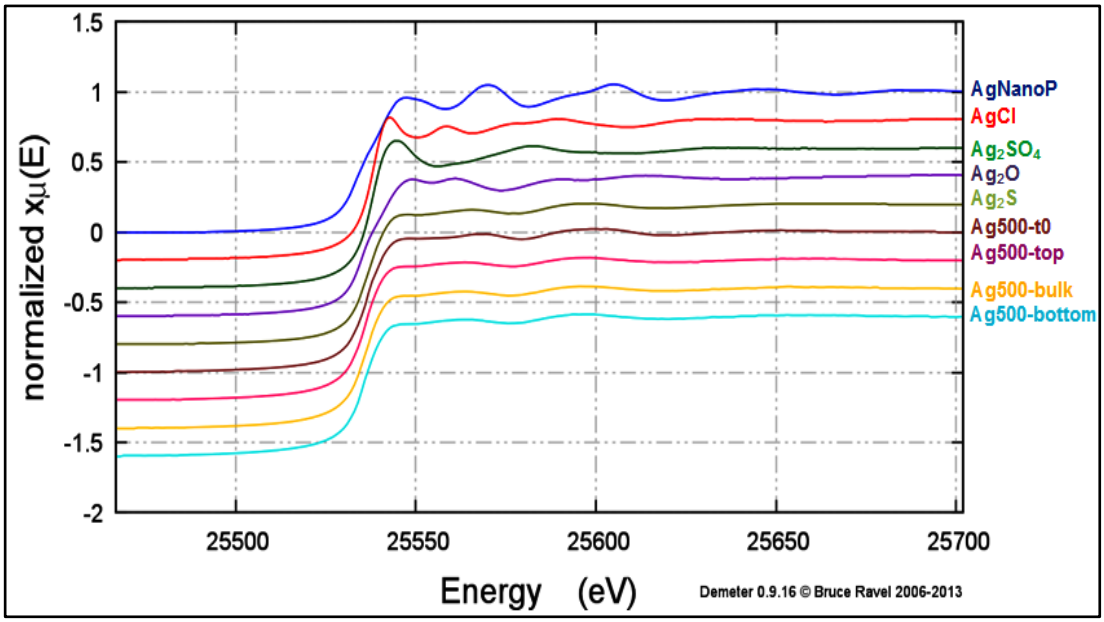

Figure 5-4a: Normalized XANES of sediments exposed to silver nanoparticle at 500 ppm. Samples frozen immediately after adding nanoparticles (t0), along major strata of the microcosm (top, bulk and bottom).

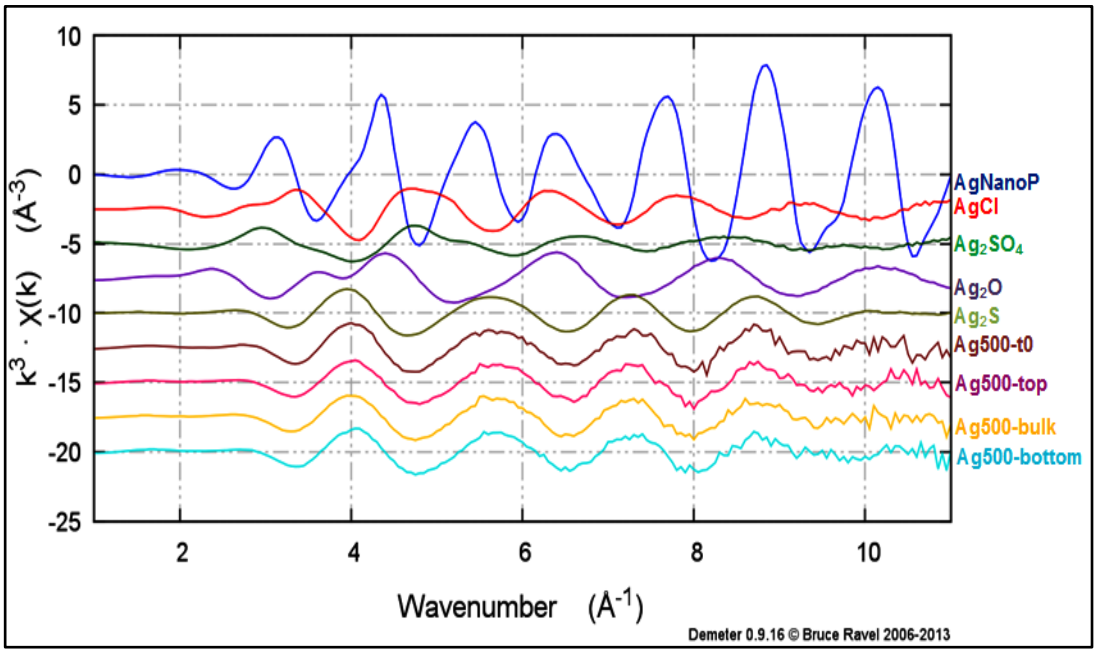

Figure 5-4b:K^3 weighted EXAFS spectra for the standards and the sediments dosed with silver nanoparticles 500 ppm.

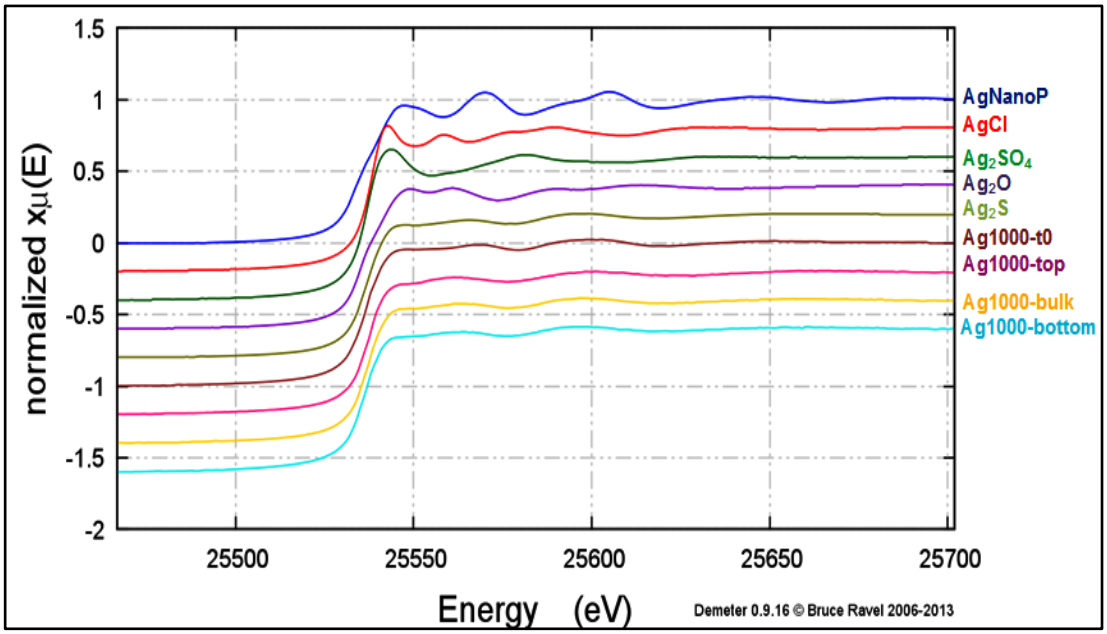

Figure 5-4c Normalized XANES spectra for the standards and the sediments dosed with silver nanoparticles at 1000 ppm

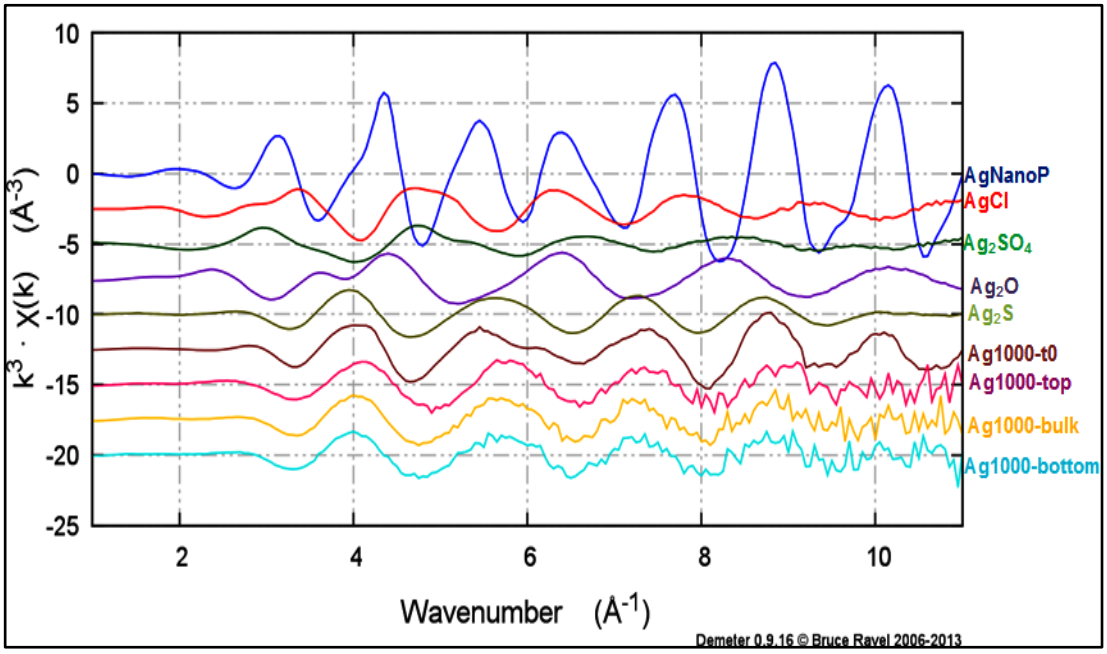

Figure 5-4d: K^3 weighted EXAFS spectra for the standards and the sediments dosed with silver nanoparticles 1000 ppm. Samples frozen immediately after adding nanoparticles (t0) and along major strata of the microcosm (top, bulk and bottom).

From the results presented in Figure 5-4, it is very difficult to conclude that a sample or a group of samples is identical to one of the standards. In particular, spectra of microcosm samples show slight deviation from the pure Ag_2S, notably in the oscillation at 4 and $5.5A^{-1}$ (Fig 5-4b and 5-4d), suggesting either incomplete transformation or the presence of other transformed products. Therefore, a linear combination analysis was conducted by fitting unknown spectra of each of the sample to the standards analysed alongside the samples. This evaluates the species and quantities of the standards in each of the heterogenous samples. The results of the linear combination fitting for some selected samples are shown in table 5-2, and fitted spectra are displayed in Figures 5-5 and 5-6 for 500 and 1000 ppm Ag nanoparticles respectively.

	Ag2O	**Ag2S**	**AgCl**	**Ag2SO4**	**Ag np**	**R**	**Chisqr**
Ag500 t0	16.01	84	0.000186	0.000004	0	0.00082	0.014
Ag500 top	14.45	85	2.8	0.000633	0	0.00066	0.011
Ag500 bulk	14.42	85	0.000047	0.000045	0	0.00056	0.01
Ag500 bottom	18.38	82	0.000075	0.0000416	0	0.00128	0.02
Ag1000 t0	12.55	87	0.00003	0.0000054	0	0.00044	0.008
Ag1000 top	8.91	91	0.00002.	0.0000136	0	0.00023	0.004
Ag1000 bulk	7.36	93	0.000067	0.0000147	0	0.00022	0.0041
Ag1000 bottom	10.55	89	0.00013	0.000039	0	0.00032	0.0059

Table 5-2 the table shows the percentage weight of each of the standards in the microcosms.

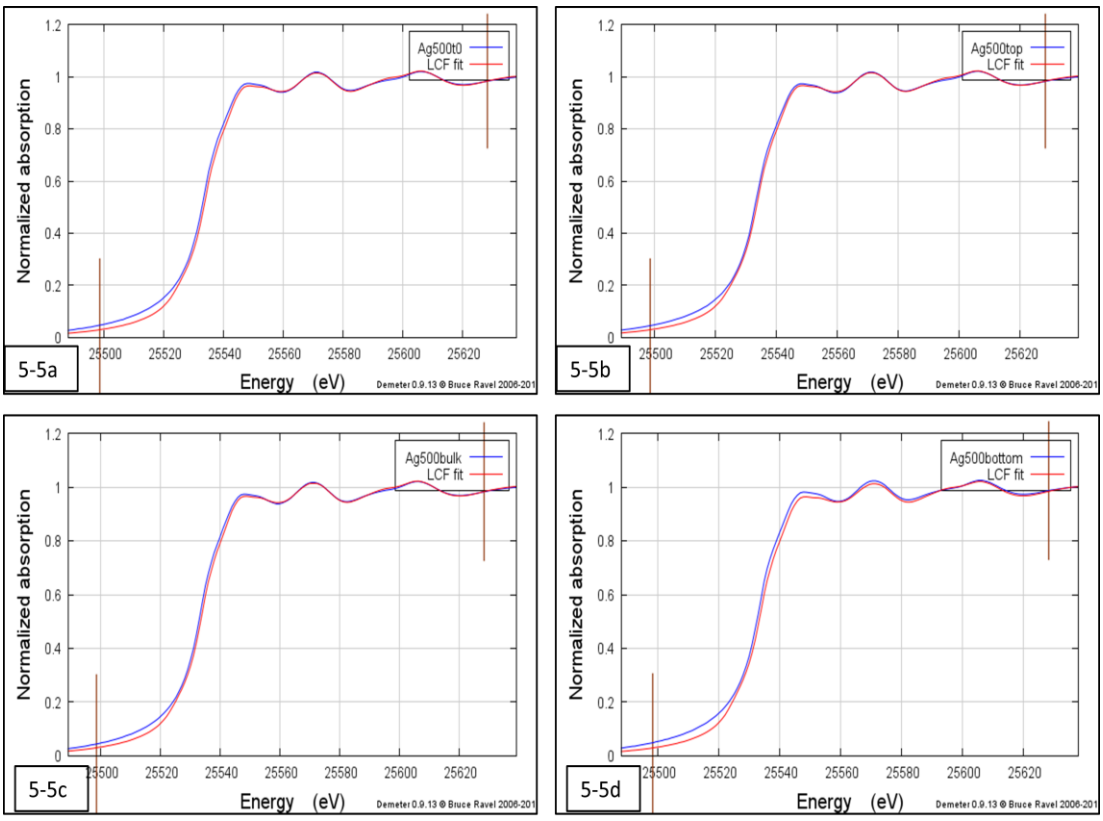

Figure 5-5: Diagrammatic presentation of LCF results of silver standards to sample sediment microcosm exposed to 500 ppm of silver nanoparticles at time zero (t0) and at three major strata of the microcosm (top bottom and mixture of layers)

.

The results of the percentage weight contribution in the samples are graphically presented in Figure 5-7a and 5-7b.

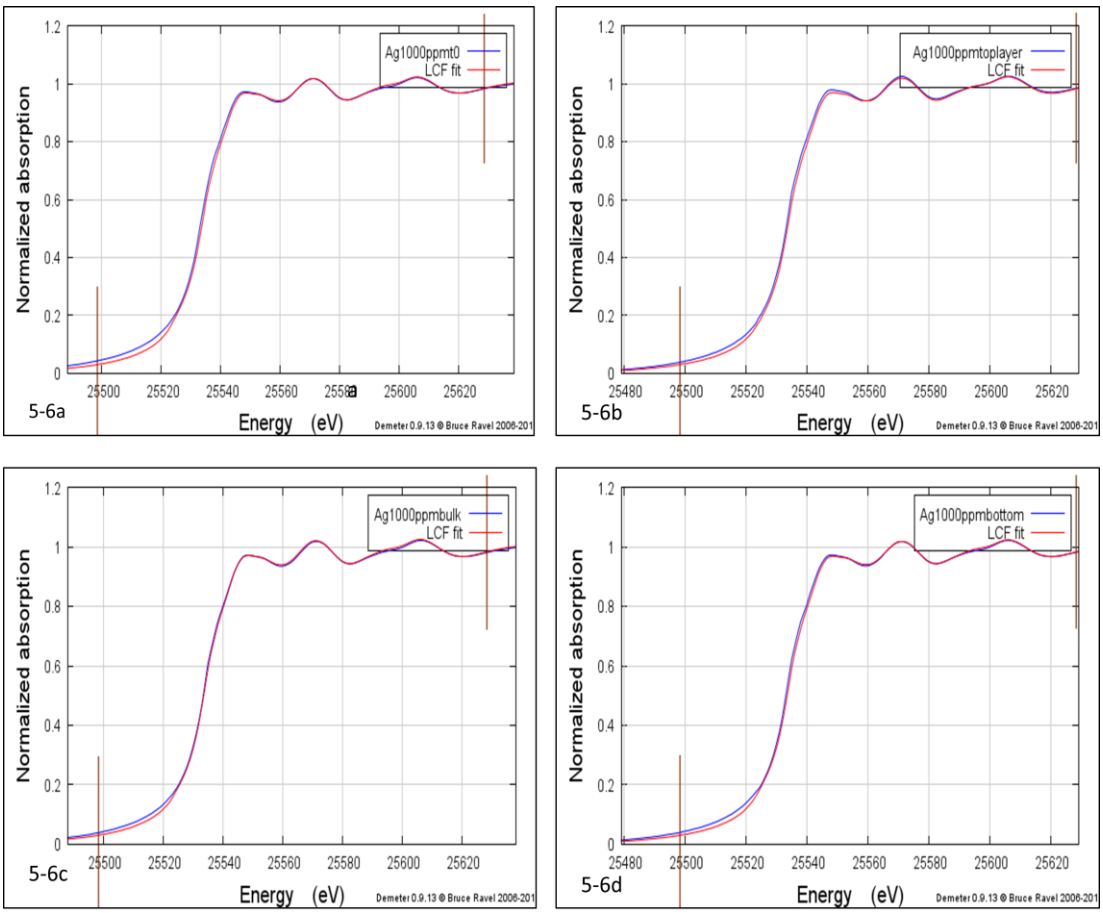

Figure 5-6: LCF modelling for the microcosms dosed with silver nanoparticles (1000 mg/l). The absorbance has been plotted against energy. The standards were initially fitted and then samples (amended) analysed. LCF fit modelled using Ag2S, Ag2O and Ag_2SO4.

The LCF modelling of the normalized spectral data for the samples (silver 500 ppm and 1000 ppm) shows that the microcosms dosed with silver nanoparticles (all three zones) contain significant levels of silver as silver sulphides (80-85%) and (average of 15%) as silver oxide for 500 ppm samples (Figure 5-7a). There is no significant contribution of silver chloride and silver sulphates at all as evident by LCF analysis (Table 5-2) hence these have been omitted while determining the weighted average of each of the species as shown in Figure 5-7a and 5-7b. More importantly, there was no contribution from the added Ag nanoparticles, implying complete

transformation within a few hours even without microbial intervention. Lastly, there are some variations between treatments; for instance, microcosms amended with 1000 ppm silver nanoparticle have relatively lower levels of silver as oxide (9% average) than the ones at 500 ppm (Figure 5-7a, b). This difference may be related to the lack of microbial activities at higher concentration of nanoparticles (see later).

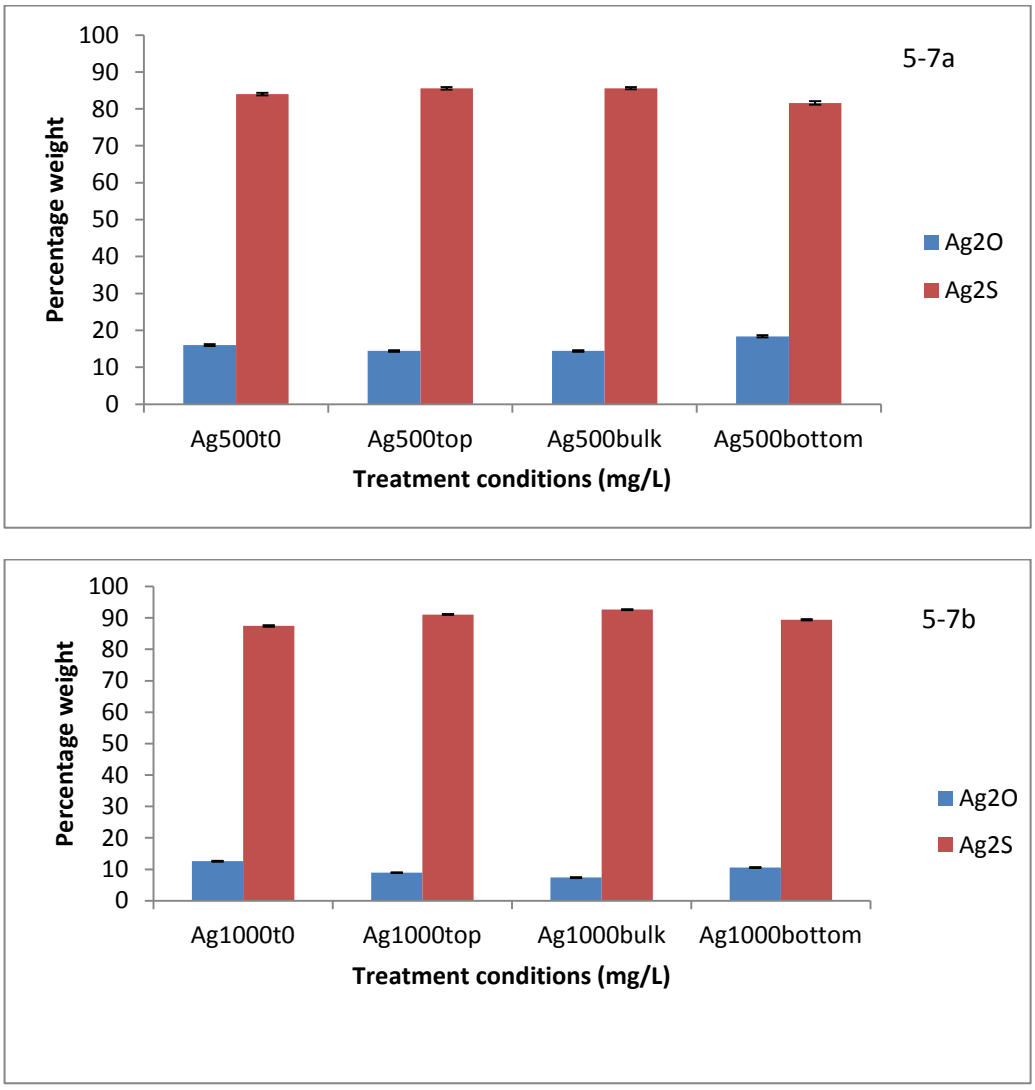

Figure 5-7a and 5-7b: Speciation rate of silver in different treatment conditions represented as the percentage weight of silver oxide and silver sulphide in each sample, the silver sulphate was statistically insignificant proportion hence ignored

5.3.2.2 XAFS for microcosms amended with zinc oxide nanoparticles

The microcosms dosed with zinc oxide nanoparticles were analysed by the X ray absorption spectroscopy in a similar manner using zinc oxide, zinc carbonate and zinc sulphide as standards.

The XANES and EXAFS spectra of the sediment and standards (Figure 5-8a and 5-8b) show that ZnO nanoparticles have transformed into zinc sulphide. However, it was difficult to determine the contribution of individual species to the spectra especially, time zero and sterile samples, hence linear combination fitting (LCF) was further conducted.

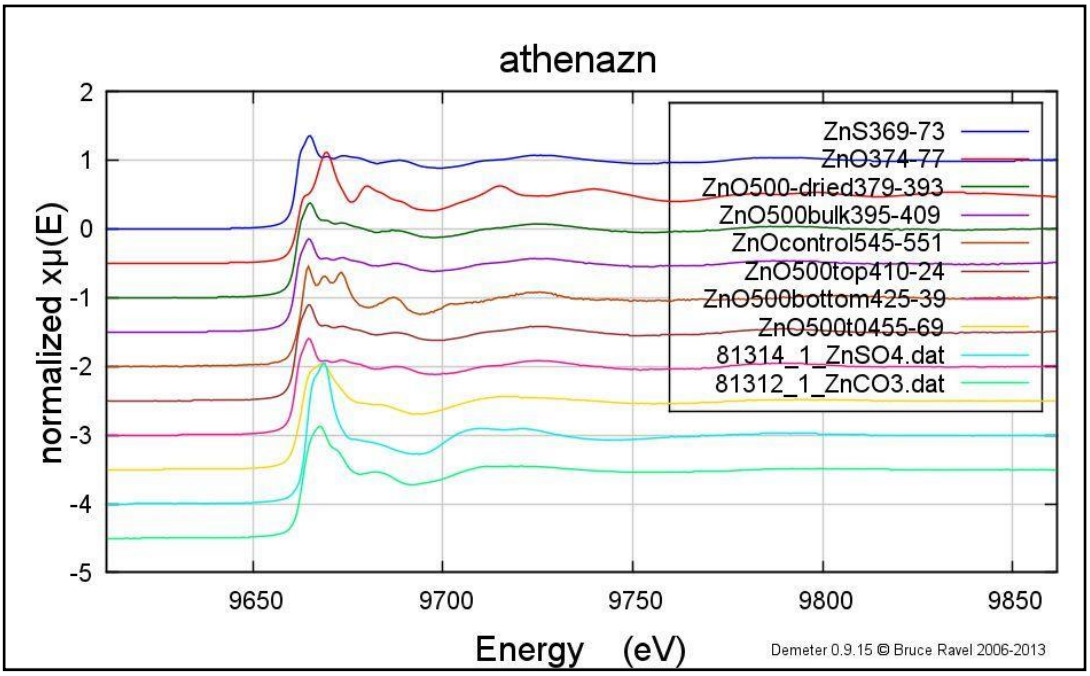

Figure 5-8a: Normalized K-edge XANES of sediment microcosm exposed to 500 ppm of ZnO nanoparticle. Samples analysed immediately after collection (t0) and along major strata of the microcosm (top, bulk and bottom) after incubation.

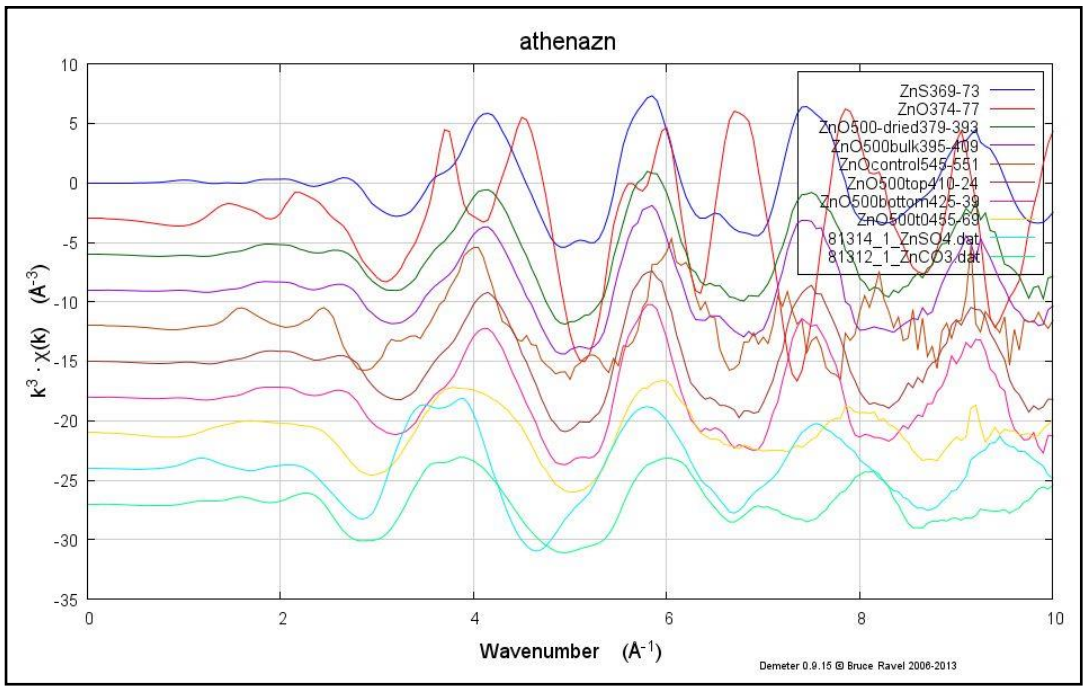

Figure 5-8b: K^3 weighted EXAFS of selected Zn standards and samples of sediment microcosm exposed to 500 ppm of ZnO nanoparticles.

The LCF modelling results are shown in Figure 5-9. They showed that speciation rate of zinc significantly varied between treatment conditions.

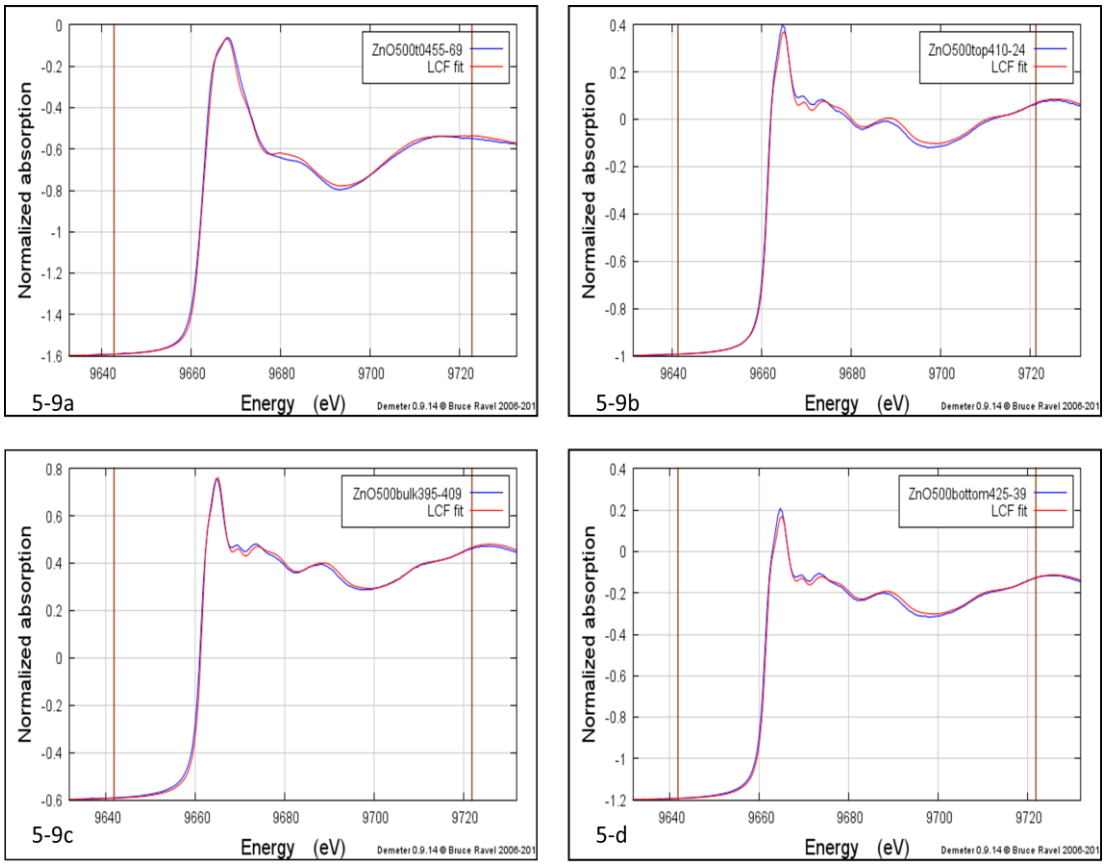

5-9: LCF modelling for the microcosms dosed with ZnO nanoparticles (500 ppm). The absorbance vs. energy. The standards were initially fitted and then samples (amended) analysed. The graphs for treatments that showed significant differences (T0, sterile and ZnO bottom have been shown).

The T0 non-sterilized sample shows a significant presence of all the zinc species (highest being zinc carbonate, followed by zinc sulphide and zinc sulphate. as show in Figure 5-10. The percentage weight of each species has been listed in Table 5-3. The samples extracted from different zones from the microcosm showed a

prominence of zinc sulphides as shown in Figure 5-10. This figure clearly indicates that sulfidation process is dominant process in speciation of zinc (within the incubation period of microcosms) irrespective of the extraction zones. ZnO amended nanoparticles freeze dried immediately after amendments (t0), were dominated by ZnCO3 with approximately 30% ZnO still remaining while ZnSO4 also precipitated. Apart from demonstrating that different nanoparticles will transform at different rates, the presence of $ZnCO_3$ and $ZnSO_4$ also implies that transformation occurs via rapid dissolution- mediated pathway to allow these salts to precipitate.

	$ZnCO_3$	**ZnO**	**$ZnSO_4$**	**ZnS**	**R**	**chisqr**
ZnO500t0	49	6.2	17.16	27	0.0023	0.07
ZnO500sterile	3.44	3.18	10.65	83	0.0043	0.11
ZnO500top	0	0	1.17	99	0.0018	0.04
ZnO500bulk	0	0	0	100	0.0017	0.04
ZnO500bottom	0	0	0.60	99.4	0.0024	0.06

Table 5-3: Linear combination fitting results (LCF) of XANES spectra shows the percentage weight of ZnO, ZnS and ZnSO4 present in the treated microcosms. The R factor and chi square have been shown. The samples have been taken from three zones within a microcosm

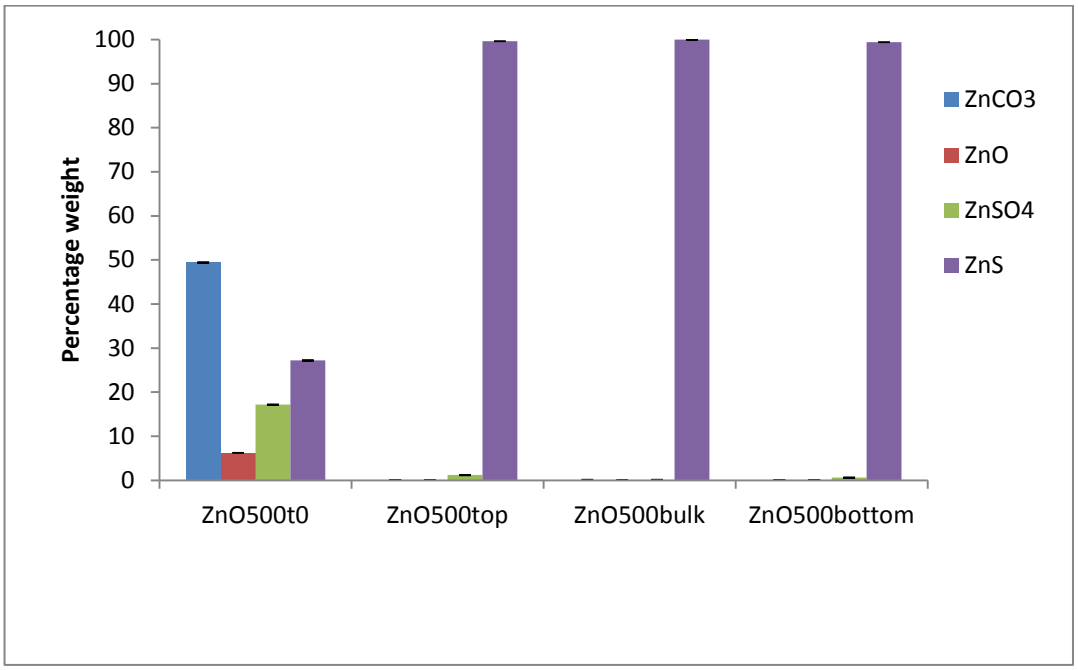

Figure 5-10 weighted average of major species of zinc present in the microcosm exposed to 500 ppm of ZnO. Graph shows the rapid change in the speciation rate of zinc in different treatment conditions

The LCF showed that transformation patterns of silver and zinc oxide nanoparticles were different especially at time zero, where speciation showed varied proportions of zinc carbonate, zinc sulphate, zinc oxide and lowest concentration of zinc sulphide. The $ZnCO_3$ has been omitted from figure 5-10, as it was negligible for other samples.

5.3.3. Analysis of the variable region of 16SrRNA genes amplified from the DNA derived from water and sediment collected from the microcosms

5.3.3.1 Analysis of the variable V3 region of the 16S rRNA amplified from the DNA derived from water samples

The DNA was extracted from sediment samples and used to amplify the V3 region of the 16S rRNA and this process was done in a two-step amplification process as

described in the methods section. The DNA recovered from sediment was also used to determine the presence of sulphate reducing bacteria by using specific primers as discussed earlier. Visual examination of the gel image showed the presence of few extra bands in some lanes; however, the overall band pattern was similar in the gel as shown in Figure 5-11. This gel was further analysed using the Bionumerics. The band intensity data showed that there was no significant change in total number of bands within each set and across the concentration gradient of the nanoparticle treatments.

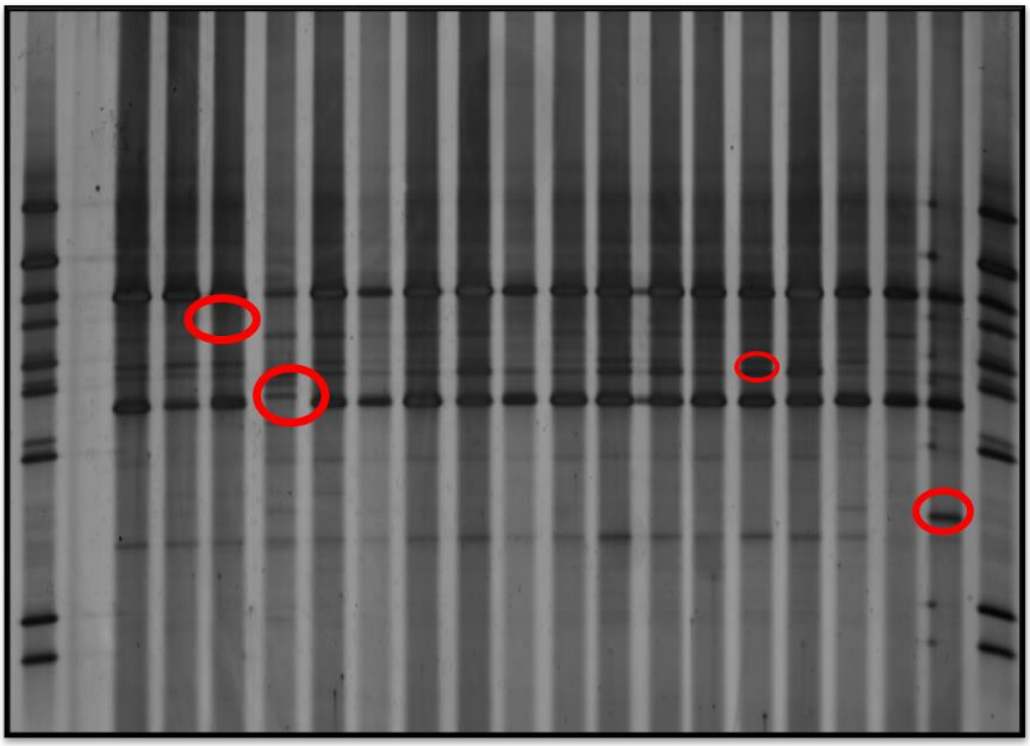

Figure 5-11: Visual analysis of the DGGE gel (water) and the lanes that show different bands. Lane 1,2,21 (read from left had side of gel onwards) is the DGGE marker. A (silver) and Z (ZnO) nanoparticles. Marked from left to right, lane 2-4 A100, 5-6 (A200), 7-9 (A500), 10-12(A1000), Z 100(13), Z200 (15), Z500 (16), C1-C3 (17-19). The numbers 100, 200, 500, 1000, denote the concentration in mg/L for nanoparticles. Highlighted areas denote extra bands

The gel image was processed by Bionumerics and the band intensity data was further analyzed by Primer 6. The resemblance matrix is shown in Figure 5-12.

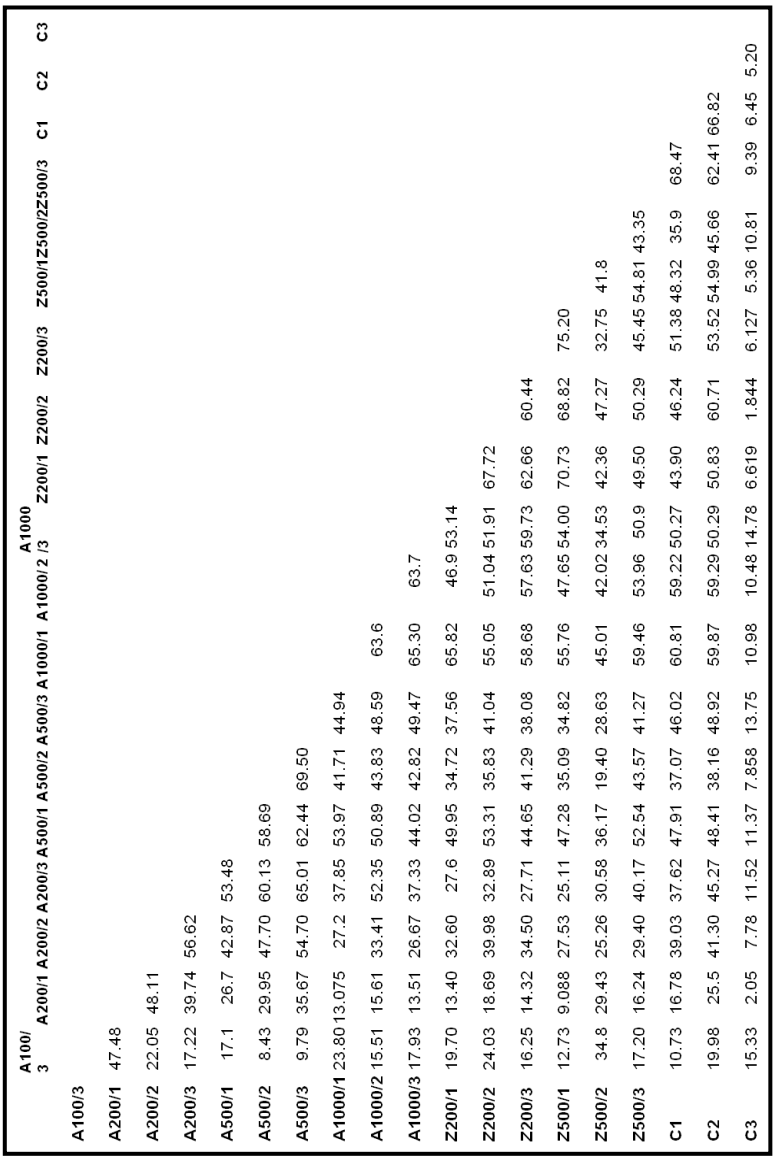

	A100/3	A200/1	A200/2	A200/3	A500/1	A500/2	A500/3	A1000/1	A1000/2	A1000/3	Z200/1	Z200/2	Z200/3	Z500/1	Z500/2	Z500/3	C1	C2	C3
A100/3																			
A200/1	47.48																		
A200/2	22.05	48.11																	
A200/3	17.22	39.74	56.62																
A500/1	17.1	26.7	42.87	53.48															
A500/2	8.43	29.95	47.70	60.13	58.69														
A500/3	9.79	35.67	54.70	65.01	62.44	69.50													
A1000/1	23.80	13.075	27.2	37.85	53.97	41.71	44.94												
A1000/2	15.51	15.61	33.41	52.35	50.89	43.83	48.59	63.6											
A1000/3	17.93	13.51	26.67	37.33	44.02	42.82	49.47	65.30	63.7										
Z200/1	19.70	13.40	32.60	27.6	49.95	34.72	37.56	65.82	46.9	53.14									
Z200/2	24.03	18.69	39.98	32.89	53.31	35.83	41.04	55.05	51.04	51.91	67.72								
Z200/3	16.25	14.32	34.50	27.71	44.65	41.29	38.08	58.68	57.63	59.73	62.66	60.44							
Z500/1	12.73	9.088	27.53	25.11	47.28	35.09	34.82	55.76	47.65	54.00	70.73	68.82	75.20						
Z500/2	34.8	29.43	25.26	30.58	36.17	19.40	28.63	45.01	42.02	34.53	42.36	47.27	32.75	41.8					
Z500/3	17.20	16.24	29.40	40.17	52.54	43.57	41.27	59.46	53.96	50.9	49.50	50.29	45.45	54.81	43.35				
C1	10.73	16.78	39.03	37.62	47.91	37.07	46.02	60.81	59.22	50.27	43.90	46.24	51.38	48.32	35.9	68.47			
C2	19.98	25.5	41.30	45.27	48.41	38.16	48.92	59.87	59.29	50.29	50.83	60.71	53.52	54.99	45.66	62.41	66.82		
C3	15.33	2.05	7.78	11.52	11.37	7.858	13.75	10.98	10.48	14.78	6.619	1.844	6.127	5.36	10.81	9.39	6.45	5.20	

Figure 5-12: Resemblance matrix for water samples derived from microcosms. The treated samples are labellled as A (silver np) and Z (ZnO) np and the numbers represent their concentration (mg/L)

The resemblance matrix reveals that there is little difference between the replicates of each of the treatments**.** Statistical analysis of the Bray Curtis coefficients by using Welch t test indicates no differences amongst the samples ($p>0.05$) except C3 and Z 500/2/. Sample C3 shows a low resemblance with other replicates and that could be due to heterogeneity of microcosms. The NMDS plot (Figure 5-13) generated by Primer 6 showed that apart from C3 (control), A (100) and A (200), most of the samples form two clusters however, this is trend does not follow concentration gradient of nanoparticle amendments. The metal extraction study conducted on the water recovered from columns showed that most of the nanoparticles had fractionated into the sediments so this could partially explain lack of significant impact on the microbial diversity (data not shown).

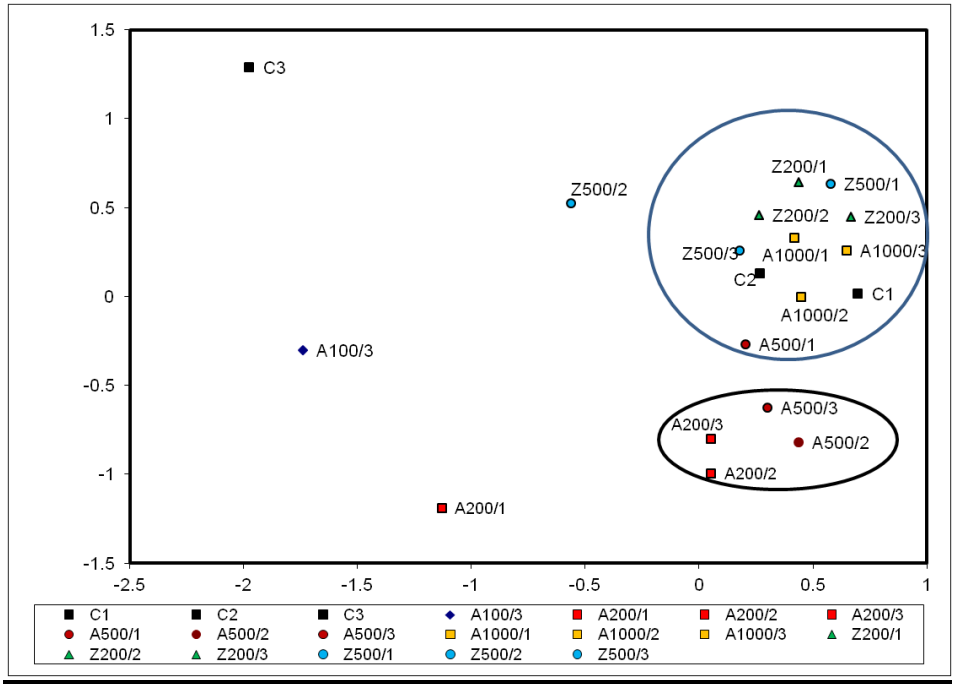

Figure 5-13: NMDS analysis of the pair-wise sequence dissimilarity scores of the samples with and without nanoparticles. Euclidean space is a function of dissimilarity and the samples close indicate resemblance to each other. (The ‘‘stress’ ’a measure of lack of fit and in this case it is 0.13

5.3.3.2. Analysis of the variable V3 region of 16SrRNA amplified from the DNA derived from sediment

The DNA fingerprinting study conducted on the sediments dosed with silver and zinc oxide nanoparticles shows some effect in terms of variation in band patterns (Figure 5-14). The highlighted lanes indicate the samples with some dissimilar (additional) bands.

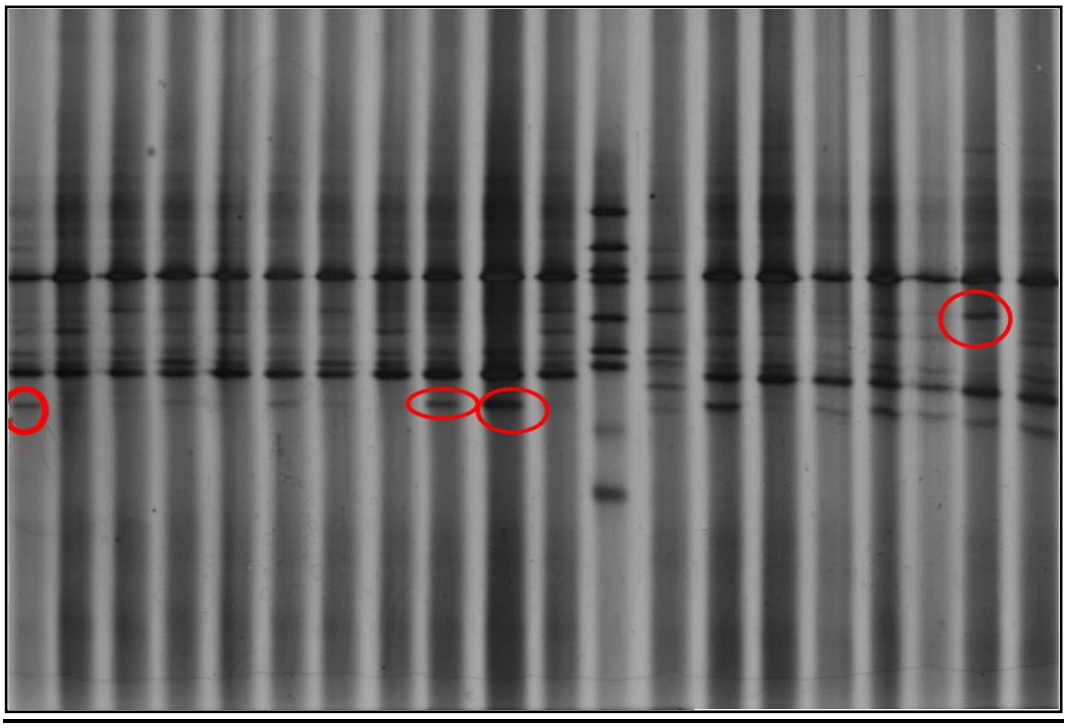

Figure 5-14: DGGE gel image for sediment samples. Order of the samples (read from left hand side of gel image) is lane 1-3 (C1-C3), 4-6 (A200), 7-9 (A500), 10, 11, 13 (A1000), 15-17 (Z200) and 18-20 (Z500). Highlighted lanes show extra bands (visual analysis). C (controls), A (microcosms with silver NP and Z (microcosms with ZnO NP).The numbers 100, 200, 500, 1000 denote the concentration in mg/L for nanoparticles

The band intensity pattern generated by the Bionumerics showed that apart from Z (500), most of the lanes showed similar number of bands. There was no significant

difference between the replicates of the treatments. This suggests that addition of nanoparticles did not significantly affect the total microbial community composition. At high concentration of zinc oxide nanoparticles, a reduction in number of microbial species was observed.

The resemblance matrix generated by Primer 6 (Figure 5-15) indicates that some replicates within a treatment condition show some variation like the control samples, A (500) and Z 500 show quantitative differences with their own replicates. The NMDS plot generated using Primer 6 shows that addition of nanoparticles does produce a shift in the pattern of distribution at higher concentration of zinc (500 ppm) and silver (1000 ppm) (Figure 5-16a). It suggests that adddition of nanoparticles produced some perturbation within the microcosms.

	C1	C2	C3	A200/1	A200/2	A200/3	A500/1	A500/2	A500/3	A100/1	A1000/2	A1000/3	Z200/1	Z200/2	Z200/3	Z500/1	Z500/2	Z500/3
C1																		
C2	40.42																	
C3	46.4	67.17																
A200/1	53	61.7	74.8															
A200/2	63.29	61	63.8	65														
A200/3	66.98	46.8	51.8	56.65	66.1													
A500/1	61.4	53.2	65.9	66.6	77.8	67												
A500/2	65.50	60.9	66.5	62.95	89.5	69.2	77.61											
A500/3	51.24	56.64	54.52	57.3	52.9	57	54.9	53.67										
A100/1	30.84	33.57	31.56	35.3	24.7	34	30	25.13	47.9									
A1000/2	54.63	67.46	71.48	70.7	77	61.4	77.89	76.5	62.83	37.4								
A1000/3	39.68	36.75	53.88	53.9	39.9	37.6	43.8	42.54	39.6	29.2	47.15							
Z200/1	52.23	57.34	50.9	58.69	57.6	56.5	57.1	55.84	68.1	64	66	35.6						
Z200/2	38.34	67.91	64.34	66.86	59.3	45.8	57.74	58.53	52.8	37.36	67.57	36.4	65.6					
Z200/3	62.42	47.39	56.35	59.94	54.9	66.7	57.2	58.17	52.87	32.97	53.63	43	51.6	49.7				
Z500/1	56.58	55.33	50.8	59.2	66.2	57.5	63.1	66.15	65.46	41.8	69.93	37.31	76.4	60	55.6			
Z500/2	59.43	56.56	56.52	62.93	59.7	60.1	60.1	60.4	51.20	29.8	59.83	45	58	57.58	74.3	70.84		
Z500/3	62.40	41.1	52.78	54.6	59.8	65.4	62.7	62.24	53.05	36.43	59.13	34.98	55.6	47.93	64.5	66.52	61.2	

Figure 5-15: Resemblance matrix for sediment analysis

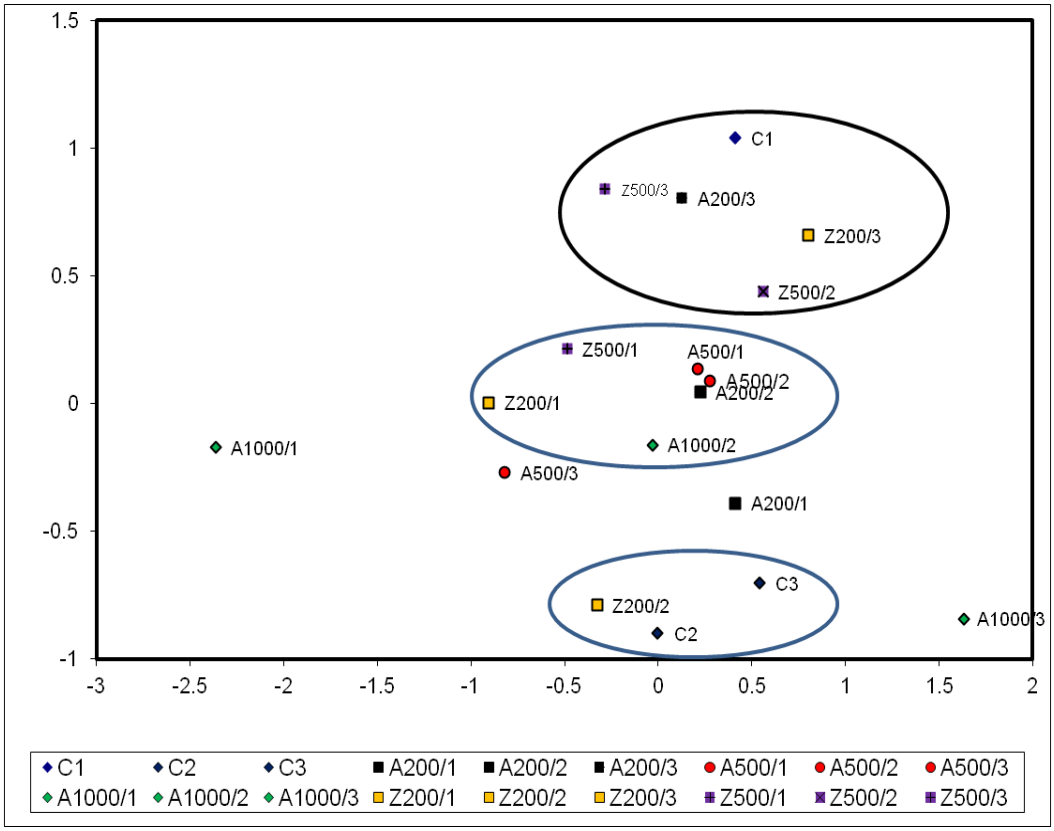

Figure 5-16a: NMDS analysis of the pair-wise sequence dissimilarity scores of the samples with and without nanoparticles. Euclidean space is a function of dissimilarity and the samples closeness indicate resemblance to each other. Stress associated is 0.15

It can be seen that the samples highlighted in the DGGE gel image (5-15) are the ones with dissimilarity in the band pattern when compared with their replicates. These samples show a wide scatter on the NMDS plot too (Fig. 5-16a).

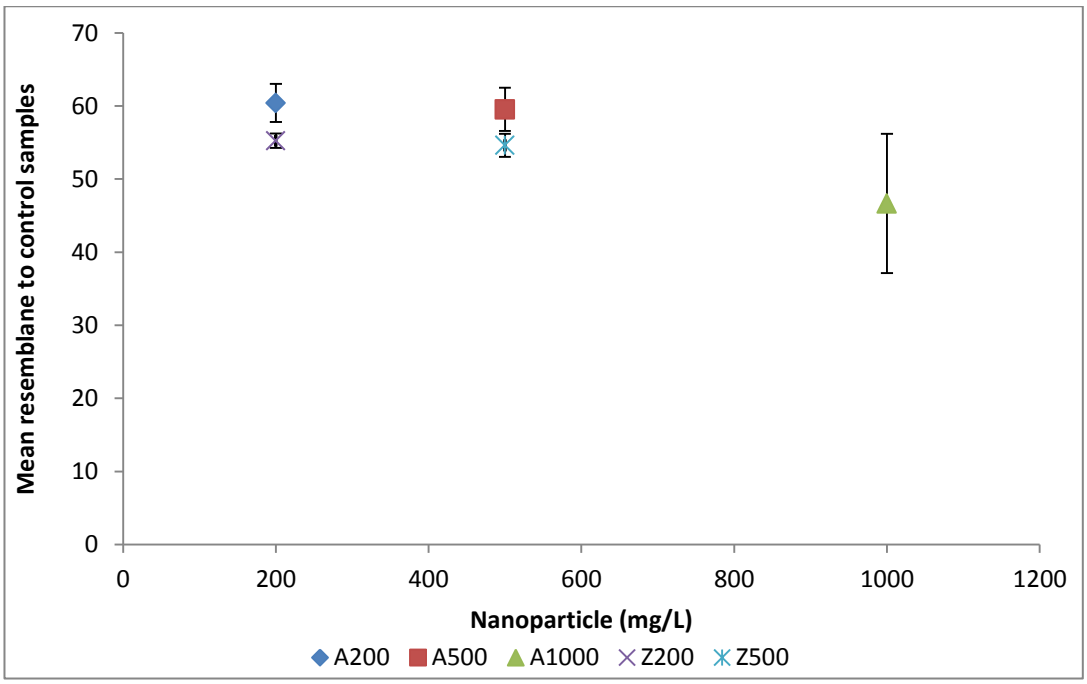

Figure 5-16b: the mean resemblance values of amended samples to the control samples. The y -axis shows the mean resemblance and y-axis concentration gradient (mg/L)

However, the addition of nanoparticles does lead to some changes in the dynamics within the microcosms (Fig. 5-16 b). The samples with amendment at 1000 ppm equivalent silver nanoparticles show a low similarity index with the rest of the samples. The Welch t test done on the Bray Curtis coefficients indicates that A 1000 has very low similarity ($p=0.02$) with control samples C ($p=0.01$) and with A200. This indicates that addition of silver nanoparticles at high concentration causes perturbation in the microbial community structure. However, the samples dosed with zinc oxide nanoparticles show variation in resemblance values that are not statistically significant. Besides, the samples within a replicate set also show a low similarity to each other.

5.3.3.3 Presence of sulphate reducing bacteria and diversity in community composition

The presence of sulphate reducing bacteria was confirmed by PCR reaction using a set of specific primers that could anneal and amplify only the variable regions associated with DSR bacteria (Geets et al., 2006). The presence of a pcr product confirmed the presence of sulphate reducing bacteria in the microcosms. Figure 5-17 shows the image of the DGGE gel.

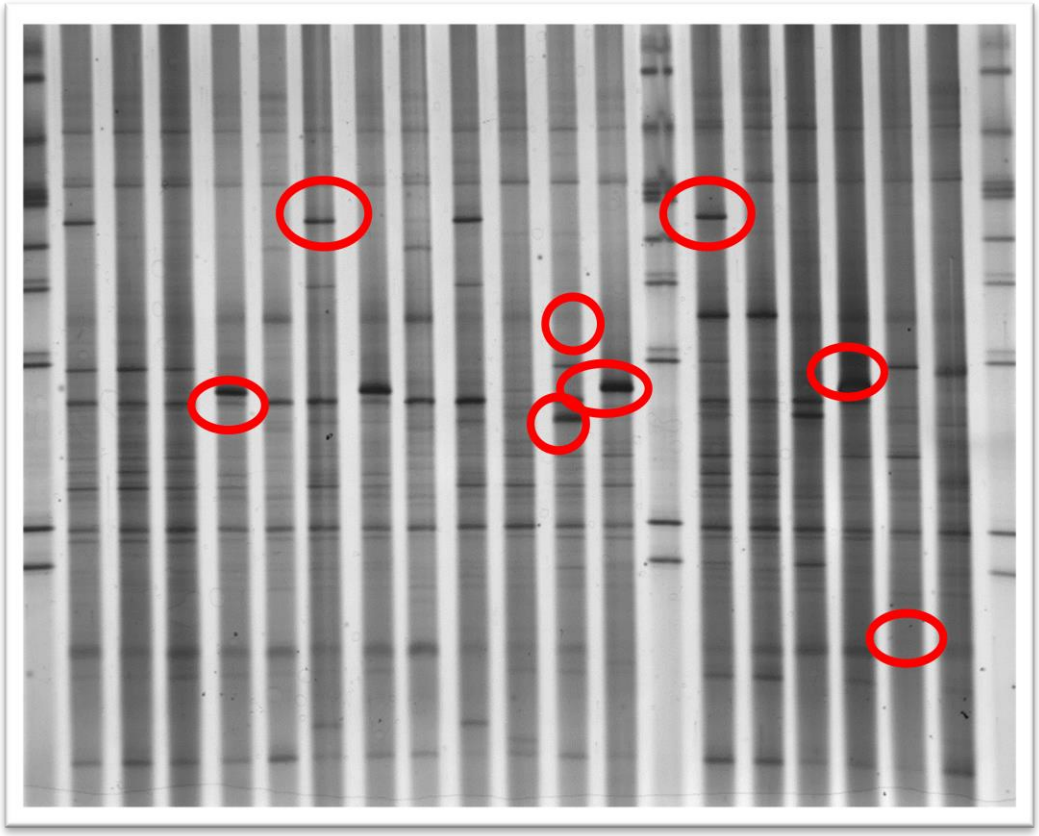

Figure 5-17: DGGE finger printing profiles of dsrB in sediment treated with nanoparticles. Lane 1, 14, 21 markers, 2-4 (C1-C3), 5-7 (A200), 8-10 (A500), 11-13(A1000), 15-17 (Z200), 18-20 (Z500). The highlighted areas indicate the presence of additional bands in specific lanes. Numbers in brackets indicate nanoparticle concentration in ppm.

It can be seen that some lanes have significant presence of additional bands. This variation increases linearly with concentration of nanoparticles. For instance, the samples with higher concentration of silver (1000/500 ppm) and ZnO (500 ppm) show additional distinct bands compared with the rest of the subset and have been highlighted in Figure 5-17.

The band intensity matrix generated by the Bionumerics (not included) showed that addition of nanoparticles (Ag 1000 ppm) and ZnO (500 ppm) significantly reduced the number of bands from mean 18 bands observed in control samples to about 9 in both cases (analysis of band intensity data has been done for this purpose). This suggests that addition of nanoparticles produced a significant change in the microbial community composition of the dsrB members, in contrast to the total community analysis. It is worth mentioning that, for both silver and zinc oxide, the intrareplicate similarity was lower at higher concentration of nanoparticles as well. The resemblance matrix generated by Primer 6 shows that there is a higher degree of variability between the replicates of the treatments for instance A 200, A500 and Z500 show some variation in the relatedness based on the resemblance values shown in Figure 5-18.

.

	C1	C2	C3	A200/1	A200/2	A200/3	A500/1	A500/2	A500/3	A1000/1	A1000/2	A1000/3	Z200/1	Z200/2	Z200/3	Z500/1	Z500/2	Z500/3
C1																		
C2	72.18																	
C3	80.6	80.46																
A200/1	62.9	63.88	73.9															
A200/2	63.13	51.96	64.6	66.														
A200/3	69.3	52	57.77	54.1	53.45													
A500/1	65.59	63.02	69.28	82.96	61.54	53.41												
A500/2	62	51.68	57.69	59.79	78.57	48.67	68.0											
A500/3	57.7	46.4	44.25	45.1	39.58	81.2	49.40	46.68										
A1000/1	40.95	56.6	56.06	43.66	31.48	38.23	39.81	36.58	38.72									
A1000/2	63.83	49.33	59.68	42.37	42.8	49	42.85	42.2	40.97	30.8								
A1000/3	37.65	28.26	36.96	36.3	19.03	38.35	37	17.41	24.1	36.8	56.35							
Z200/1	59.59	49.83	52.2	45.66	47.78	50.77	48.8	44.13	40.90	28.5	61.22	47.83						
Z200/2	58.57	48.36	58.3	51.64	54.8	39.9	55.58	50.72	28.92	30.6	157.19	41.55	77					
Z200/3	56.37	41.4	58.57	48.55	52.26	50.79	51.96	48.1	36.23	27.4	63	38.69	57	69				
Z500/1	43	26.83	42.98	39	35.15	35.18	41	33.64	23.5	16.3	56.57	58.4	46.86	55.45	60			
Z500/2	35.64	36.5	45.30	28.6	28.9	31.32	20.33	21.46	8.95	31.44	45.87	45.76	35.4	36	43.44	55.78		
Z500/3	43.52	38.36	45.35	32.1	23.8	40.64	27.6	23.17	26.26	41.7	44.36	48.28	39.41	49.22	53.86	49.47	53.33	

Figure 5-18: Resemblance matrix for the dsrB analysis

.

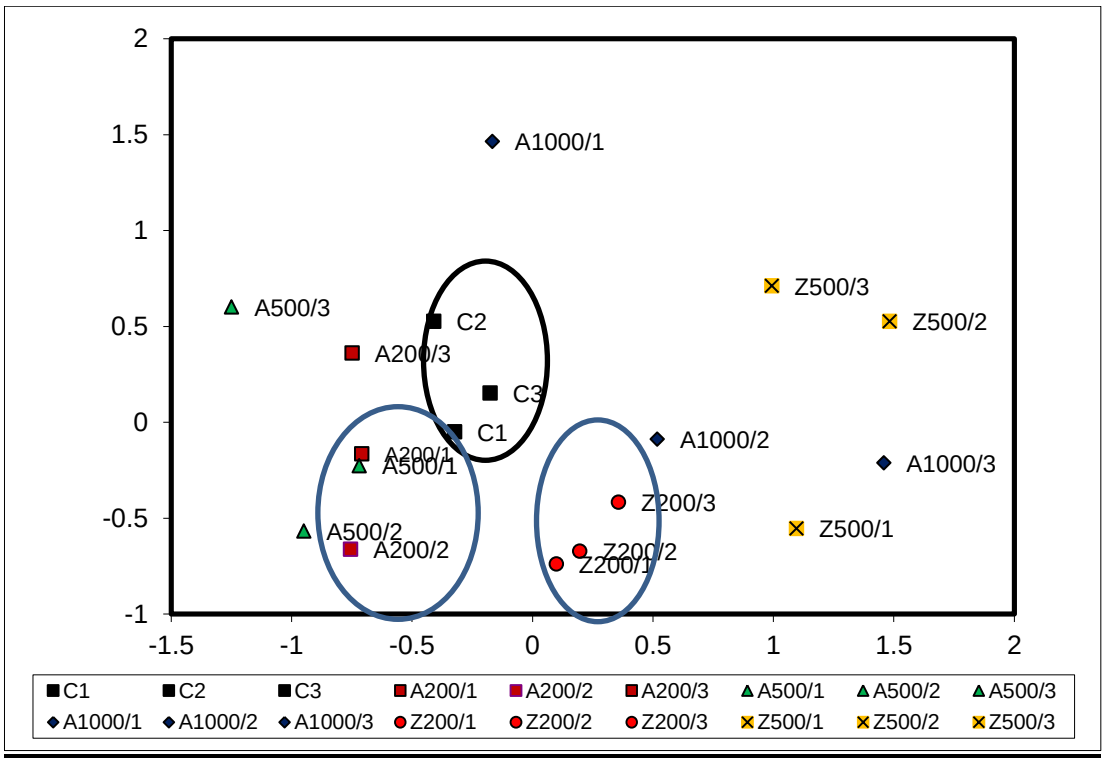

Figure 5-19a: NMDS analysis of the pair-wise sequence dissimilarity scores of the samples with and without nanoparticles. Euclidean space is a function of dissimilarity and the samples close indicate resemblance to each other. (The ‘‘stress’’, associated with this is 0.14).

The NMDS plot (Figure 5-19a) also suggests two possibilities (a) the high degree of variability is due to variation in the population structure of sulphate reducing bacteria or (b) this variation is due to the addition of nanoparticles. Quantitative analysis of the bands suggests that this variation is largely due to the presence of nanoparticles

The data points of Bray Curtis analysis (coefficients) along x axis were thereafter analysed using a Welch t-test and were found to be statistically different (p=0.004). From the Bray Curtis resemblance matrix the mean resemblance of the treated samples with respect to the controls was plotted against the concentration gradient of amendments. It was observed that with increase in the concentration of nanoparticles, the samples showed a consistent divergence away from the control samples as shown

in Figure 5-19b and 5-19c. This clearly indicates that high concentration of nanoparticles is producing some perturbation and the samples show a greater divergence from the rest of the samples. This is an important observation.

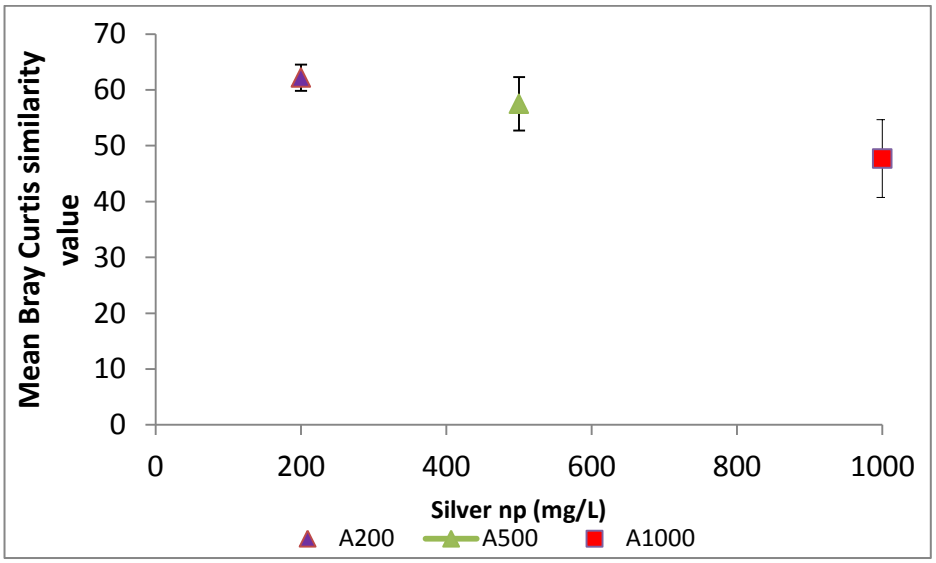

Figure 5-19b: The resemblance matrix plotted against the concentration gradient of silver nanoparticles. The y -axis shows the mean resemblance of samples to control samples.

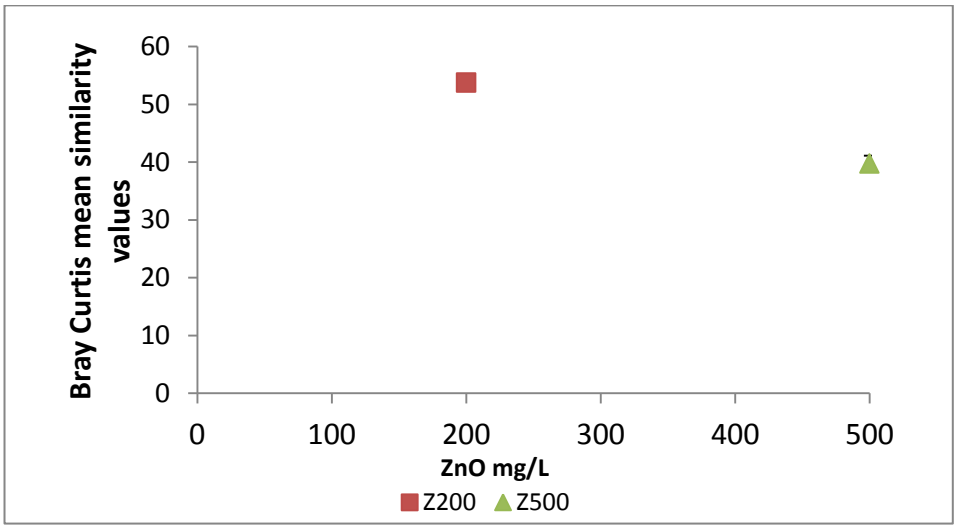

Figure 5-19c: The resemblance matrix plotted against the concentration gradient of zinc oxide nanoparticles. The y-axis shows the mean resemblance of samples to control and x-axis ZnO (mg/L).

The DNA finger print analysis shows that within the community of sulphate reducing bacteria, some degree of heterogeneity exists and high concentration of nanoparticles could be an important factor contributing to it.

5.4 Discussion

The nanoparticle exposure studies conducted by developing microcosms bring out a different picture in comparison to the controlled lab experiments discussed in other chapters. There is no denying the fact that the nanoparticles are toxic to living organisms.

5.4.1 Major transformation pathways of silver nanoparticles

The LCF analysis showed that silver nanoparticles rapidly transformed into silver sulphide and silver oxide. In contrast to other findings (Lowry et al., 2012), the transformation rates observed in this study were quite high so much that the time zero freeze dried samples also showed a high percentage of sulphides. This could be because the nanoparticle used in the current study lacked any stabilizing coating on their surface and were prone to chemical transformations.

The presence of silver sulphide in time zero samples clearly shows that this phenomenon had little to do with added sulphate levels. In fact, the driving force for sulphidation could have been the basal levels of sulphides present in the sediment. Ag nanoparticles have been shown to transform to sulphide under laboratory conditions where H_2S levels are in the ppb range (Bennett et al., 1969), hence any traces of sulphide in the original sediment either in dissolved or solid form is likely to transform silver into sulphides (the sediment used was very dark and hence likely

reducing). Besides sulphates, traces of sulphides may form due to biological activities mainly due to presence of amino acids like methionine (Brock, 1978) and population of bacteria that can convert cysteine into sulphides (Jones, 1982). The sediment collected and analysed at time 0 certainly was not incubated and experienced no further bacterial growth but the possibility of presence of minimal levels of compounds of biological origin cannot be completely ruled out. This study can certainly be further optimized by estimation of native sulphate levels in water and the amount of acid volatile sulphides present, both of which could have contributed to the presence of sulphides and partially explain the transformation of unstabilized nanoparticles. Transformation of silver into silver sulphides has been shown to reduce the toxicity of silver nanoparticles (Choi et al., 2009, Reinsch et al., 2012) and this could partially explain the absence of drastic impact of nanoparticles on the total microbial community composition in the sediments.

5.4.2 Major transformation pathways of ZnO nanoparticles

Microcosms amended with ZnO also demonstrated transformation to ZnS with trace (and likely statistically insignificant) amounts of $ZnSO_4$ in the top layer where the microcosms may have maintained oxic conditions. However, ZnO amended nanoparticles freeze-dried immediately after amendment (time zero), were dominated by $ZnCO_3$ with ~30% of ZnO still remaining while $ZnSO_4$ also precipitated. Apart from demonstrating that different nanoparticles will transform at different rates, the presence of $ZnCO_3$ and $ZnSO_4$ also implies that transformation occurs *via* a rapid dissolution-mediated pathway to allow these salts to precipitate.

5.4.3 Chemical pathways of transformation of nanoparticles in the environment

In this work, LCF modelling showed that sediment samples amended with nanoparticles showed a significant amount of silver as silver sulphide and silver oxide. Silver oxide forms due to dissolution from nanoparticles (Levard et al., 2011, Xiu et al., 2011). Silver sulphide on the other hand could have possibly formed due to sulphidation reactions (dissolution-precipitation reaction). The sulphidation process can also produce changes in the surface charges of the nanoparticles and their interaction with organic ligands present in the sediment. These can affect the stability of nanoparticles and restrict their movement in the porous medium like soil (Levard et al., 2011). The high temperature and pressure used for sterilization could have produced reduced aeration (most of air bubbled could have escaped/ bubbled out). Anoxic conditions together with high temperatures could possibly accelerate the precipitation reactions like sulphidation.

This work demonstrates that presence of ions and sulphate rich environment (that ensures growth of specific bacterial communities/dsrB) can drive changes in the speciation and fate of nanoparticles (Peralta-Videa et al., 2011). This transformation could be due to the chemical composition of sediment matrix like presence of sulphides. The formation of sulphide shell on the nanoparticles can further restrict the solubility and ionization hence checks the effect of silver nanoparticles (Levard et al., 2012).

Hence, the environmental variables that can affect the silver precipitation in favour of chlorides, sulphates or complexation with organic matter, will invariably

shift the toxicity levels and in case of microcosms the minor changes will not create enough stress to bring a drastic change in community composition. As seen in this study, most of the ionic silver formed by nanoparticles was transformed into silver sulphide. If this observation is corelated to natural habitats like estuary, water logged areas and acidic soils and urban water bodies (all of which can be a possible sink of nanoparticles), microbial communities will not be drastically affected. Apart from sulphides, the presence of silver oxide that form largely because of dissolution from silver nanoparticles also exist (Levard, 2012). The presence of ions and organic matter will complex the nanoparticles and greatly restrict the mobility and toxicity of nanoparticles like silver and zinc oxide. A similar observation was reported by Kaegi et al. (2013) that silver nanoparticles released in the waste water were rapidly transformed into silver sulphide and were efficiently recovered irrespective of the surface and size of the nanoparticles.

The speciation analysis of microcosms dosed with zinc oxide nanoparticles clearly shows a significant pattern, the initial presence of high amounts of zinc carbonates and sulphates was replaced by dominant zinc sulphide with increase in incubation time. This indicates that speciation pattern of nanoparticles is initially dependent on the chemical properties of the metal they are constituted of but later the presence of common ion and the mineralogy of the soil can shift the transformations in a specific direction, in this case sulphides**.** This also suggests that short-term exposure studies using ZnO and silver nanoparticles will certainly produce different outcomes but in the longer run can also produce similar results.

A similar observation was reported by Ma et al. (2010) when ZnO amended microcosms showed hundred percent transformation of ZnO nanoparticles to ZnS

nanoparticles which led to aggregation of nanoparticles and greatly restricted their dissolution rates. The immediate impacts will be very different from long term exposure of urban water bodies to engineered nanoparticles.

5.4.4 Microbial activities that influence speciation of nanoparticles

The 16 S rRNA finger printing analysis show that addition of silver and zinc oxide nanoparticles produces distinct perturbations apparent from the presence of additional bands in gel and this effect is consistent in the subsequent Bray Curtis resemblance matrix (in case of sediments derived from microcosm). The analysis of water sub sampled from these microcosms however show inconclusive outcomes. This could be partially explained by the fact that the added nanoparticles had migrated to the sediment zone as confirmed by total metal extraction (BCR extraction) conducted on water samples extracted from these microcosms. This fractionation possibly due to sedimentation leaves insignificant amount of nanoparticles, insufficient to produce any effect on microbial community in the supernatant.

The addition of nanoparticles marginally affected the overall distribution of the microbial community in sediment as evident by the quantitative analysis of the band intensity matrix. However, in case of sediment analysis overall no statistically significant effect was observed. This observation is in agreement with other findings. For instance, both, Bradford (2009) and Muhling (2009) showed that silver nanoparticles did not bring about much change in the microbial community structure.

A number of studies have shown that Ag nanoparticles oxidise rapidly in most aqueous environments, affording a mechanism for oxidative dissolution to generate Ag+ (Xiu et al., 2011). Transformation of Ag nanoparticles to Ag_2S has recently been shown to reduce toxicity of Ag nanoparticles (Choi et al., 2009, Reinsch et al., 2012), apparently due to reduced solubility of the Ag_2S (Levard et al.2011). Presence of even low levels of sulphides in freshwater systems can therefore effectively check the impact of incidental release of metal based nanoparticles by promoting their transformation into lesser toxic forms.

However, the dsrB profile analysis shows that high concentration of nanoparticles affected the microbial diversity more than that observed in the total community analysis using 16S RNA. Sulfidation of silver has been shown to reduce its toxicity significantly (Reinsch, 2012). However, this could not be said of the silver oxides that account for approximately 15% as shown by LCF analysis. These could be instrumental in producing effect on sulphate reducing bacteria.

Bray Curtis similarity index of dsrB shows that nanoparticles amendment at high concentrations did produce statistically significant change. For instance, samples Ag 500 or Ag1000 mg/L forms a subset with wide scatter from the rest of the samples (Figure 5-19a). The Welch t test also showed that along the X ordinate the values produced significant difference in case of dsrB analysis. The mean resemblance of the treated samples showed an inverse relation to the concentration gradient of nanoparticles (Figure 5-19 b, c).

5.4.5 Implications for toxicity of nanoparticles to the environment

In other studies, it has been shown that the environmental variables, plants, organic matter and ions can drive changes in the speciation and fate of nanoparticles. For instance, Bradford et al. (2009) used estuarine brackish water (higher levels of chlorides) for microcosm studies. This could have complexed most of the silver as silver chloride and reduced the bioavailability of ionic silver formed from nanoparticulate surface. Hence, no drastic impact on community structure was observed. Similarly, Bone et al. (2012) showed how the plant and bacterial amendments can reduce the toxicity levels of silver nanoparticles and influence the transformation of silver into sulphides. In this work too, sulphidation of silver greatly altered the availability of ionic silver and thereby influenced the toxicity levels as evident from insignificant changes in the overall microbial community structure. However, the presence of nanoparticles did produce some perturbation within the population structure. In contrast, Das et al. (2012) used fresh water samples for microcosm development and found that in fresh water with apparently low levels of ions (chlorides and sulphates), ionic silver significantly affected bacterial cell viability and in long term, the community composition.

The rapid transformation of silver in wastewater systems and ZnO nanoparticles in sediment microcosms has shown that engineered nanoparticles will be subjected to abiotic processes with a strong potential to render them insoluble hence less toxic. The microcosms certainly provide a demonstrable model to show transformation of engineered nanoparticles however, this study can greatly be improved by development of mesocosms that can perhaps enable better stratification

and mimic terrestrial system and by use of higher range of nanoparticle concentration. Both long term and short-term incubation strategy coupled with sample analysis at regular time intervals can help to get more information about toxicity and net impact of nanoparticles on the biota.

References

1. Battin , T., Frank, V. D., Weilhartner, A., Ottofuelling, S. & Hofmann, T. 2009. Nanostructured TiO2: transport behavior and effects on aquatic microbial communities under environmental conditions. *Environ. Sci. Technol.,* 43**,** 8098-8104.

2. Becker, J., Parkin, T., Nakatsu, C., Wilbur, J. & Konopka, A. 2006. Bacterial activity, community structure, and centimeter-scale spatial heterogeneity in contaminated Soil. *Microbial Ecology,* 51**,** 220-231.

3. Bennett, H. E., Peck, R. L., Burge, D. K. & Bennett, J. M. 1969. Formation and growth of tarnish on evaporated silver films. *J. Appl. Phys.,* 40**,** 3351.

4. Bone, A. J., Colman, B. P., Gondikas, A. P., Newton, K. M., Harrold, K. H., Cory, R. M., Unrine, J. M., Klaine, S. J., Matson, C. W. & Di Giulio, R. T. 2012. Biotic and abiotic interactions in aquatic microcosms determine fate and toxicity of Ag nanoparticles: part 2-toxicity and Ag speciation. *Environ. Sci.Technol.,* 46(13)**,** 6925-33.

5. Choi, O., Clevenger, T. E., Deng, B., Surampalli, R. & Hu, Z. 2009. Role of sulfide and ligand strength in controlling nanosilver toxicity. *Water Res.,* 43**,** 1879-1886.

6. Dimkpa, C., Calder, A., Gajjar, P., Merugu, S., Huang, W., Britt, D., McLean, J., Johnson, W. & Anderson, A. J. 2011. Interaction of silver nanoparticles with an environmentally beneficial bacterium, *Pseudomonas chlororaphis*. *J.Hazard.Mater,* Volume 188**,** 428-435.

7. Fabrega, J., Shona, R., Fawcett, S., Renshaw, J. C. & Lead, J. R. 2009. Silver nanoparticle impact on bacterial growth: effect of pH, concentration, and organic matter. *Environ. Sci. Technol.,* 43(19)**,** 7285-90.

8. Gajjar, P., Pettee, B., Britt, D., Huang, W., Johnson, W. & Anderson, A. 2009. Antimicrobial activities of commercial nanoparticles against an environmental soil microbe, *Pseudomonas putida* KT2440. *J Biol.Eng.,* 3**,** 1611-1754.

9. Ge, Y., Schimel, J. P. & Holden, P. A. 2011. Evidence for Negative Effects of TiO(2) and ZnO Nanoparticles on Soil Bacterial Communities. *Environ. Sci.Technol.,* 45**,** 1659-1664.

10. Geets, J., Borremans, B., Diels, L., Springael, D., Vangronsveld, J., van der Lelie, D. & Vanbroekhoven, K. 2006. DsrB gene-based DGGE for community and diversity surveys of sulfate-reducing bacteria. *J Microbiol Methods.,* 66(2)**,** 194-205.

11. Gondikas, A. P., Morris, A., Reinsch, B. C., Marinakos, S. M., Lowry, G. V. & Hsu-Kim, H. 2012. Cysteine-induced modifications of zero-valent silver nanomaterials: implications for particle surface chemistry, aggregation, dissolution, and silver speciation. *Environ. Sci.Technol.,* 46**,** 7037-45. .

12. He, D., Garg, S. & Waite, T. D. 2012. H2O2-mediated oxidation of zero-valent silver and resultant interactions among silver nanoparticles, silver ions, and reactive oxygen species. *Langmuir,* 28(27)**,** 10266-75.

13. Huang, Z., Zheng, X., Yan, D., Yin, G., Liao, X., Kang, Y., Yao, Y., Huang, D. & Hao, B. 2008. Toxicological effect of ZnO nanoparticles based on bacteria. *Langmuir,* 24**,** 4140-4144.

14. Jones, J.G., Simon, B.M., Roscoe, J.V. 1982. Mirobiological sources of sulphides in fresh water sediments. J.Gen.Microbiol., 128, 2833-2839.

15. Kanaly, R. A., Maeda, A. H., Kunihiro, M. & Hamamura, N. 2011. Application of Denaturing Gradient Gel Electrophoresis as an Ecotoxicological Tool to Investigate the Effects of aqu-Fullerene on a Bacterial Community. *Interdisciplinary Studies on Environmental Chemistry—Environmental Pollution and Ecotoxicology***,** 79-88.

16. Kasemets, K., Ivask, A., Dubourguier, H.-C. & Kahru, A. 2009. Toxicity of nanoparticles of ZnO, CuO and TiO2 to yeast *Saccharomyces cerevisiae*. *Toxicology in Vitro,* 23**,** 1116-1122.

17. Levard, C., Hotze, E. M., Lowry, G. V. & Brown, G. E. 2012. Environmental transformations of silver nanoparticles: impact on stability and toxicity. *Environ. Sci.Technol.,* 46**,** 6900-6914.

18. Levard, C., Reinsch, B., Michell, F., Oumachi, C., Lowry, G. V. & Brown, G. E. 2011. Sulfidation processes of pvp-coated silver nanoparticles in aqueous solution: Impact on dissolution rate *Environ Sci Technol.,* 45**,** 5260−5266.

19. Levard, C. et al., 2011. Sulfidation processes of pvp-coated silver nanoparticles in aqueous solution: Impact on dissolution rate. *Environ. Sci. Technol*., 45, 5260−5266.

20. Li, M., Zhu, L. & Lin, D. 2011. Toxicity of ZnO nanoparticles to *Escherichia coli*: mechanism and the influence of medium components.*Environ. Sci.Technol.,* 45**,** 1977-1983.

21. Liu, Y., Li, J., Qiu, X. & Burda, C. 2007. Bactericidal activity of nitrogen-doped metal oxide nanocatalysts and the influence of bacterial extracellular polymeric substances (EPS). *J Photochem Photobiol A: Chemistry,* 190**,** 94-100.

22. Ma, R., Koksharova, O. A. & Khmel, I. A. 2009. Antibacterial effects of silver ions: effect on gram-negative bacteria growth and biofilm formation]. *Mol Gen Mikrobiol Virusol.,* 4**,** 27-31.

23. Morones, J. R., Elechiguerra, J., Camacho, A., Holt, K., Kouri, J., Ramrez, J. T. & Yacaman, J. 2005. Bactericidal impact of silver nanoparticles. *Nanotechnol.,* 16**,** 2346-2353

24. Nagy, A., Harrison, A., Sabbani, S., Munson, R. S., Jr., Dutta, P. K. & Waldman, W. J. 2011. Silver nanoparticles embedded in zeolite membranes: release of silver ions and mechanism of antibacterial action. *Int J Nanomedicine. ,* 6**,** 1833-52.

25. Nel, A., Xia, T., Mädler, L. & Li, N. 2006. Toxic Potential of Materials at the Nanolevel. *Science,* 311**,** 622-627.

26. Park, H. J., Kim, J. Y., Kim, J., Lee, J. H., Hahn, J. S., Gu, M. B. & Yoon, J. 2009. Silver-ion-mediated reactive oxygen species generation affecting bactericidal activity. *Water Res.,* 43(4)**,** 1027-32.

27. Peralta-Videa, J. R., Zhao, L., Lopez-Moreno, M. L., de la Rosa, G., Hong, J. & Gardea-Torresdey, J. L. 2011. Nanomaterials and the environment: A review for the biennium 2008-2010. *J Hazard Mater.,* 186**,** 1-15.

28. Ravel, B. & Newwille, M. 2005. ATHENA, ARTEMIS, HEPHAESTUS: Data analysis for X ray absorption spectroscopy using IFEFFIT. *J. Synchrotron. Radiation,* 12**,** 537-541.

29. Reinsch, B. C., Levard, C., Li, Z., Ma, R., Wise, A., Gregory, K. B., G. E. Brown, J. & Lowry, G. V. 2012. Sulfidation of silver nanoparticles decreases *Escherichia coli* growth inhibition. *Environ. Sci. Technol.,* 46**,** 6992-7000.

30. Rousk, J., Ackermann, K., Curling, S. F. & Jones, D. L. 2012. Comparative toxicity of nanoparticulate CuO and ZnO to soil bacterial communities. *PLoS ONE,* 7(3)**,** e34197.

31. Sondi, I. & Sondi, B. S. 2004. Silver nanoparticles as antimicrobial agent: a case study on *E. coli* as a model for Gram-negative bacteria. *J.Colloid. Interphase Sci.,* 275**,** 177-182.

32. Tong, Z., Bischoff.M, Nies, L., Applegate, B. & Turco, R. F. 2007. Impact of Fullerene (C60) on a Soil Microbial Community. *Environ. Sci.Technol.,* 41**,** 2985-2991.

33. Van de Peer, Y., Chapelle, S. & De, W. R. 1996. A quantitative map of nucleotide substitution rates in bacterial rRNA. *Nucleic Acids Res,* 24**,** 3381–3391.

34. Verhoef, H. A. 1996. The role of soil microcosms in the study of ecosystem processes. *Ecology,* 72**,** 685-90.

35. Xiu, Z.-M., Ma, J. & Alvarez, P. J. J. 2011. Differential Effect of Common Ligands and Molecular Oxygen on Antimicrobial Activity of Silver Nanoparticles versus Silver Ions. *Environ Sci Technol.*, 45**,** 9003-9008.

36. Xiu , Z. M., Zhang, Q. B., Puppala, H. L., Colvin, V. L. & Alvarez, P. J. 2012. Negligible particle-specific antibacterial activity of silver nanoparticles. *Nano Letters*, 12(8)**,** 4271-5.

37. Yuan, G., Joshua P, S. & Holden, P. A. 2011. Evidence for Negative Effects of TiO2 and ZnO Nanoparticles on Soil Bacterial Communities. *Environ. Sci. Technol.*, 45**,** 1659–1664.

38. Zinder, S.H and Brock, T.D. 2011. Methane, carbon dioxide, and hydrogen sulfide production from the terminal methiol group of methionine by anaerobic lake sediments. Appl Environ Microbiol., 35(2): 344–352.

Chapter 6

Synthesis and conclusion

Engineered nanoparticles find many applications and therefore will be manufactured in increased quantities in the near future. Inevitably, they will be released in the environment and interact with biota. Controlled laboratory experiments have shown that nanoparticles including Ag, TiO_2, ZnO and CuO and C60 fullerene produce adverse impacts on living organisms (Lam et al., 2004, Sondi and Sondi, 2004, Heinlaana et al., 2008, Kasmets et al., 2009). These studies span a wide variety of living organisms including bacteria, yeast, invertebrates, mammalian cell lines and plants.

The adverse impacts of nanoparticles vary depending on the nanoparticle in question and the model organisms. Nanoparticles in general, have been shown to cause DNA damage (Bhabra et al., 2009), impaired physiological functions in invertebrates like *Daphnia magna* and *Mytilus* (Cattaneo et al., 2009) and reduction in cell viability (Sondi, 2004). Laboratory findings form an important basis for assessment of nanoparticles but when their possible risks to environment are considered, the observed response is not consistent with laboratory predictions. The terrestrial and aquatic environment is compositionally and biologically variable and is in a state of constant flux. Biotic metabolic exudates, cycling of ions and abiotic factors, can all affect the stability and behaviour of nanoparticles. Thus, it is important to investigate nanotoxicity under environmentally realistic conditions.

In this research work, it was found that silver nanoparticle produce toxicity to bacteria by multiple pathways and this in agreement with other works (Gou et al., 2010, Horie et al., 2011). Bacteria can resist nanotoxicity by production of extracellular polymeric substance (EPS), and microcosm's studies demonstrate that nanoparticles undergo transformation in the environment, which can significantly alter their toxicity levels.

6.1 Nanotoxicity operates by multiple pathways

Recently, attempts have been made to understand the mechanism of nanotoxicty but this has produced some seemingly contradictory results. This situation has arisen due to variations in the experimental design, choice of nanomaterial and the model organism under study. Engineered metal and metal oxide nanoparticles release ions that form a major contributor to toxicity as shown in many studies with silver, zinc oxide and copper oxide nanoparticles (Kasemets et al., 2009, Bondarenko et al., 2012, Ma et al., 2012, Xiu et al., 2012, Ya-Nan et al., 2012).

However, the exposure assays using eukaryotoic cell lines clearly show that oxidative stress also contributes to nanotoxicity (Hussain et al., 2005, Carlson et al., 2008, Xia et al., 2008, Liu et al., 2011, Napierska et al., 2012). These studies made use of specific probes that detect and bind to reactive oxygen species (ROS) and enzyme assays to measure elevated levels of gene expression. This was comparatively easy in higher organisms because the cells are highly differentiated and ROS can be detected with ease. However, in the case of microorganisms it was a challenging task. Nevertheless, many studies conducted on bacteria now indicate that

nanoparticles definitely contribute to oxidative stress (Inoue et al., 2002, Choi and Hu, 2008, He et al., 2012, Ivask et al., 2012).

In this work too, it was found that deletion mutants of *E. coli* lacking genes that mediate processes like ion efflux and resistance to oxidative stress, showed increased sensitivity towards silver nanoparticles. Furthermore, addition of catalase conferred some resistance against nanotoxicity. The bioreporter that responds to copper and silver ions was not induced on exposure to silver nanoparticles, yet a significant drop in cell viability was observed. It was a very important observation, which proved that silver nanoparticles express their toxicity by more than one mechanism. The current work showed that deletion mutant strains without genes like *katG, sodA* (OxyR and SoxR regulon) and Δ *cueR, Δ copA* (involved in the effux of ionic silver) both show sensitivity to silver nanoparticles. By making use of a GFP fusion library, Gou et al.(2010) also demonstrated that exposure to silver nanoparticles, induced an increase in gene expression for OxyR, SoxR regulon and altered expression of genes including *bolA* (related to biofim formation) and membrane permeability (*cyoA*). Therefore, there are multiple factors instrumental in nanotoxicty as shown in this work and others (Gou, 2010).

6.2 Oxidative stress and nanotoxicity

The oxidative stress biosensors did not show a significant response to silver nanoparticles due to which the nature of reactive oxygen species (ROS) could not be identified. However, this does not imply that oxidative stress is not involved in silver nanotoxicity. There is sufficient evidence in the available literature confirming the

role of oxidative stress in nanotoxicity, yet, there is no agreement about the exact nature of toxicity. This suggests that there could be a mix of radicals that might form and highly specific promoters perhaps not serve as best indicators to detect them, as shown in the current study.

Secondly, the overexpression strains for superoxide dismutase and glutathione peroxidase do show a consistent but low cell count during exposure studies, unlike the control strain that showed a sharp decline in cell viability in presence of silver np. This suggests that the strategy of using cell viability test is perhaps not the best one for overexpression strains. Similarly, the strains that overproduce prefoldin and Dps show greater cell viability than the controls suggesting that silver nanoparticles cause damage to DNA and also contribute to loss of membrane integrity. This again suggests that nanotoxicity operates by multiple pathways.

6.3 Presence of EPS and analogues protects bacteria against nanotoxicity

Bacteria growing in a biofilm show better survival against environmental stress conditions like osmotic shock and presence of toxins. It was observed that bacteria that produce copious amount of extracellular polymeric substances (EPS) show a better survival against nanotoxocity. For instance, Liu (2007) demonstrated that bacteria with intact EPS showed higher cell viability on exposure to TiO_2 and ZrO_2 nanoparticles than the ones without EPS. EPS has been shown to protect

bacteria against a wide range of metal nanoparticles (Moreau et al., 2007, Fabrega et al., 2009a, Liu et al., 2007, Dimkpa et al., 2011).

In this work, the engineered bacteria *E.coli* JM109 /pRcsA2 that overproduced colanic acid (a type of EPS) showed a better survival than the control strain on exposure to silver nanoparticles. The EPS released by bacteria protects it in many ways, most commonly by encapsulating the cells and acting as a physical barrier (Battin et al., 2009, Joshi et al., 2012). Secondly, EPS has many functional groups that can essentially bind released ions (Omoike and Chorover, 2006, Kiser et al., 2010) or simply adsorb the nanoparticles on their surface (Sahle-Demessie and Tadesse, 2011). Furthermore, the presence of EPS has been shown to promote aggregation of nanoparticles (Moreau et al., 2007, Fabrega et al., 2009) and reduce the mobility of nanoparticles by reducing their diffusion coefficient (Peulen and Wilkinson, 2011). EPS analogues like xanthan have been shown to alleviate nanotoxicty (Miao et al., 2009, Joshi et al., 2012) and addition of EPS preparation has been found to protect cells irrespective of its source. This indicates that the protection provided by EPS is partially physical and to some extent related to surface chemistry but quite nonspecific (Fabrega et al., 2009a).

6.4 Nanoparticles transformation in the environment alleviates nanotoxicity

Engineered nanoparticles are stabilized entities and their impact on the environment is dependent on factors like pH, presence of ions (Limbach et al., 2005), organic matter (Fabrega et al., 2009), all which can affect their stability, size and

speciation and promote their transformation into less toxic forms (Lowry, 2012, Wirth et al., 2012). Recent studies show that nanoparticles behave quite differently in sediment and aquatic habitats. Chemical transformations like sulphidation and oxidation can change the speciation of metals released from nanoparticulate surfaces to form precipitates (Levard et al., 2012, Ma et al., 2012). Microcosm studies using fullerene (Tong et al., 2007), silver (Lowry et al., 2012) and zinc oxide nanoparticles (Yuan et al., 2011) demonstrate that these nanomaterials produce impact ranging from insignificant (silver, C60) to negative (ZnO and silver NP in fresh water microcosm) on microbial communities. The outcomes are dependent on the physicochemical properties of the medium. For instance, presence of chlorides, sulphates and plant matter essentially reduces their toxicity and promotes adsorption on plant surface and precipitation of nanoparticles as chlorides and sulphides (Bone et al., 2012, Dinesh et al., 2012, Unrine et al., 2012).

In this work, addition of uncapped silver and zinc oxide nanoparticles to microcosms did not drastically alter the microbial community composition. The nanoparticles were prone to rapid transformation into silver sulphide and zinc sulphide. The transformation process is shown in Figure 6-1. There was significant variation in the speciation rates and silver demonstrated a high propensity to form sulphides at the onset of the experiment whereas samples amended with ZnO nanoparticles had fractions of sulphides, carbonates and oxides, although long term exposure resulted in formation of sulphides in all samples. This result shows that not all nanoparticles will demonstrate similar transformation rates hence nanoparticles will have different fates in environment.

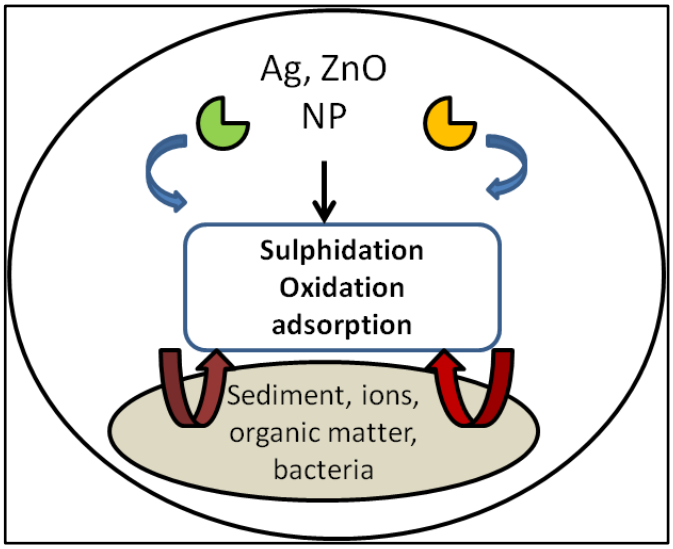

Figure 6-1 Transformation of nanoparticles in a microcosm (this study)

The point to note is that naoparticles like silver will show a higher toxicity impact than ZnO in controlled laboratory experiments but in environment such as sediments, considering that ZnO resists transformation much more than silver NP, the results could be different.

6.5 Future work

Microarray techniques to investigate the response of bacteria against nanoparticles

Molecular biology techniques such as microarrays can be used to measure the gene expression levels in bacteria on exposure to known oxidative stress producing agents and the most widely used engineered nanoparticles. For instance, Pelletier et al. (2010) used transcriptional profiling of bacteria (*E. coli*, *Bacillus subtilis* and *Shwenaella oneidensis*) exposed to cerium oxide nanoparticles. This study has

provided vital clues about the nanotoxicity pathways. This method can be used to determine the toxicity pathways of other nanoparticles like silver and zinc oxide.

Mass spectroscopy has been used to investigate the pattern of gene expression in many bacteria under different stress conditions (Leverrier et al., 2004, Hemm et al., 2010). It could be used to analyse the protein expression of bacterial strains resistant to oxidative stress and silver toxicity on exposure to engineered nanoparticles. This technique can provide a choice to compare patterns (at the proteomic level) for specific and diffused stress agents such as nanoparticles.

Development of biosensors against a wide range of environmental stress

Furthermore, sensitive biosensors can be constructed with a wide range of promoters specific to stresses including heat shock and starvation (*rpoH, dnak, groE dps*); reactive oxygen species (*katG, ahpf, katE and sodA*) by using synthetic biology techniques. These could be tested in conjunction with flow cytometry and microarray techniques. The promoters could be combined together and their net response can also be tested by making use of novel assembly methods and use of reverse transcription polymerase chain reaction (RT-PCR) can help to investigate the gene expression during nanoparticle exposure assays (Mo, 2012). This method will provide a global approach required to detect the nature of nanotoxicity.

Microcosm and mesocosms analysis

Microcosm experiments can be further optmized for two levels of exposures, a short-term impact and a long-term exposure analysis with respect to speciation of metals and impact on microbial community composition. Mesocosms can be designed to provide a realistic assessment of impact of nanoparticles. This can have certain advantages over the microcosms namely; (a) provide an increased spatial heterogeneity and (b) development of stratifications/zones that can mimic terrestrial habitat.

The toxicity of nanoparticles requires significant research with improved experimental designs and a multivariable scenario involving communities of plants and microorganisms. A combination of biochemical and ecological experimental designs can certainly improve our current knowledge about nanoparticles and provide vital information about the fate of nanoparticles and their toxicity mechanisms.

References

1. Battin , T., Frank, V. D., Weilhartner, A., Ottofuelling, S. & Hofmann, T. 2009. Nanostructured TiO2: transport behavior and effects on aquatic microbial communities under environmental conditions. *Environ. Sci. Technol.,* 43**,** 8098-8104.

2. Bhabra, G., Sood, A., Fisher, B., Cartwright, L., Saunders, M., Evans, W. H., Surprenant, A., Castejon, G., Mann, S., Davis, S. A., Hails, L. A., Ingham, E., Verkade, P., Lane, J., Heesom, K., Newson, R. & Case, C. P. 2009. Nanoparticles can cause DNA damage across a cellular barrier. *Nature Nanotechnol.,* 873-883.

3. Bondarenko, O., Ivask, A., Käkinen, A. & Kahru, A. 2012. Sub-toxic effects of CuO nanoparticles on bacteria: kinetics, role of Cu ions and possible mechanisms of action. *Environ. Pollut.,* 169**,** 81-90.

4. Bone, A. J., Colman, B. P., Gondikas, A. P., Newton, K. M., Harrold, K. H., Cory, R. M., Unrine, J. M., Klaine, S. J., Matson, C. W. & Di Giulio, R. T. 2012. Biotic and abiotic interactions in aquatic microcosms determine fate and toxicity of Ag nanoparticles: part 2-toxicity and Ag speciation. *Environ. Sci.Technol.,* 46(13)**,** 6925-33.

5. Carlson, C., Hussain, S. M., Schrand, A. M., K. Braydich-Stolle, L., Hess, K. L., Jones, R. L. & Schlager, J. J. 2008. Unique cellular interaction of silver nanoparticles: size-dependent generation of reactive oxygen species. *J.Phys.Chem.B,* 112**,** 13608-13619.

6. Cattaneo, A., Gornati, R., Chiriva-Internati, M. & Bernardini, G. 2009. Ecotoxicology of nanomaterials: the role of invertebrate testing *ISJ 6* 6**,** 78-97.

7. Choi, O. & Hu, Z. 2008. Size Dependent and Reactive Oxygen Species Related Nanosilver Toxicity to Nitrifying Bacteria. *Environ Sci Technol.,* 42**,** 4583-4588.

8. Dimkpa, C., Calder, A., Gajjar, P., Merugu, S., Huang, W., Britt, D., McLean, J., Johnson, W. & Anderson, A. J. 2011. Interaction of silver nanoparticles with an environmentally beneficial bacterium, *Pseudomonas chlororaphis*. *J.Hazard.Mater,* Volume 188**,** 428-435.

9. Dinesh, R., Anandaraj, M., Srinivasan, V. & Hamza, S. 2012. Engineered nanoparticles in the soil and their potential implications to microbial activity. *Geoderma,* 173-174**,** 19-27.

10. Fabrega, J., Renshaw, J. C. & Lead, J. R. 2009a. Interactions of silver nanoparticles with *Pseudomonas putida* biofilms. *Environ. Sci Technol,* 43**,** 9004-9009.

11. Fabrega, J., Shona, R., Fawcett, S., Renshaw, J. C. & Lead, J. R. 2009b. Silver nanoparticle impact on bacterial growth: effect of pH, concentration, and organic matter. *Environ. Sci. Technol.,* 43(19)**,** 7285-90.

12. Gou, N., Onnis-Hayden, A. & Gu, A. Z. 2010. Mechanistic toxicity assessment of nanomaterials by whole-cell array stress genes expression analysis. *Environ. Sci. Technol.,* 44**,** 5964–5970.

13. Lowry, G.V., Espinasse, B.P., Badireddy, A.R., Richardson, C.J., Reinsch, B.C., Bryant, L.D., Bone, A.J., Deonarine, A, Chae, S., Therezien, M., Colman, B.P., Hsu-Kim H., Bernhardt, E.S., Matson, C.W., Wiesner, M.R 2012. Long-term transformation and fate of manufactured Ag nanoparticles in a simulated large scale freshwater emergent wetland. *Environ.Sci.Technol.,* 46**,** 7027-36.

14. He, D., Garg, S. & Waite, T. D. 2012. H2O2-mediated oxidation of zero-valent silver and resultant interactions among silver nanoparticles, silver ions, and reactive oxygen species. *Langmuir,* 28(27)**,** 10266-75.

15. Heinlaana, M., Ivaska, A., Blinovaa, I., Dubourguier, H.C. & Kahru, A. 2008. Toxicity of nanosized and bulk ZnO, CuO and TiO2 to bacteria *Vibrio fischeri* and crustaceans *Daphnia magna* and *Thamnocephalus platyurus*. *Chemos.,* 71**,** 1308–1316.

16. Hemm, M. R., Paul, B. J., Miranda-Ríos, J., Zhang, A., Soltanzad, N. & Storz, G. 2010. Small stress response proteins in *Escherichia coli*: proteins missed by classical proteomic studies. *J. Bacteriol.,* 196**,** 46-58.

17. Horie, M., Kato, H., Fujita, K., Endoh, S. & Iwahashi, H. 2011. In vitro evaluation of cellular response induced by manufactured nanoparticles. *Chem. Res.Toxicol.,* 25**,** 605-619.

18. Hussain, S. M., Hess, K. L., Gearhart, J. M., Geiss, K. T. & Schlag, J. J. 2005. In vitro toxicity of nanoparticles in BRL 3A rat liver cells. *Toxicity invitro,* 19**,** 975–983.

19. Inoue, Y., Hoshino, M., Takahashi, H., Noguchi, T., Murata, T., Kanzaki, Y., Hamashima, H. & Sasatsu, M. 2002. Bactericidal activity of Ag-zeolite mediated by reactive oxygen species under aerated conditions. *J Inorg Biochem.,* 30**,** 37-42.

20. Ivask, A., Suarez, E., Patel, T., Boren, D., Ji, Z., Holden, P., Telesca, D., Damoiseaux, R., Bradley, K. A. & Godwin, H. 2012. Genome-wide bacterial toxicity screening uncovers the mechanisms of toxicity of a cationic polystyrene nanomaterial. *Environ. Sci. Technol.*46**,** 2398–2405.

21. Joshi, N., Ngwenya, B. & French, C. E. 2012. Enhanced resistance to nanoparticle toxicity is conferred by overproduction of extracellular polymeric substances. *J Hazard. Mater.,* 241–242**,** 363-370.

22. Kasemets, K., Ivask, A., Dubourguier, H.-C. & Kahru, A. 2009. Toxicity of nanoparticles of ZnO, CuO and TiO2 to yeast *Saccharomyces cerevisiae*. *Toxicology in Vitro,* 23**,** 1116-1122.

23. Kasmets, K., Ivask, A., Dubourgier, H. & Kahru, A. 2009. Toxicity of nanoparticles TiO2,ZnO,SiO2 to yeast *Saccharomyces cerevisiae*. *Toxicity invitro,* 23**,** 1116-1122.

24. Kiser, M. A., Ryu, H., Jang, H., Hristovski, K. & Westerhoff, P. 2010. Biosorption of nanoparticles to heterotrophic wastewater biomass. *Water Res.,* 42**,** 4104-4114.

25. Lam, C., James, J. T., McCluskey, R. & Hunter, R. L. 2004. Pulmonary toxicity of single-wall carbon nanotubes in mice 7 and 90 days after intratracheal instillation. *Toxicol. Sci.,* 77**,** 126-134.

26. Levard, C., Hotze, E. M., Lowry, G. V. & Brown, G. E. 2012. Environmental transformations of silver nanoparticles: impact on stability and toxicity. *Environ. Sci.Technol.,* 46**,** 6900-6914.

27. Leverrier, P., Vissers, J. P., Rouault, A., Boyaval, P. & Jan, G. 2004. Mass spectrometry proteomic analysis of stress adaptation reveals both common and distinct response pathways in *Propionibacterium freudenreichii*. *Arch. Microbiol,* 181**,** 215-233.

28. Limbach, L., Y.Li, R.Grass, Brunner, T. J., Hintermann, M., M.Muller, Gunther, D. & Stark, W. 2005. Cerium oxide nanoparticle uptake in human lung fibroblasts: effects of particle size, agglomeration and diffusion at low concentrations. *Environ. Sci.Technol.,* 39**,** 9370-9376.

29. Liu, S., Zeng, T. H., Hofmann, M., Burcombe, E., Wei, J., Jiang, R., Kong, J. & Chen, Y. 2011. Antibacterial activity of graphite, graphite oxide, graphene oxide, and reduced graphene oxide: membrane and oxidative stress. *ACS Nano,* 5**,** 6971-6980.

30. Liu, Y., Li, J., Qiu, X. & Burda, C. 2007. Bactericidal activity of nitrogen-doped metal oxide nanocatalysts and the influence of bacterial extracellular polymeric substances (EPS). *J Photochem Photobiol A: Chem,* 190**,** 94-100.

31. Ma, R., Levard, C., Marinakos, S. M., Cheng, Y., Liu, J., Michel, F. M., Brown, G. E. & Lowry, G. V. 2012. Size-controlled dissolution of organic-coated silver nanoparticles. *Environ Sci Technol,* 46**,** 752-759.

32. Miao, A. J., Schwehr, K. A., Xu, C., Zhang, S. J., Luo, Z., Quigg, A. & Santschi, P. H. 2009. The algal toxicity of silver engineered nanoparticles and detoxification by exopolymeric substances. *Environ. Pollut.,* 157(11)**,** 3034-41.

33. Moreau, J., Weber, P., Michael, C., Martin, M., Gilbert, B., Hutcheon, I. & Banfield, J. F. 2007. Extracellular proteins limit the dispersal of biogenic nanoparticles. *Science,* 316**,** 1600-1603.

34. Mo Y, Wan R, Zhang Q.2012. Application of reverse transcription-PCR and real-time PCR in nanotoxicity research.*Methods Mol.Biol.926,* 99-112.

35. Napierska, D., Rabolli, V., Thomassen, L. C. J., Dinsdale, D., Princen, C., Gonzalez, L., Poels, K. L. C., Kirsch-Volders, M., Lison, D., Martens, J. A. & Hoet, P. H. 2012. Oxidative stress induced by pure and iron-doped amorphous silica nanoparticles in subtoxic conditions. *Chem Res. Toxicol.* 25(4):828-37.

36. Omoike, A. & Chorover, J. 2006. adsorption of geothite to extracellular polymeric substances from *Bacillus subtilis*. *Geochem.Cosmochim.Acta,* 70**,** 827-838.

37. Pelletier, D. A., Suresh, A. K., Holton, G. A., McKeown, C. K., Wang, W., Gu, B., Mortensen, N. P., Allison, D. P., Joy, D. C., Allison, M. R., Brown, S. D., Phelps, T. J. & Doktycz, M. J. 2010. Effects of engineered cerium oxide nanoparticles on bacterial growth and viability. *Appl Environ Microbiol.,* 76**,** 7981–7989.

38. Peulen, T. O. & Wilkinson, K. J. 2011. Diffusion of nanoparticles in a biofilm. *Environ. Sci Technol.,* 45**,** 3367-3373.

39. Sahle-Demessie, E. & Tadesse, H. 2011. Kinetics and equilibrium adsorption of nano-TiO2 particles on synthetic biofilm. *Surface Science,* 605**,** 1177-1184.

40. Sondi, I. & Sondi, B. S. 2004. Silver nanoparticles as antimicrobial agent: a case study on *E. coli* as a model for Gram-negative bacteria. *J.Colloid. Interphase Sci.,* 275**,** 177-182.

41. Tong, Z., Bischoff.M, Nies, L., Applegate, B. & Turco, R. F. 2007. Impact of Fullerene (C60) on a Soil Microbial Community. *Environ. Sci.Technol.,* 41**,** 2985-2991.

42. Unrine, J. M., Colman, B., Bone, A. J., Gondikas, A. P. & Matson, C. W. 2012. Biotic and abiotic interactions in aquatic microcosms determine fate and toxicity of Ag nanoparticles. Part 1. aggregation and dissolution. *Environ. Sci.Technol.,* 46**,** 6915–6924.

43. Wirth, S. M., Lowry, G. V. & Tilton, R. D. 2012. Natural organic matter alters biofilm tolerance to silver nanoparticles and dissolved silver. *Environ. Sci.Technol.,* 46 (22)**,** 12687–12696.

44. Xia, T., Kovochich, M., Liong, M., Mädler, L., Gilbert, B., Shi, H., Yeh, J. I., Zink, J. I. & Nel, A. E. 2008. Comparison of the mechanism of toxicity of

zinc oxide and cerium oxide nanoparticles based on dissolution and oxidative stress properties. *ACS Nano,* 2**,** 2121-2134.

45. Xiu , Z. M., Zhang, Q. B., Puppala, H. L., Colvin, V. L. & Alvarez, P. J. 2012. Negligible particle-specific antibacterial activity of silver nanoparticles. *Nano Letters,* 12(8)**,** 4271-5.

46. Ya-Nan, C., Mingyi, Z., Lin, X., Jun, Z. & Gengmei, X. 2012. The toxic effects and mechanisms of CuO and ZnO nanoparticles. *Materials,* 5**,** 2850-2871.

47. Yuan, G., Joshua P, S. & Holden, P. A. 2011. Evidence for negative effects of TiO2 and ZnO nanoparticles on soil bacterial communities. *Environ. Sci. Technol.,* 45**,** 1659–1664.

Appendix

1.Statistical analysis for the data presented in chapter 2 and 4 respectively using Annova and Tukey test (HSD).

Tukey analysis for chapter 2

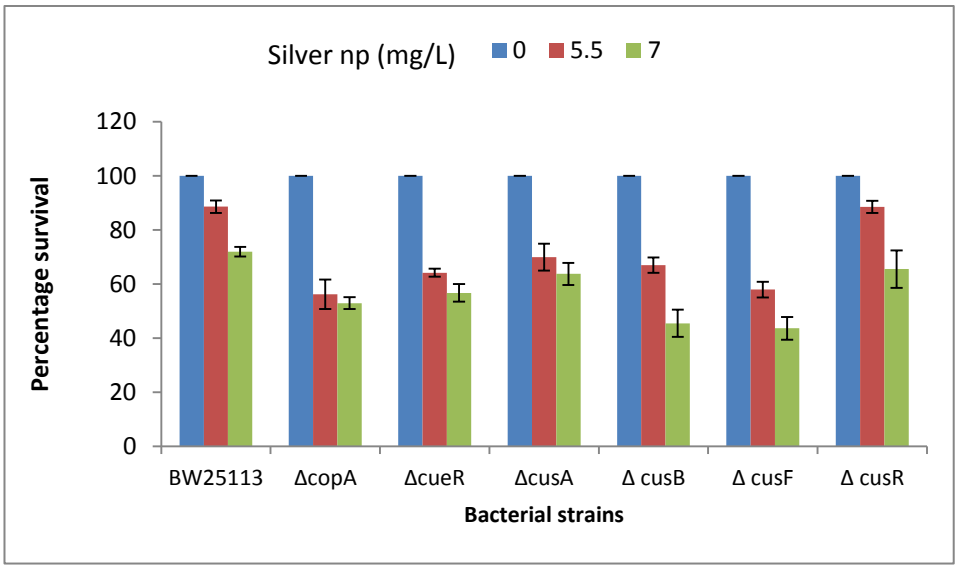

Figure 2-2b in chapter 2 as shown on page 97

The post hoc test analysis on the percentage survival was conducted after Annova. Different letter indicate that's the associated treatments are statistically different $p<0.05$

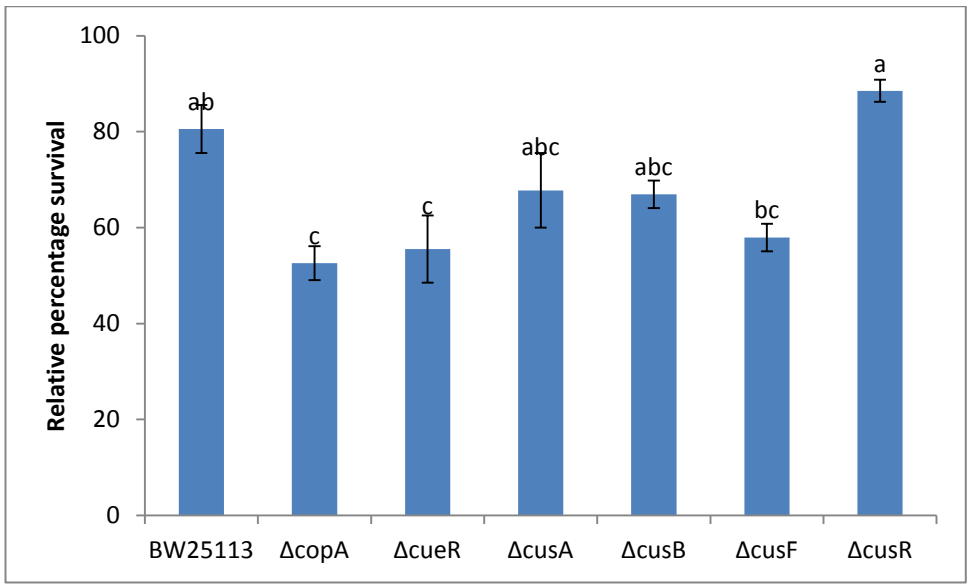

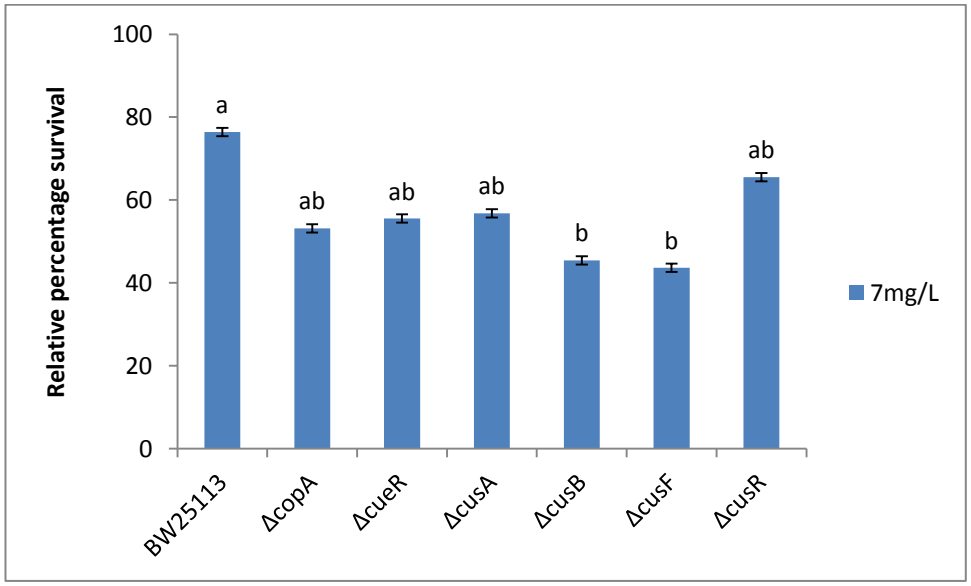

Tukey analysis at 5.5 and 7 mg/L Ag np exposure

Figure: 2-3b in chapter 2

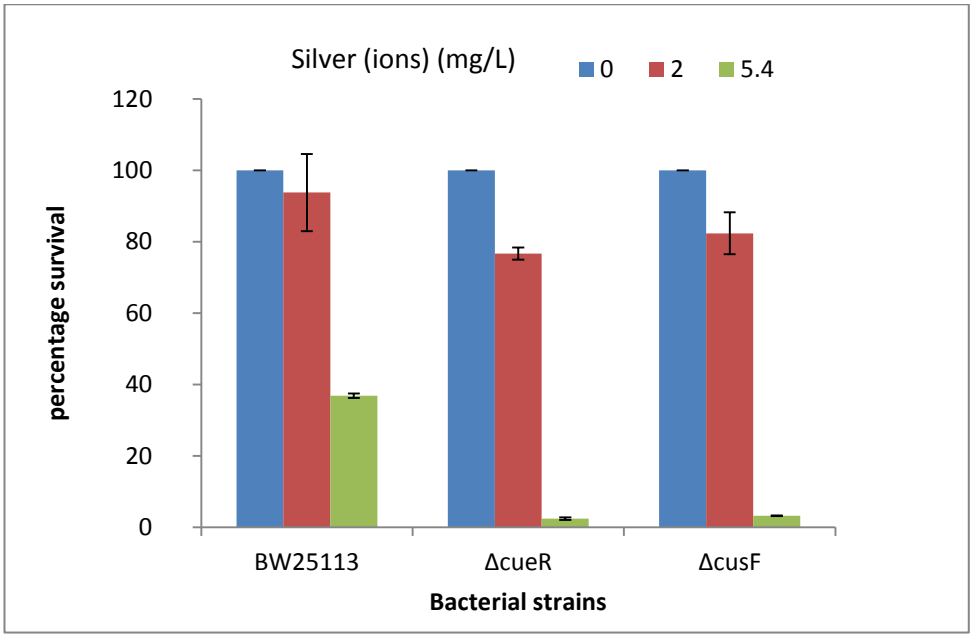

Annova analysis on the data at 2 mg/L showed $p>0.05$. However at 5.4 mg/L silver ions, $p<0.05$ hence Post Hoc Tukey test analysis (below) was conducted

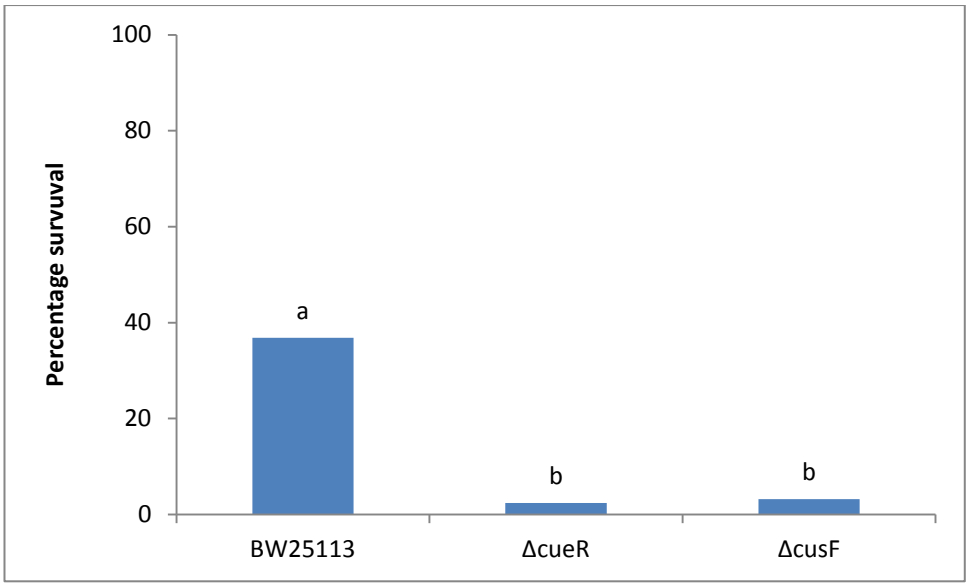

Figure 2-9 b in chapter 2

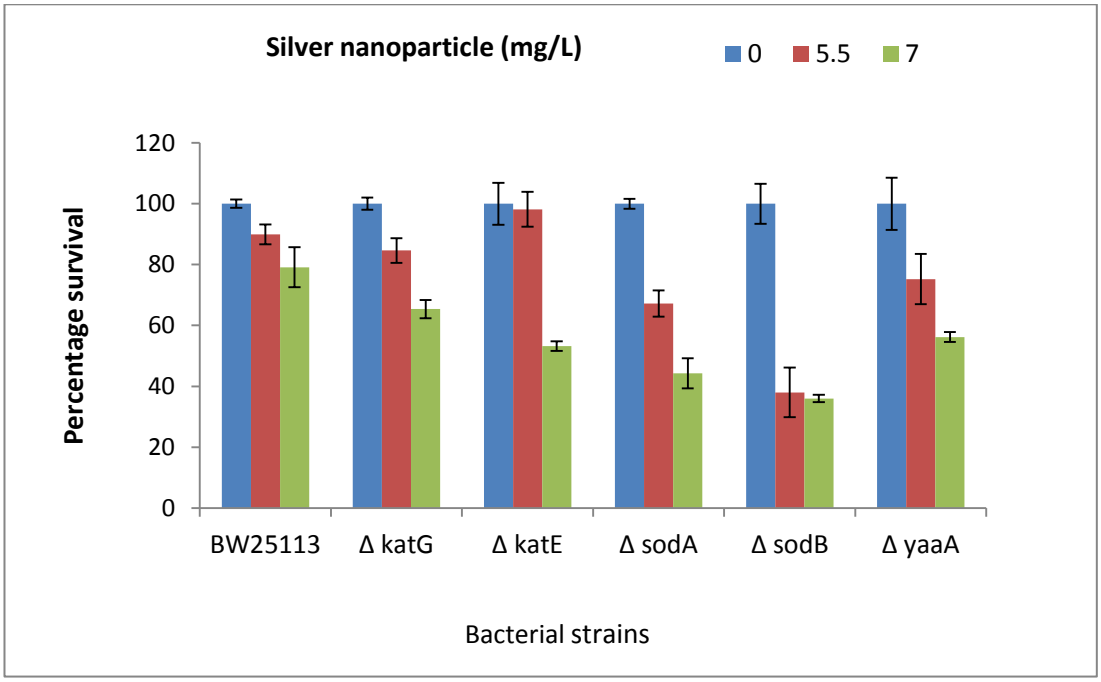

Now the Annova and Tukey analysis were conducted on the above

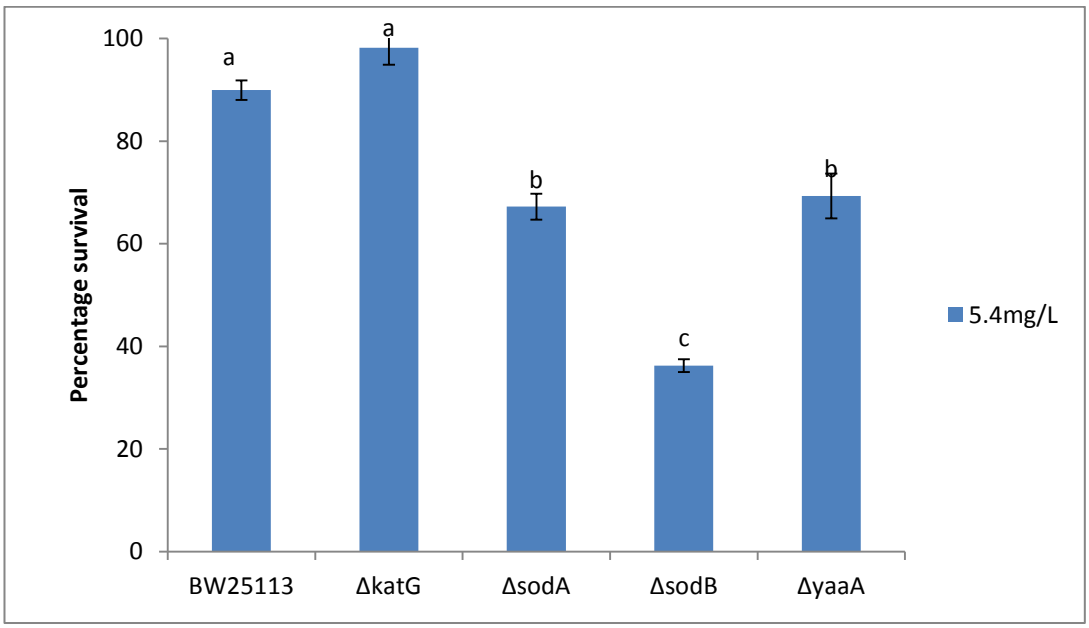

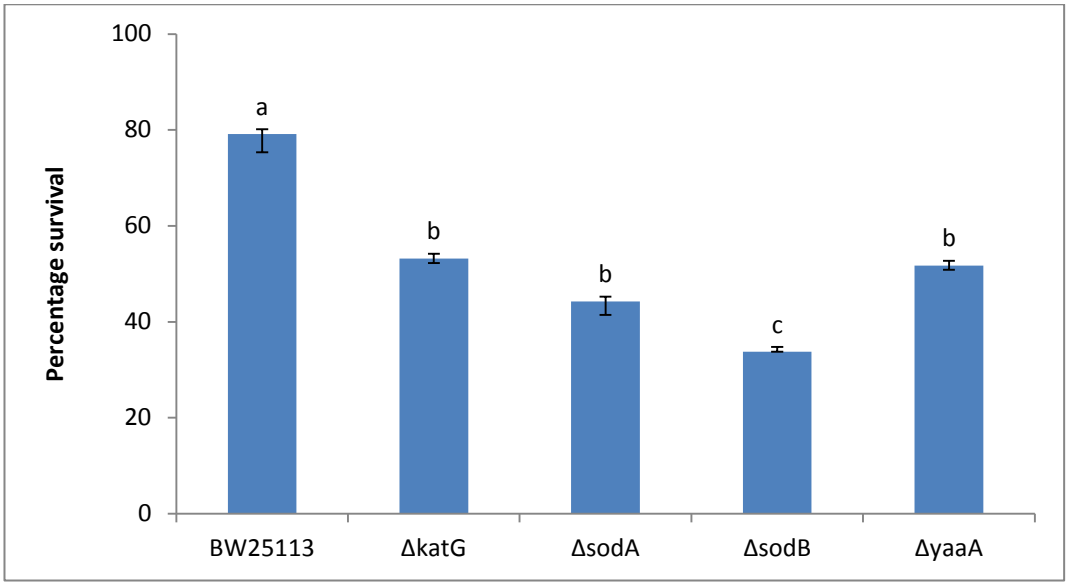

Figure 2-9c in chapter 2

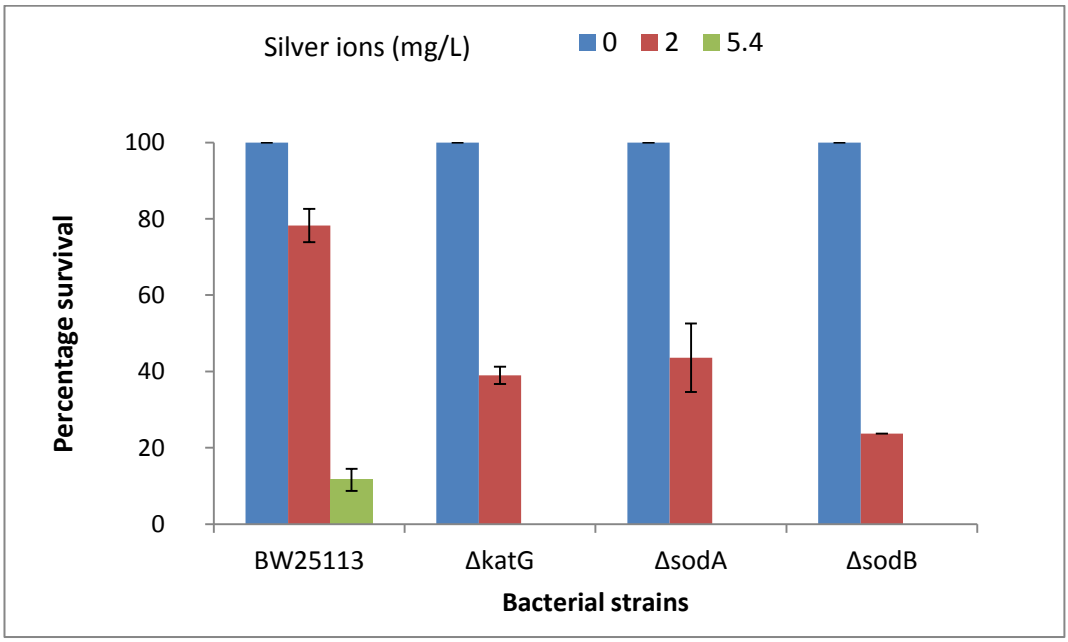

Tukey and Annova analysis below

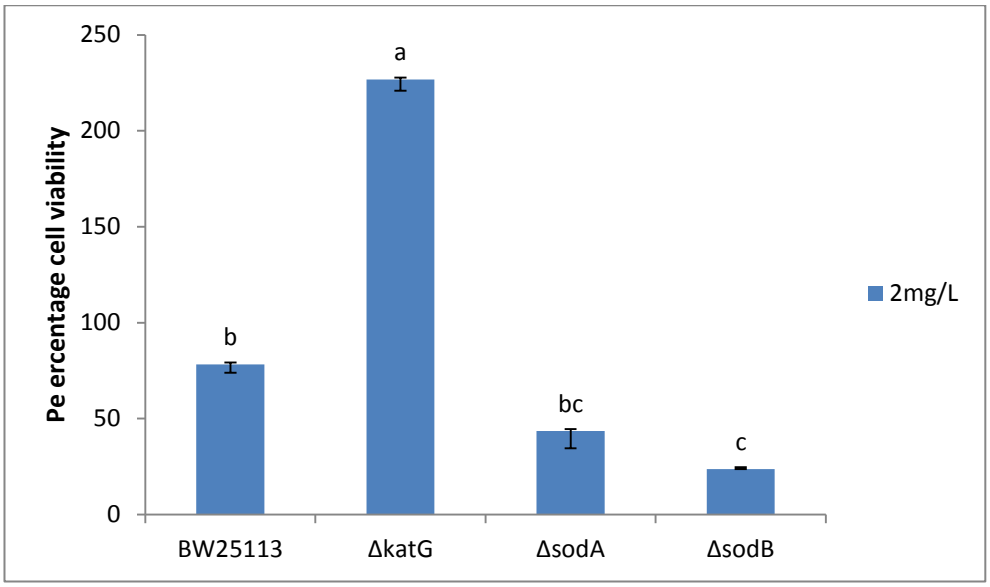

Figure 2-11 in chapter 2

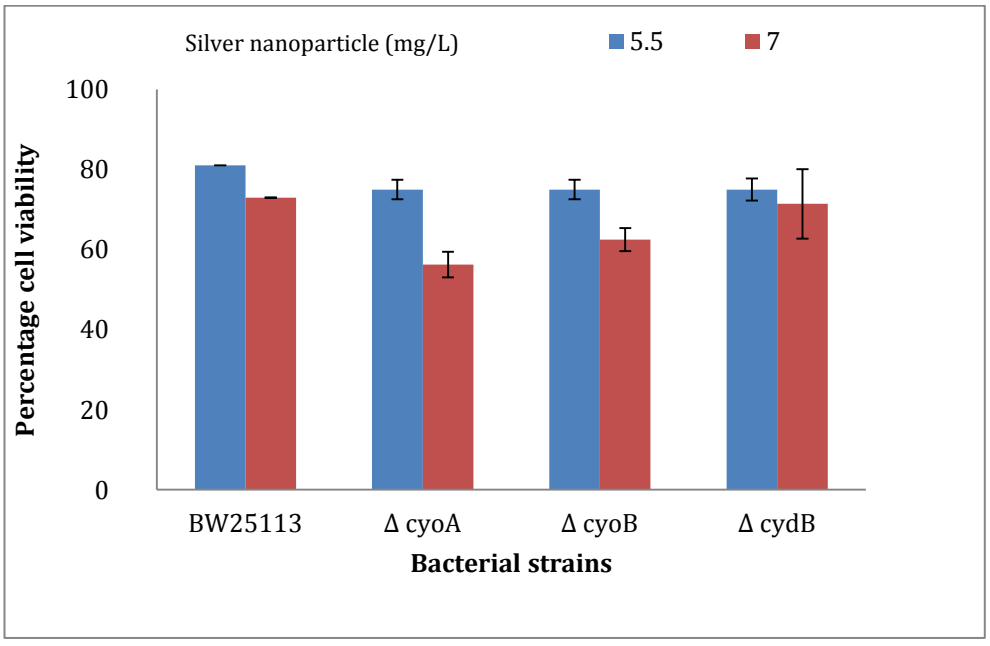

Annova and tukey on above graph

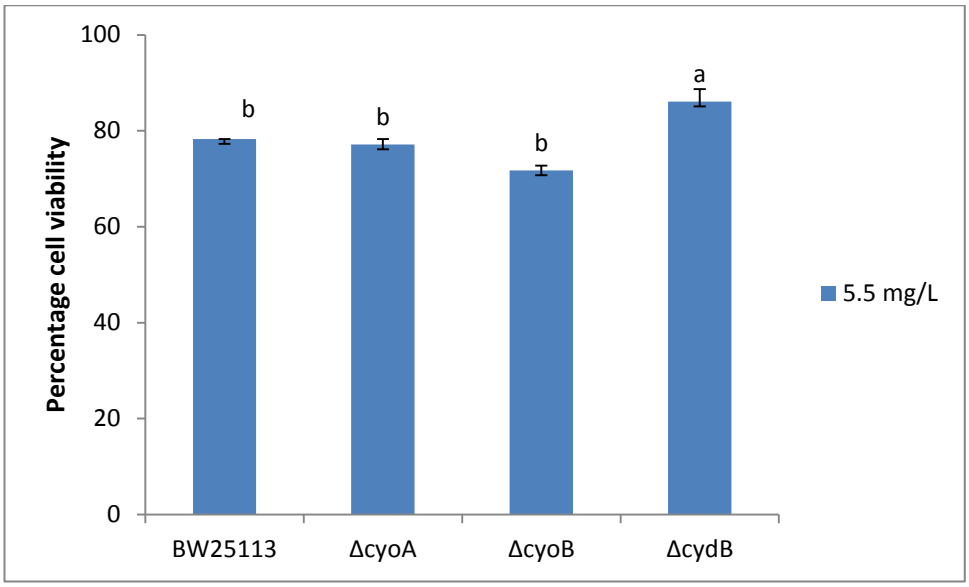
100
80
60
40
20
0
Percentage cell viability
b
b
b
a
BW25113
ΔcyoA
ΔcyoB
ΔcydB
5.5 mg/L

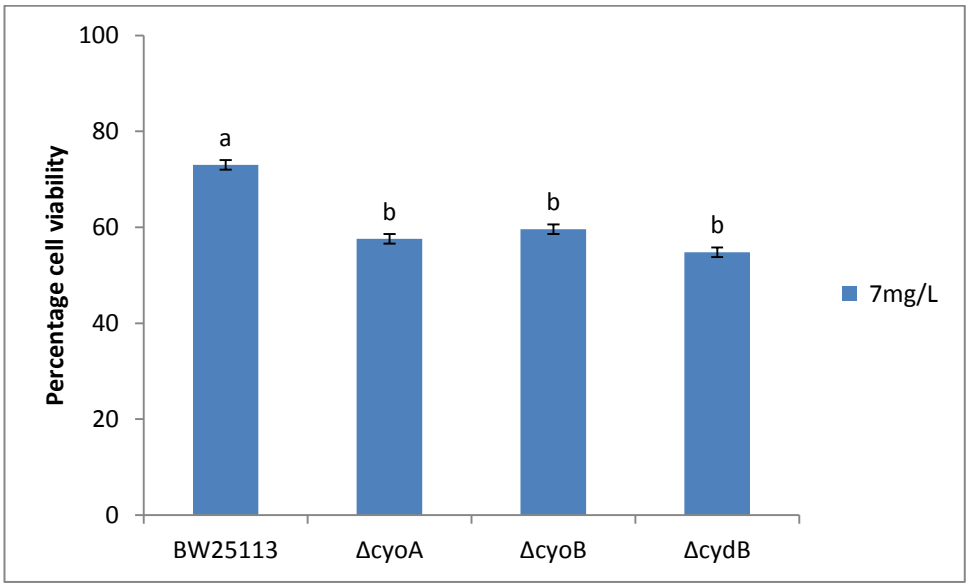
100
80
60
40
20
0
Percentage cell viability
a
b
b
b
BW25113
ΔcyoA
ΔcyoB
ΔcydB
7mg/L

Tukey analysis for Figure 2-12 in chapter 2

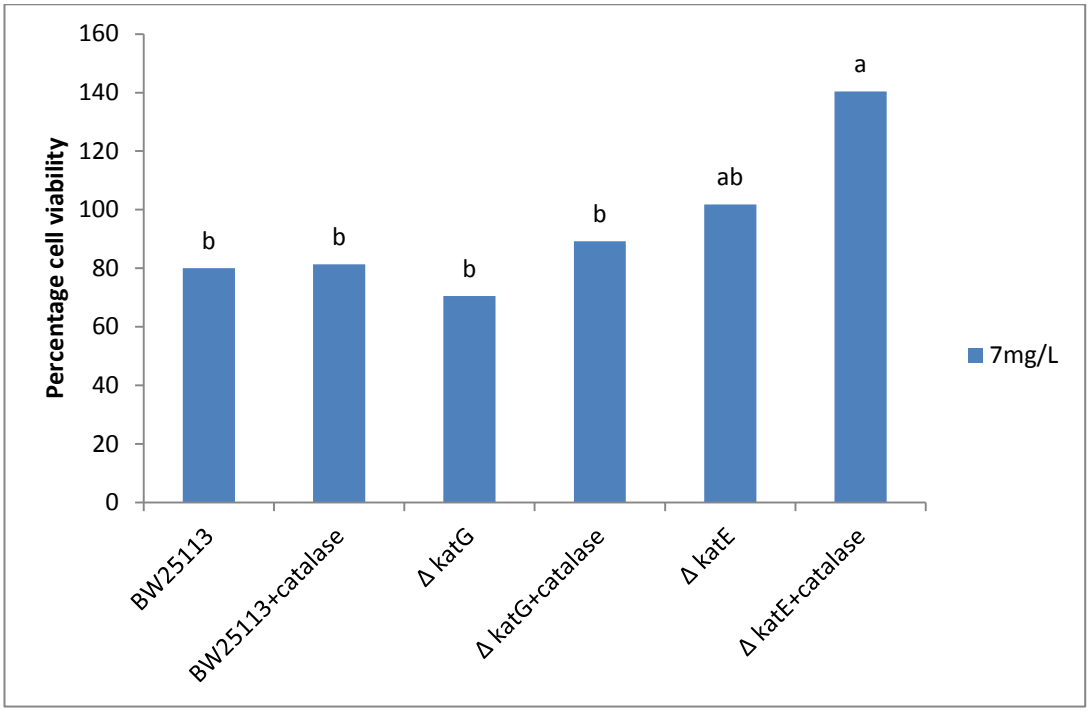

Tukey analysis for Figure 2-4 (a-d)

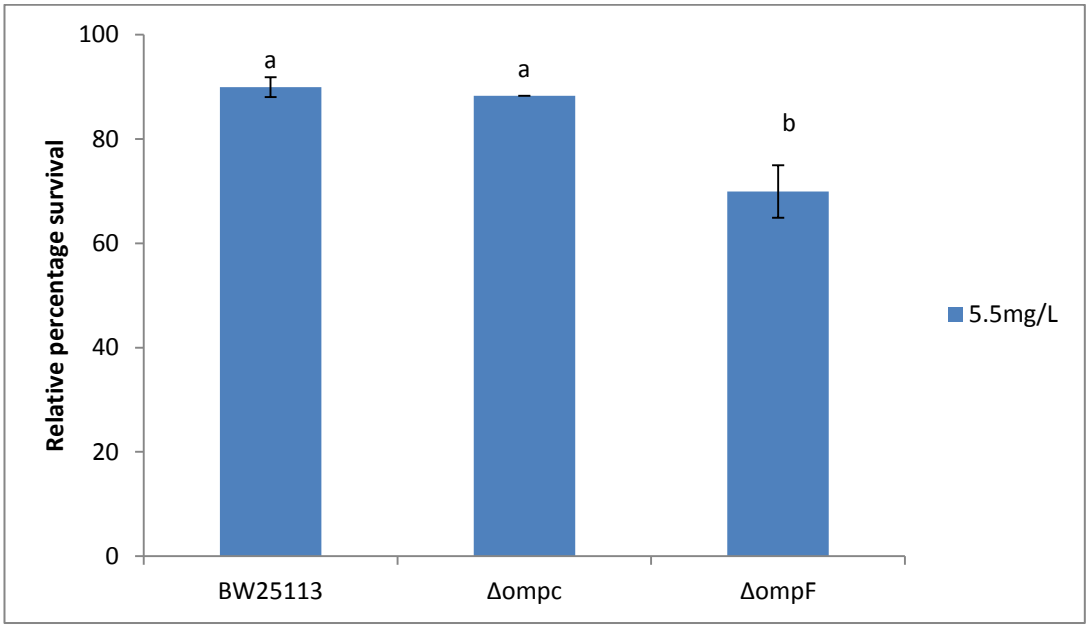

Porins And silver ions at low concentration

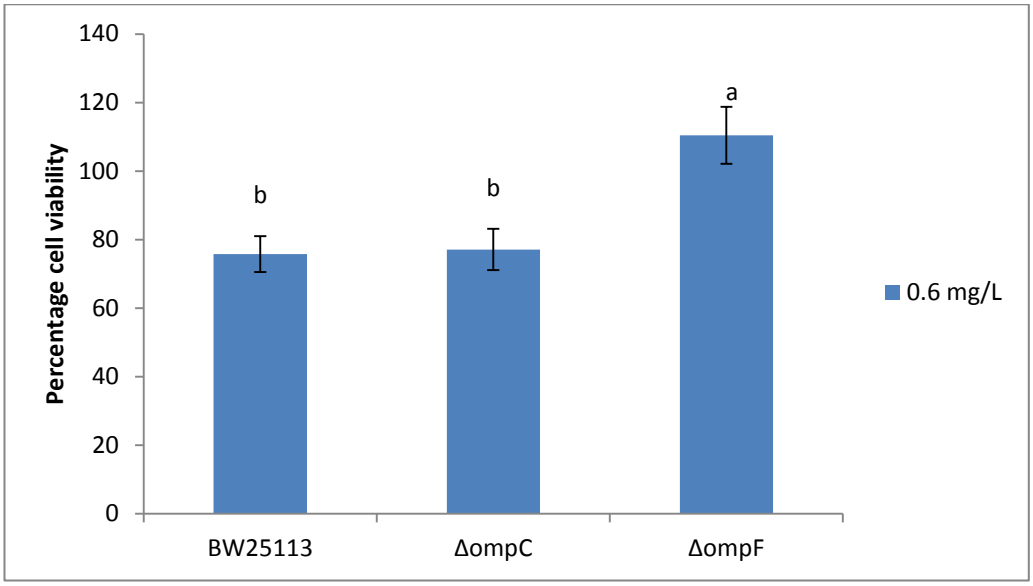

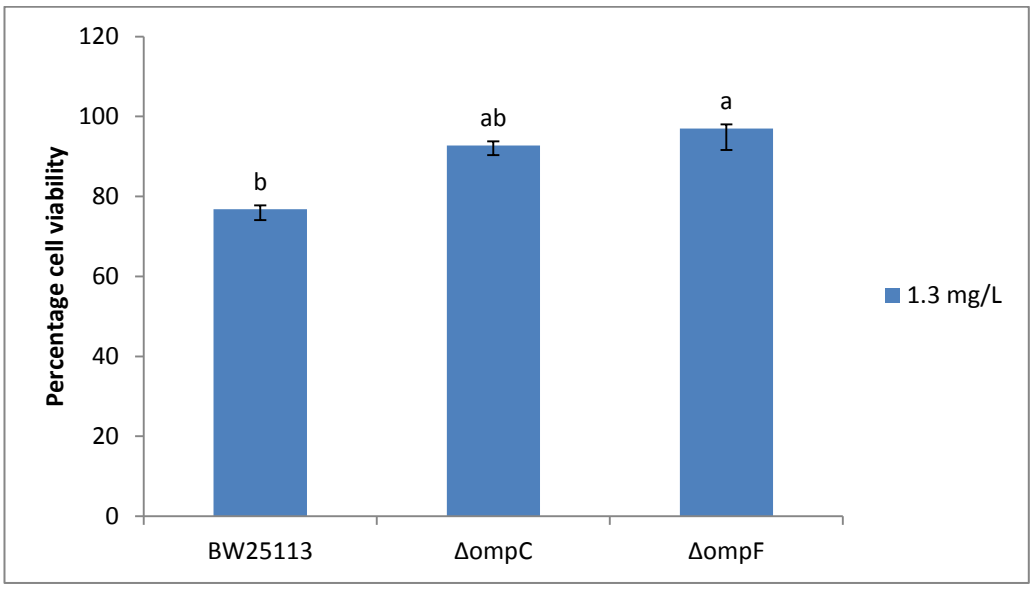

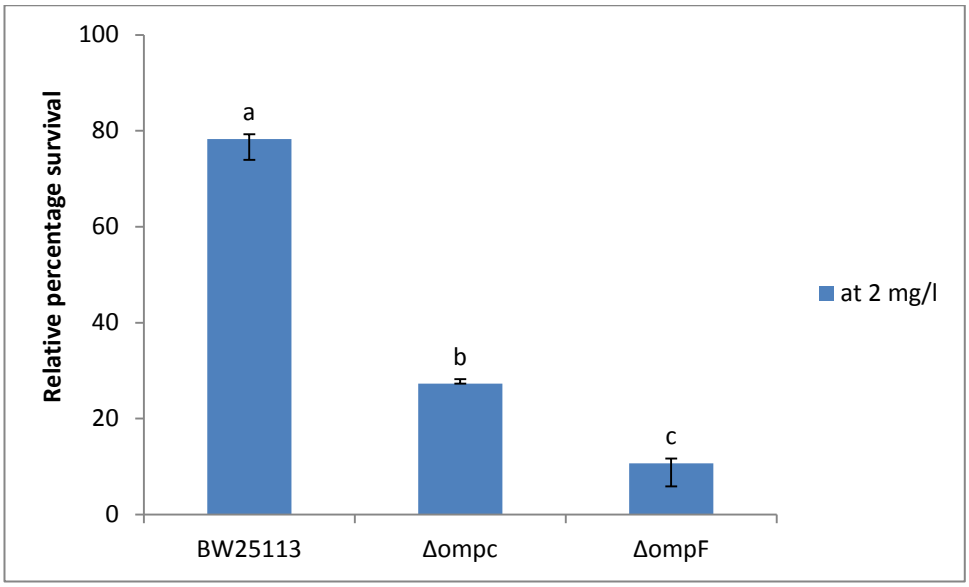
Relative percentage survival
100
80
60
40
20
0
a
b
c
BW25113
Δompc
ΔompF
at 2 mg/l

Tukey analysis for chapter 4

1. Impact of grain size and protective role of EPS

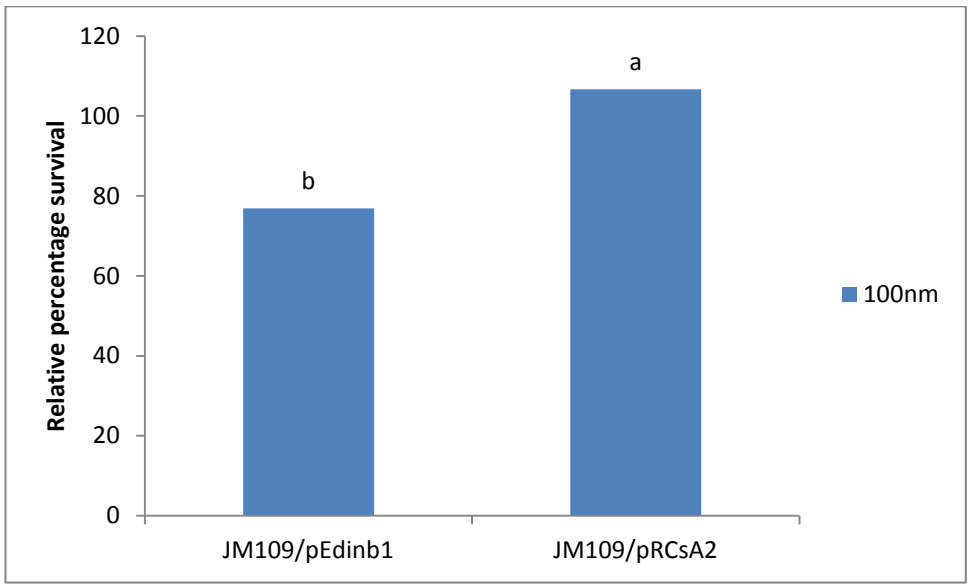

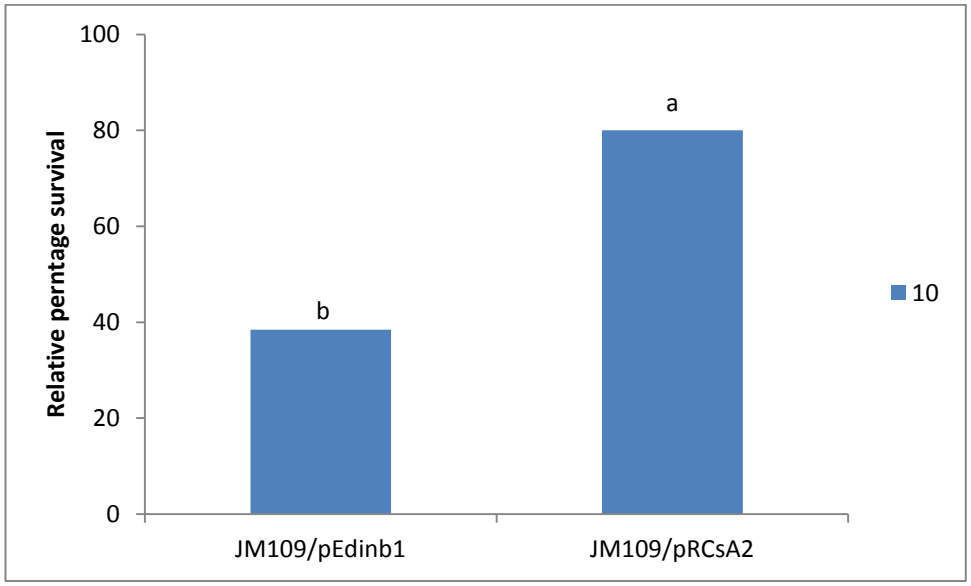

Impact of addition of xanthan

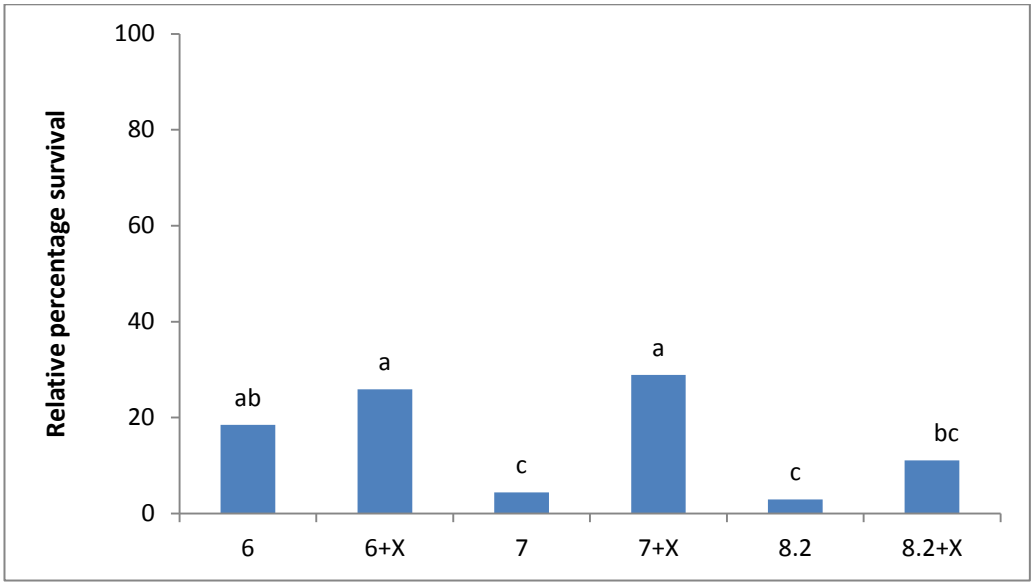

Adding EPS

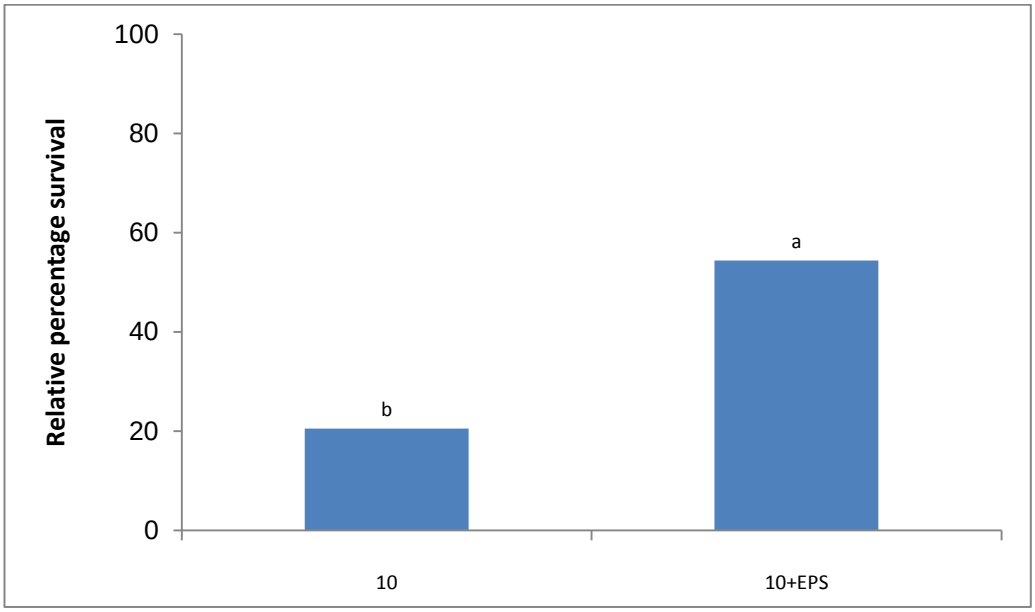

II. Experiment files for XAS analysis of the microcosm samples (Chapter5)

13/04/2013 18:07 <DIR> .

13/04/2013 18:07 <DIR>

10/10/2012 11:04 39,298 70163_Ag_nanoparticles_test_1.dat

10/10/2012 11:08 39,297 70164_Ag_nanoparticles_test_1.dat

10/10/2012 11:18 81,768 70165_Ag_nanoparticles_test_1.dat

10/10/2012 11:21 81,798 70166_Ag_nanoparticles_test_2.dat

10/10/2012 11:25 81,778 70167_Ag_nanoparticles_test_3.dat

10/10/2012 11:29 81,765 70168_Ag_nanoparticles_test_4.dat

10/10/2012 11:33 81,769 70169_Ag_nanoparticles_test_5.dat

10/10/2012 11:41 81,726 70170_Ag_nanoparticles_test_1.dat

10/10/2012 11:45 81,396 70171_Ag_nanoparticles_test_2.dat

10/10/2012 11:48 81,422 70172_Ag_nanoparticles_test_3.dat

10/10/2012 11:52 81,236 70173_Ag_nanoparticles_test_4.dat

10/10/2012 11:56 81,140 70174_Ag_nanoparticles_test_5.dat

10/10/2012 12:18 80,905 70179_Ag1000ppm microcosm test_1.dat

10/10/2012 12:26 80,203 70183_Ag1000ppm microcosm test_1.dat

10/10/2012 12:27 80,183 70184_Ag1000ppm microcosm test_1.dat

10/10/2012 12:31 82,681 70185_Ag1000ppm microcosm test_1.dat

10/10/2012 12:55 211,727 70189_Ag1000ppm microcosm test_1.dat

10/10/2012 13:12 213,735 70190_Ag1000ppm microcosm test_1.dat

10/10/2012 13:21 213,615 70191_Ag1000ppm microcosm test_2.dat

10/10/2012 13:30 213,505 70192_Ag1000ppm microcosm test_3.dat

10/10/2012 13:40 213,353 70194_Ag1000ppm microcosm test_4.dat

10/10/2012 13:49 213,205 70195_Ag1000ppm microcosm test_5.dat

10/10/2012 13:58 213,097 70196_Ag1000ppm microcosm test_6.dat

10/10/2012 14:07 213,061 70197_Ag1000ppm microcosm test_7.dat

10/10/2012 14:16 213,041 70198_Ag1000ppm microcosm test_8.dat

10/10/2012 14:25 213,006 70199_Ag1000ppm microcosm test_9.dat

10/10/2012 14:35 212,947 70200_Ag1000ppm microcosm test_10.dat

10/10/2012 17:47 39,221 70204_Ag2Sstd_1.dat

10/10/2012 17:55 78,169 70205_Ag2Sstd_1.dat

10/10/2012 18:07 80,296 70207_Ag2Sstd_1.dat

10/10/2012 18:14 80,283 70208_Ag2Sstd_2.dat

10/10/2012 18:21 80,278 70209_Ag2Sstd_1.dat

10/10/2012 18:36 124,865 70210_Ag1000ppmbulk_1.dat

10/10/2012 18:42 124,878 70211_Ag1000ppmbulk_2.dat

10/10/2012 18:47 124,872 70212_Ag1000ppmbulk_3.dat

10/10/2012 18:52 124,907 70213_Ag1000ppmbulk_4.dat

10/10/2012 18:58 124,911 70214_Ag1000ppmbulk_5.dat

10/10/2012 19:03 124,924 70215_Ag1000ppmbulk_6.dat

10/10/2012 19:09 124,937 70216_Ag1000ppmbulk_7.dat

10/10/2012 19:14 124,948 70217_Ag1000ppmbulk_8.dat

10/10/2012 19:20 124,945 70218_Ag1000ppmbulk_9.dat

10/10/2012 19:25 124,950 70219_Ag1000ppmbulk_10.dat

10/10/2012 19:31 126,046 70220_Ag1000ppmtoplayer_1.dat

10/10/2012 19:36 126,045 70221_Ag1000ppmtoplayer_2.dat

10/10/2012 19:41 126,032 70222_Ag1000ppmtoplayer_3.dat

10/10/2012 19:47 126,040 70223_Ag1000ppmtoplayer_4.dat

10/10/2012 19:52 126,022 70224_Ag1000ppmtoplayer_5.dat

10/10/2012 19:58 126,014 70225_Ag1000ppmtoplayer_6.dat

10/10/2012 20:03 126,032 70226_Ag1000ppmtoplayer_7.dat

10/10/2012 20:09 126,005 70227_Ag1000ppmtoplayer_8.dat

10/10/2012 20:14 126,000 70228_Ag1000ppmtoplayer_9.dat

10/10/2012 20:20 125,989 70229_Ag1000ppmtoplayer_10.dat

10/10/2012 20:25 124,850 70230_Ag1000ppmbottom_1.dat

10/10/2012 20:30 124,835 70231_Ag1000ppmbottom_2.dat

10/10/2012 20:36 124,836 70232_Ag1000ppmbottom_3.dat

10/10/2012 20:41 124,825 70233_Ag1000ppmbottom_4.dat

10/10/2012 20:47 124,840 70234_Ag1000ppmbottom_5.dat

10/10/2012 20:52 124,844 70235_Ag1000ppmbottom_6.dat

10/10/2012 20:58 124,842 70236_Ag1000ppmbottom_7.dat

10/10/2012 21:03 124,865 70237_Ag1000ppmbottom_8.dat

10/10/2012 21:09 124,860 70238_Ag1000ppmbottom_9.dat

10/10/2012 21:14 124,873 70239_Ag1000ppmbottom_10.dat

10/10/2012 21:19 127,842 70240_Ag1000ppmsterile_1.dat

10/10/2012 21:25 127,837 70241_Ag1000ppmsterile_2.dat

10/10/2012 21:44 125,030 70242_Ag1000ppmt0_1.dat

10/10/2012 21:49 125,041 70243_Ag1000ppmt0_2.dat

10/10/2012 21:55 125,037 70244_Ag1000ppmt0_3.dat

10/10/2012 22:00 125,024 70245_Ag1000ppmt0_4.dat

10/10/2012 22:06 125,056 70246_Ag1000ppmt0_5.dat

10/10/2012 22:11 125,039 70247_Ag1000ppmt0_6.dat

10/10/2012 22:17 125,068 70248_Ag1000ppmsterile_1.dat

10/10/2012 22:22 125,041 70249_Ag1000ppmsterile_2.dat

10/10/2012 22:27 125,065 70250_Ag1000ppmsterile_3.dat

10/10/2012 22:33 125,064 70251_Ag1000ppmsterile_4.dat

10/10/2012 22:38 125,034 70252_Ag1000ppmt0_1.dat

10/10/2012 22:44 125,032 70253_Ag1000ppmt0_2.dat

10/10/2012 22:49 125,019 70254_Ag1000ppmt0_3.dat

10/10/2012 22:55 125,016 70255_Ag1000ppmt0_4.dat

10/10/2012 23:00 125,011 70256_Ag1000ppmt0_5.dat

10/10/2012 23:06 125,006 70257_Ag1000ppmt0_6.dat

10/10/2012 23:11 125,004 70258_Ag1000ppmt0_7.dat

10/10/2012 23:16 124,971 70259_Ag1000ppmt0_8.dat

10/10/2012 23:22 124,991 70260_Ag1000ppmt0_9.dat

10/10/2012 23:27 124,992 70261_Ag1000ppmt0_10.dat

11/10/2012 00:15 125,205 70262_Ag2Sstd_1.dat

11/10/2012 00:21 124,927 70263_Ag2Sstd_2.dat

11/10/2012 00:27 125,014 70264_Ag500top_1.dat

11/10/2012 00:33 125,009 70265_Ag500top_2.dat

11/10/2012 00:38 124,999 70266_Ag500top_3.dat

11/10/2012 00:44 125,006 70267_Ag500top_4.dat

11/10/2012 00:49 125,034 70268_Ag500top_5.dat

11/10/2012 00:55 125,035 70269_Ag500top_6.dat

11/10/2012 01:00 125,022 70270_Ag500top_1.dat

11/10/2012 01:05 125,024 70271_Ag500top_2.dat

11/10/2012 01:11 125,011 70272_Ag500top_3.dat

11/10/2012 01:16 125,012 70273_Ag500top_4.dat

11/10/2012 01:22 125,015 70274_Ag500top_5.dat

11/10/2012 01:27 125,017 70275_Ag500top_6.dat

11/10/2012 01:33 125,005 70276_Ag500top_7.dat

11/10/2012 01:38 125,015 70277_Ag500top_8.dat

11/10/2012 01:44 125,012 70278_Ag500top_9.dat

11/10/2012 01:49 125,009 70279_Ag500top_10.dat

11/10/2012 01:58 125,007 70280_Ag500top_11.dat

11/10/2012 02:03 125,023 70281_Ag500top_12.dat

11/10/2012 02:09 125,018 70282_Ag500top_13.dat

11/10/2012 02:14 125,016 70283_Ag500top_14.dat

11/10/2012 02:20 125,006 70284_Ag500top_15.dat

11/10/2012 02:25 124,979 70285_Ag500bulk_1.dat

11/10/2012 02:31 124,970 70286_Ag500bulk_2.dat

11/10/2012 02:36 124,972 70287_Ag500bulk_3.dat

11/10/2012 02:41 124,969 70288_Ag500bulk_4.dat

11/10/2012 02:47 124,958 70289_Ag500bulk_5.dat

11/10/2012 02:52 124,957 70290_Ag500bulk_6.dat

11/10/2012 02:58 124,953 70291_Ag500bulk_7.dat

11/10/2012 03:03 124,935 70292_Ag500bulk_8.dat

11/10/2012 03:09 124,937 70293_Ag500bulk_9.dat

11/10/2012 03:14 124,919 70294_Ag500bulk_10.dat

11/10/2012 03:19 124,914 70295_Ag500bulk_11.dat

11/10/2012 03:25 124,906 70296_Ag500bulk_12.dat

11/10/2012 03:30 124,906 70297_Ag500bulk_13.dat

11/10/2012 03:36 124,929 70298_Ag500bulk_14.dat

11/10/2012 03:41 124,915 70299_Ag500bulk_15.dat

11/10/2012 03:47 123,693 70300_Ag500bottom_1.dat

11/10/2012 03:52 123,791 70301_Ag500bottom_2.dat

11/10/2012 03:58 123,690 70302_Ag500bottom_3.dat

11/10/2012 04:03 123,692 70303_Ag500bottom_4.dat

11/10/2012 04:09 123,779 70304_Ag500bottom_5.dat

11/10/2012 04:14 123,670 70305_Ag500bottom_6.dat

11/10/2012 04:19 123,646 70306_Ag500bottom_7.dat

11/10/2012 04:25 123,661 70307_Ag500bottom_8.dat

11/10/2012 04:30 123,817 70308_Ag500bottom_9.dat

11/10/2012 04:36 123,462 70309_Ag500bottom_10.dat

11/10/2012 04:41 123,341 70310_Ag500bottom_11.dat

11/10/2012 04:47 123,305 70311_Ag500bottom_12.dat

11/10/2012 04:52 123,184 70312_Ag500bottom_13.dat

11/10/2012 04:57 123,142 70313_Ag500bottom_14.dat

11/10/2012 05:03 123,074 70314_Ag500bottom_15.dat

11/10/2012 05:08 124,927 70315_Ag500airdry_1.dat

11/10/2012 05:14 124,930 70316_Ag500airdry_2.dat

11/10/2012 05:19 124,903 70317_Ag500airdry_3.dat

11/10/2012 05:25 124,882 70318_Ag500airdry_4.dat

11/10/2012 05:30 124,865 70319_Ag500airdry_5.dat

11/10/2012 05:36 124,869 70320_Ag500airdry_6.dat

11/10/2012 05:41 124,825 70321_Ag500airdry_7.dat

11/10/2012 05:46 124,873 70322_Ag500airdry_8.dat

11/10/2012 05:52 124,839 70323_Ag500airdry_9.dat

11/10/2012 05:57 124,887 70324_Ag500airdry_10.dat

11/10/2012 06:03 124,856 70325_Ag500airdry_11.dat

11/10/2012 06:08 124,849 70326_Ag500airdry_12.dat

11/10/2012 06:14 124,646 70327_Ag500airdry_13.dat

11/10/2012 06:19 124,631 70328_Ag500airdry_14.dat

11/10/2012 06:25 124,474 70329_Ag500airdry_15.dat

11/10/2012 06:30 124,826 70330_Ag500t0bulk_1.dat

11/10/2012 06:36 124,793 70331_Ag500t0bulk_2.dat

11/10/2012 06:41 124,776 70332_Ag500t0bulk_3.dat

11/10/2012 06:46 124,721 70333_Ag500t0bulk_4.dat

11/10/2012 06:52 124,448 70334_Ag500t0bulk_5.dat

11/10/2012 06:57 124,404 70335_Ag500t0bulk_6.dat

11/10/2012 07:03 124,248 70336_Ag500t0bulk_7.dat

11/10/2012 07:08 124,360 70337_Ag500t0bulk_8.dat

11/10/2012 07:14 124,180 70338_Ag500t0bulk_9.dat

11/10/2012 07:19 124,336 70339_Ag500t0bulk_10.dat

11/10/2012 07:24 124,253 70340_Ag500t0bulk_11.dat

11/10/2012 07:30 124,188 70341_Ag500t0bulk_12.dat

11/10/2012 07:35 124,169 70342_Ag500t0bulk_13.dat

11/10/2012 07:41 124,149 70343_Ag500t0bulk_14.dat

11/10/2012 07:46 124,102 70344_Ag500t0bulk_15.dat

11/10/2012 07:52 124,000 70345_Ag500sterile_1.dat

11/10/2012 07:57 123,934 70346_Ag500sterile_2.dat

11/10/2012 08:03 124,056 70347_Ag500sterile_3.dat

11/10/2012 08:08 123,914 70348_Ag500sterile_4.dat

11/10/2012 08:13 123,789 70349_Ag500sterile_5.dat

11/10/2012 08:19 123,685 70350_Ag500sterile_6.dat

11/10/2012 08:24 123,688 70351_Ag500sterile_7.dat

11/10/2012 08:30 123,632 70352_Ag500sterile_8.dat

11/10/2012 08:35 123,621 70353_Ag500sterile_9.dat

11/10/2012 08:41 123,494 70354_Ag500sterile_10.dat

11/10/2012 08:46 123,788 70355_Ag500sterile_11.dat

11/10/2012 08:52 123,702 70356_Ag500sterile_12.dat

11/10/2012 08:57 123,409 70357_Ag500sterile_13.dat

11/10/2012 09:02 123,517 70358_Ag500sterile_14.dat

11/10/2012 09:08 123,343 70359_Ag500sterile_15.dat

11/10/2012 11:27 352,488 70365_Zn reference test_1.dat

11/10/2012 11:29 356,850 70366_Zn reference test_1.dat

11/10/2012 12:00 116,338 70369_ZnS_1.dat

11/10/2012 12:06 116,337 70370_ZnS_2.dat

11/10/2012 12:12 116,340 70371_ZnS_3.dat

11/10/2012 12:19 116,337 70372_ZnS_4.dat

11/10/2012 12:25 116,339 70373_ZnS_5.dat

11/10/2012 12:50 116,401 70374_ZnO_1.dat

11/10/2012 12:56 116,402 70375_ZnO_2.dat

11/10/2012 13:02 116,403 70376_ZnO_3.dat

11/10/2012 13:08 116,403 70377_ZnO_4.dat

11/10/2012 13:15 93,657 70378_ZnO_5.dat

11/10/2012 13:21 293,698 70379_ZnO_500ppm_dried_1.dat

11/10/2012 13:27 293,697 70380_ZnO_500ppm_dried_2.dat

11/10/2012 13:33 293,698 70381_ZnO_500ppm_dried_3.dat

11/10/2012 13:39 293,699 70382_ZnO_500ppm_dried_4.dat

11/10/2012 13:46 293,704 70383_ZnO_500ppm_dried_5.dat

11/10/2012 13:52 293,702 70384_ZnO_500ppm_dried_6.dat

11/10/2012 13:58 293,703 70385_ZnO_500ppm_dried_7.dat

11/10/2012 14:04 293,697 70386_ZnO_500ppm_dried_8.dat

11/10/2012 14:10 293,698 70387_ZnO_500ppm_dried_9.dat

11/10/2012 14:17 293,701 70388_ZnO_500ppm_dried_10.dat

11/10/2012 14:23 293,697 70389_ZnO_500ppm_dried_11.dat

11/10/2012 14:29 293,692 70390_ZnO_500ppm_dried_12.dat

11/10/2012 14:35 293,695 70391_ZnO_500ppm_dried_13.dat

11/10/2012 14:41 293,697 70392_ZnO_500ppm_dried_14.dat

11/10/2012 14:47 293,694 70393_ZnO_500ppm_dried_15.dat

11/10/2012 16:05 293,400 70395_ZnO500bulk_1.dat

11/10/2012 16:12 293,453 70396_ZnO500bulk_2.dat

11/10/2012 16:18 276,287 70397_ZnO500bulk_3.dat

11/10/2012 16:24 293,500 70398_ZnO500bulk_4.dat

11/10/2012 16:30 293,467 70399_ZnO500bulk_5.dat

11/10/2012 16:36 293,468 70400_ZnO500bulk_6.dat

11/10/2012 16:43 293,503 70401_ZnO500bulk_7.dat

11/10/2012 16:49 293,408 70402_ZnO500bulk_8.dat

11/10/2012 16:55 293,429 70403_ZnO500bulk_9.dat

11/10/2012 17:01 293,405 70404_ZnO500bulk_10.dat

11/10/2012 17:07 293,392 70405_ZnO500bulk_11.dat

11/10/2012 17:14 293,419 70406_ZnO500bulk_12.dat

11/10/2012 17:20 293,396 70407_ZnO500bulk_13.dat

11/10/2012 17:26 293,403 70408_ZnO500bulk_14.dat

11/10/2012 17:32 293,360 70409_ZnO500bulk_15.dat

11/10/2012 17:38 292,220 70410_ZnO500top_1.dat

11/10/2012 17:44 292,227 70411_ZnO500top_2.dat

11/10/2012 17:51 292,212 70412_ZnO500top_3.dat

11/10/2012 17:57 292,209 70413_ZnO500top_4.dat

11/10/2012 18:03 292,221 70414_ZnO500top_5.dat

11/10/2012 18:09 292,217 70415_ZnO500top_6.dat

11/10/2012 18:15 292,220 70416_ZnO500top_7.dat

11/10/2012 18:22 292,211 70417_ZnO500top_8.dat

11/10/2012 18:28 292,227 70418_ZnO500top_9.dat

11/10/2012 18:34 292,233 70419_ZnO500top_10.dat

11/10/2012 18:40 292,218 70420_ZnO500top_11.dat

11/10/2012 18:46 292,223 70421_ZnO500top_12.dat

11/10/2012 18:52 291,983 70422_ZnO500top_13.dat

11/10/2012 18:59 291,982 70423_ZnO500top_14.dat

11/10/2012 19:05 291,983 70424_ZnO500top_15.dat

11/10/2012 19:11 290,704 70425_ZnO500bottom_1.dat

11/10/2012 19:17 290,541 70426_ZnO500bottom_2.dat

11/10/2012 19:23 290,025 70427_ZnO500bottom_3.dat

11/10/2012 19:30 290,207 70428_ZnO500bottom_4.dat

11/10/2012 19:36 290,405 70429_ZnO500bottom_5.dat

11/10/2012 19:42 290,369 70430_ZnO500bottom_6.dat

11/10/2012 19:48 290,376 70431_ZnO500bottom_7.dat

11/10/2012 19:54 290,583 70432_ZnO500bottom_8.dat

11/10/2012 20:00 290,645 70433_ZnO500bottom_9.dat

11/10/2012 20:07 290,434 70434_ZnO500bottom_10.dat

11/10/2012 20:13 290,170 70435_ZnO500bottom_11.dat

11/10/2012 20:19 289,769 70436_ZnO500bottom_12.dat

11/10/2012 20:25 289,532 70437_ZnO500bottom_13.dat

11/10/2012 20:31 289,501 70438_ZnO500bottom_14.dat

11/10/2012 20:38 289,521 70439_ZnO500bottom_15.dat

11/10/2012 20:44 292,931 70440_ZnO500sterile_1.dat

11/10/2012 20:50 292,935 70441_ZnO500sterile_2.dat

11/10/2012 20:56 292,970 70442_ZnO500sterile_3.dat

11/10/2012 21:02 292,984 70443_ZnO500sterile_4.dat

11/10/2012 21:09 292,982 70444_ZnO500sterile_5.dat

11/10/2012 21:15 292,967 70445_ZnO500sterile_6.dat

11/10/2012 21:21 292,999 70446_ZnO500sterile_7.dat

11/10/2012 21:27 293,066 70447_ZnO500sterile_8.dat

11/10/2012 21:33 293,041 70448_ZnO500sterile_9.dat

11/10/2012 21:39 293,039 70449_ZnO500sterile_10.dat

11/10/2012 21:46 293,071 70450_ZnO500sterile_11.dat

11/10/2012 21:52 293,069 70451_ZnO500sterile_12.dat

11/10/2012 21:58 293,135 70452_ZnO500sterile_13.dat

11/10/2012 22:04 293,103 70453_ZnO500sterile_14.dat

11/10/2012 22:10 292,995 70454_ZnO500sterile_15.dat

11/10/2012 22:17 294,744 70455_ZnO500t0_1.dat

11/10/2012 22:23 294,739 70456_ZnO500t0_2.dat

11/10/2012 22:29 294,788 70457_ZnO500t0_3.dat

11/10/2012 22:35 294,785 70458_ZnO500t0_4.dat

11/10/2012 22:41 294,772 70459_ZnO500t0_5.dat

11/10/2012 22:47 294,829 70460_ZnO500t0_6.dat

11/10/2012 22:54 294,831 70461_ZnO500t0_7.dat

11/10/2012 23:00 294,834 70462_ZnO500t0_8.dat

11/10/2012 23:06 294,841 70463_ZnO500t0_9.dat

11/10/2012 23:12 294,848 70464_ZnO500t0_10.dat

11/10/2012 23:18 294,855 70465_ZnO500t0_11.dat

11/10/2012 23:25 294,856 70466_ZnO500t0_12.dat

11/10/2012 23:31 294,843 70467_ZnO500t0_13.dat

11/10/2012 23:37 294,845 70468_ZnO500t0_14.dat

11/10/2012 23:43 294,855 70469_ZnO500t0_15.dat

11/10/2012 23:49 293,716 70470_ZnO500bulk_1.dat

11/10/2012 23:56 293,661 70471_ZnO500bulk_2.dat

12/10/2012 00:02 293,658 70472_ZnO500bulk_3.dat

12/10/2012 00:08 293,677 70473_ZnO500bulk_4.dat

12/10/2012 00:14 293,715 70474_ZnO500bulk_5.dat

12/10/2012 00:20 293,690 70475_ZnO500bulk_6.dat

12/10/2012 00:27 293,680 70476_ZnO500bulk_7.dat

12/10/2012 00:33 293,729 70477_ZnO500bulk_8.dat

12/10/2012 00:39 293,683 70478_ZnO500bulk_9.dat

12/10/2012 00:45 293,651 70479_ZnO500bulk_10.dat

12/10/2012 00:51 293,573 70480_ZnO500bulk_11.dat

12/10/2012 00:57 293,620 70481_ZnO500bulk_12.dat

12/10/2012 01:04 293,662 70482_ZnO500bulk_13.dat

12/10/2012 01:10 293,692 70483_ZnO500bulk_14.dat

12/10/2012 01:16 293,723 70484_ZnO500bulk_15.dat

12/10/2012 01:22 292,240 70485_ZnO500top_1.dat

12/10/2012 01:28 292,246 70486_ZnO500top_2.dat

12/10/2012 01:35 292,244 70487_ZnO500top_3.dat

12/10/2012 01:41 292,220 70488_ZnO500top_4.dat

12/10/2012 01:47 292,228 70489_ZnO500top_5.dat

12/10/2012 01:53 292,244 70490_ZnO500top_6.dat

12/10/2012 01:59 292,270 70491_ZnO500top_7.dat

12/10/2012 02:05 292,228 70492_ZnO500top_8.dat

12/10/2012 02:12 292,251 70493_ZnO500top_9.dat

12/10/2012 02:18 292,193 70494_ZnO500top_10.dat

12/10/2012 02:24 292,225 70495_ZnO500top_11.dat

12/10/2012 02:30 292,210 70496_ZnO500top_12.dat

12/10/2012 02:36 292,223 70497_ZnO500top_13.dat

12/10/2012 02:43 292,203 70498_ZnO500top_14.dat

12/10/2012 02:49 292,197 70499_ZnO500top_15.dat

12/10/2012 02:55 291,749 70500_ZnO500bottom_1.dat

12/10/2012 03:01 291,728 70501_ZnO500bottom_2.dat

12/10/2012 03:07 291,774 70502_ZnO500bottom_3.dat

12/10/2012 03:14 291,812 70503_ZnO500bottom_4.dat

12/10/2012 03:20 291,876 70504_ZnO500bottom_5.dat

12/10/2012 03:26 291,753 70505_ZnO500bottom_6.dat

12/10/2012 03:32 291,658 70506_ZnO500bottom_7.dat

12/10/2012 03:38 291,628 70507_ZnO500bottom_8.dat

12/10/2012 03:44 291,611 70508_ZnO500bottom_9.dat

12/10/2012 03:51 291,525 70509_ZnO500bottom_10.dat

12/10/2012 03:57 291,657 70510_ZnO500bottom_11.dat

12/10/2012 04:03 291,685 70511_ZnO500bottom_12.dat

12/10/2012 04:09 291,730 70512_ZnO500bottom_13.dat

12/10/2012 04:15 291,794 70513_ZnO500bottom_14.dat

12/10/2012 04:21 291,731 70514_ZnO500bottom_15.dat

12/10/2012 04:28 293,583 70515_ZnO500sterile_1.dat

12/10/2012 04:34 293,615 70516_ZnO500sterile_2.dat

12/10/2012 04:40 293,578 70517_ZnO500sterile_3.dat

12/10/2012 04:46 293,592 70518_ZnO500sterile_4.dat

12/10/2012 04:52 293,606 70519_ZnO500sterile_5.dat

12/10/2012 04:59 293,584 70520_ZnO500sterile_6.dat

12/10/2012 05:05 293,640 70521_ZnO500sterile_7.dat

12/10/2012 05:11 293,606 70522_ZnO500sterile_8.dat

12/10/2012 05:17 293,635 70523_ZnO500sterile_9.dat

12/10/2012 05:23 293,668 70524_ZnO500sterile_10.dat

12/10/2012 05:30 293,646 70525_ZnO500sterile_11.dat

12/10/2012 05:36 293,685 70526_ZnO500sterile_12.dat

12/10/2012 05:42 293,699 70527_ZnO500sterile_13.dat

12/10/2012 05:48 293,714 70528_ZnO500sterile_14.dat

12/10/2012 05:54 293,704 70529_ZnO500sterile_15.dat

12/10/2012 06:00 294,869 70530_ZnO500t0_1.dat

12/10/2012 06:07 294,883 70531_ZnO500t0_2.dat

12/10/2012 06:13 294,882 70532_ZnO500t0_3.dat

12/10/2012 06:19   294,881 70533_ZnO500t0_4.dat

12/10/2012 06:25   294,880 70534_ZnO500t0_5.dat

12/10/2012 06:31   294,877 70535_ZnO500t0_6.dat

12/10/2012 06:38   294,883 70536_ZnO500t0_7.dat

12/10/2012 06:44   294,883 70537_ZnO500t0_8.dat

12/10/2012 06:50   294,885 70538_ZnO500t0_9.dat

12/10/2012 06:56   294,886 70539_ZnO500t0_10.dat

12/10/2012 07:02   294,883 70540_ZnO500t0_11.dat

12/10/2012 07:08   294,883 70541_ZnO500t0_12.dat

12/10/2012 07:15   294,884 70542_ZnO500t0_13.dat

12/10/2012 07:21   294,881 70543_ZnO500t0_14.dat

12/10/2012 07:27   294,880 70544_ZnO500t0_15.dat

12/10/2012 08:41   288,638 70545_ZnOcontrol_1.dat

12/10/2012 08:47   288,588 70546_ZnOcontrol_2.dat

12/10/2012 08:53   288,581 70547_ZnOcontrol_3.dat

12/10/2012 08:59   288,596 70548_ZnOcontrol_4.dat

12/10/2012 09:05   288,596 70549_ZnOcontrol_5.dat

12/10/2012 09:11   288,593 70550_ZnOcontrol_6.dat

13/04/2013 18:07   0 print.txt

366 File(s)   74,547,851 bytes

Journal of Hazardous Materials 241–242 (2012) 363–370

Contents lists available at SciVerse ScienceDirect

Journal of Hazardous Materials

journal homepage: www.elsevier.com/locate/jhazmat

Enhanced resistance to nanoparticle toxicity is conferred by overproduction of extracellular polymeric substances

Nimisha Joshi [a,*], Bryne T. Ngwenya [a], Christopher E. French [b]

[a] School of GeoSciences, Microbial Geochemistry Laboratory, University of Edinburgh, West Mains Road, Edinburgh EH9 3JW, United Kingdom
[b] School of Biological Sciences, Institute of Cell Biology, Darwin Building, University of Edinburgh, Mayfield Road, Edinburgh EH9 3JR, United Kingdom

HIGHLIGHTS

- Demonstration that bacteria engineered for EPS overproduction have better survival against Ag nanotoxicity.
- EPS destabilises Ag nanoparticles and promotes their aggregation.
- TEM demonstration that EPS traps the Ag nanoparticles outside the cell.
- EPS from overexpressing strains offers protection to non-EPS strains of bacteria.
- EPS polymer analogues such as xanthan also produce a similar response.

ARTICLE INFO

Article history:
Received 28 June 2012
Received in revised form
19 September 2012
Accepted 22 September 2012
Available online 29 September 2012

Keywords:
Nanotoxicity
Xanthan
Exopolysaccharides
Viability
Aggregation

ABSTRACT

The increasing production and use of engineered nanoparticles, coupled with their demonstrated toxicity to different organisms, demands the development of a systematic understanding of how nanoparticle toxicity depends on important environmental parameters as well as surface properties of both cells and nanomaterials. We demonstrate that production of the extracellular polymeric substance (EPS), colanic acid by engineered *Escherichia coli* protects the bacteria against silver nanoparticle toxicity. Moreover, exogenous addition of EPS to a control strain results in an increase in cell viability, as does the addition of commercial EPS polymer analogue xanthan. Furthermore, we have found that an EPS producing strain of *Sinorhizobium meliloti* shows higher survival upon exposure to silver nanoparticles than the parent strain. Transmission electron microscopy (TEM) observations showed that EPS traps the nanoparticles outside the cells and reduces the exposed surface area of cells to incoming nanoparticles by inducing cell aggregation. Nanoparticle size characterization in the presence of EPS and xanthan indicated a marked tendency towards aggregation. Both are likely effective mechanisms for reducing nanoparticle toxicity in the natural environment.

1. Introduction

Due to their small size, composition and reactivity, engineered nanoparticles are widely used in a variety of applications, including sunscreens, clothes and advanced targeted drug delivery for cancer treatments [1]. Whereas their unique physicochemical properties account for their versatile uses, the very same features raise considerable concern about their possible impact on the environment. As a result many studies have investigated the possible impact of engineered nanoparticles, including carbon nanotubes, metal and metal oxide nanoparticles on human cell lines, yeasts, bacteria and aquatic organisms [2–5]. Silver (Ag) nanoparticles have been reported to be toxic to many bacteria including *Escherichia coli*, *Pseudomonas chlororaphis*, and *Pseudomonas putida* [6–10]. Suggested causes of nanoparticle toxicity include death via injury to cells, membrane damage [8–11] and oxidative stress promoted by the formation of reactive oxygen species (ROS).

The objective of these studies is to be able to predict the behaviour and impact of engineered nanoparticles on organisms in the natural environment. However, this goal is not attainable without taking into consideration environmental variables such as pH, presence of dissolved salts, shape of nanoparticles, type of organic matter and type of medium under study [11–17]. The dynamic interaction with environmental variables can lead to changes in, and loss of properties associated with reactivity and toxicity of the nanoparticles. Moreover, intrinsic properties of the nanoparticles themselves, including surface charge and coatings, can have a significant impact on their reactivity. As a result, recent studies on microbe–nanoparticle interactions have begun to systematically examine these aspects. For instance, it was found that

* Corresponding author. Tel.: +44 790 122 9576; fax: +44 131 668 3184.
E-mail address: joshi.nimisha@gmail.com (N. Joshi).

0304-3894/$ – see front matter © 2012 Elsevier B.V. All rights reserved.
http://dx.doi.org/10.1016/j.jhazmat.2012.09.057

the toxicity of silver nanoparticles was dependent on the surface charge of these particles and that capping agents like citrate and organic compounds like humic acid can reduce the toxicity of silver nanoparticles [15,18].

Surface properties of bacteria could also play an important role in influencing the net toxicity of nanoparticles. Bacteria are known to secrete exopolysaccharides (EPS), particularly while growing in a biofilm mode [19–21]. EPS could play an important role in controlling the toxicity of nanoparticles in the environment [6,22–25]. For example it has been shown that bacteria exposed to nanoparticles in the biofilm mode and planktonic mode show different behaviour, with bacteria in planktonic mode being more vulnerable to nanoparticle toxicity [23]. In another study [22], bacteria covered with EPS showed a lower inactivation rate in the presence of titanium oxide (TiO_2) nanoparticles. The addition of EPS to *P. chlororaphis* eliminated silver nanoparticle toxicity at lower concentrations of nanoparticles [6].

Most of this work has hypothesized that EPS acts as a physical barrier or interacts with nanoparticles and competes with cell surfaces thereby reducing nanoparticle toxicity. In order to demonstrate this, EPS was either removed from the cells by mechanical means, cation exchange resins or glass beads. All these methods can affect the metabolic state of bacteria [26]. Secondly, the process of EPS extraction by using resins, ethanol precipitation or sonication produce quite variable outcomes with some loss in cell viability [27]. This can interfere indirectly with the nanoparticle toxicity results, particularly those that rely on cell viability testing. In order to investigate further the potential protective role of EPS, we developed a strain of *E. coli* that produces excess colanic acid, an extracellular polysaccharide produced by most strains of *E. coli*, which plays an important role in its protection against desiccation, osmotic and oxidative stress [19,28–30]. We also used an environmental isolate of *Sinorhizobium meliloti* and its EPS overproducing mutants and tested the impact of xanthan as a biopolymer analogue of EPS. This combination of tests allowed us to pose and investigate the following hypotheses: (i) EPS and associated biopolymers will alter the behaviour of nanoparticles and influence their toxicity by promoting their aggregation under natural conditions and (ii) such a mechanism will also extend to protection of non-EPS producing cells growing in co-culture with EPS-producing strains.

2. Materials and methods

2.1. Bacterial strains and growth conditions

In order to investigate the protective role of EPS on the impact of silver nanoparticles *E. coli* (JM109) and *S. meliloti* were used [29,31–34] (Table 1). Three strains of *S. meliloti*, a nitrogen fixing and hence environmentally significant bacterium were used to explore the environmental relevance of our findings [35].

E. coli was genetically modified to overproduce capsular polysaccharide. The capsule synthesis (cps) in *E. coli* is controlled by a complex network of genes. *rcsA* has been shown to act as a positive regulator of the *cps* operon in *E. coli* and shown to activate its own expression [30,36,37]. The primer sequences for the promoter and coding sequence of the *rcsA* gene were designed and sourced from Sigma–Aldrich, UK.

For *E. coli*, exposure studies were carried out in Minimal Davidson Medium (MDM) for which salts (and antibiotics) were sourced from Sigma–Aldrich, UK. Minimal medium (64 g/L $Na_2HPO_4{\cdot}7H_2O$, 15 g/L KH_2PO_4, 5 g/L NH_4Cl, and 2.5 g/L NaCl) was diluted four times and supplemented with 0.2% Casamino acids, 1 mM thiamine hydrochloride and 0.4% (w/v) glycerol as a carbon source. Ampicillin (100 μg/ml) was used to maintain plasmids when required in *E. coli*. For *S. meliloti*, M9 supplemented medium (recipe as above) with 2.5 mM calcium chloride and magnesium sulphate was used together with streptomycin at 500 μg/ml. For the incubations, an overnight culture was prepared in M9 medium. Cultures were incubated at 37 °C for *E. coli* and 30 °C for *S. meliloti* with rotary shaking at 200 rpm.

Table 1
Bacterial strains and plasmids.

Bacterial strains	Genotype/characteristics	Source
1. *E. coli*		
E. coli JM109/pRcsA2	Laboratory strain modified to overproduce colanic acid	This work
E. coli JM109/pEdinbrick1	Vector control strain	[38]
2. *Sinorhizobium meliloti*		
Rm1021	Parent strain	[31,33]
Rm7096	Rm1021 *exoS*::Tn5 EPS overproducing strain	[30–32]
Rm7210	Rm1021 *exoY*:: Tn5 Lacks EPS production	[31,32]
3. *E. coli JW3077-1*	*yhaK725*(del)::kan	[42]
Plasmid: pEdinbrick1		[38]

2.2. Construction of a colanic acid over producing strain of E. coli and colanic acid analysis

Primers for promoter and the coding sequence of *rcsA* were designed in a standard BioBrick format RFC10 as defined by the Registry of Standard Biological parts [38]. The promoter of *rcsA* and corresponding coding sequence were amplified using KOD polymerase from Invitrogen according to the manufacturer's protocol. The following primers were used.

Forward primer with BioBrick prefix: TCTgaattcgcggccgcttctaga gAAGCTCACTCACATATCGCAA and reverse primer ctgcagcggccgctactagta TTAGCGCATGTTGACAA. The generated Bio Brick P_{rcsA}+*rcsA* was cloned in pSB1A2 to generate pRcsA1 and then Bba_J33207 (*lac* promoter) was inserted upstream to generate pRcsA2.

EPS was quantified by the anthrone sulphuric acid assay. The cells were scraped from LB agar plates (approx. 30–40 mg) and suspended in 1 ml of water and the method of Mendrygal et al. [29,39] was followed. The supernatant recovered after centrifugation was used for assay [35,39]. Total carbohydrate was determined using a glucose standard and final values were normalized to corresponding OD600 values of the bacterial suspensions. Total EPS and colanic acid recovery from *E. coli* JM109/pRcsA2 was carried out as described by Obadia et al. [39]. The presence of fucose is an indicator of the presence of colanic acid produced by *E. coli* so a fucose standard curve in the range of 5–100 μg/ml was used to determine the concentration of fucose in the modified strains [40].

2.3. Nanoparticles source, sample preparation, characterization and speciation analysis

Silver nanoparticles of 100 nm (Catalog no. 576832) diameter were obtained from Sigma–Aldrich, UK. In order to prepare a silver dispersion (100 nm), the method of Fabrega et al. [15] was used. The final concentration of silver in the sample was determined in triplicate using ICP-OES and found to be 70 mg/L. A 10 nm silver nanoparticle dispersion 20 mg/L was obtained from Sigma–Aldrich, UK (Catalog no. 730785).

Size characterization of silver nanoparticles was carried out in the presence of water, growth media (Luria Bertani or minimal medium) with or without EPS and an EPS analogue (xanthan). Both the silver dispersion (10 nm) and 100 nm water suspensions were

used. A median concentration of 100 mg/L was used for xanthan as a substitute for EPS and 9 mg/L of glucose equivalent of the EPS preparation recovered from JM109/pRcsA2 was used. Particle size distribution was analysed by dynamic light scattering (DLS) using a Zeta PALS 90 Plus submicron size analyzer (Brookhaven Instruments Corporation, Holtsville, NY, USA). The samples were sonicated for 5 min prior to use. The data were collected in triplicate at a temperature of 25 °C.

In order to determine the extent of ion dissolution/speciation for the exposure period chosen for experiments (120 min), a background study was conducted. The nanoparticles were suspended in M9 supplemented medium and incubated on a shaker at 200 rpm. Suspensions were centrifuged at 22,000 × *g* for 60 min at 4 °C following incubation for 2 h [41]. The supernatant was acidified with 2% nitric acid and total silver concentration was determined by ICP-OES analysis. Samples for each of the concentration were in duplicates, and there was no change in pH during this treatment.

2.4. Nanoparticle exposure and viability study

Bacteria were grown overnight in minimal medium (described above) with suitable antibiotics and the next day, exposure was carried out after adjusting the OD600 to 0.2 by diluting with fresh medium. All experiments were conducted using 10 nm silver nanoparticles, except for the experiment investigating the effects of nanoparticle size on toxicity, where 100 nm silver nanoparticles were also used. The nanoparticle treated samples were incubated in the dark for 120 min on a rotary shaker at 37 °C for *E. coli* and *S. meliloti*. Cell viability was tested by determining colony forming units (CFU/ml) following serial dilution. An incubation temperature of 37 °C was used for *E. coli* grown on LB-agar plates. For *S. meliloti*, LB agar supplemented with 2.5 mM magnesium sulphate and calcium chloride was used and incubated at 30 °C.

A Bactiter-Glo microbial cell viability kit (Promega Catalog no. G8230) was used to determine the number of viable cells in bacterial cultures based on the quantization of ATP content (in terms of luminescence values) after exposure to silver nanoparticles. The exposure method was as described above and the kit was used as per the manufacturer's protocol. The luminescence was determined by using a modulus single tube multimode reader (BS040271 Turner Biosystems). The possible interference by silver nanoparticles and the background noise was also assessed and the final luminescence (relative luminescence value/RLU) was obtained after deducting the background (supporting information).

The potential role of EPS produced by one strain of bacteria on the other strain was also tested. The EPS recovered from *E. coli*/JM109/pRcsA2 culture was used to test protection of non mucoid cells against nanoparticle toxicity. A different strain of *E. coli*/BW25113/*ΔyhaK* strain was used to investigate if the EPS produced by one strain can provide cross protection to another [42]. A 6.5 mg/L final silver nanoparticles concentration (10 nm diameter silver nanoparticles) was used. The method was as described above. An EPS preparation (9 mg/L of glucose equivalent) was added per ml of bacterial culture.

In order to study the impact of xanthan on cell viability a xanthan suspension in water (100 mg/L) was used (50 μl per ml of culture) with silver nanoparticles of 10 nm diameter. All the experiments were conducted in triplicate and also conducted at different time intervals to ensure the reproducibility of the data. The data analysis was done using Excel 2007 and Student's *t* test was used to determine the statistical significance of the data.

2.5. Microscopy and image analysis

A Phillips CM120 Transmission Electron Microscope (FEI UK Ltd, Cambridge, England) operated at 80 kV was used to study the fate and spatial distribution of Ag nanoparticles in/around bacteria. The bacterial samples, both the control strain and the EPS overproducing strain of *E. coli*, were exposed to silver nanoparticles as described above and then used for sample preparation for TEM imaging. Representative images were taken on a Gatan Orius CCD camera (Gatan UK, Oxon, England). Sample preparation for TEM was conducted according to the method of Bechtel et al. [43] and as detailed in the supporting information (S4).

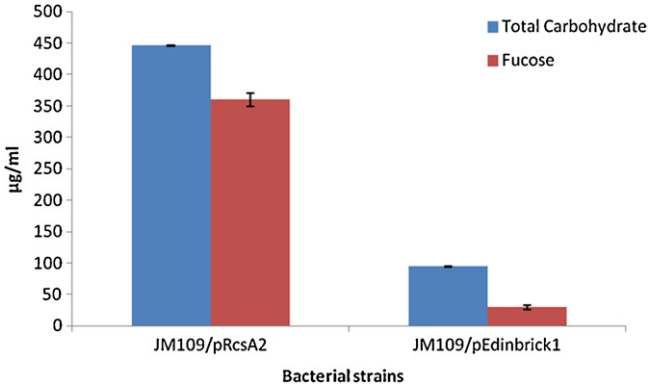

Fig. 1. Determination of total carbohydrate content and fucose content (representing colanic acid) in *E. coli* JM109/pRcsA2 cells as compared to JM109/pEdinbrick1 cells. Bacterial strains illustrated on *x* axis and their corresponding carbohydrate and fucose content described on the *y* axis in μg/ml.

3. Results

3.1. A colanic acid overexpressing strain was successfully constructed

A colanic acid overproducing strain of *E. coli*, JM109/pRcsA2 was developed and characterized. This strain showed enhanced mucoidy and glossy texture when grown on LB agar plates supplemented with IPTG and ampicillin. These samples were tested for total carbohydrate production and presence of colanic acid based on fucose content [40]. The total carbohydrate content of JM109/pRscSA2 strain was found to be about five times higher than that of the control strain JM109/pEdinbrick1 (Fig. 1), and the colanic acid content of JM109/pRcsA2 was fourteen times greater than that of the control strain.

3.2. E. coli JM109 pRcsA2 shows better survival upon exposure to nanoparticles

The response of JM109/pRcsA2 towards nanoparticles was investigated by exposing the cells to both 100 nm and 10 nm silver nanoparticles at the same concentration of 6 mg/L. This experiment provided an insight into the protective role of EPS and at the same time, the effect of grain size on the toxic potential of nanoparticles. It was found that the EPS overproducing strain JM109/pRcsA2 showed higher cell viability than the control strain JM109/pEdinbrick1. The marginal increase in CFU/ml for JM109/pRcsA2 at 100 nm exposure is not statistically significant relative to controls without nanoparticles. For the 10 nm exposure condition, there was a statistically significant decrease in cell growth between controls and nanoparticle-treated samples between the strains ($p = 0.02$). Fig. 2 also shows that the 10 nm Ag nanoparticles were more toxic than the 100 nm ($p = 0.02$). Similarly JM109/pEdinbrick 1 shows a higher drop in cell viability when exposed to 10 nm particles ($p = 0.01$) than the JM109/pRcsA2.

The Bactiter microbial cell viability kit was used to determine the cell viability in another experiment where both strains were

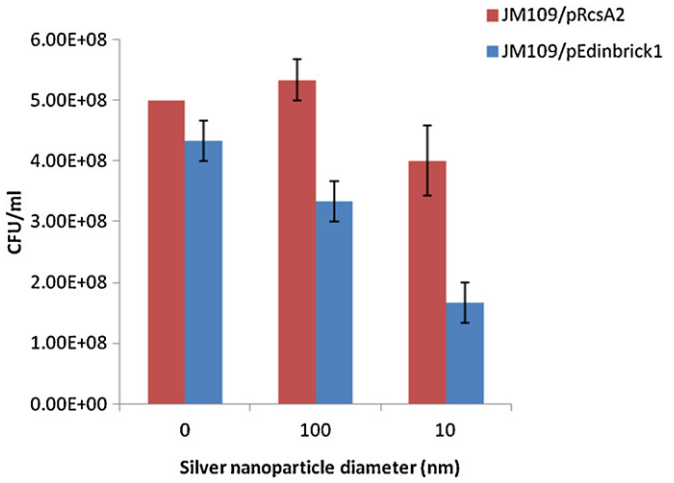

Fig. 2. Effect of nanoparticle exposure on *E. coli* EPS overproducing strain JM109/pRcsA2 and control strain JM109/pEdinbrick1 using 100 and 10 nm diameter silver nanoparticles at 6 mg/L. Silver nanoparticle size (diameter) in nm shown on *x* axis and cell viability of bacteria in CFU/ml on *y* axis. Error bars indicate one standard error.

exposed to 10 nm silver nanoparticles. The control strain showed a decrease in luminescence (Relative luminescence units/RLU) while the mucoid strain JM109/pRcsA2 shows a marginal change (statistically insignificant), indicative of the fact that it shows a resistance towards nanoparticle toxicity (Fig. S1a and b in supporting information).

3.3. Rm7096, a succinoglycan overproducing strain of S. meliloti shows better survival than the parent strain Rm1021 and non EPS producing mutant strain Rm7210

The impact of silver nanoparticles on the parent strain RM1021 that produces EPS (Type 1 succinoglycan) was compared with two mutant forms: Rm7096, an EPS overproducing strain and Rm7210 that does not produce any EPS [29,31–34]. The EPS overproducing mutant Rm7096 strain showed higher cell viability at all three different silver nanoparticle concentrations (Fig. 3a and b) compared with the mutant strain Rm7210. Rm7210 shows similar survival to the parent strain at 7 mg/L and 8.2 mg/L silver nanoparticle concentrations. The statistical data based on *t*-test is provided in point S5 in supporting information.

3.4. Speciation of silver from silver nanoparticles

ICP analysis indicated that a small fraction of silver ions were being released into the medium in a 2 h exposure period (accounting for 0.27 mg/L or 4.5% of initial concentration of silver nanoparticle dispersion added to the medium). Exposure of cells to the equivalent 0.27 mg/L silver nitrate solutions does not lead to an appreciable drop in cell count (Fig. S3 in supporting information), suggesting that release of silver ions from nanoparticle surface cannot alone explain all the toxicity observations. This supports the hypothesis that the loss in cell viability was primarily due to the nanoparticles that could have entered the cells rather than just ionic silver released into the medium. However, the impact of silver ions cannot be totally negated because media used for exposure studies also contained chloride, which potentially led to precipitation of AgCl [6,44], thereby reducing total bio-available ionic silver. To fully account for this removal requires determining the relative rates of silver nanoparticle dissolution and silver chloride precipitation in order to demonstrate whether the residence time of silver ions in the media is long enough to

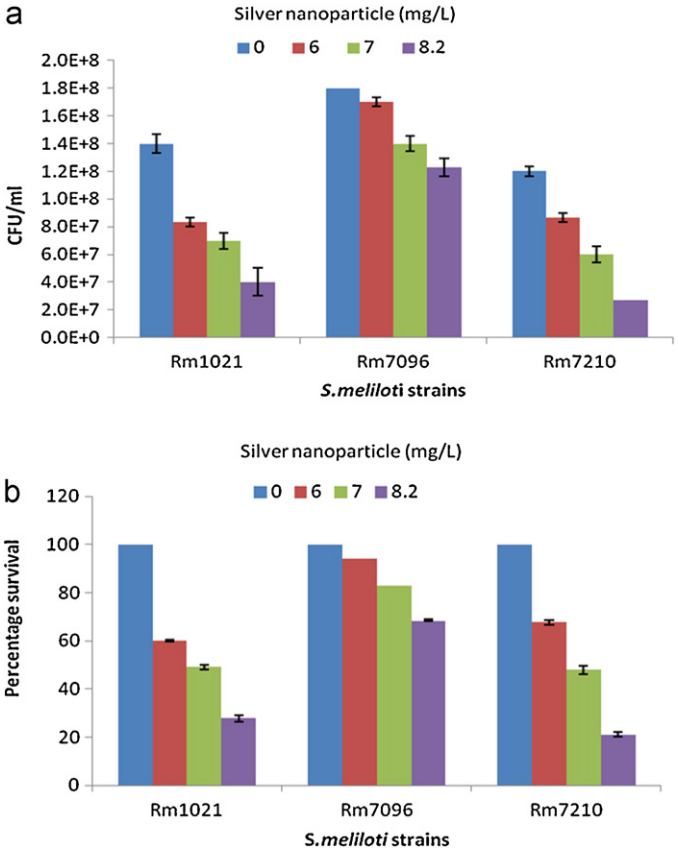

Fig. 3. Impact of silver nanoparticles on different strains of *S. meliloti* exposed to different concentrations of 10 nm diameter silver nanoparticles. (a) Post-exposure viability determined by colony count and (b) percentage survival relative to the control which was not exposed to nanoparticles. The strains of *S. meliloti* have been shown on *x*-axis and their corresponding cell viability (CFU/ml or percentage survival) on the *y*-axis. Error bars indicate one standard error. Error bars in (b) are too small to be visible.

make it bioavailable. While this was beyond the scope of this study, we can estimate the concentration of Ag^+ ions in equilibrium with 0.0343 mol/L total chloride in the media, based on the solubility product constant of 1.77×10^{-10} mol^2 L^{-2} for AgCl [45]. Using the extended Debye–Huckel equation for activity correction (and ignoring organic compounds in the ionic strength calculation) yields an equilibrium ionic silver concentration of about 5.15×10^{-9} mol/L or 5.56×10^{-4} mg/L. This is several magnitudes lower than the average 0.3 mg/L we can detect, suggesting that some of the silver detected is probably still nanoparticulate. The probable presence of silver nanoparticles in the supernatant was also implied by residual absorbance at 400 nm using a UV–visible spectrometer. Together, these analyses suggest that most of the Ag^+ ions are precipitated out of the media [6] and hence that all/most of the toxicity we see is due to nanoparticles. Perhaps the separation method used, adapted from [41] is not as effective as suggested. This is an important observation regarding the protective role of extracellular polymeric substance (EPS) to nanoparticle toxicity since ionic silver may well diffuse through the EPS barrier.

3.5. EPS and xanthan protect non-EPS containing cells against nanoparticle toxicity

Further nanoparticle exposure experiments were carried out with addition of the well-characterized polymer xanthan to investigate whether it plays a protective role against nanoparticle toxicity, using the control strain JM109/pEdinbrick1, which does not

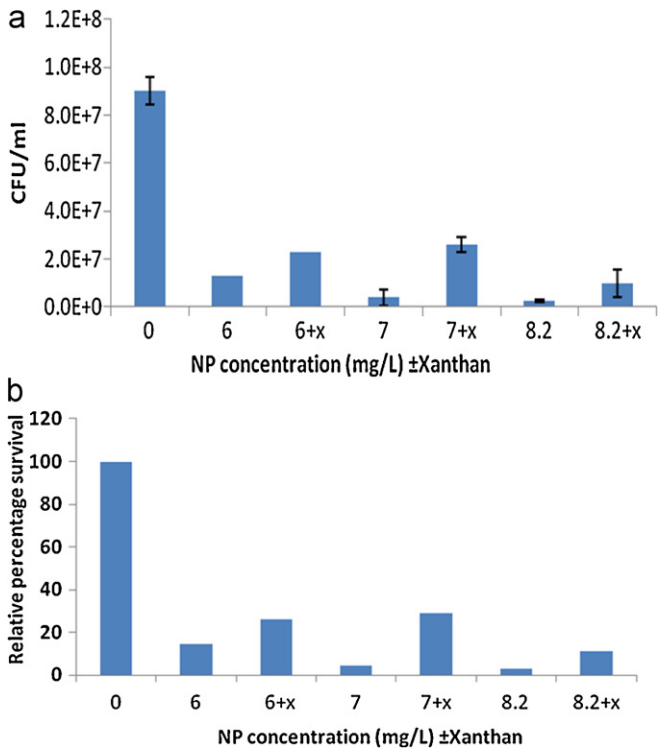

Fig. 4. Impact of xanthan on silver nanoparticle toxicity. (a) Viability as determined by colony count following exposure to 6, 7 and 8.2 mg/L silver nanoparticles, with or without addition of 100 mg/L xanthan and (b) percentage survival for the same samples. Error bars indicate one standard error. The *x*-axis describes the treatment conditions and the *y*-axis the cell viability in each condition (CFU/ml or percentage survival). Error bars in (b) are too small to be visible.

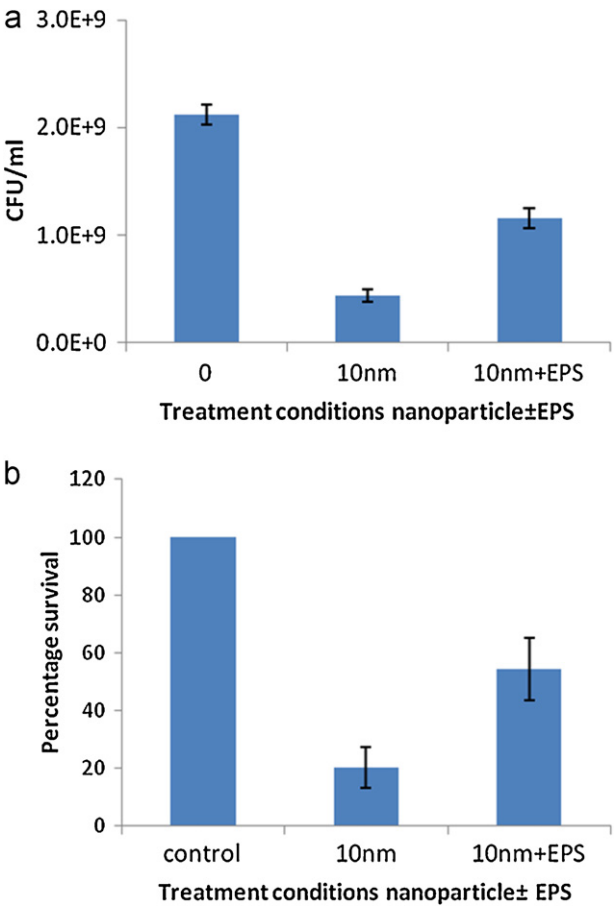

Fig. 5. The protective effect of EPS on bacteria. (a) Differential survival of *E. coli*/BW25113/Δyhak on addition of EPS following exposure to silver nanoparticles (10 nm diameter) at 6.5 mg/L and (b) percentage survival normalized to the control samples not exposed to nanoparticles.

produce a significant level of colanic acid. The cell viability was found to be higher when xanthan was added during exposure (Fig. 4). For each silver nanoparticle concentration, the addition of xanthan results in better growth in terms of CFU (Fig. 4a) and survival percentage (Fig. 4b). While the difference in CFU is not statistically significant for exposure to 6 mg/L nanoparticles ($p = 0.23$) a significant difference exists at 7 mg/L ($p = 0.0001$) and 8.2 mg/L ($p = 0.0004$). A similar protective response was also observed when EPS purified from JM109/pRcsA2 was added to another strain of *E. coli*, BW25113/*Δyhak*, which also produces minimal levels of polysaccharides. The result was statistically significant ($p = 0.03$) (Fig. 5a and b).

3.6. TEM analysis shows silver nanoparticle invasion of JM109/pEdinbrick1 control cells

In order to study the fate of nanoparticles and their spatial relationship to cells, TEM was performed on samples of JM109/pRcsA2 and control strain JM109/pEdinbrick1 exposed to 7 mg/L silver nanoparticles (10 nm). Fig. 6 compares sections of the two strains when exposed to nanoparticles. After exposure to silver nanoparticles, JM109/pEdinbrick1 cells show diffuse cell membranes, with the occasional dark spots representing silver nanoparticles inside cells (Fig. 6a). Nanoparticles outside cells appear to have been washed away during preparation and mounting in the case of the control strain (Fig. 6b); however, the EPS released by the JM109/pRcsA2 seems to have trapped much of the nanoparticulate silver in the matrix as seen in Fig. 6c. Secondly, JM109/pRcsA2 cells show a marked tendency towards clumping/aggregation, with the nanoparticles trapped on/outside a relatively intact membrane (Fig. 6c), while cells of the control strain do not show this.

3.7. Polysaccharide increases the hydrodynamic diameter of silver nanoparticles

Particle size analysis shows that both sets of nanoparticles used in this study (10 nm and 100 nm diameter) maintained their nominal sizes when dispersed in water and M9 medium (Fig. 7a and b). Moreover, no change in size was evident when polysaccharides were added to nanoparticles dispersed in water. However, addition of polysaccharides to nanoparticle suspensions in M9 medium had a significant effect, particularly on the 10 nm nanoparticle dispersion where measured particle sizes more than doubled, while 100 nm nanoparticles increased their apparent size by 20%. The nanoparticles also show a greater aggregation depending on the length of time they were left suspended in the medium (data not shown).

4. Discussion

4.1. EPS encapsulates the cells and reduces exposed surface area

EPS production by microbial cells serves a number of different functions including stabilization and protection of the biofilm structure through increasing resistance to dehydration and biocides, facilitating adhesion to surfaces [46–48] and promoting cell aggregation and biofilm accumulation [49]. The protective role of EPS to different biocides, including metals, is well established. Our results are therefore consistent with the few recent studies in the literature [6,23–25]. What remain unclear are the

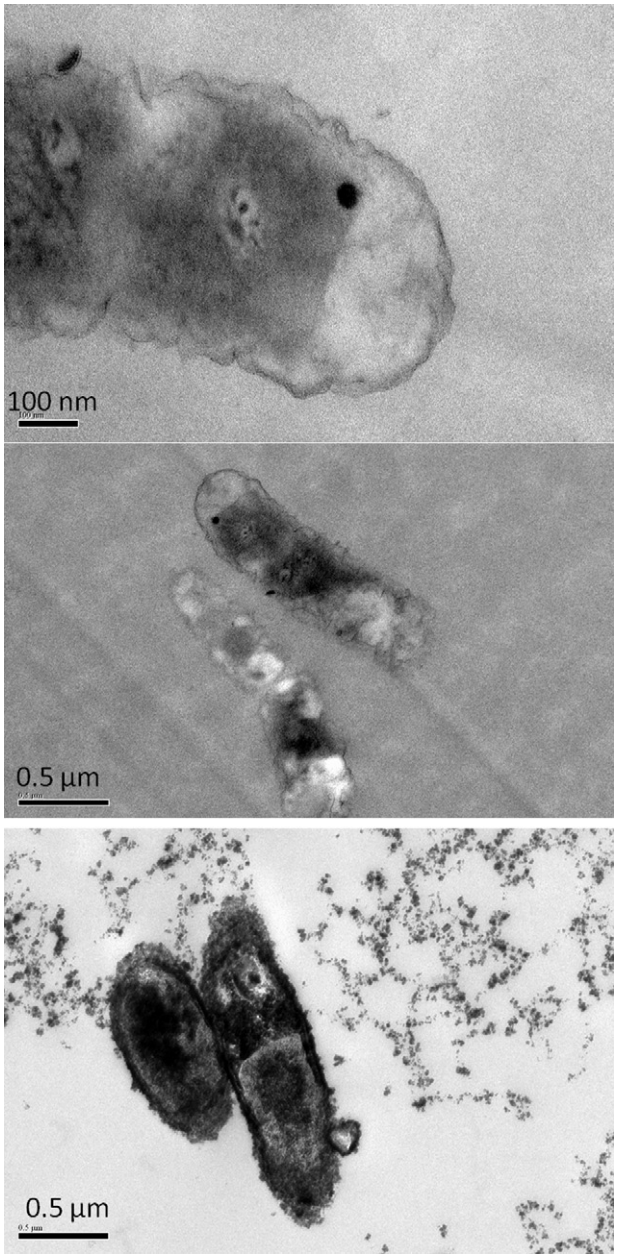

Fig. 6. TEM analysis of *E. coli* cells treated with silver nanoparticles. The cells were exposed to silver nanoparticles at 7 mg/L for 2 h. TEM images of *E. coli* JM109/pEdinbrick1 (control strain (a) and (b)). The cell membrane is less defined indicating possible damage, and cells are not clumped/aggregated together. (c) *E. coli* JM109/pRcsA2 (EPS-overproducing strain). Cells are aggregated and show intact membranes with most of the nanoparticles trapped outside the cell membrane.

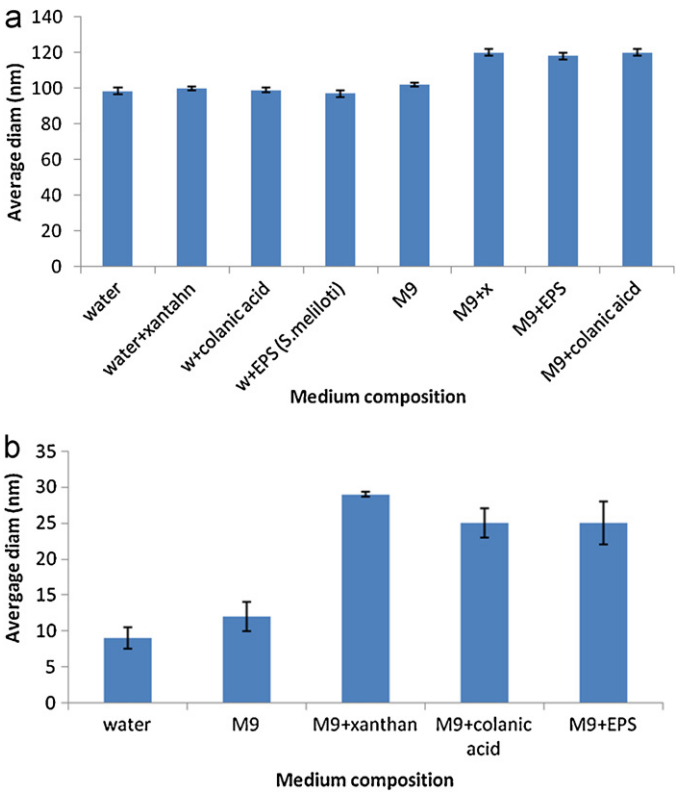

Fig. 7. (a) Average diameter of nominally 100 nm silver nanoparticles in different media and with the addition of xanthan or EPS and colanic acid extracted from *S. meliloti* and *E. coli* JM109/pRcsA2 respectively. (b) Similar data for the nominally 10 nm silver nanoparticle suspension. Bars represent one standard error. The *x*-axis highlights the different mediums used and the *y*-axis shows the average diameter of silver nanoparticle in nm.

mechanisms by which EPS mediates cell survival. Most previous studies have demonstrated the protective role of EPS either by comparing toxicity of nanoparticles between planktonic cells (which produce less EPS) and biofilms [7] or by extracting the EPS using physicochemical methods [6]. However, planktonic and biofilm cells have other physiological differences which may affect the results, and use of physical methods to remove EPS can in itself compromise cell viability or result in partial removal of EPS. Taking advantage of the fact that JM109/pRcsA2 produces excess EPS [20,39] we found that strain JM109/pRcsA2 cells had a higher percentage survival than the control strain when exposed to silver nanoparticles of two different sizes, 100 and 10 nm diameter (Fig. 2). This observation clearly supports the fact that EPS protects the cells against nanoparticle toxicity. A statistically significant difference between both the samples at 6 mg/L silver (10 nm diameter) was observed ($p = 0.0002$). One possible reason is that EPS encapsulates the bacteria and provides a protective layer against incoming nanoparticles, which is consistent with the TEM observations in Fig. 6c. Moreover, EPS has been shown to be an efficient adsorbent for all nanoparticles, but especially for silver nanoparticles [50,51]. By keeping nanoparticles distant from the cells, EPS may also act as a protective barrier by localising reactive oxygen species (ROS) away from cells. It is well known that ROS have very short lifetimes, about 3 ns [23,24] and are only effective if produced close to or inside the cell membrane.

4.2. EPS reduces toxicity by inducing aggregation of silver nanoparticles

Based on TEM observations, we hypothesized that EPS may also protect cells by inducing aggregation of nanoparticles in the liquid [52] thus reducing both their solubility and propensity to penetrate cell walls [53]. In order to test this hypothesis, we measured the hydrodynamic diameter of the silver nanoparticles in different media, comparing the mean particle size between suspensions with and without EPS isolated from *E. coli* and *S. meliloti*, and by using the synthetic EPS analogue xanthan. The results supported our hypothesis, showing a statistically significant increase in hydrodynamic diameter in the presence of EPS and xanthan (Fig. 7), but only when nanoparticles were dispersed in minimal medium. Moreau et al. [21] have also shown that extracellular proteins of microbial origin have the potential to induce aggregation of metal sulphide nanoparticles.

EPS and xanthan also caused silver nanoparticle aggregation when sodium citrate stabilized silver nanoparticles (10 nm) were used in a similar experimental set. Aggregation was not observed when EPS or xanthan were added to nanoparticle suspensions in water. By contrast, Khan et al. [50] reported significant aggregation of silver nanoparticles after 4 h of dispersion in water, which decreased with increasing concentration of EPS extracted from *Bacillus pumilus*. These differences may reflect differences in the composition and hence charge characteristics of the EPS. For example, Dimkpa et al. [6] showed that EPS consisting of neutral sugars did not significantly affect the zeta potential of silver nanoparticles, although particle size data was not reported.

Intuitively, colloidal stabilisation of nanoparticle suspensions should lead to increased toxicity [54]. However, surface coatings can also reduce toxicity of silver nanoparticles by reducing oxidative dissolution of nanoparticles, which is now considered to be an important mechanism for increasing bioavailability of ionic silver [55]. The effects of EPS are therefore likely to be complex; however, the observed aggregation in the presence of EPS/xanthan, coupled with higher survival of cells in the presence of these macromolecules, suggests that EPS-induced nanoparticle aggregation is an important protective mechanism in our study.

4.3. Environmental implications

An outstanding question to be addressed by in vitro toxicity findings is whether they have environmental relevance given the tendency for nanoparticles to aggregate under natural environmental conditions and the possible transformations like oxidation, dissolution and biotransformation that could happen in the environment. The fact that only a fraction of silver ions were released in the medium suggests that the primary toxicity was due to the silver nanoparticles that could either be disrupting the cell membrane or ionic silver released in the cytoplasm following nanoparticle invasion. The finding that silver nanoparticles aggregate in the presence of EPS, and consequently display reduced toxicity in this and other studies [14,15,22,23], has important implications for the environment where bacteria occur in the form of biofilms consisting of consortia of microbes. Our results suggest that adding xanthan or extracted EPS to cultures that do not produce EPS leads to some degree of co-protection, at lower concentrations of nanoparticles, by influencing nanoparticle size and stability. However, studies have also shown that when mixed culture biofilms are exposed to nanoparticles, some of the strains show better survival than others, leading to shifts in community composition [14,23]. It is therefore not possible to extrapolate observed EPS co-protection effects on monoculture studies directly to the natural environment. One accepted source of differential susceptibility to toxins is growth rate; wherein cells that grow slowly appear to show better survival [20,21]. *E. coli* JM109/pRcsA2 shows a slightly lower growth rate relative to the control strain (supporting information, Fig. S2), which is associated with enhanced protection from nanoparticles (Fig. S2a). Thus, the slower growth rate may be due to EPS overexpressing cells diverting effort into EPS synthesis rather than being due to susceptibility to added nanoparticles.

Finally, it should be noted that many studies are consistent with EPS acting as a physical barrier that traps nanoparticles and prevents entry into cells. Moreover, some studies have demonstrated that components of EPS often lead to aggregation of nanoparticles [21], with consequent reduction in mobility of nanoparticles, while others report enhanced stability of nanoparticles in the presence of EPS [50]. These discrepancies likely reflect the diversity of EPS composition, and suggest that the effects of EPS may not be amenable to generalisations.

Acknowledgements

This work was supported by the Scottish Overseas Research Students Award Scheme (SORSAS) and funding from the School of Geosciences, University of Edinburgh. We would like to thank Steve Mitchell of the Institute of Molecular Plant Sciences, School of Biological Sciences, University of Edinburgh for assistance with TEM and Steve Mowbrey (School of Geosciences, University of Edinburgh) for assistance with lyophilisation. *S. meliloti* strains were generously provided by Dr. Gary Dorken, School of Physics and Astronomy, University of Edinburgh. We would also like to thank Dr David Radford, School of Biological Science and Prof. Nick Christofi of Recyclatech Group Ltd, for providing feedback during manuscript preparation.

Appendix A. Supplementary data

Supplementary data associated with this article can be found, in the online version, at http://dx.doi.org/10.1016/j.jhazmat.2012.09.057.

References

[1] B. Nowack, T.D. Bucheli, Occurrence, behavior and effects of nanoparticles in the environment, Environ. Pollut. 150 (2007) 5–22.
[2] T.M. Scown, M.E. Santos, M. Eduarda, B.D. Johnston, B. Gaiser, M. Baalousha, S. Mitov, J.R. Lead, V. Stone, T.F. Fernandes, M. Jepson, R. Aerle, C.R. Tyler, Effects of aqueous exposure to silver nanoparticles of different sizes in rainbow trout, Toxicol. Sci. 115 (2) (2010) 521–534.
[3] X. Hu, S. Cook, P. Wang, H.M. Hwang, In vitro evaluation of cytotoxicity of engineered metal oxide nanoparticles, Sci. Total Environ. 407 (2009) 3070–3072.
[4] L.K. Adams, D.Y. Lyon, P.J.J. Alvarez, Comparative eco-toxicity of nanoscale TiO_2, SiO_2 and ZnO water suspensions, Water Res. 40 (2006) 3527–3532.
[5] K. Kasmets, A. Ivask, H. Dubourgier, A. Kahru, Toxicity of nanoparticles TiO_2, ZnO, SiO_2 to yeast *Saccharomyces cerevisiae*, Toxicol. In Vitro 23 (2009) 1116–1122.
[6] C. Dimkpa, A. Calder, P. Gajjar, S. Merugu, W. Huang, D. Britt, J. McLean, W. Johnson, A.J. Anderson, Interaction of silver nanoparticles with an environmentally beneficial bacterium, *Pseudomonas chlororaphis*, J. Hazard. Mater. 188 (2011) 428–435.
[7] J. Fabrega, J.C. Renshaw, J.R. Lead, Interactions of silver nanoparticles with *Pseudomonas putida* biofilms, Environ. Sci. Technol. 43 (2009) 9004–9009.
[8] P. Gajjar, B. Pettee, D. Britt, W. Huang, W. Johnson, A. Anderson, Antimicrobial activities of commercial nanoparticles against an environmental soil microbe, *Pseudomonas putida* KT2440, J. Biol. Eng. 3 (2009) 1611–1754.
[9] O. Choi, Z. Hu, Size dependent and reactive oxygen species related nanosilver toxicity to nitrifying bacteria, Environ. Sci. Technol. 42 (2008) 4583–4588.
[10] I. Sondi, B.S. Sondi, Silver nanoparticles as antimicrobial agent: a case study on *E. coli* as a model for Gram-negative bacteria, J. Colloid Interface Sci. 275 (2004) 177–182.
[11] J.R. Morones, J. Elechiguerra, A. Camacho, K. Holt, J. Kouri, J.T. Ramrez, J. Yacaman, Bactericidal impact of silver nanoparticles, Nanotechnology 16 (2005) 2346–2353.
[12] S. Pal, Y. Tak, J.M. Song, Does the antibacterial activity of silver nanoparticles depend on the shape of the nanoparticle? A study of the Gram-negative bacterium *Escherichia coli*, Appl. Environ. Microbiol. 73 (2007) 1712–1720.
[13] M. Auffan, W.R.J. Achouak, M. Roncato, C. Chaneac, D. Waite, A. Masion, J. Woicik, M.R. Wiesner, J.Y. Bottero, Relation between the redox state of iron-based nanoparticles and their cytotoxicity toward *Escherichia coli*, Environ. Sci. Technol. 42 (2008) 6730–6735.
[14] M. Li, L. Zhu, D. Lin, Toxicity of ZnO nanoparticles to *Escherichia coli*: mechanism and the influence of medium components, Environ. Sci. Technol. 45 (2011) 1977–1983.
[15] J. Fabrega, R. Shona, S. Fawcett, J.C. Renshaw, J.R. Lead, Silver nanoparticle impact on bacterial growth: effect of pH, concentration, and organic matter, Environ. Sci. Technol. 43 (19) (2009) 7285–7290.
[16] X. Jin, M. Li, J. Wang, C. Marambio-Jones, F. Peng, X. Huang, R. Damoiseaux, E.M.V. Hoek, High-throughput screening of silver nanoparticle stability and bacterial inactivation in aquatic media: influence of specific ions, Environ. Sci. Technol. 44 (2010) 7321–7328.
[17] G.V. Lowry, K.B. Gregory, S.C. Apte, J.R. Lead, Transformations of nanomaterials in the environment, Environ. Sci. Technol. (2012), http://dx.doi.org/10.1016/j.jhazmat.2012.09.057
[18] A. El Badawy, R.G. Silva, B. Morris, K.G. Scheckel, M. Suidan, T.M. Tolaymat, Surface charge-dependent toxicity of silver nanoparticles, Environ. Sci. Technol. 45 (2011) 283–287.
[19] H. Flemming, J. Wingender, The biofilm matrix, Nat. Rev. 8 (2010) 623–633.

[20] D.G. Allison, I.W. Sutherland, T.R. Neu, EPS: what's an acronym? in: A. McBain, D. Allison, M. Brading, A. Rickard, J. Verran, J. Walker (Eds.), Biofilm communities: order from chaos?, BioLine, Cardiff, 2003, pp. 381–387.
[21] J. Moreau, P. Weber, C. Michael, M. Martin, B. Gilbert, I. Hutcheon, J.F. Banfield, Extracellular proteins limit the dispersal of biogenic nanoparticles Science 316 (2007) 1600–1603.
[22] G. Jiang, Z. Shen, J. Niu, Y. Bao, J. Chen, T. He, Toxicological assessment of TiO_2 nanoparticles by recombinant *Escherichia coli* bacteria, J. Environ. Monit. 13 (2011) 42–48.
[23] T. Battin, V.D. Frank, A. Weilhartner, S. Ottofuelling, T. Hofmann, Nanostructured TiO_2: transport behavior and effects on aquatic microbial communities under environmental conditions, Environ. Sci. Technol. 43 (2009) 8098–8104.
[24] Y. Liu, J. Li, X. Qiu, C. Burda, Bactericidal activity of nitrogen-doped metal oxide nanocatalysts and the influence of bacterial extracellular polymeric substances (EPS), J. Photochem. Photobiol. A: Chem. 190 (2007) 94–100.
[25] C. Dimkpa, A. Calder, D. Britt, J.E. McLean, A. Anderson, Responses of a soil bacterium, *Pseudomonas chlororaphis* O6 to commercial metal oxide nanoparticles compared with responses to metal ions, Environ. Pollut. 159 (2011) 1749–1756.
[26] Y. Hong, D.G. Brown, Variation in bacterial ATP level and proton motive force due to adhesion to a solid surface, Appl. Environ. Microbiol. 75 (2009) 2346–2353.
[27] A.S. Gong, C.H. Bolster, M. Benavides, S.L. Walker, Extraction and analysis of extracellular polymeric substances: comparison of methods and extracellular polymeric substance levels in *Salmonella pullorum* SA 1685, Environ. Eng. Sci. 26 (2009) 1523–1532.
[28] J. Chen, S.M. Lee, Y. Mao, Protective effect of exopolysaccharide colanic acid of *Escherichia coli* O157:H7 to osmotic and oxidative stress, Int. J. Food Microbiol. 3 (2004) 281–286.
[29] X. Zhang, R. Garcia-Contreras, T.K. Wood, *Escherichia coli* transcription factor YncC (McbR) regulates colanic acid and biofilm formation by repressing expression of periplasmic protein YbiM (McbA), The ISME 2 (2008) 615–631.
[30] M. Wehland, F. Bernhard, The RcsAB box. Characterization of a new operator essential for the regulation of exopolysaccharide biosynthesis in enteric bacteria, J. Biol. Chem. 275 (1999) 7013–7020.
[31] D. Doherty, J.A. Leigh, J. Glazebrook, G.C. Walker, *Rhizobium meliloti* mutants that overproduce the *R. meliloti* acidic calcofluor-binding exopolysaccharide, J. Bacteriol. 170 (9) (1988) 4249–4256.
[32] S. Yao, L. Luo, K.J. Har, A. Becker, S. Ruberg, G.Q. Yu, J.B. Zhu, H.P. Cheng, *Sinorhizobium meliloti* ExoR and ExoS proteins regulate both succinoglycan and flagellum production, J. Bacteriol. 186 (18) (2004) 6042–6049.
[33] T. Reuber, G.C. Walker, Biosynthesis of succinoglycan, a symbiotically important exopolysaccharide of *Rhizobium meliloti*, Cell 74 (2) (1993) 269–280.
[34] H. Meade, S.R. Long, G.B. Ruvkun, S.E. Brown, F.M. Ausubel, Physical and genetic characterization of symbiotic and auxotrophic mutants of *Rhizobium meliloti* induced by transposon Tn5 mutagenesis, J. Bacteriol. 149 (1) (1982) 114–122.
[35] K.E. Mendrygal, J.E. Gonzalez, Environmental regulation of exopolysaccharide production in *Sinorhizobium meliloti*, J. Bacteriol. 182 (2000) 599–606.
[36] V. Stout, A. Torres-Cabassa, M.R. Maurizi, D. Gutnick, S. Gottesman, RcsA, an unstable positive regulator of capsular polysaccharide synthesis, J. Bacteriol. 173 (1991) 1738–1747.
[37] W. Ebel, J.E. Trempy, *Escherichia coli* RcsA, a positive activator of colanic acid capsular polysaccharide synthesis, functions to activate its own expression, J. Bacteriol. 181 (2) (1999) 577–584.
[38] Design of BioBricks, http://syntheticbiology.org/BioBricks/Part_fabrication.html
[39] B. Obadia, S. Lacour, P. Doublet, A.J. Baubichon-Cortay, C. Cozzone, Grangeasse, influence of tyrosine-kinase Wzc activity on colanic acid production in *Escherichia coli* K12 cells, J. Mol. Biol. 367 (2007) 42–53.
[40] I. Sutherland, Structural studies on Colanic acid, the common exopolysaccharide found in the Enterobacteriaceae, by partial acid hydrolysis, J. Biol. Chem. 115 (1969) 935–945.
[41] R.P. Singh, P. Ramarao, Cellular uptake, intracellular trafficking and cytotoxicity of silver nanoparticles, Toxicol. Lett. 213 (2) (2012) 249–259.
[42] T. Baba, T. Ara, M. Hasegawa, Y. Takai, Y. Okumura, M. Baba, K.A. Datsenko, M. Tomita, B.L. Wanner, H. Mori, Construction of *Escherichia coli* K-12 in-frame, single-gene knockout mutants: the Keio collection, Mol. Syst. Biol. 2 (2006) 2006.0008.
[43] D. Bechtel, L.A. Bulla Jr., Electron microscope study of sporulation and parasporal crystal formation in *Bacillus thuringiensis*, J. Bacteriol. 127 (1976) 1472–1481.
[44] A. Calder, C. Dimkpa, J. McLean, D. Britt, W. Johnson, A. Anderson, Soil components mitigate the antimicrobial effects of silver nanoparticles towards a beneficial soil bacterium, *Pseudomonas chlororaphis* O6, Sci. Total Environ. 429 (2012) 215–222.
[45] C. Levard, E.M. Hotze, G.V. Lowry, G.E. Brown, Environmental transformations of silver nanoparticles: impact on stability and toxicity, Environ. Sci. Technol. 46 (2012) 6900–6914.
[46] A. Omoike, J. Chorover, Spectroscopic study of extracellular polymeric substances from *Bacillus subtilis*: aqueous chemistry and adsorption effects, Biomacromolecules 5 (2004) 1219–1230.
[47] A. Omoike, J. Chorover, Adsorption of goethite to extracellular polymeric substances from *Bacillus subtilis*, Geochem. Cosmochim. Acta 70 (2006) 827–838.
[48] T. Perry, C. Klepac, X.V. Zhang, C.J. McNamara, M.F. Polz, S.T. Martin, N. Berk, R. Mitchell, Binding of harvested bacterial exopolymers to the surface of calcite, Environ. Sci. Technol. 39 (2005) 8770–8775.
[49] M.C. Cammarota, G.L. Sant anna, Metabolic blocking of exopolysaccharide synthesis: effects on microbial adhesion and biofilm accumulation, Biotechnol. Lett. 20 (1998) 1–4.
[50] S. Khan, A. Mukherjee, N. Chandrasekaran, Silver nanoparticles tolerant bacteria from sewage environment, J. Environ. Sci. 23 (2) (2011) 346–352.
[51] M.A. Kiser, H. Ryu, H. Jang, K. Hristovski, P. Westerhoff, Biosorption of nanoparticles to heterotrophic wastewater biomass, Water Res. 42 (2010) 4104–4114.
[52] A. Lankoff, W. Sandberg, A. Wegierek-Ciuk, H. Lisowska, M. Refsnes, B. Sartowska, P. Schwarze, S. Meczynska-Wielgosz, M. Wojewodzka, M. Kruszewski, The effect of agglomeration state of silver and titanium dioxide nanoparticles on cellular response of HepG2, A549 and THP-1 cells, Toxicol. Lett. 208 (2012) 197–213.
[53] L. Limbach, Y. Li, R. Grass, T.J. Brunner, M. Hintermann, M. Muller, D. Gunther, W. Stark, Cerium oxide nanoparticle uptake in human lung fibroblasts: effects of particle size, agglomeration and diffusion at low concentrations, Environ. Sci. Technol. 39 (2005) 9370–9376.
[54] M. Valodkar, A. Bhadoria, J. Pohnerkar, M. Mohan, S. Thakore, Morphology and antibacterial activity of carbohydrate-stabilized silver nanoparticles, Carbohydrate Res. 345 (2010) 1766–1773.
[55] E. Navarro, F. Piccapietra, B. Wagner, F. Marconi, F. Marconi, R. Kaegi, N. Odzak, L. Sigg, R. Behra, Toxicity of silver nanoparticles to *Chlamydomonas reinhardtii*, Environ. Sci. Technol. 42 (2008) 8959–8964.